PNNL-11096
UC-810
Project Technical Information

HWVP Pilot-Scale Vitrification System Campaign - LFCM-8 Summary Report

J. M. Perez
L. D. Whitney
W. C. Buchmiller
J. T. Daume
G. A. Whyatt

April 1996

Prepared for
the U.S. Department of Energy
under Contract DE-AC06-76RLO 1830

Pacific Northwest National Laboratory
Richland, Washington 99352

Battelle

MASTER

PNNL-11096
UC-810
Project Technical Information

HWVP Pilot-Scale Vitrification System Campaign - LFCM-8 Summary Report

JM Perez
LD Whitney
WC Buchmiller
JT Daume
GA Whyatt

April 1996

Prepared for
the U.S. Department of Energy
under Contract DE-AC06-76RLO 1830

Pacific Northwest National Laboratory
Richland, Washington 99352

DISCLAIMER

PACIFIC NORTHWEST NATIONAL LABORATORY
operated by
BATTELLE
for the
UNITED STATES DEPARTMENT OF ENERGY
under Contract DE-AC06-76RLO 1830

Printed in the United States of America

Available to DOE and DOE contractors from the
Office of Scientific and Technical Information, P.O. Box 62, Oak Ridge, TN 37831;
prices available from (615) 576-8401.

Available to the public from the National Technical Information Service,
U.S. Department of Commerce, 5285 Port Royal Rd., Springfield, VA 22161


The document was printed on recycled paper.

Acronyms and Initialisms

AA	atomic absorption spectroscopy
amu	atomic mass units
DAS	data acquisition system
DF	decontamination factor
DOE	U.S. Department of Energy
DOS	disk operating system
DOV	direct operating value
DRE	organic destruction and removal efficiency
DWPF	Defense Waste Processing Facility
EAA	electrical aerosol analyzer
ESM	engineering-scale melter
FY	fiscal year
GF	gradient furnace
HEME	high efficiency mist eliminator
HEMF	high efficiency metal fiber
HEPA	high efficiency particulate air filter
HB	high bay
HLW	high-level radioactive waste
HWVP	Hanford Waste Vitrification Plant
IC	ion chromatography
ICP-AES	inductively coupled plasma atomic emission spectroscopy
ICP-MS	inductively coupled plasma mass spectroscopy
IDMS	Integrated DWPF Melter System
KfK	Kernforschungszentrum Karlsruhe Institute
KVA	kilovolt ampheres
LEL	lower explosive limits
LFCM	liquid-fed ceramic melter
MFT	melter feed tank
M&TE	measuring and testing equipment
NCAW	neutralized current acid waste
OLC	off-gas line cleaner
PC	personal computer
PHTD	PNL HWVP Technology Development Project
PNL	Pacific Northwest Laboratory
POG	process off-gas
PSCM	Pilot-Scale Ceramic Melter
QA	quality assurance
SBS	submerged bed scrubber
SCFM	standard volumetric flow
SCR	silicon controlled rectifier
SIPT	slurry integrated process test
SME	slurry mix evaporator
SOP	safe operating procedure
SRAT	slurry receipt and adjustment tank
TRU	transuranic
VVS	vessel vent system
WC	water column
WHC	Westinghouse Hanford Company
WSRC	Westinghouse Savannah River Company
WVDP	West Valley Demonstration Project
XRF	X-ray diffraction

Acknowledgments

Besides the authors identified, a significant number of PNL staff supported this work. We wish to acknowledge staff of the Applied Melter Technologies Section and other members of the Engineering Technology Center. These staff took time from their own critical work to support this work by filling the shift assignments or conducting sampling or measurement activities. Staff include Jeff Higginson, Mike Elliott, Kathy Whittington, Ken Eliason, Matt Cooper, Gene Whittington, Dave Lamar, Rick Merrill, Gary Sevigny, Chuck Hymas, Roy Lundgren, and Charlie Freeman.

Steve Halstead and Jim Davis of the Process Technology Department are cited for their support throughout the campaign coordinating SIPT interfaces, principally the slurry sampling system and feed pump control.

Dana Widrig, Bob Barbera, and Frank Hara are thanked for performing the sample characterization of the glass and slurry samples. Eric Wyse and Ron Sanders of the Materials and Chemical Sciences Center performed ICP-MS and X-ray Fluorescence analyses, respectively.

Dr. D. S. Kim evaluated the cold cap samples and reported the results for inclusion in this report.

Task Managers George Jensen and Don Larson of the PHTD Project provide technical and management support of this work throughout the planning and testing phases of this work.

Finally, the presentation of this work has been enhanced significantly by the technical editing and publications support provided by Barbara Eaton and Hyo Morgan.

Summary

The Hanford Waste Vitrification Plant (HWVP) is being designed to treat the high-level radioactive waste (HLW) stored in underground storage tanks as an alkaline sludge. Tank wastes will first be retrieved and pretreated to minimize the solids requiring vitrification as HLW. The glass product resulting from HWVP operations will be stored onsite in sealed stainless steel canisters until the HLW repository is available for final disposal. The first waste stream scheduled to be processed by the HWVP is the neutralized current acid waste (NCAW) stored in double-shell storage tanks.[(a)] The Pacific Northwest Laboratory (PNL) is supporting Westinghouse Hanford Company (WHC) by providing research, development, and engineering expertise in defined areas. As a part of this support, pilot-scale testing is being conducted to support closure of HWVP design and development issues. Testing results will verify equipment design performance, establish acceptable and optimum process parameters, and support product qualification activities.

The HWVP-16/LFCM-8 campaign was performed in fiscal year (FY) 1993 by the PNL HWVP Technology Development Project (PHTD) to obtain data to support specific process and design data needs. Operation at defined plant conditions of temperatures, pressures, and flow rates were duplicated as closely as possible during the campaign. Principal components evaluated included components comprising the feed delivery system, off-gas treatment system, and glass discharge control system. The feed delivery system components included recirculation loop, feed line, cross-flow strainer, and feed nozzle. To obtain this data, testing was integrated with the Slurry Integrated Process Test (SIPT) system. Off-gas treatment systems for which data was required included the film cooler, control air injection position, and submerged bed scrubber (SBS) and high efficiency metal fiber (HEMF) filter. Glass discharge system components included the prototypic glass sampler/canister throat protector and differential pressure glass pour system.

In addition to design data, process data was required to assess the production performance of the liquid-fed ceramic melter (LFCM) processing the revised NCAW flowsheet. This included assessment of the impact of adding a simulated HWVP recycle waste to the melter feed, the effectiveness of plenum heaters to boost production rates, and the effectiveness of the melter and off-gas system to destroy and remove organics from the off-gas stream. Finally, data on glass and feed samples were provided to other PHTD activities to support their laboratory studies.

The LFCM-8 campaign began on April 17 and concluded on May 16. All required data necessary to support design objectives were successfully obtained. Because of the failure of key analyzer equipment, the LFCM was idled between April 29 and May 10. On May 10 the campaign resumed and continued until May 16. For reporting purposes, the two segments of the campaign have been defined as LFCM-8A and LFCM-8B. The combined LFCM-8A and LFCM-8B campaign times totaled

(a) The revision of the Hanford Tri-Party Agreement may revise the processing sequence of wastes through the HWVP.

439 hours. This consisted of 433 hours of melter feeding and 6 hours of downtime. A total on-line efficiency of >98% was achieved. The total volume of feed slurry processed was estimated to be 23,113 liters. This resulted in 11,105 kg of glass being produced and discharged into full-scale West Valley Demonstration Project (WVDP) canisters.

Although there was a 10-day idle period the performance of the pilot-scale vitrification system was outstanding with one exception. The SBS packing was retained in the housing by a screen that was tack-welded to the bed housing. During the latter part of the campaign (i.e., LFCM-8B), some of the tack welds failed and the packing was ejected from the bed by the off-gas stream. Nonetheless, particulate scrubbing performance of the SBS was not measurably affected by the loss of the packing material.

The prototypic feed system, consisting of recirculation loop, cross flow strainer, feed line, and three-way valve, performed very well for the most part. No plugging of the feed line or strainer occurred. Water flushes performed when the feed flow rate began dropping and were successful in restoring the feed rate. The control of the feed rate into the melter was significantly affected by the feed's physical properties. In order to reduce the feedrate within the LFCM process range, the feed line had to be replaced with tubing. The tubing had about 50% of the original line's inner diameter and was over 50% longer. The three-way valve operation was very good until the final days of the campaign. Erratic behavior is believed to be due to solids that accumulated in the valve housing throughout the campaign.

The processing rates in the melter were well below expectations, based on previous pilot-scale melter runs. Nominal feed process rates were 55 to 60 L/h as compared to the expected 80 to 85 L/h. A combination of poor slurry behavior in the melter and cold cap melt rate is believed to be responsible for the low processing rate.

All primary and a majority of the secondary objectives were achieved within the constraints of the campaign. They are summarized in the Conclusion and Recommendations Section of this report. Of the primary objectives, the evaluation of the glass sampler could not be fully completed. This was caused by the glass bonding to the sample cup during the fourth sampler test.

All of the off-gas system objectives were completed. Of the more critical objectives of the campaign, evaluation of the HEMF filter and initial determination of the organic destruction and removal efficiency (DRE) of the melter and off-gas treatment system were both successfully completed. The HEMF filter was extremely efficient, and the off-gas particulate concentration downstream of the filter was always below the detection limit of the electrical aerosol analyzer. The results indicate that the filter exceeded the 10^5 decontamination factor when evaluated using the full particle size distribution. For particles having approximately 0.1 μm diameter, the results are not conclusive that a 10^5 performance standard was met because of the detection limit constraint. However, every indication was that the filter was functioning properly from a particle removal standpoint.

Formic acid DRE test results indicate that the formic acid destruction in the melter is roughly 99.95% complete. The variability in the SBS formate concentration makes estimation of downstream formate removal and subsequent DRE values questionable. This uncertainty resulted in the overall vitrification system DRE being set at 99.8%. It is expected that the average DRE will very nearly equal the melter destruction efficiency.

Contents

Figures

Tables

1.0 Introduction

Vitrification testing activities by the Hanford Waste Vitrification Plant (HWVP) Project are required to support closure of HWVP design and development issues. Results will verify equipment design, establish acceptable and optimum process parameters, and support product qualification activities. This campaign summary presents the results of the HWVP-16/liquid-fed ceramic melter (LFCM)-8 test. The HWVP-16/LFCM-8 campaign was performed specifically to 1) develop data necessary for Fluor-Daniel, Inc. to complete the vitrification system design; 2) perform flowsheet testing to demonstrate acceptability of the melter feed composition, including addition of a simulated HWVP recycle stream; 3) operate and evaluate prototypic feed nozzle, glass sampler, air injection for melter vacuum control, differential pressure glass pour control, and plenum heaters; and 4) operate and evaluate prototypic off-gas treatment equipment.

The HWVP-16 campaign was performed in the LFCM between April 17 and May 16, 1993. This was the first HWVP pilot-scale melter campaign in which lid heaters were used to boost production rates. Two previous engineering-scale melter tests were performed in FY 1992 with which results could be compared--one at the Kernforschungszentrum Karlsruhe Institute (KfK) and the second by the Westinghouse Savannah River Company (WSRC). This activity was conducted under the direction of the Pacific Northwest Laboratory (PNL)[a] Project Work Plan and FY 1992 Statement of Work. The technical requirements for pilot-scale testing by the HWVP project are defined by May (1992). The specific test objectives for LFCM-8 were transmitted to PNL through the FY 1993 Statement of Work [U.S. Department of Energy (DOE) 1992] and are further defined in the PNL HWVP Technology Development (PHTD) Project Work Plan for FY 1993 (Creer 1992). The specific data requirements, test approach, and testing constraints are defined in the HWVP-16/LFCM-8 Test Plan (Janke 1991).

The conclusions and recommendations of the LFCM-8 campaign are provided in Section 2. Test objectives, test methodology, equipment descriptions, and testing highlights are given in Section 3. Test results are presented and discussed in detail in Section 4.

(a) Pacific Northwest Laboratory is operated for the U.S. Department of Energy by Battelle Memorial Institute under Contract DE-AC06-76RLO 1830.

2.0 Conclusions and Recommendations

The conclusions and recommendations resulting from the HWVP-16/LFCM-8 campaign are presented in this chapter. Each is stated in brief bulleted format. Detailed data presentations and discussions supporting the findings stated here are provided in Chapter 4.

2.1 Conclusions

2.1.1 Slurry Integrated Process Test Equipment Performance

- The slurry integrated process test (SIPT) recirculation loop and cross-flow strainer provided a steady, uninterrupted supply of melter feed to the LFCM. Modifications to the feed line to increase its length and reduce its diameter were required, however. This was necessary to increase the line pressure; thereby dropping the feed rate to the LFCM to within the required range.

- The Everlasting® three-way feed line flush valve performed well for the majority of the campaign. Reduced performance was indicated during the final days of the LFCM-8A by the fact that repeated flush operations were sometimes required and valve alignment appeared to be offset. Solids accumulations were found in the three-way valve after the campaign. This may explain operational difficulties experienced toward the end of the campaign.

- The melter feed nozzle performed well, with the exception of solids accumulation on the outside of the nozzle. The solids extended down to the cold cap surface. This was because the insulation on the outside of the nozzle allowed the exterior surface to operate hot.

2.1.2 Melter Equipment Performance

- The current HWVP reference feed has very poor cold cap behavior and a slow melting rate. This contributes to the achievement of only 64% to 70% of the HWVP design criteria process rate of 200 L/h based on the scale up of LFCM-8 results.

- The use of plenum heaters may have had a detrimental affect on melter process rate based on visual observations of the cold cap, cold cap probing and comparisons to current modeling prediction results.

- The differential pressure glass discharge system operation was stable and controllable with no observable effect on the glass pour stream.

- The combination throat protector/glass sampler apparatus successfully obtained samples with minimum interaction with the glass pour stream. However, the sample cup can not be fully retracted when the glass is allowed to completely fill the cup due to an excessive amount of glass in the cup.

- Cadmium deposits in the off-gas line were found to be no more significant than other semivolatile feed constituents such as sodium and potassium. A melter decontamination factor (DF) for cadmium was measured to be approximately 350.

2.1.3 Off-Gas Treatment Equipment Performance

- The average mass DF for the melter was 1520 (based on metal oxides). The concentration and size distribution of aerosols were fairly uniform over the cross-section of the off-gas line. (i.e., aerosol concentration or size distribution did not vary significantly between the inside, center, and outside of bend in off-gas jumper.)

- Concentrations of potentially explosive gases (H_2 and CO) were greater than 10 times below the lower explosive limits (LELs) throughout LFCM-8.

- An adequate nitrogen balance across the melter could not be achieved. NO_x emissions account for only approximately 65% of the nitrogen entering the melter in the feed. It is likely that ammonia or other compounds account for the balance, but this could not be confirmed during LFCM-8.

- The average mass DF for the submerged bed scrubber (SBS) was 5.0 (based on metal oxides). The SBS DFs did not noticeably change throughout LFCM-8, despite the loss of packing in the SBS that occurred during the latter portion of the run. Essentially no scrubbing of NO_x occurred in the SBS.

- Pressure/flow oscillations in the off-gas line originating from the SBS were observed. These SBS pressure drop oscillations exhibited a frequency of 2.7 Hz and a magnitude of 2.5 in. water column (WC) (peak-to-peak).

- Formic acid destruction and removal efficiency for the melter and off-gas system was estimated to be 99.8%. The maximum melter destruction efficiency was measured to be 99.95%. However, variability of SBS formate analyses require that the lower, more conservative result be used at this time.

- The average mass DF for the high efficiency mist (HEME) determined from cascade impactor samples was 107. The HEME DF determined from electrical aerosol analyzer (EAA) measurements was 324.

- The high efficiency metal fiber (HEMF) filter was substantially loaded with particulate during LFCM-8, and exhibited a corresponding increase in pressure drop from 2.5 to 50 in. WC. The clean pressure drop was restored after completion of a backflush procedure supplied by the vendor. The overall mass DF was 10^5 or greater for all sampling periods.

2.2 Recommendations

- The alternative Fujikin feed system flush valve should be considered as a replacement for the Everlasting® valve because the Everlasting® valve has a tendency to accumulate solids that interfere with its operation. WSRC's experience with both valves should be re-examined to determine if an acceptable operating procedure for the Fujikin valve can be developed.

- The method of controlling the feed rate to the melter should be re-evaluated. The current system allowed a very limited range of control (modification of the feed line and installation of an upstream restrictor were required), was highly dependant on slurry rheology, and as tank level dropped the range of control also dropped.

- The HWVP reference melter feed flowsheet should be investigated to determine the variable or variables contributing to its poor processing performance. These include: optimum plenum space temperature, frit composition, recycle waste stream composition, and slurry properties.

- The glass sampling device should be redesigned to improve its operation and ensure that it can be withdrawn back into the flange after use. Redesign of the device is also recommended to ensure its operability in the plant during remote operations.

- Pressure oscillations in the SBS should be studied further to determine the variables that contribute to this behavior and to determine methods of dampening or eliminating the oscillations.

- During future melter campaigns, aerosol sampling should be conducted for longer periods of time if compositional analyses are required. A larger sample mass is needed for accurate analysis.

- Gas analysis equipment needs to include accurate analyzers for NH_3 and, possibly, other nitrogen compounds. This will make it possible to achieve a nitrogen balance across the melter.

3.0 Experimental Approach

The LFCM-8 campaign was performed according to the LFCM-8 Test Plan (Janke 1991). The plan identified the specific test objectives, the data required during the campaign to successfully complete the objectives, the equipment and procedures to be used during the campaign, and the test schedule. This section describes the objectives and the degree to which they were completed, the method or approach to complete the objectives, descriptions of the test equipment, the test schedule, and test highlights of the campaign.

3.1 Test Objectives

Presented below are the test objectives defined by the test plan. The experimental approach used to complete each objective is stated after each objective. The degree to which each was completed, and the section in this report where the results are located are also given. In cases where data or samples were obtained for another HWVP development activity, results were not reported in this summary report. Where appropriate, this fact is identified. Primary objectives were of highest priority. The level to which secondary objectives were completed depended on completion of the primary objectives if there was a testing conflict, actual length of the test, ability to maintain steady state, and remaining resources and funds.

- Determine glass properties and compare them with laboratory glasses of identical compositions as well as with property values predicted from empirical models - Secondary objective.

  Approach - Obtain glass samples during LFCM-8 as the glass composition in the melter is converted from the composition of the startup glass to that of the target glass composition.

  Partially completed - Glass samples were obtained at the beginning and during the campaign for performing this comparison by PHTD glass development staff.

- Correlate glass redox of melter glasses as functions of plenum temperature, recycle addition, and process time; and compare results to laboratory results - Secondary objective.

  Approach - Obtain glass samples throughout the test period and evaluate against measured changes in melter and feed composition parameters.

  Partially Completed - Glass samples were analyzed to determine glass redox, and process data is available (see section 4.2). However, changes in plenum temperature and recycle addition did not occur (this was not planned for LFCM-8).

- Evaluate performance of melter feed recirculation loop and cross-flow strainer (Fluor Data Need No. 1.4a) - Primary objective.

Approach - Monitor pressure and flow parameters throughout the campaign as well as feed properties, such as density and solids concentration. Based on entire test period, determine whether loop or strainer performance changed over time.

Completed - The SIPT staff performed this system evaluation during the LFCM-8 campaign and obtained sufficient data to complete this objective for the nominal feed case.

- Evaluate melter feed loop pressure drop (Fluor Data Need No. 1.4b) - Primary objective.

  Approach - Monitor pressure and flow parameters throughout the campaign as well as feed properties, such as density and solids concentration. Also, monitor the frequency of line pluggages that occur. Based on entire test period, determine whether feed loop performance changed over time.

  Completed - The SIPT staff performed this system evaluation during the LFCM-8 campaign and obtained sufficient data to complete this objective for the nominal feed case.

- Establish melter processing rates using plenum heaters for preliminary confirmation of Defense Waste Processing Facility (DWPF) melter design - Primary objective.

  Approach - Establish steady state feeding and melting conditions and assess nominal and maximum feed rate processing. Characterize cold cap conditions via routine visual observations.

  Completed - The results are reported in Section 4.1.

- Obtain preliminary data on impact of zeolite and diatomaceous earth from transuranic (TRU) recycle on melter throughput rate - Primary objective.

  Approach - Characterize process conditions, e.g., cold cap thickness, cold cap melting rate, cold cap coverage, and power consumption and assess results against previous process tests.

  Partially completed - Process results of the composite feed are reported in Section 4.1. There were no variations in recycle composition or relative concentration in the feed planned for LFCM-8. Therefore, any differences in process results that may be observed, which were different from previous tests could not be directly attributed to the inclusion of recycle in the melter feed.

- Evaluate feed flow control and potential for melter feed nozzle clogging using the Fluor melter feed line design (Fluor Data Needs Numbers 1.4a and 1.4b) - Primary objective.

  Approach - Evaluate effect of cooling water flow on frequency of feed nozzle pluggages. Measure feed line pressure stability as a function of feed rate.

  Completed - Results are reported in Section 4.3.

- Assess glass pour stream stability and interaction with the DWPF-designed throat protector/ glass sampler (excludes manipulator testing) - Primary objective.

  Approach - Document glass pour stream characteristics during starting, pouring, and stopping glass pour actions. Conduct glass sampling tests to assess sampler performance as a function of sample time, pour rate and overflow section temperature.

  Partially Completed - The test matrix defined in the test plan could not be completed because glass became bonded to the sample cup. Results are reported in Section 4.3.

- Evaluate the performance of the HWVP melter differential pressure glass-pouring system using the prototypic SBS design (supports Fluor Data Needs No. 3.6a) - Primary objective.

  Approach - Document operating characteristics of pour control system on glass pour stream stability and determine operating parameters, i.e., discharge section pressure, injection air rate, and effect of SBS tube submergence.

  Partially Completed - Data at two of the three submergence settings for the SBS vent pipe were attained. Results are reported in Section 4.4.

- Evaluate melter pressure control with air injection placement either near the melter or after the HEMF filter (Fluor Data Needs No. 3.6a) - Primary objective.

  Approach - Testing was performed prior to LFCM-8 to evaluate this objective. Measure melter and off-gas system pressures throughout LFCM-8 to determine any differences from the previous testing.

  Completed - Results are reported in Section 4.5.

- Obtain film cooler pressure drop data (Fluor Data Needs No. 3.1a) - Primary objective.

  Approach - Testing was performed prior to LFCM-8 to evaluate this objective. Measure film cooler flow, temperature and pressure drop throughout LFCM-8 to determine any differences from the previous testing.

  Completed - This objective was completed during SBS testing conducted before the LFCM-8 campaign (Whyatt et al. 1992). Additional data obtained during LFCM-8 is discussed in Section 4.8.

- Determine the DF of the SBS for aerosol particles with aerodynamic diameters $> 1\mu m$ and $< 1\mu m$ - Primary objective.

  Approach - Perform aerosol sampling of the inlet and outlet submerged bed scrubber (SBS) gas streams during steady-state operating periods of the test. Quantify mass and constituent fractions of aerosol the particles.

  Completed - Results are reported in Section 4.10.

- Determine the NO_x removal performance of the melter off-gas system - Primary objective.

  Approach - Continuously monitor off-gas stream and measure the concentration of NO and NO_x in the stream. Sampling is to occur at the inlet and exit of the SBS and at the end of the off-gas treatment systems.

  Completed - Results are reported in Section 4.9.

- Determine the melter and off-gas decontamination factors for the following elements: cadmium, lead, tellurium, selenium, tin, antimony, and iodine - Primary objective.

  Approach - Perform particulate and aerosol sampling between the LFCM and each off-gas treatment system during steady-state operation. Quantify mass and constituent fractions and estimate capture efficiency of the equipment for these feed constituents.

  Completed - Results are reported in Section 4.10.

- Characterize the off-gas from the LFCM and associated off-gas system during the run - Primary objective.

  Approach - Perform continuous gas monitoring throughout the test to track and characterize non-condensible gas concentrations. Sampling is to occur after each piece of process equipment.

  Completed - This objective was partially completed during SBS testing conducted before the LFCM-8 campaign (Whyatt et al. 1992). Additional data obtained during LFCM-8 is discussed in Section 4.8.

- Provide size distribution characterization of aerosols throughout the melter off-gas system - Primary objective.

  Approach - Sample aerosols using cyclone separator sampling equipment to classify particulate mass. Determine relative mass fraction in each separator and obtain elemental analyses of the captured materials.

  Completed - Results are reported in Section 4.10.

- Determine the operating history of off-gas equipment including circulation rate within the SBS bed (data needs defined in change request HWVP-0517 and in Fluor needs 3.1a, 3.2b, 3.2c, 3.2e) - Primary objective.

  Approach - Monitor long-term operation of the off-gas treatment equipment, i.e., measure temperature, flow, pressure, and liquid level variables and determine changes over time.

  Completed - This objective was completed during SBS testing conducted before the LFCM-8 campaign (Whyatt et al. 1992). Additional data obtained during LFCM-8 is discussed in Section 4.8.

- Determine if pressure drop across the HEMF filter increases over the duration of the run. If pressure drop increase is noted, evaluate the ability of a water wash to restore the clean pressure drop. Evaluate the effectiveness of the filter to remove small particulates from the gas stream. (Requirement in change request HWVP-0517) - Secondary objective.

  Approach - Monitor HEMF filter differential pressure over time and perform water flush procedure to restore operational efficiency. Determine HEMF filter DF during steady-state operating periods to assess filter efficiency.

  Completed - Results are reported in Section 4.8.

- Determine the amount of solids buildup, especially cadmium, occurring in the off-gas lines during the melter run (Fluor Data Need No. 3.9a) - Primary objective.

  Approach - At the conclusion of LFCM-8 disassemble off-gas line jumper and measure solids accumulation. Sample solids to quantify cadmium concentration in the solid.

  Completed - Results are reported in detail by Perez et al. (1993). Results have been summarized in Section 4.10.

- Determine the concentration of soluble and insoluble solids in the thermosyphon concentrator bottoms - Secondary objective.

  Approach - Sample bottoms generated by thermosyphon and analyze to determine composition and weight fraction of soluble and insoluble materials.

  Not completed - Due to testing priorities, this work was not performed.

- Determine the effectiveness of the HEMF filter to operate as part of the vessel vent system (VVS) by operating the LFCM off-gas treatment system with the HEME filter valved out - Primary Objective.

  Approach - Characterize filtration performance for aerosols over time and determine any decrease in performance throughout the test period.

  Completed - Results are reported in Sections 4.8 and 4.10.

- Operate the West Valley Demonstration Project (WVDP) prototypic off-gas line cleaner during LFCM-8 as a routine operation and evaluate its effectiveness - Secondary Objective.

  Approach - Operate cleaning device routinely throughout campaign. Document changes to any performance characteristics. At end of test remove device and inspect it and the film cooler to determine effectiveness.

  Partially completed - Results are reported in detail by Buchmiller et al. (1993) and are summarized in Section 4.6.

- Obtain initial characterization on the organic thermal destruction and removal efficiency of the LFCM and off-gas treatment system for formate - Primary Objective.

  Approach - Perform specific sampling of the melter and SBS offgas streams and SBS condensate. Quantify formate concentration in these streams and correlate to melter feed concentrations.

  Completed - Results are presented in Section 4.11.

3.2 General Operations

3.2.1 General

The success of a pilot-scale system campaign depends on the preparations and planning that precede startup and the disciplined execution of the test plan. Success is, therefore, based on ensuring that the following key activities are completed:

1. All required equipment and data gathering preparations are complete.
2. Shift operations staff are properly briefed on their duties and responsibilities.
3. The required testing materials are on hand.
4. Scheduled operational activities are identified and tracked.
5. Quality assurance requirements are satisfied.

Pre-test and operational activities performed as part of LFCM-8 in these areas are described in the following paragraphs.

The LFCM and off-gas treatment equipment are composed of over 125 pieces of measuring and testing equipment (M&TE). These are identified and tracked using the control listing form presented in Appendix A. Each item is assigned a unique control number, and key information such as calibration interval and calibration level requirement (i.e., "Category") is defined. The fact that the M&TE calibration intervals spanned the LFCM-8 campaign period was verified for each equipment piece just before the start of LFCM-8. The operational readiness of the process equipment itself was determined during pre-LFCM-8 shakedown tests that were conducted in the months before LFCM-8.

Execution of a major campaign such as LFCM-8 requires staff who are assigned shift support duties. These staff were specifically trained to ensure that they adequately understood the test objectives, equipment operations, and duties. A training record prepared to document minimum required staff training is presented in Appendix B. Training consisted of reading assignments, briefings, and hands-on operation of the equipment before LFCM-8. Reading assignments included the test plan and all applicable procedures. The procedure list is presented in Table 3.1. Before LFCM-8, a pre-run briefing was conducted during which the test plan and schedule were reviewed, shift schedules were discussed, and any questions concerning execution were answered. The final major documents

Table 3.1. LFCM-8 Operations Procedures

SOP-21	Auxillary Off-Gas System Safe Operating Procedure (SOP)
SOP-53	Thermosyphon Evaporator SOP
SOP-57	Process Off-Gas System SOP
SOP-67	SIPT Feed Preparation Test System SOP
SOP-68	Liquid-Fed Ceramic Melter SOP
WTC-006-31	Non-Condensible Gas Sampling Procedure
WTC-006-34	SIPT, LFCM, and Off-Gas System Performance Characterization
LFCM-1	Glass Pouring Procedure
LFCM-2	Glass Sampling Procedure
LFCM-3	Off-Gas Cleaner Operating Procedure
LFCM-4	Tank-60 Feed System Operating Procedure
LFCM-5	LFCM Over-Pressure Vent Operating Procedure
LFCM-6	Discharge, Plenum, and Electrode Over-Temperature Alarm Operation Procedure
LFCM-7	Electrode Transformer Cooling Water Alarm Operation Procedure
LFCM-8	LFCM Electrode, Plenum Heater, and Discharge Heater Process Controller Operating Procedure
LFCM-9	Operational Guidelines for the LFCM Data Acquisition System

required before commencement of the campaign were the pre-run checklist and the operational readiness checklist. These checklists, shown in Appendix C, provided a final review to ensure that all previous planning and preparations had been completed. They also ensured that the required sampling and test materials were on hand and that spare parts and safety-related equipment were available.

Data collection, sampling activities, and equipment operations were completed following a set routine. A daily activities schedule and log, shown in Appendix D, was used to ensure that routine tasks were completed on schedule. Data not automatically stored by the data acquisition system (DAS) were recorded on data and status sheets. These sheets are reproduced in Appendix E. To ensure that the system was functioning properly, DAS data were reviewed each day by recording and reviewing key data on Status Sheet No. 2.

3.2.2 Off-Gas Sampling and Analysis Equipment

Off-gas sampling for noncondensible gases occurred during LFCM-8 to determine production rates of H_2, CO_2, and NO_x in the melter and the concentration of these gases in the off-gas lines. Attempts were made to measure concentrations of CO, N_2O, CH_4, and NH_3 as well, but concentrations were too low to accurately measure with the available equipment. Aerosol sampling was also conducted to determine the concentration, size distribution, and chemical composition of aerosols present at various locations throughout the off-gas system.

Gas Sampling. Sampling was performed at three locations in the off-gas system for non-condensible gases, NO and NO_2 (NO_x). These locations were as follows:

1. Before SBS: Sample drawn from the off-gas line before entering the SBS.

2. After SBS: Sample drawn from the line between the SBS and the HEME.

3. After HEMF: Sample drawn from the off-gas line just downstream of the HEMF but before the downstream control air injection.

Sampling occurred continuously after the HEMF filter, except for brief periods daily when samples were taken at the other two locations.

The gas sampling train is shown in Figure 3.1. Helium was injected into the off-gas line near the film cooler at a known flow rate using a mass flow controller. The helium was used as a tracer gas to determine the relative concentration of sampled gases to the concentration present in the off-gas line. The gas to be sampled was drawn from the appropriate location through stainless steel tubing, initially, and then through polypropylene. The gas passed through a condenser (ice bath) to remove most of the water. This condensate is analyzed to determine the quantity of gas scrubbed out in the condensate prior to measurement. Argon was then injected at a known flow rate to lower the dew point and avoid condensation in the sampling lines entering the analytical equipment. The diluted sample gas was sampled by the mass spectrometer and the gas chromatograph before being routed through the infrared analyzers and the NO_x analyzer. The accuracy of the other analyzers exceeds the accuracy of the mass spectrometer; therefore, the mass spectrometer was used during LFCM-8 testing only to detect the presence or absence of gases with atomic masses less than 50 amu. The gas chromatograph was used to analyze for H_2, He, N_2, and O_2. Separate infrared analyzers were used to analyze for CO_2, CO, N_2O, CH_4, and NH_3. The NO_x analyzer automatically switched to NO mode for one minute out of every ten so that the NO:NO_2 ratio could be determined.

Aerosol Sampling. Evaluation of total mass DFs for the melter and off-gas components throughout the system were evaluated. Elemental DFs were also calculated for the melter and the SBS. Where possible, size distributions of the off-gas were determined.

To characterize the off-gas leaving the melter and SBS, samples were taken from the off-gas line after the melter and after the SBS, using the aerosol sampling train shown in Figure 3.2. Isokinetic sampling was attempted for these samples. The sampled melter effluent stream was drawn through heat-traced tubing and through a cyclone separator, which separates the particulate by aerodynamic diameter. The nominal cutpoints were 16, 6, and 1 μm. However, the actual cutpoints differed from these because the sample flow had to be adjusted for process conditions and available nozzle sizes to achieve isokinetic flow. Particulate smaller than approximately 1 μm were collected on a final filter. The gas was then scrubbed in three consecutive NaOH scrubbers.

Sampling after the SBS was performed in the same way as that before the SBS, except a cascade impactor was used rather than a cyclone separator, because of lower concentrations of particulate in this stream. Sampling was performed on most days during the run and was done during relatively steady conditions. The sample duration was generally 2 hours, although certain samples were taken over longer periods to acquire more particulate.

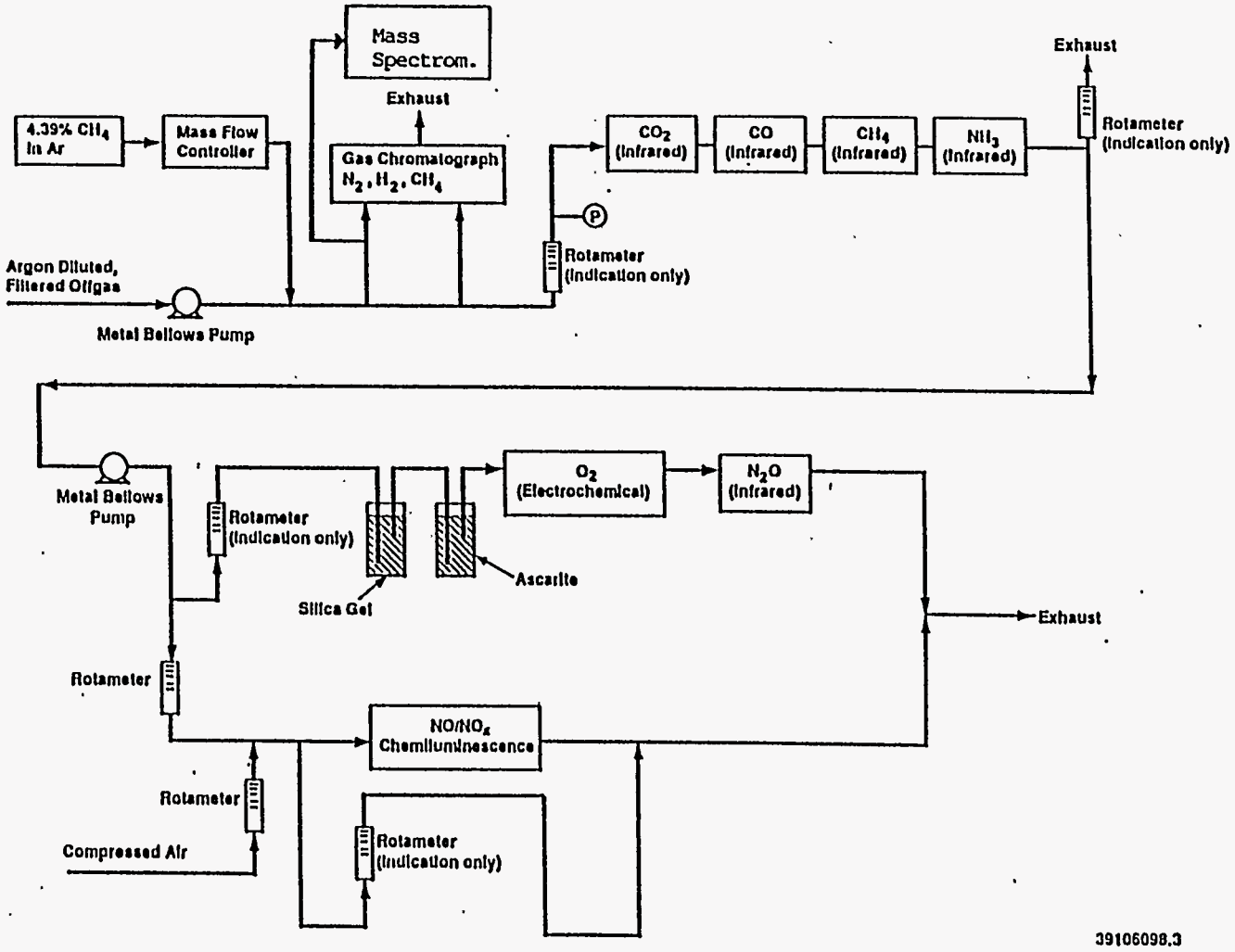

Figure 3.1. Gas Sampling Train

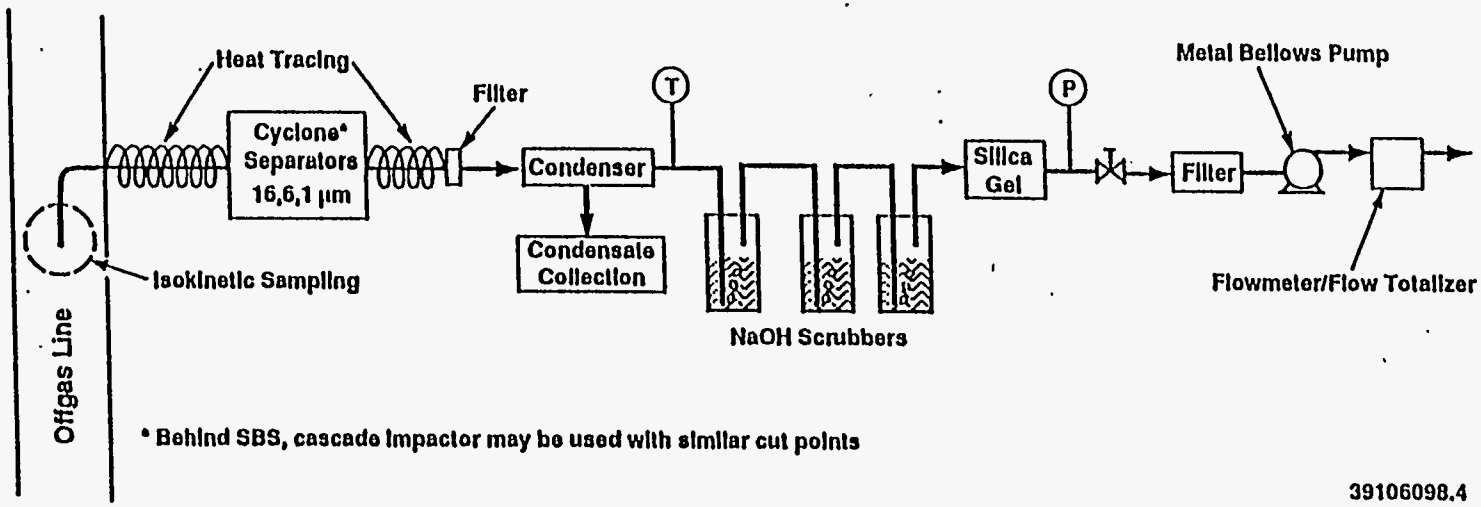

Figure 3.2. Aerosol Sampling Train

One sample of the gas exiting the HEME was taken. This sample was taken using the sampling train used for post-SBS samples. For all of these aerosol samples, the mass of aerosol collected in each cyclone, impactor stage, or filter was measured. The cyclone, filter, and scrub solution samples were analyzed for composition. Most cations were analyzed using X-ray diffraction (XRF) or inductively coupled plasma atomic emission spectroscopy (ICP-AES). Ion chromatography (IC) was used for anions (except I). Inductively coupled plasma mass spectroscopy (ICP-MS) was used to analyze for I, Cd, Pb, Te, Se, Sn, and Sb.

Electrical Aerosol Analyzer (EEA). A TSI Model 3030 EAA was used to measure the concentration and size distribution of aerosols before and after the HEMF filter. A schematic of the instrument is provided in Figure 3.3. The aerosol sample enters the analyzer at a known flow rate determined by a mass flow meter within the instrument and controlled by a manual valve. The aerosol particles are charged by the corona discharge of a tungsten wire contained in the charger section. The charger sheath is supplied through a rotameter to provide a buffer of clean air between the aerosol particles and the charger wire/screen assembly to ensure a uniform charging of the aerosols. After charging of the particles, the sample enters the analyzer section. A high-voltage rod positioned in the center is set to one of a number of preset voltages. Analyzer sheath air passes up the center of this rod and is directed downward, providing a sheath of clean air around the rod. The charged particles are attracted to the rod and migrate through the clean sheath of air, and may or may not deposit on the rod. After leaving the analyzer section the air is filtered, and a sensitive electrometer measures the rate of charge transferred to the electrometer by the remaining aerosol particles. Finally, the flow rate of the air is measured by a mass flow meter. A manual valve is used to adjust the total flow through the instrument.

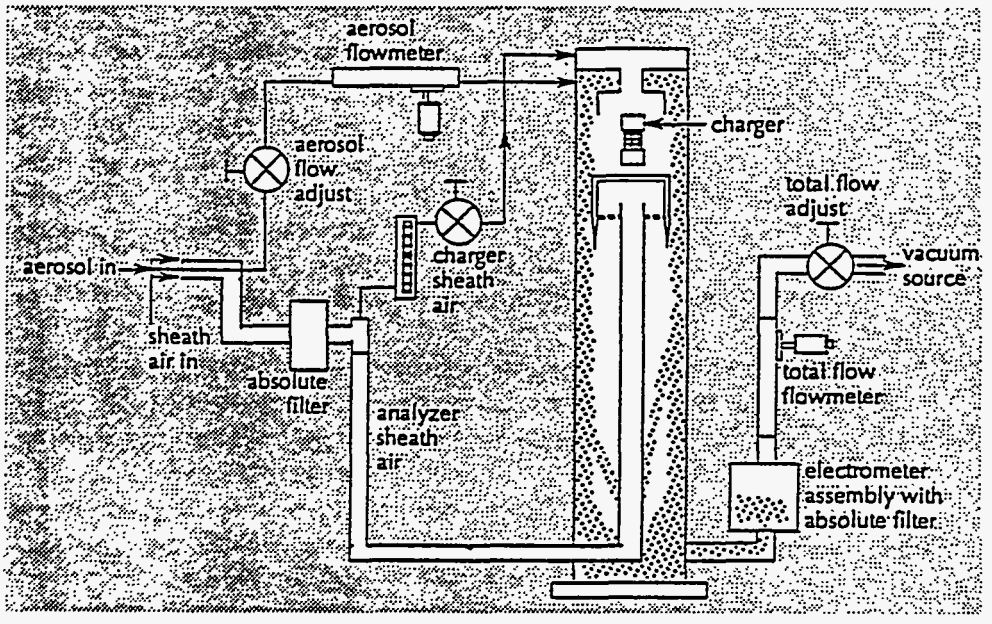

Figure 3.3. Electrical Aerosol Analyzer

The current collected on the electrometer depends on the total rate of charge transferred by aerosol particles escaping the analyzer section. The ability of a particle to escape the analyzer section primarily depends on the size of the particle in question and the voltage on the collector rod. Other factors contribute to the capture of the particle on the rod but will not be discussed here. The voltage on the collector rod is initially set at a low value, and the total current being collected at the electrometer is measured. Then the voltage is increased through a number of preset voltages, and the changes in current at the electrometer are noted. Each time the voltage is increased, more particles of increasingly larger size are collected on the high-voltage rod, and the current measured at the electrometer decreases. From the observed decreases, the number and size of the aerosol particles can be deduced.

The particle size cut-points and sensitivities (the amount of electrometer current per particle collected of a given size) for the electrical aerosol analyzer instrument is well established for operation at near-ambient pressure. However, changes in pressure affect the sensitivity of the analyzer and have a small effect on the mobility of the aerosol particles in the analyzer section of the instrument. The pressure of the off-gas in the vicinity of the HEMF filter was substantially sub-ambient. To allow collection of data at sub-ambient pressure, the EAA was sent to the University of Minnesota and the sensitivities and cutpoints were determined at absolute pressures of 0.901, 0.878, and 0.853 atm. The typical pressure at the inlet to the EAA while sampling from the off-gas line near the HEMF during LFCM-8 was approximately 0.85 atm, although some variation occurred depending upon the operating conditions of the melter system. The instrument calibration that developed for 0.853 atm was used directly for all calculations, and differences between the actual inlet pressure and the calibration value of 0.853 atm were neglected. Changes in pressure from the calibration point have a small effect on the particle size cut point boundaries and alter the sensitivity at the new cut points. For example in changing pressure from 0.853 atm to 0.878 atm the cut point boundary near the 0.1 μm particle size changes from 0.118 μm to 0.114 m. The sensitivity (units of $pA/10_6$ particles/cm_3) at the new boundary is changed from 103 (0.853 atm, 0.114 μm) to 90.5 (0.878 atm, 0.118 μm).

Measurements Made Using the Electrical Aerosol Analyzer. The EAA was used to determine total concentration and particle size distribution of aerosols entering and leaving the HEME and HEMF filter. The experimental configuration of the EAA with sample ports located on either side of the HEMF filter is provided in Figure 3.4. The sample ports used to extract the sample from the off-gas line were directed into the oncoming off-gas, and the nozzles were sized at 0.490 diameter upstream and 0.295 downstream to roughly approximate isokinetic conditions. However, the sample flow was not adjusted to attempt to achieve isokinetic conditions. The errors involved due to non-isokinetic sampling are negligible due to the submicron size of the aerosols of interest.

For measurements of HEME performance, sampling was performed from the port upstream of the HEMF filter. To sample the aerosol concentration entering the HEME, the off-gas leaving the SBS was rerouted to bypass the HEME, pass through the heat exchanger and then measured at the HEMF inlet. Because of this, the inlet concentration would not include any potential line losses between the HEME and HEMF and does not include the liquid volume of any mist particles that evaporate when passing through the heat exchanger. To sample downstream of the HEME, the sample point was maintained constant, and the off-gas was rerouted to pass through the HEME.

The sample was drawn out of the off-gas line through heat-traced stainless steel tubing. Dry dilution air was then added to the sample to prevent condensation in the sample lines or analyzer. Later, the amount of dilution air added was taken into account in determining the concentration in the off-gas line. The dilution air was supplied by a compressed air cylinder and was then filtered twice

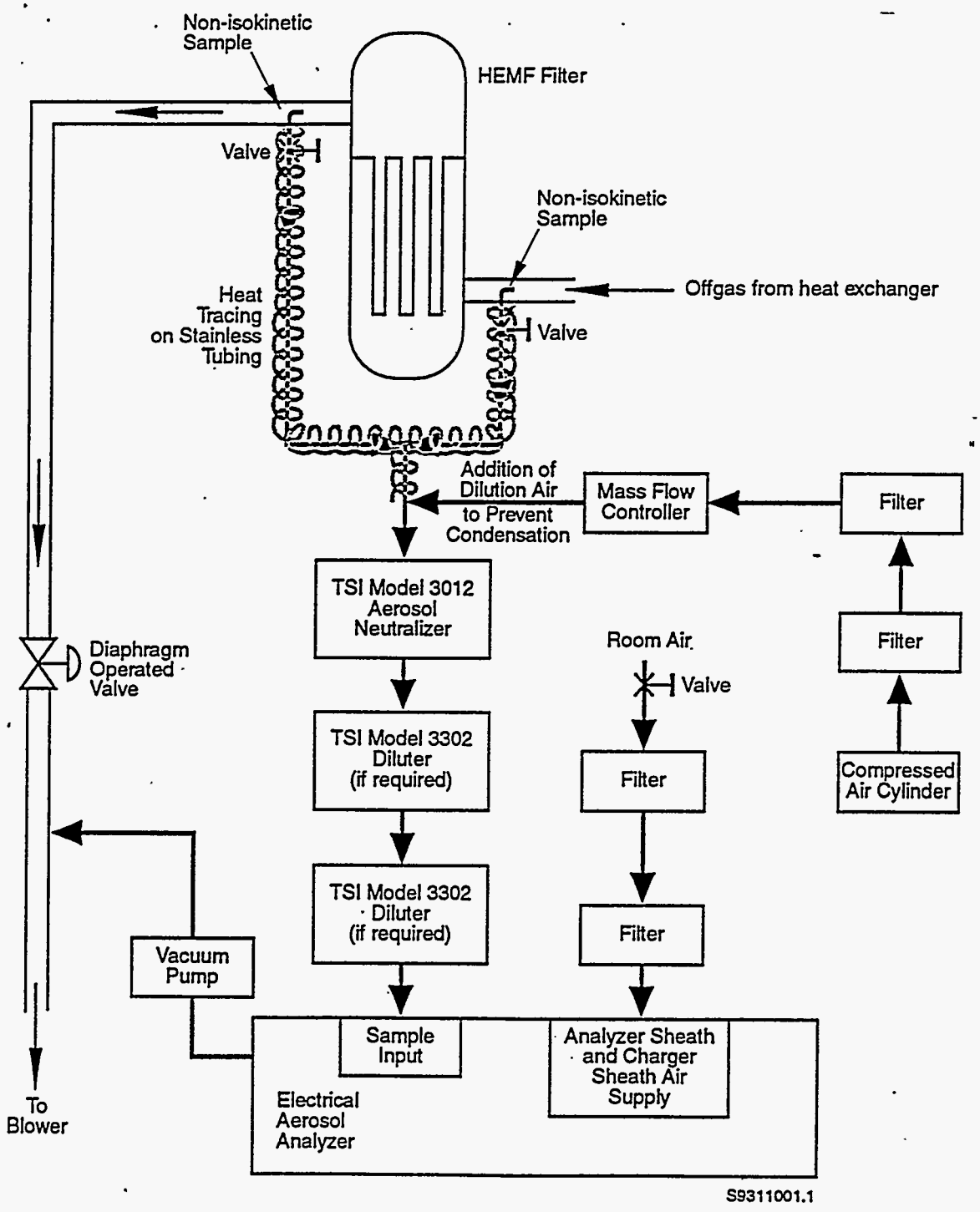

Figure 3.4. Electrical Aerosol Analyzer Sampling Arrangement at HEMF Filter

before being introduced into the sample line. The absence of aerosol particles in this stream was verified by increasing the flow of the dilution air so that only dilution air was supplied to the analyzer. If the analyzer detected any aerosols, it indicated either contamination in the dilution air (never found) or a leak within the system that allowed unfiltered room air into the sample line (this was checked periodically, and occasionally leaks were found).[a]

The off-gas then passed through a TSI Model 3012 aerosol neutralizer, which eliminated existing charges on the aerosol particles. The gas was then passed through tygon tubing to one or more TSI Model 3302 diluters. The diluters isokinetically sampled the inlet gas, filtered the remainder of the inlet gas, and then recombined the sample with the filtered inlet gas. The effect was to reduce the inlet concentration by a known amount. The diluters could be configured for 20:1 or 100:1 reduction in the aerosol concentration by the use of different capillary tubes. Placing diluters in series provided other dilutions (i.e., a 20:1 followed by a 100:1 = a 2000:1 dilution). The diluters were necessary because the high concentration of aerosols leaving the SBS was greater than was optimal for the EAA. No diluters were used when measuring concentrations downstream of the HEMF filter due to the low concentration of the aerosols.

After passing through the diluters, the sample was introduced to the EAA. The sample was drawn through the system using a vacuum pump, which discharged into the off-gas line downstream of the direct operating value (DOV). The supply of air provided to the sheath air inlet was drawn from room air and filtered through two filters before being introduced into the instrument. Although filtering of this stream is not required (the stream is filtered within the EAA instrument), the filtering was performed to avoid possible detection limit problems that might have resulted from ambient air aerosols penetrating the internal filter of the EAA and entering the charging section as charger sheath air.

Formic Acid Destruction and Removal Efficiency (DRE) Measurements. The destruction and removal efficiency (DRE) of the melter and offgas system for formic acid was determined. The DRE was determined from analysis of condensate samples obtained during aerosol sampling. No condensate samples were obtained from aerosol sampling trains which included a caustic scrubber. Samples were obtained from before and after the SBS and from downstream of the HEME. Typically, the offgas was drawn through an aerosol sampling device such as a cascade impactor or cyclone train, was filtered, and was then passed through a condenser consisting of an empty 500 mL gas scrubber submerged in an ice bath. For larger volumes of condensate, a large filter flask was used in place of the empty gas scrubber. The exit temperature of the condenser was not measured. However, in some cases the quantity of condensate and the weight gain in downstream desiccant columns were recorded to determine the fraction of water condensed. Additional information on formic acid destruction was obtained by tracking the concentration of formic acid in the SBS over time and evaluating the concentration of formate in offgas deposits obtained after the conclusion of the melter test.

In addition to the data described above, measurements were attempted using sorption tubes according to the modified National Institute for Occupational Safety and Health (NIOSH) Method S173 described in Appendix F. These off-gas samples were not successful in determining the organic destruction and removal efficiency (DRE) for the melter system. The off-gas was sampled from the line at points before the SBS and after the HEMF filter. The formic acid concentration entering the melter

---

(a) Leak checks were performed after EAA measurements were taken. If the setup failed the leak check, the results of the analysis were discarded.

was determined through IC analysis of the feed. The off-gas was sampled non-isokinetically through the flow train shown in Figure 3.5. The gas passed through a condenser in an ice bath, followed by two sorbent tubes connected in series, before passing through a mass flow controller and returning to the off-gas line. The second tube is intended to determine the extent of breakthrough in the first tube. The flow rate was adjusted to 0.200 std L/min., and all samples were taken for 2 hour periods. The tubes were desorbed with high purity water, and the liquid was analyzed by IC. Several problems prevented this approach from providing adequate data. First, the amount of formate in the samples was approximately at the detection limit of the IC. In addition, interference problems with fluoride were experienced that decreased the precision at low concentrations. Finally, breakthrough was observed in all of the samples so that there may be some amount of formate leaving the second tube. The flow rate selected probably contributed to this. The flow rate selected for sampling was 0.200 std L/min. while the maximum flow for the tubes was 0.200 actual L/min. Due to the significant sub-ambient pressure, this difference may have contributed to the breakthrough observed.

3.2.3 Process Flow Measurement

Control Air Injection Flow Rate. Air used for melter plenum pressure control can be injected at either of two locations. The first location is directly past the film cooler (referred to as melter air injection). The other location is downstream of the HEMF (referred to as downstream air injection). Air injected at either location comes from one common header and passes through a pressure regulator and an automatic control valve (Fisher Governor Co. Serial No. 3560502, Type 510-GR, 3/4 in.). Just downstream from the control valve, the air can be routed to either air injection location. The flow rate of control air injected is measured at each location by a Pitot tube in the injection line, a reading of the static pressure in the line, and the temperature of the air being injected.

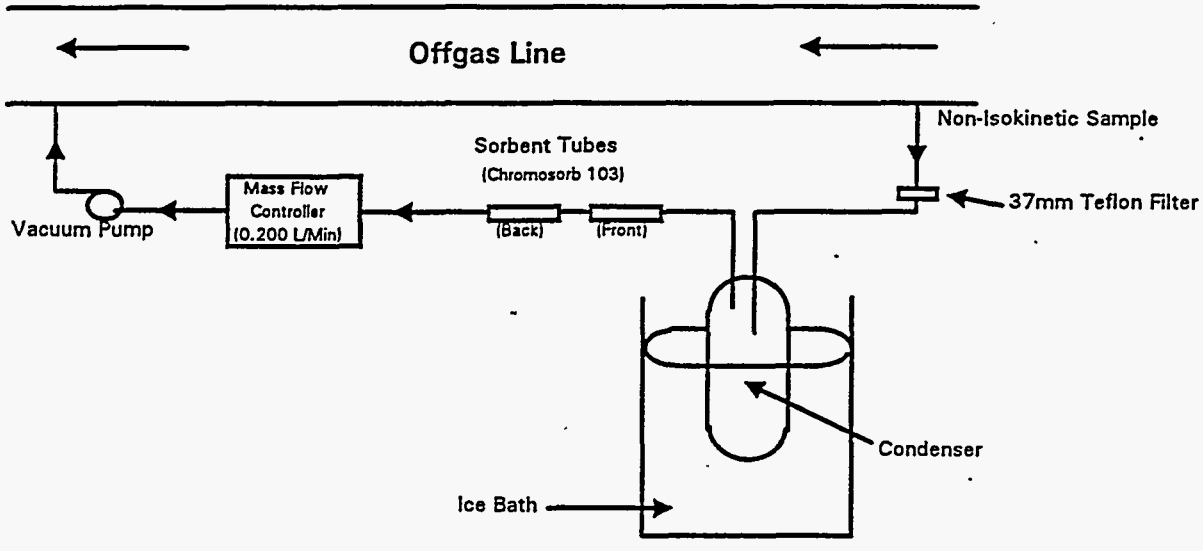

Figure 3.5. Formic Acid Off-Gas Sampling Arrangement

Off-Gas Flow Rate. The off-gas flow rate refers to the total flow (including steam) in the off-gas jumper (between the film cooler and the SBS). The off-gas flow rate is measured by a Pitot tube located in the off-gas jumper, and uses a calculation of the estimated static pressure at the measurement point, and a measurement of the off-gas temperature. This flow rate includes melter source gas, in leakage, film cooler air injection, and possibly melter control air injection (if used).

Final Flow Rate. The final flow rate is measured at the end of the off-gas system, past the downstream control air injection location. The final flow rate is measured using a pitot tube, a reading of the static pressure, and the temperature of the gas.

The SBS exit flow (which equals the flow through the demister, HEME, heat exchanger, and HEMF) can be determined by subtracting the downstream control air injection flow rate from the final flow rate.

3.3 Equipment Description

This section contains general descriptions and design specifications of the pilot-scale systems operated during the test.

3.3.1 Prototypic Feed System

The full scale prototypic feed system used during the LFCM-8 campaign to test the performance of the DWPF design with HWVP feeds is described below. This equipment, representing the HWVP feed preparation system being designed by Fluor-Daniel, Inc., is composed of a feed makeup tank, a test vessel (evaporator), condenser, slurry transfer pump, sample pump, sample station, and feed deliv ery system. A detailed equipment description is presented in the SIPT Test Plan by McKay (1992).

Feed Makeup Tank. Tank High Bay (HB)-13 was used to make up initial concentrations of simulated feed for transfer to the feed preparation test vessel (Tank HB-15). Tank HB-13 is a baffled, stainless steel tank that is equipped with a 20-hp agitator and has a maximum operating volume of 4,300 gallons. The Tank HB-13 bottom drain is piped to a double diaphragm air-driven pump (P-1300) for transfer of tank contents to HB-15 or Tank 60 (the backup feed system).

Feed Preparation Test Vessel. Tank HB-15 is a full-scale representation of the DWPF slurry receipt and adjustment tank/slurry mix evaporator/melter feed tank (SRAT/SME/MFT) with the exception of remote features. The function of the test vessel is to receive, hold, and process the simulated slurries and maintain slurry homogeneity. The vessel, which has a maximum capacity of 10,200 gallons, is constructed from Carpenter 20 Cb-3 steel. The agitator motor is a 100-hp TEFC high efficiency motor that drives two 36-in. dia. impellers. The bottom impeller is a 4 blade vertically flat (radial) type that is located approximately 7 in. above the vessel floor. A second impeller, located 60 in. above the radial impeller, is a 3-blade hydrofoil or turbine-type impeller. Tank HB-15 is equipped with a double set of steam coils and a single cooling coil assembly. Although the HWVP MFT does not have steam coils, during LFCM-8 the steam coils remained in the tank.

Condenser. Vapors produced in the test vessel are condensed with a full-scale representative prototype of the DWPF SRAT/SME condenser (excluding remote features). The condenser has an overall height of 14 ft. and is constructed from stainless steel. The condenser shell, which is 24 in. in diameter, encloses vertical 14 BWG 314 stainless steel tubes that are 0.75 in. dia by 88 in. long.

Slurry Transfer Pump. The slurry transfer pump is a vertical cantilevered centrifugal type variable speed pump that is used to transfer feed out of the vessel. The transfer pump, also used as the melter feed pump, is driven by a 20-hp TEFC electric motor and has a 100 gpm design transfer capacity. The pump impeller and casing are constructed from Stellite,® while the remainder of the pump is fabricated from stainless steel.

Sample Pump. The sample pump is used to recirculate slurry through the sample system and is similar in construction to the transfer pump. The pump is driven by a 15-hp TEFC electric motor and has a maximum capacity of 58 gpm. The variable speed pump is designed in such a way that a majority of the slurry is discharged directly back into the vessel through a recirculation line fitted with a ceramic restriction orifice. During maximum operating speed, it is expected that approximately 10 gpm is circulated through the sample station.

Sample Station. The sample station consists of one 2-way and one 3-way Everlasting® valve, one standard ball valve, a Hydragard® in-line sampler, a flow meter, and a pressure gauge. Slurry is transferred to the station through a 1/2 in. Schedule 40 stainless steel line through the sample pump. This line is connected to the 3-way Everlasting valve. From the valve the slurry is routed to the Hydragard sampler. Between the valve and the sampler are the pressure gauge and the flow element. The 1/2 in. Schedule 40 return line exits the station through the 2-way Everlasting valve and is routed back to the vessel through a connection on the sample pump flange. When the sampler is engaged to draw a sample, the slurry flows through the sampler to a separate line that is tied into the return line. The 3-way Everlasting and standard ball valves are operated as required to either obtain a sample or back-flush the lines with water.

Feed Delivery System. The feed delivery system consists of five components besides the feed pump described above (see Figure 3.6). These components are the recirculation loop, the cross-flow strainer, the melter feed line, the restriction orifice, and the feed nozzle

The first component, a recirculation loop, is approximately 300 ft. long and is constructed from 2-in. Schedule 40 stainless steel pipe. This loop is routed from the slurry transfer pump outlet to a point near the LFCM before returning to the vessel. The loop is equipped with in-line pressure, temperature, and flow-sensing elements.

The second component of the system is the cross-flow strainer. The strainer, installed approximately in the middle of the recirculation loop (the portion of the loop nearest the melter), functions as a transition piece to divert slurry from the 2-in. line to a 3/8-in. line that feeds the melter. The strainer also protects the 3/8-in. line against plugging by preventing any particles greater than 0.05 in. in size from entering the feed line.

The third component of the system is the 3/8-in. Schedule 80 stainless steel melter feed line. This line is equipped with pressure and flow-sensing elements as well as a 3-way Everlasting valve. The valve is used to divert a water flush through the line in both directions.

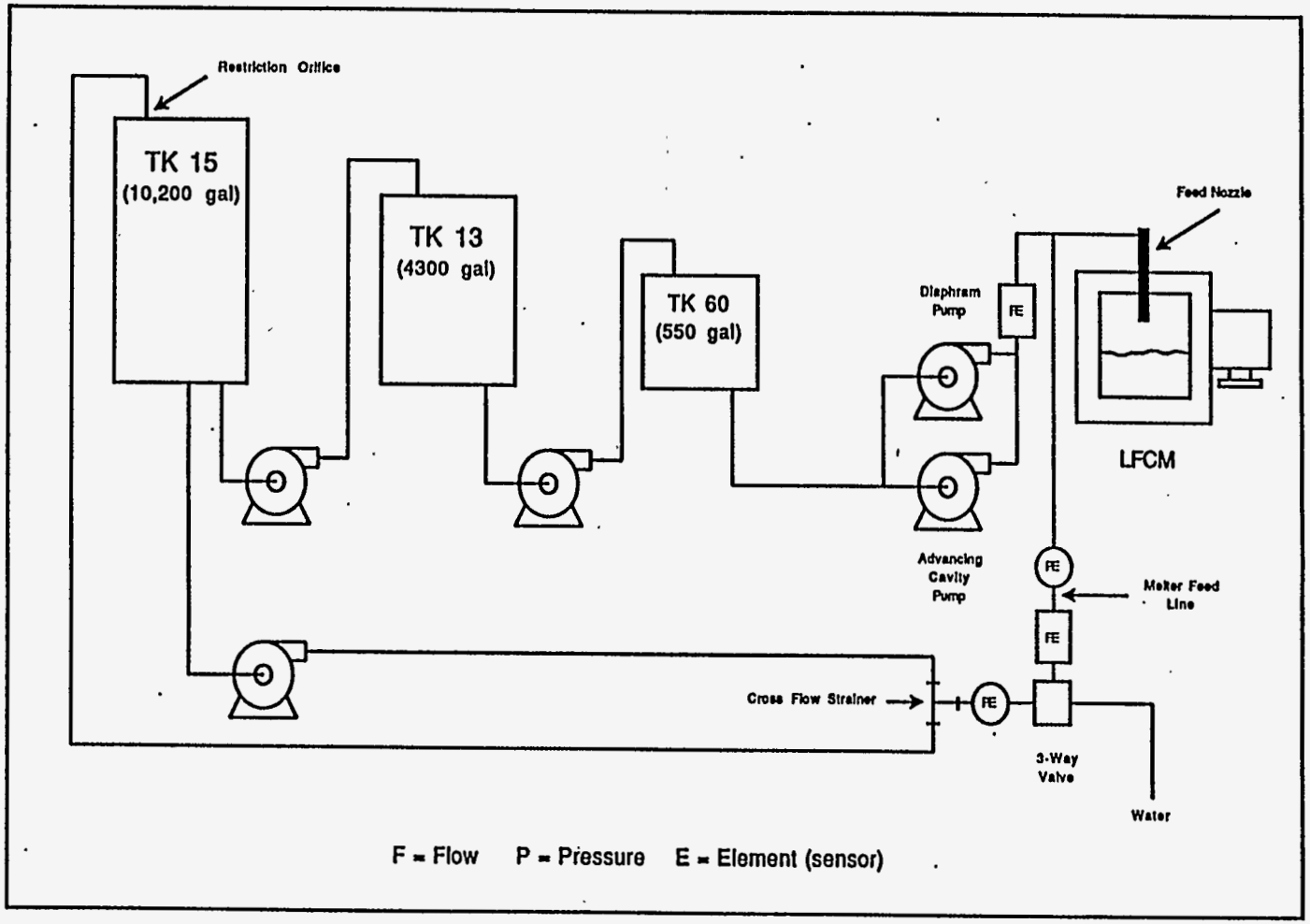

Figure 3.6. Schematic of LFCM/SIPT Feed Preparation and Delivery Equipment

The fourth system component is the restriction orifice that is installed in the recirculation loop at the vessel termination. The function of the restriction orifice is to maintain back pressure on the recirculation loop so that feed is forced through the cross-flow strainer, the feed line, and ultimately into the melter. The inside diameter of the orifice is one inch.

The final component is the melter feed nozzle assembly (see Figure 3.7). The feed nozzle is a prototypic design of the DWPF nozzle with one minor design change. The tip of the feed nozzle has been tapered to a 45° tip. This differs from the DWPF's flat tip design. A sharply angled tip design minimized slurry drops from separating from the stream and traveling across the nozzle face. This minimizes the buildup of solids and potential plugging of the nozzle. The overall length of the prototypic assembly is 9.4 ft. with the in-melter length being 37.5 in. To prevent the feed from drying, the nozzle has both insulation and water cooling. The outer shell of the feed nozzle is fabricated of Inconel®-600. Approximately 0.5 in. of Fiberfrax® insulation surrounds the water cooling jacket that in turn surrounds the 0.75-in. (0.43-in. ID) feed tube. Cooling water for the feed nozzle enters and exits through a set of flexible rubber hoses; the inlet and exit temperatures were measured with type J thermocouples.

Before beginning LFCM-8, it was determined that the feed rate could not be adjusted down to the expected LFCM processing range. The feed rate is controlled by the feed pump speed. However, the pressure in the feed loop at the feed line was too high even with minimum feed pump speed and the feed loop restriction orifice removed. To increase the pressure drop between the recirculation loop and the feed nozzle, the prototypic spool piece and feed line after the 3-way Everlasting valve were replaced with 17 ft. of 3/8-in.-dia, 0.065-wall stainless steel tubing (.245 in. ID). The final 10 ft. of line was coiled into a 6-in.-dia helix because of space constraints (see Figure 3.7). The original jumper was made of Schedule 80, 3/8 in. nominal stainless steel pipe (0.423 in. ID) and was 5 ft. long. The prototypic spool piece was also schedule 80, 3/8 in. nominal stainless steel pipe and 5 ft. long. As the Tank HB-15 liquid level dropped, decreasing the resultant feed loop pressure, the 10 ft. coiled helix was replaced by an 8 ft. helix and later by a 6 ft. helix.

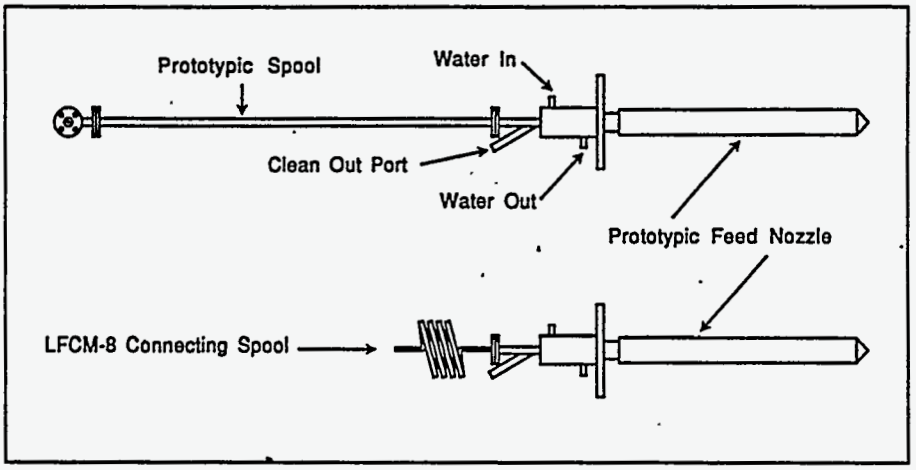

Figure 3.7. LFCM Prototypic Feed Nozzle

Once the liquid level in Tank HB-15 dropped below the minimum design agitation level, the melter feed heel was transferred to Tank HB-13. From Tank HB-13, the feed was transferred to a an alternate backup feed system. This system consisted of a holding tank (Tank 60), a primary feed pump, and a backup feed pump. The primary pump is a Neptune Model 562-T-N7® tubular diaphragm pump. The backup pump is a Moynor advancing cavity pump. Both pumps were installed so that either pump could be valved out and the other valved in as necessary. Adequate flushing capabilities were added that allowed either back flushing to Tank 60 or flushing through the feed pump and into the melter. Tank 60, a 550 gal stainless steel tank, is equipped with a variable speed 3.5 hp Lightning® agitator. Batch transfers of feed from Tank HB-13 to Tank 60 were made as necessary while continuously pumping feed to the LFCM through the secondary feed system. Flow indication for the backup feed system were generated by a separate Krona Altoflux X-1000® flow sensor located near the pump discharge. A feed rate calibration curve was generated for this flowmeter and the straight line curve-fit coefficients were entered into the DAS software. Feed rates were displayed on the DAS computer screen in the melter control room and stored in the DAS data package.

3.3.2 Liquid Fed Ceramic Melter

The LFCM is a ceramic brick-lined, joule-heated glass melter (see Figure 3.8) with a glass surface area that is 40% of the HWVP reference melter. The melt cavity consists of fused, high chrome/ alumina refractory up to the nominal level of glass inventory and a high alumina castable refractory in the lid or plenum space. The floor refractory is backed by a layer of alumina/zirconia/silica brick, and the wall refractory is backed by a layer of high alumina castable refractory. The melter has a nominal operating depth of 56 cm at a plenum vacuum of 7 in. WC, a surface area of 1.05 m^2, and a plenum space height (above the glass) of 94 cm. Three of the walls (two electrode walls and the back wall) have a 45° slope. The front, or discharge wall, is vertical. With this configuration, the nominal glass volume is calculated to be approximately 0.34 m^3 (851 kg glass, $\rho \approx 2.5$). The tank walls are equipped with water jackets to provide cooling. The lid was constructed with nine flanged ports (see Figure 3.9). The feed nozzle uses the center port. The remaining ports are used for off gas removal, viewing, and instrumentation.

The glass is kept in its molten state by resistance heating, produced as 1Φ electrical current passes between three Inconel® 690 electrodes submerged below the glass surface (see Figure 3.10). Power to the electrodes is supplied by two Kirkoff® 250 kilovolt ampheres (KVA) multi-tap transformers, which are controlled by a single Halmar® 650 amp silicone controlled rectifier Silicon Controlled Rectifiers power controller and a Research Incorporated® Model 640UD process controller. The feed-back signal for the electrode process controller is taken from the primary side of the SCR. A target bulk glass operating temperature of 1150°C is maintained by manually increasing or decreasing melter power as required. By varying the voltage between either the east or west electrode and the bottom electrode (tap changes on one or both electrode transformers), it is possible to skew the electrical current path in the glass and affect the direction and magnitude of the glass roll cells. Plenum and glass temperatures are measured using Type K thermocouples. Thermocouples of varying lengths are placed into protective Inconel 690 thermowells (see Figure 3.11) that are inserted through the lid.

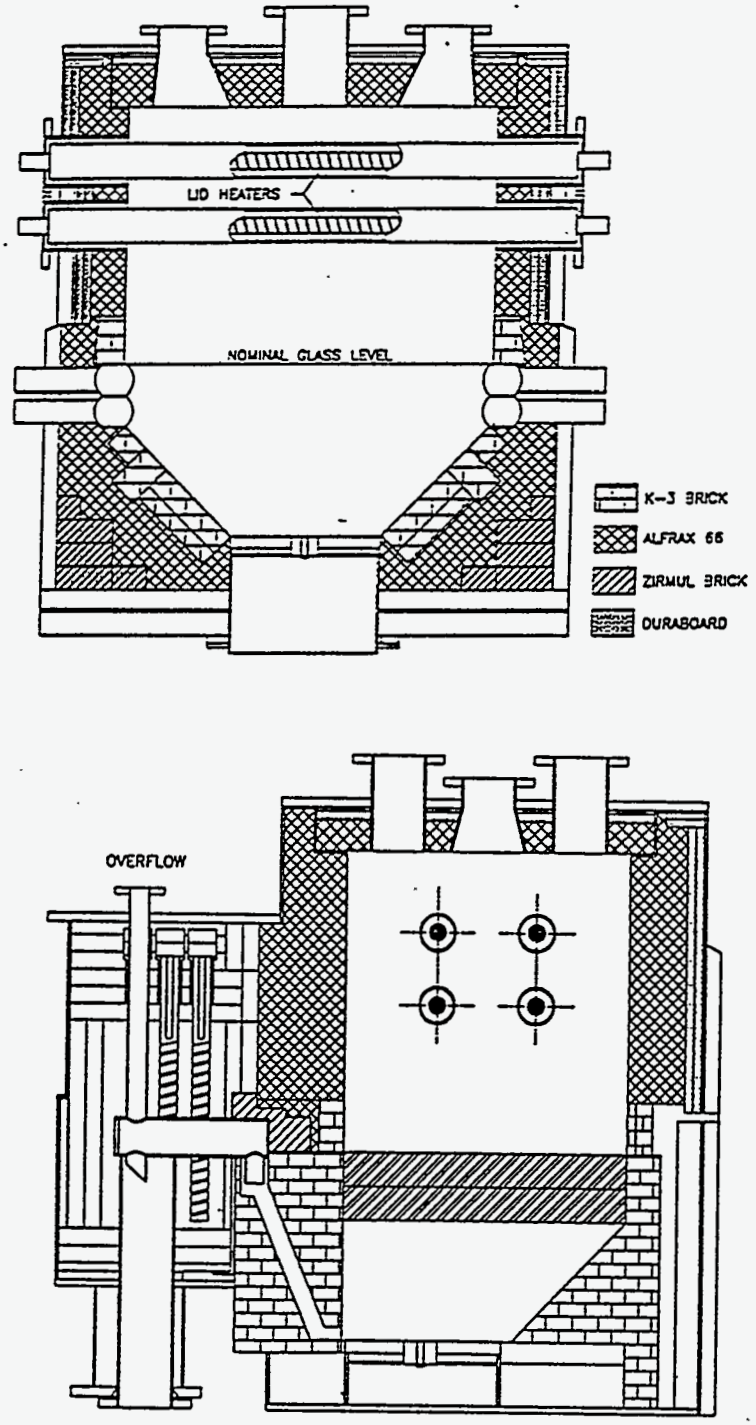

Figure 3.8. Liquid-Fed Ceramic Melter

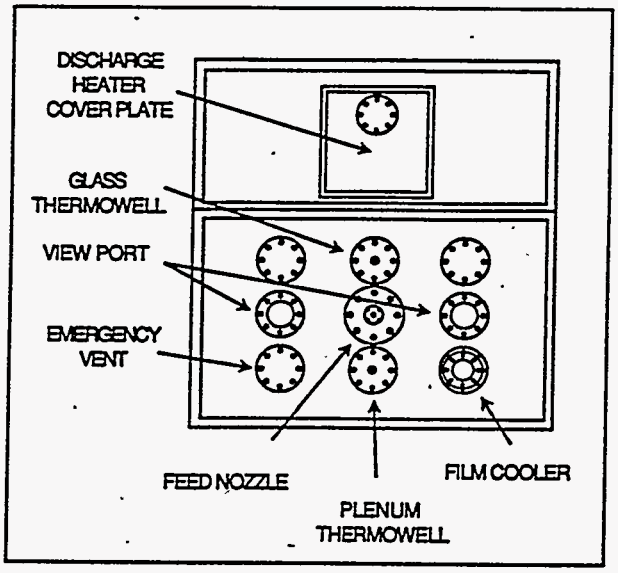

Figure 3.9. LFCM Lid Nozzle Identification and Locations

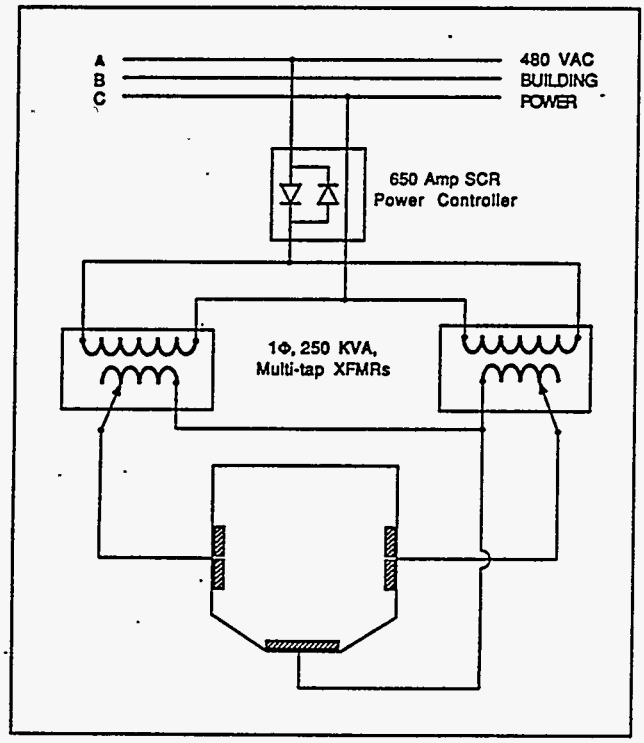

Figure 3.10. LFCM Electrode Power Supply Arrangement

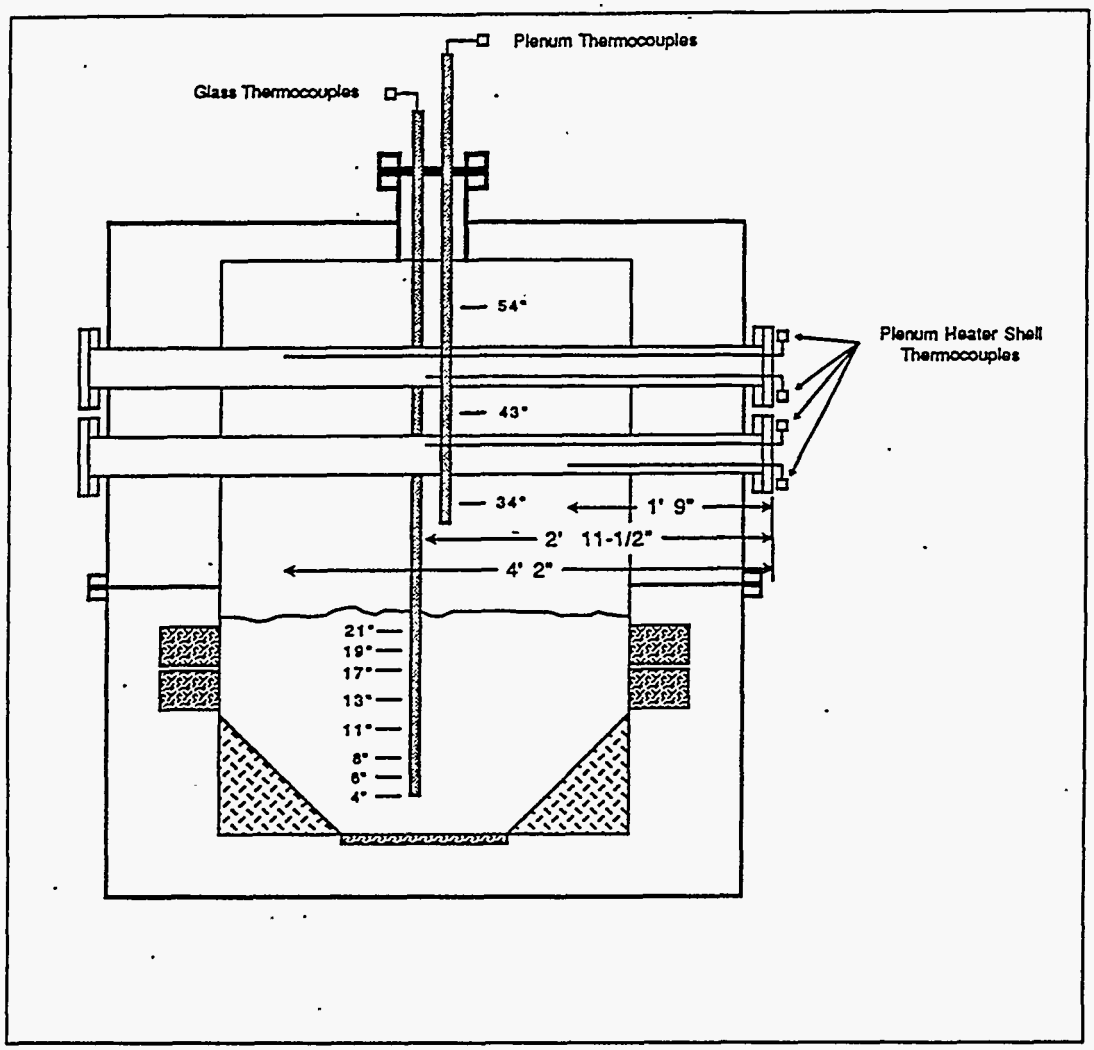

Figure 3.11. LFCM Thermowell and Plenum Heater Thermocouple Locations

Plenum Heater System. The LFCM has a plenum heater system that is used to initiate melter startup and to provide plenum heater boosting during feeding operations. The plenum heaters are powered by a single Halmar 650 amp SCR power controller, and controlled by a Research Incorporated Model 640UD process controller using plenum temperature as feedback for automatic control. The four plenum heaters are 2-1/8 in. O.D. Carborundum® silicon carbide heaters, Model Globar Type LL, with an overall length of 84 in., and an effective heating length of 46 in. Each heater is rated for 22.4 kW at 0.674 ohms and is enclosed by a 4 in. dia. Haynes 214® metal pipe sheath. Haynes 214 is similar to Inconel 690 in composition and was readily available when the LFCM was rebuilt. The heater assemblies are mounted horizontally in the melter plenum through four 6 in. dia nozzles located on the sides of the melter lid. Two thermocouples have been placed within each sheath to monitor pipe wall temperature. To prevent the metal sheath from creeping, a maximum plenum heater pipe temperature limit, for extended operation, has been set at 1000°C.

Differential Pressure Glass Pour System. The differential pressure glass pour system (see Figure 3.12) used during LFCM-8 testing uses the same vacuum pouring concept as adapted by the HWVP from the DWPF. However, the LFCM system and the HWVP design differs from DWPF on the discharge vacuum source. The SBS provides vacuum for the LFCM glass discharge pour system through a 20-ft. long, 1-in. dia, stainless steel vent line between the SBS and the melter-to-canister connecting section; DWPF uses an eductor. Manual regulation of air injection into the vent line near the canister-connecting section controls the glass pouring rate. The vent line outlet was submerged below the liquid surface in the SBS during the LFCM-8 campaign to scrub and cool the discharge section offgas.

3.3.3 Off-Gas Treatment System Equipment

The LFCM off-gas treatment system consists of a film cooler, SBS, chevron demister, HEME, heat exchanger, and HEMF filter. The purpose of each of these pieces of equipment will be described, as well as the process data collected for each piece during LFCM-8.

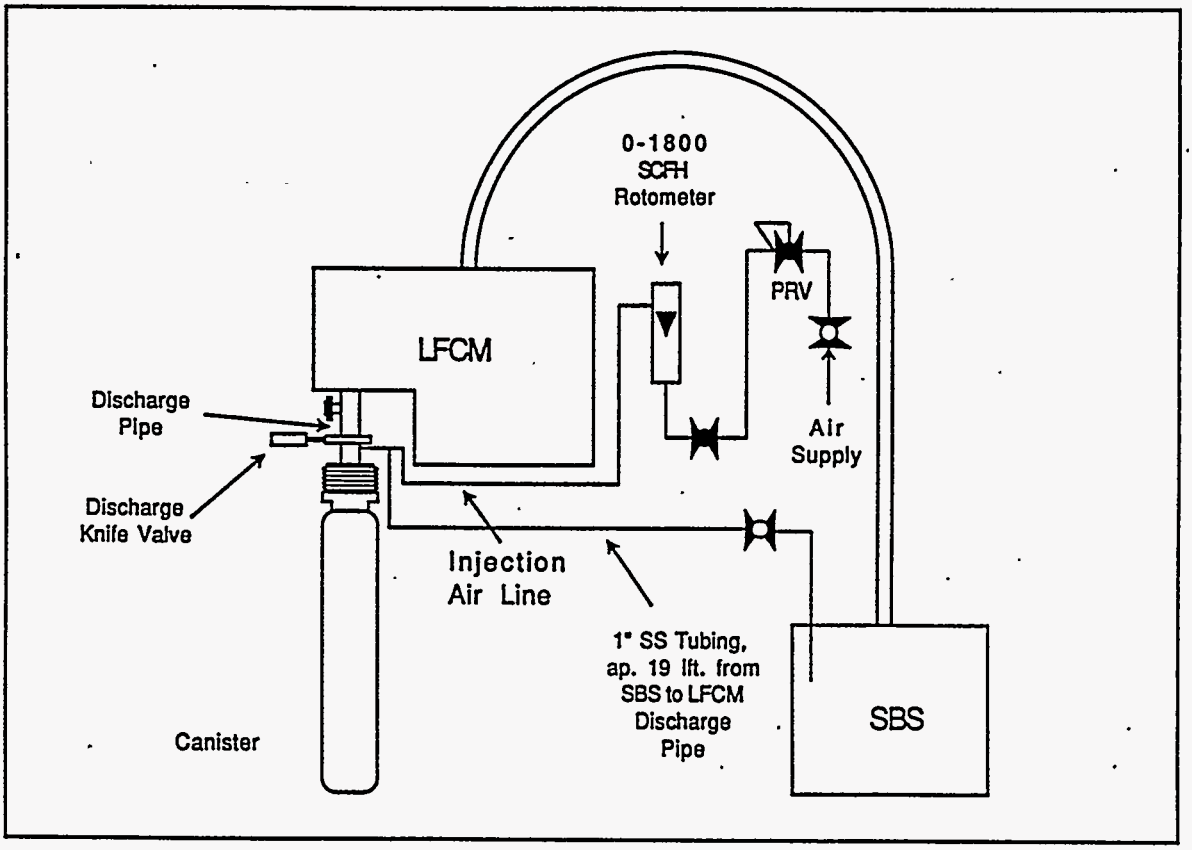

Figure 3.12. Glass Discharge Differential Pressure Pour Arrangement

Film Cooler. A slotted film cooler (see Figure 3.13) placed in a 5-in. dia pipe forms the plenum exhaust port in the lid of the melter. The injection air used with this device cools the melter exhaust stream below the softening point of glass (~400°C) and maintains off-gas velocities above 60 ft./sec. to minimize off-gas line deposits. Both of these functions are intended to ensure that the off-gas jumper between the melter and the SBS remains clear and unobstructed. Film cooler process data collected during LFCM-8 testing include injection air temperature and flow rate and pressure drop across the film cooler. Injection air flow rate was measured by a Pitot tube in the air supply line, a reading of the static pressure in the line, and the temperature of the air being injected. The film cooler pressure drop is measured between the melter plenum and a location downstream of the film cooler, 6 in. past the reamer brush pipe section. Pressure drop in the off-gas jumper is measured between this location and a point 3.5 in. below the flange connection of the off-gas line and the SBS downcomer pipe.

Submerged Bed Scrubber. The primary off-gas system scrubber is the SBS shown in Figure 3.14. The SBS consists of a packed bed submerged in a vessel through which the off gas is bubbled. The packing consists of 1/2 in. Intalox® saddles. Buoyancy drives liquid circulation through the bed. The circulating fluid cools the hot melter exhaust and provides off-gas scrubbing and cleaning of the bed. In operation, the process exhaust is co-currently contacted and cooled by the scrubbing liquor in the SBS bed. The outer portion of the vessel is fitted with cooling coils to remove this heat. Since liquid recirculation is naturally maintained by buoyancy effects, no external pump is needed, which is a significant operational advantage in that the scrubbing liquor is abrasive due to the solids present and can be corrosive due to low pH resulting from the scrubbing of acid gases. However, the

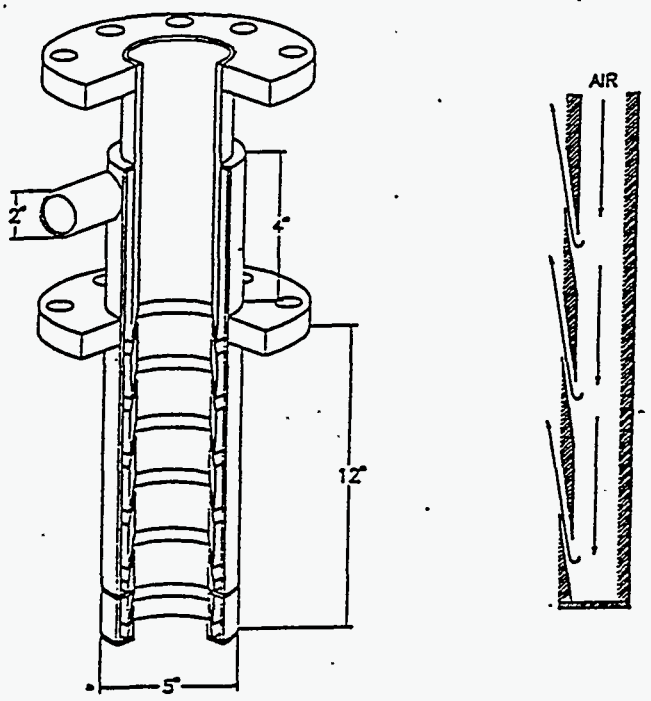

Figure 3.13. LFCM Prototypic Film Cooler Design

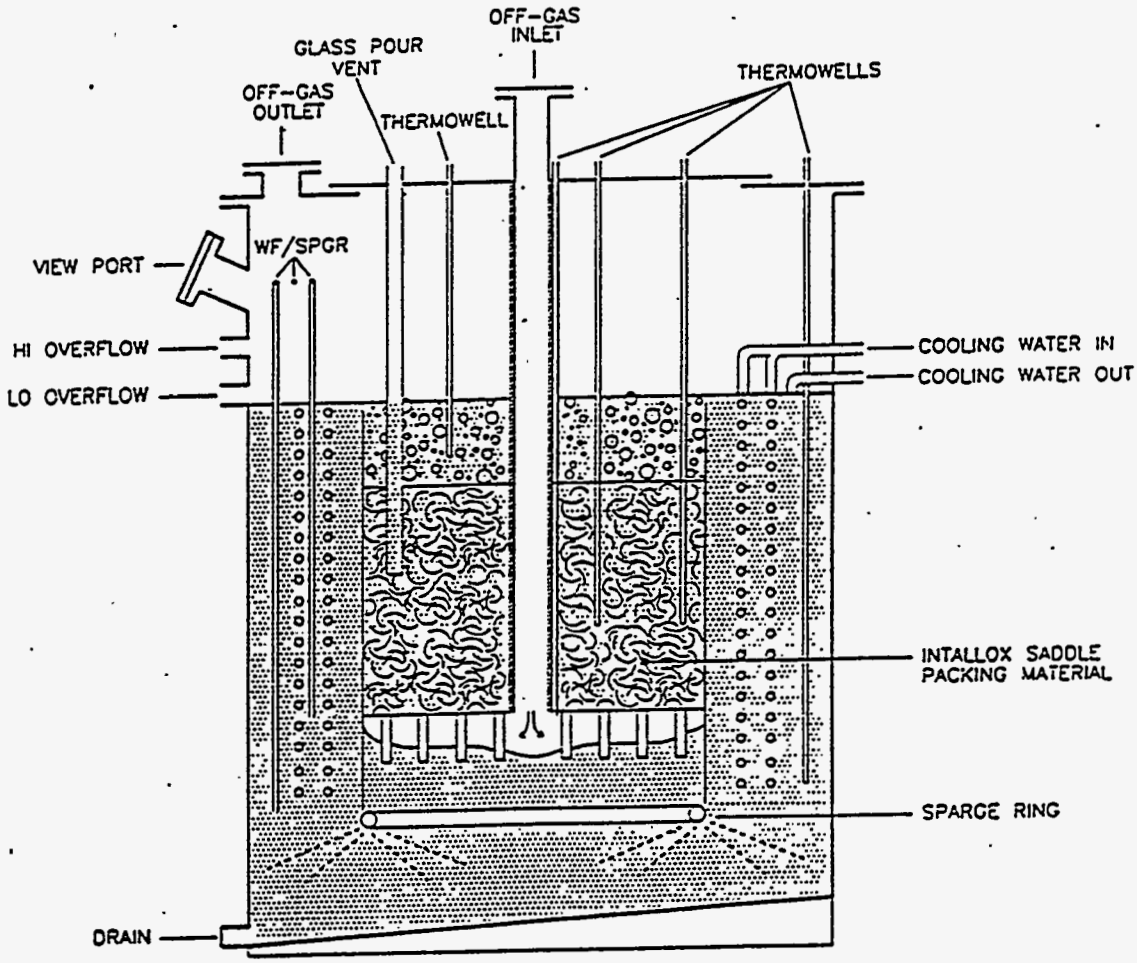

Figure 3.14. Submerged Bed Scrubber

pressure drop through the bed is high, being established by the submergence of the inlet pipe below the liquid overflow drain level. The lower overflow drain was used during LFCM-8, resulting in a 32-in. submergence.

During the melter run, the SBS was operated under cooling conditions intended to maintain the bulk temperature of the scrubbing liquor and exiting off-gas between 45°C and 50°C (115°F to 125°F). At these temperatures the steam produced from the melter feed condensed, and the accumulated condensate continuously overflowed into a condensate collection tank (Tank 20) located in the 324 Building tank pit. The off-gas flow rate through the SBS is established by the film cooler air injection rates, the air injection rate for melter vacuum control, and melter inleakage. The nominal superficial velocity for the SBS is 52 ft./min based on a bed cross-section area of 6.8 ft_2. SBS process data collected during the test include pressure drop; scrub liquor temperature; bed temperature; cooling water inlet/outlet temperatures and flow rate; and process exhaust inlet/outlet temperatures, effluent concentrations, and aerosol size distributions.

The upstream tap for SBS pressure drop measurement is located below the flange connecting the off-gas jumper to the SBS downcomer pipe. The downstream pressure tap is located in the SBS lid. The SBS inlet gas temperature is measured in the downcomer pipe a few in. above the SBS lid. The outlet gas temperature is measured in the piping between the SBS and the HEME.

Chevron Demister. A chevron demister is used at the SBS exhaust port to reduce the liquid phase aerosol loading of the SBS exhaust stream resulting from entrainment of the scrub solution. The chevron demister removes water droplets from the exhaust stream by causing the droplets to impact on corrugated plates. The impaction method of droplet removal works well for droplets larger than approximately 3 μm (depending on gas velocity) but less well on submicron droplets. The chevron demister shown in Figure 3.15 is located at the outlet of the SBS to collect the larger fluid droplets entrained in the SBS outlet gas stream. Pressure drop was the only data collected for the chevron demister. Pressure drop is measured between the melter plenum and a location a few inches past the demister.

High Efficiency Mist Eliminator. The combined effect of the SBS and the demister upon the process exhaust is to quench the off-gas stream and to remove most of the large diameter (> 1μm) condensed phase aerosols. The HEME is used as a high-efficiency filtration device designed to remove the aerosols leaving the previous, low-efficiency system components (see Figure 3.16). The HEME was operated for a portion of LFCM-8, during which time aerosol concentrations entering and leaving the HEME were measured. During the remainder of LFCM-8, the HEME was bypassed to quickly load the final HEMF filter.

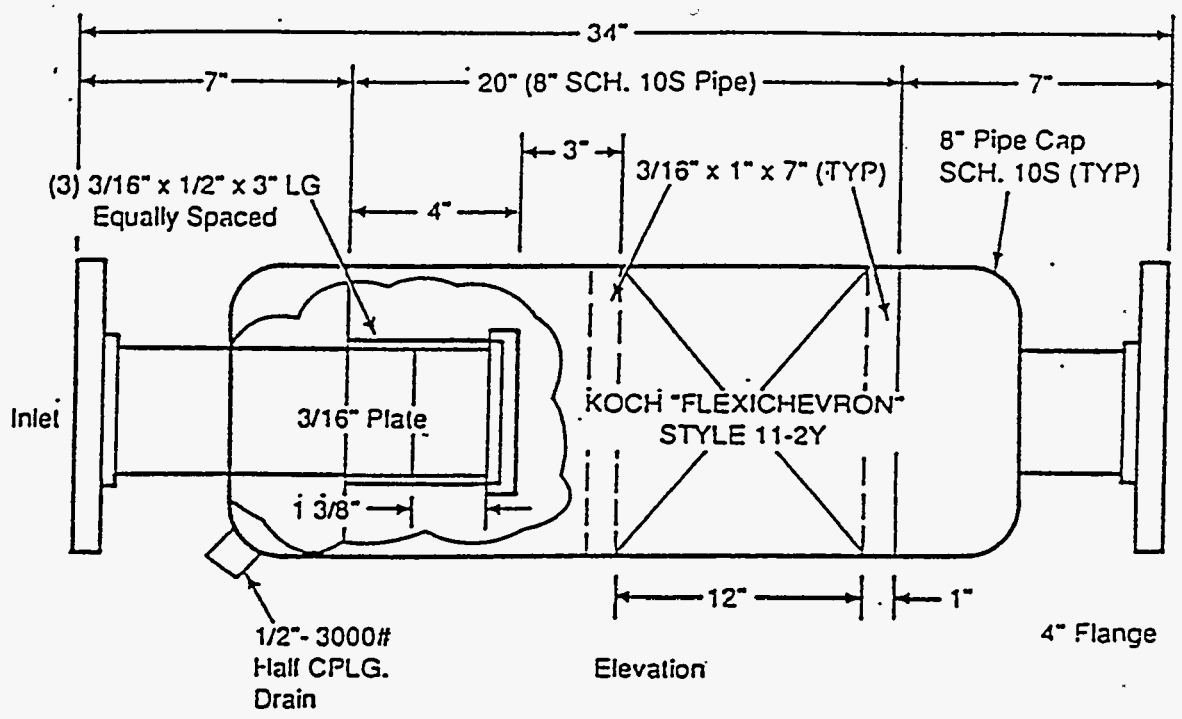

Figure 3.15. SBS Chevron Demister Schematic

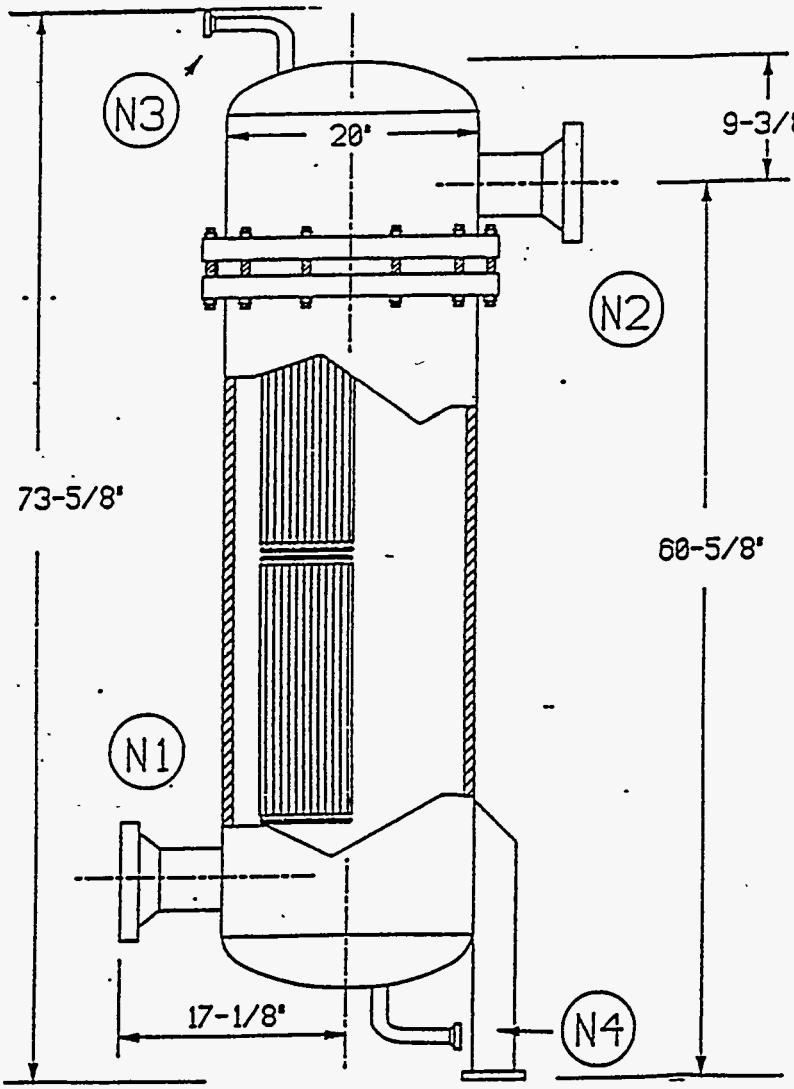

Figure 3.16. High Efficiency Mist Eliminator

Off-Gas Heat Exchanger. A heat exchanger was employed before the final filtration step to heat the gas to above its dew point. The heater is an inline, flow through, steam heated heat exchanger (Young Heat Exchanger #SSF-604-ER-1P). The off-gas heater was operated to elevate off-gas temperatures at least 10°C and usually about 30°C. Process variables to be tracked during the test include off-gas inlet and outlet temperatures. The inlet temperature is measured between the SBS and the HEME. The outlet temperature is measured just downstream from the heat exchanger.

High-Efficiency Metal Fiber Filter. The final treatment stage of the melter off-gas system to be tested is the HEMF filter which was manufactured by Pall Filter Corporation. The HEMF filter will replace the conventional high-efficiency particulate air filter (HEPA) filters in the off-gas line during LFCM-8 testing. A drawing of the HEMF is shown in Figure 3.17. The filter consists of a vessel with a tube sheet from which multiple cartridges are suspended. The filter media consists of sintered

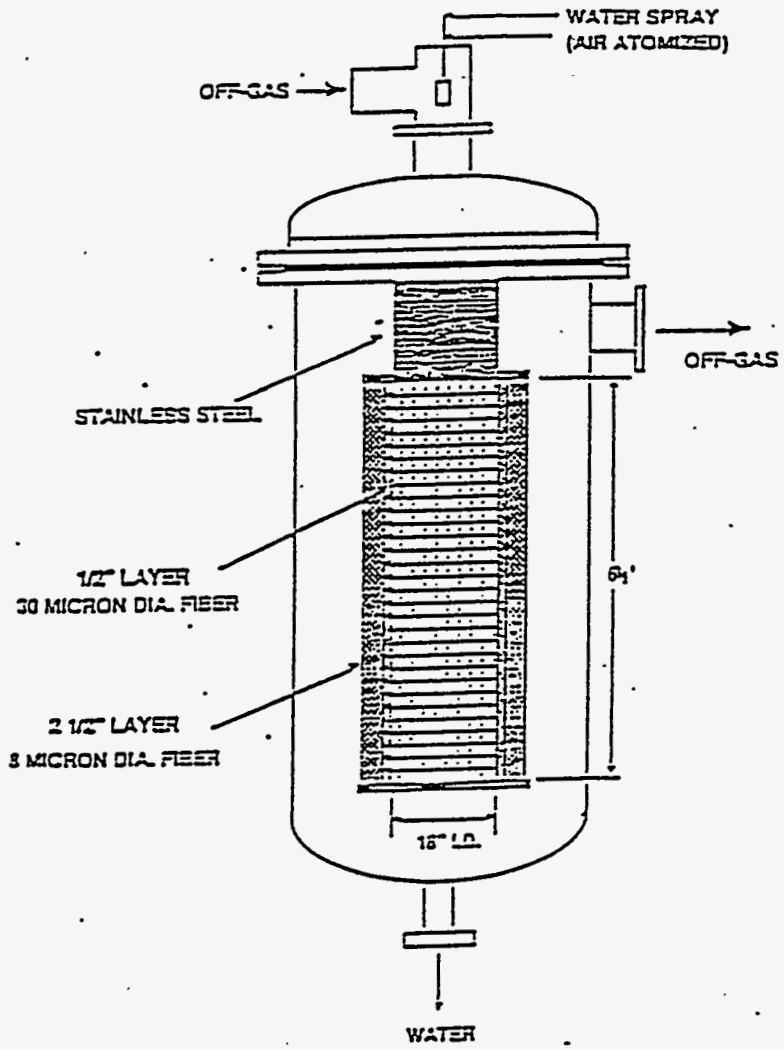

Figure 3.17. High Efficiency Metal Fiber Filter

metal fibers of approximately 2 μm diameter. The filter has advantages over conventional high efficiency particulate air (HEPA) filters in that it can withstand large differential pressures without losing integrity and can be washed in place, thus eliminating the need for frequent replacement. The vessel and filter media are all 316 stainless steel construction. The operating conditions to be monitored are pressure drop across the filter, temperature, flow rate, and aerosol concentrations in the inlet and outlet gas streams. Pressure drop is measured across the filter elements using pressure taps located in the filter housing above and below the tube sheet.

Process Off-Gas Blower. Off gas from the LFCM is drawn through the off-gas treatment equipment by the process off-gas (POG) blower. The POG blower is located in the 324 Building tank pit. The blower has an 800 scfm capacity operating at -80 in.WC. The blower exhausts to the zone two tunnel, through two sets of HEPA filters, and exits the facility stack. This blower is also used for maintaining vacuum on the feed preparation tanks in the 324 Building high bay.

3.3.4 Data Acquisition System

The DAS used a Gateway® 2000 486/33 personal computer (PC) to run a data acquisition/control software package, AIMAX-3 Plus.® Data was sent to the PC via ten duTech®, Model IOP-AD, 16 station I/O plexors; unique data inputs (thermocouple, millivolt, milliamp, digital, etc.) were wired into each I/O plexor. Once sent to the computer, data was displayed 1) in a real-time mode on a number of computer graphic displays, 2) in historical and real-time trend x-y data plots, and 3) on paper as printed by a dot-matrix printer.

Each data point was described to the computer and assigned a specific tag number. This was accomplished through a configuration program integral to AIMAX-3 Plus. Definitions of the I/O plexor terminal location, engineering units, span, scaling, alarm levels, and display format were included in the configuration process. In addition, calculation points were configured so that incoming raw data could be used to calculate, store, and/or display temperature averages, flows, power totals, etc. Data points were grouped together based on sampling period and data viewing needs. Data points with different sampling requirements could not be configured together in the same group. Once a data point was put into a group, the saved data point could be configured to be 1) the average value over the sample period, 2) the high or low value over the sample period, or 3) an initial snapshot value. Percent dead band instructions were also configured into the group description. Dead banding of data helped decrease the amount of data being stored to data files by storing additional data only if the new data value differed from the previously stored data by a user-defined percentage.

Before the LFCM-8, a check was made on all calculated points for accuracy. Verification checks were also performed on data sent to the DAS and the corresponding data displayed and stored. A complete printout of the data configuration and the system checks were put into the DAS quality assurance file. During the test, a daily data review was performed at 00:00 in which the total data for that sample period was printed out and reviewed for acceptability. Periodically raw data was stored to a Bernoulli® removable hard disk. A paper printout of the disk operating system (DOS) data file description was made for each data transfer to the Bernoulli; this printout verified that data transfer was complete.

Approximately 30 data files (groups) were created each day. At the end of the test, the daily data files were converted to text files and then imported to and saved as Excel 4.0® files. The LFCM operation data was compiled into chronological files consisting of an entire group's data for each of the April and the May segments. This data was further reduced using an averaging macro designed to create separate data sets comprised of the hourly averages of each group. The hourly averages were then evaluated using the Excel statistics package and imported into data plots.

3.4 Methods or Sample Analysis

This section describes the analytical techniques used to characterize the daily samples of glass, cold cap, and off-gas line deposit samples.

Density Determination of Slurry Samples. The density of slurry samples are measured by weighing the sample in 15 mL capacity centrifuge tube with graduated volume subdivisions of 0.1 mL. The volume in the centrifuge is read to the nearest 0.1 mL. After determining the tare weight of the tube 10 to 15 mL of slurry are pipetted into the tube. The weight and volume of the slurry are determined and the density is calculated.

Determination of Weight Percent Solids. Weight percent total solids or dissolved solids of slurries or liquids with dissolved solids are determined by this procedure. By difference, the undissolved solids fraction can d\be determined. A five to ten gram sample of slurry is weighed into a tared crucible that has been stored in a desiccator. The crucible is then placed in a conventional drying oven for between 12 and 24 hours. The oven temperature is maintained at between 103 and 108°C. Once removed from the oven the crucible is placed in a desiccator until it has cooled to room temperature. The final weight is then determined and percent solids is determined.

Determination of Total Oxides. Weight percent total oxides is determined in much the same way as percent solids. However, instead of heating the sample to around 100°C, it is heated to 1,000°C. A five to ten gram sample of slurry is weighed into a tared crucible that has been stored in a desiccator. Initially, to prevent sample loss most of the free moisture is driven off by placing the crucible under a heat lamp. The crucible is then placed in a muffle furnace for between 4 and 8 hours. Oxide concentration can also be calculated from the ICP analysis. The elements are converted to oxides and totaled. Comparison of feed samples shows that the two methods agree to within 1%. Values can be expressed as grams oxides per liter of slurry by multiplying the fractional oxide value by the slurry density.

Iron II and Total Iron Ratio Analyses of Glasses. Samples of glass are crushed to achieve a particle size of <200 mesh. They are then dissolved in a non-oxidizing condition using a mixture of sulfuric and hydrofluoric acids. Boric acid is later added to complex the phenanthroline forming an orange-red complex. The complex concentration is determined spectrophotometrically at 510 nm using a Spectronic's Model 601 Spectrophotometer. The colored solution obeys Beer's Law and its intensity is independent of pH from 3 to 9. A pH between 2.9 and 3.5 insures the rapid color development in the presence of an excess of phenanthroline. The total iron in the sample is determined by reducing the ferric ion to a ferrous ion with hydroquinone at room temperature.

Inductively Coupled Plasma - Atomic Emission Spectroscopy (ICP) Analysis. ICP/AES is a technique for the simultaneous or sequential multi-analyte determination of inorganic analytes in solution. The basis of the method is the measurement of atomic emission by an optical spectroscopic technique. the sample is nebulized and the aerosol produced is transported to the plasma torch where excitation occurs. The characteristic atomic-line emission spectra produced by the excitation energy of the plasma are dispersed by a grating spectrophotometer and the intensities of the lines are monitored by photomultiplier tubes. The photocurrent from the photomultiplier detector tubes are processed by a computer system.

Glass, condensate, and slurry samples are prepared for ICP analyses by obtaining representative aliqotes of the samples and dissolving it into a dilute acid solution. Glass and slurry samples do not readily dissolve in mineral acids, unless one of the acids is hydrofluoric acid, because they contain a large concentration of silicates and /or refractory compounds. However, hydrofluoric acid should not be used since several of the metal ions, such as rare earths, alkaline earth metals, and chromium III form fluoride compounds with low solubility products.

Fusions procedures are used to dissolve these samples. Since an alkali metal ion is added during the fusion, two fusions are performed on each sample so that all major metal ions are analyzed on each sample. The potassium hydroxide fusion is done in a nickel metal crucible and the sodium peroxide is done in a zirconium metal crucible. When specialized analyses are required, the fusion can be made using a different flux and/or a different type of crucible.

When the quantity of solids is small or it is in a very dilute concentration such that sufficient sample can not be filtered, the sample is digested in a mineral acid or a mixture of mineral acids. As stated above, not all of the sample will be dissolved if silicates or other refractory compounds are present. Unless otherwise requested the samples are digested in nitric acid.

Ion Chromatography (IC) Analyses of Soluble Anions. Ion chromatography is used for determining the concentration of several anions (i.e., F^-, Cl^-, NO_2^-, NO_3^-, PO_4^{-3}, SO_4^{-2}, HCO_2^-, and $C_2O_4^{-2}$) in aqueous samples and water leachates of solid and slurry samples using the Dionex Model 300 D. IC is a rapid, multi-ion method for analyzing anions in a small volume of aqueous solution. The method utilized by the Dionex system is based on separation of the anions on an anion exchange column, suppression of the eluent conductivity by a cation exchange membrane, and conductimetric detection of the separated anions as they pass through a sample conductivity cell. The increase in conductivity caused by each anion is recorded and the anion concentrations are determined by comparison with detector responses from standard solutions. The anions are identified by their retention time, the time required for the anion peak to appear following injection.

To prepare a sample for analysis, approximately one gram of the supernatant fraction is leached in approximately 100 grams of water. The sample is then placed on an orbital shaker from at least one hour. The sample is then left undisturbed to allow any solids to settle before obtaining an aliquotel sample for IC analysis.

3.5 Test Schedule

The test schedule or chronology under which the objectives were completed is shown in Figure 3.18. Many of the test objectives were achieved throughout the campaign, regardless of melter process conditions. Certain other test objectives required the establishment and maintenance of specific process conditions, such as steady state or maximum process rates. In some cases they precluded other objectives from being simultaneously obtained. Emphasis was on completing the objectives within the pilot-scale melter testing subtask. However, data was successfully obtained for all of the primary objectives and all but one of the secondary objectives.

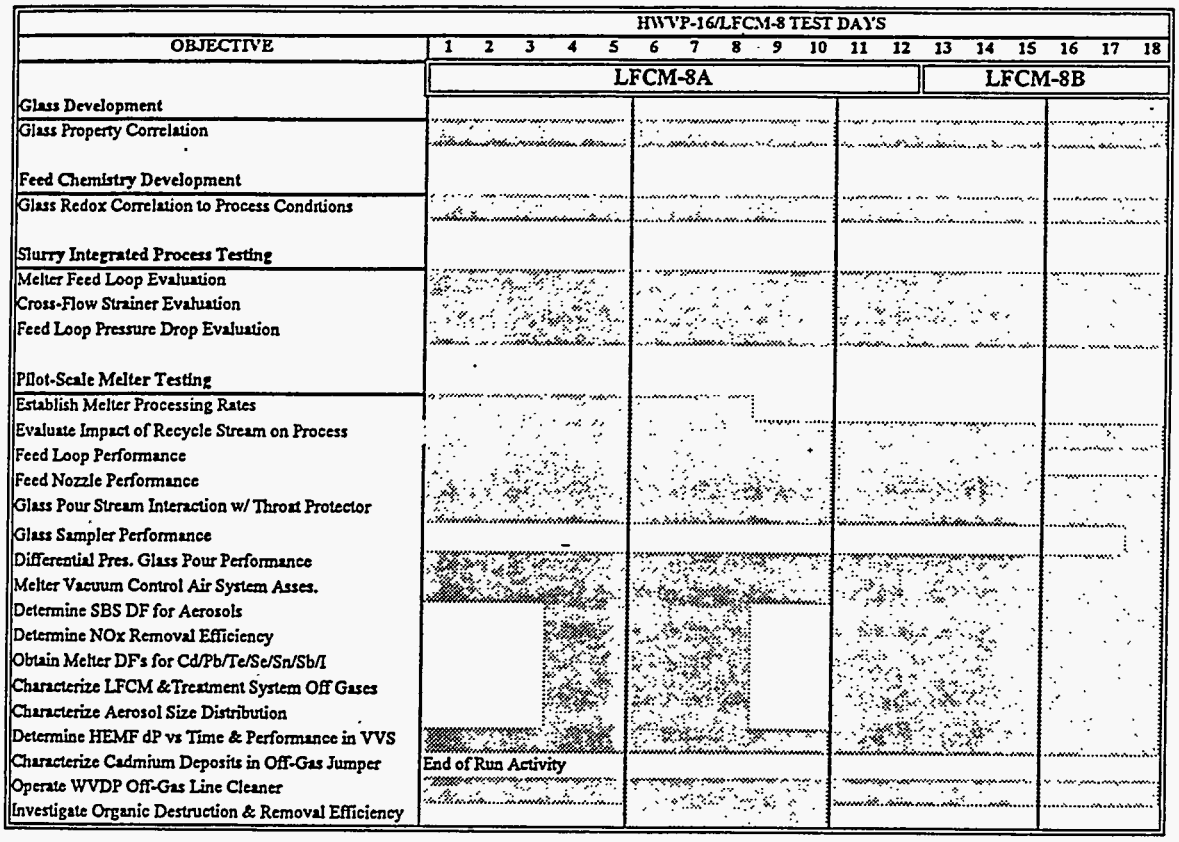

Figure 3.18. LFCM-8 Test Chronology

3.6 Testing Highlights

The LFCM-8 campaign commenced on April 17, 1993. It was anticipated that the test duration would be between 18 and 21 days, depending on the rate at which the melter feed could be processed. However, on April 29 the test had to be interrupted. The electric aerosol analyzer used to characterize HEME and HEMF performances failed, and replacement components had to be obtained from the manufacturer. As a result, the LFCM was idled between April 29 and May 10. On May 10 the campaign resumed and continued until May 16. For reporting purposes, the two segments of the campaign have been defined as LFCM-8A and LFCM-8B. Although there was a 10-day idle period, the performance of the pilot-scale vitrification system was outstanding with one exception. The SBS packing was retained by a screen that was tack-welded to the bed housing. During the latter part of the campaign (i.e., LFCM-8B), some of the tack welds failed and the packing was ejected from the bed by the off-gas stream. Particulate scrubbing performance of the SBS was not measurably affected by the loss of the packing material.

The LFCM, which had been rebuilt and restarted between 1990 and 1992, operated very well. The refractory and electrode configuration included a novel electrode power system that used a single power controller and two transformers. This system provided adequate control and also provided the ability to skew the power to one side of the melter to enhance convective mixing. The differential pressure glass pour system was also demonstrated to be reliable and quite stable. The pressure fluctuations present in the SBS did not affect the ability to control the glass pour rate, during either batch pour or continuous pour operations. One component that did have operational problems was the prototypic feed nozzle. The insulated sides allowed the outer surface to remain hot. As a result, feed material that splattered onto it became affixed. Throughout the campaign solid accumulations built up and extended downward to the cold cap. A one-hour interruption of feeding did occur during LFCM-8A to allow a feed accumulation to melt off. Frequent visual observations did establish that the accumulations interfered with the slurry stream stability. Although it did not ultimately lead to feed nozzle plugging, the potential for doing so was certainly present.

The SIPT feed system, consisting of recirculation loop, cross-flow strainer, feed line, and three-way valve, performed very well. No plugging of the feed line or strainer occurred. Several water flushes were performed when the feed flow rate began dropping. The flushes were successful in restoring the feed rate. After completion of the campaign, the three-way valve was disassembled and inspected. A significant amount of solids were found in the chambers. It was suspected, toward the end of the run, that instabilities in feed flow might be due to solids in the valve. It is recommended that the alternate valve be reconsidered for use. Water leakage problems with the Fujikin valve was reported by WSRC at water pressures above 50 psig. This might be eliminated if lower water pressures can be used. If plugging of the line by feed solids occurs, such that high pressures are required, the pressure could be increased in the gallery.

All primary objectives and a majority of the secondary objectives were achieved within the constraints of the test. Of the primary objectives, the evaluation of the glass sampler could not be fully completed. This was due to the glass bonding to the sample cup during the fourth test. As a result, the glass could not be completely removed. However, the basic purpose of the objective to determine the effect of sample time on the sampling technique was achieved. It was observed during testing that when the glass overflowed the sample cup, the glass did not drain completely down to the weir level. This is required to allow the cup to be withdrawn completely back into the throat protector. Due chiefly to rapid cooling of the glass, significant differences in LFCM and HWVP melter temperatures in this area would affect the results.

The combined operating lengths of LFCM-8A and LFCM-8B testing times totaled 439 hours. This consisted of 433 hours of melter feeding and 6 hours of downtime. Explanations of downtime are given in Table 3.1. The nine test interruptions are described in Table 3.2. A total on-line efficiency of >98% was achieved. The total volume of feed slurry processed was estimated to be 23,113 liters. This resulted in 11,105 kg of glass being produced and discharged into full-scale WVDP canisters.

Table 3.2. Description of Feeding or Operational Interruptions

Stop Date	Stop Time	Duration (hrs.)	Interruption, Explanation, and Corrective Action Taken
4/17/93	18:58	1.25	Moisture observed in discharge region, zone too cool for glass pour (approx. 980°C). Replaced blown SCR fuse, rewired discharge heaters (4 heaters instead of 6 heaters). Switched LFCM cooling jacket water from cooling tower to building process water.
4/22/93	8:10	0.433	Turned feed pump off to install conductivity probe in feed piping loop.
4/24/93	14:48	0.4	Ceased feeding and de-energized melter power to replace the glass thermowell and thermocouple assembly.
4/25/93	3:29	1	Large feed pile below feed nozzle formed and bridged to the feed nozzle. Ceased feeding to permit the mound to melt into glass bath.
4/29/93	18:01	N/A	Shut down of melter for 10 day period. Normal operation shut down, down time not included in efficiency calculation.
5/10/93	9:42	1.3	Feed flow rate decreased to zero, several unsuccessful attempts made to remove obstruction. Shift engineer concluded that the three way valve was responsible. Primary feed tubing was rerouted around the valve, all tubing thoroughly flushed.
5/10/93	14:34	0.367	Feed flow rate decreased to zero, all tubing was thoroughly flushed with no success. Blockage was tracked to pump inlet, determined to be a chip of plastic approximately 3/16"x3/16"x1/16" in size.
5/10/93	23.36	0.5	324 Bldg. suffered a complete power outage, melter power, pumps, and off-gas blower all stopped. Power was restored in approx-imately 1/2 hour, feed system was flushed and all components were restarted.
5/13/93	13:40	0.42	Feed flow rate decreased to zero, water flushing was unsuccessful. Blockage was a frit buildup. Removed obstruction from pump inlet. Power breaker for Mod 15 tripped during pump restart. Tripped breaker traced to adjacent EDL-101 and reset.
5/14/94	9:36	0.17	Power breaker for Mod 15 tripped. Breaker was reset and feed lines were flushed and feeding resumed.

4.0 Results and Discussion

Test results from LFCM-8 are presented and discussed in this section. Section 4.1 presents the melter process results. Characterization of feed, glass, and cold cap samples as well as selected condensate analyses are given in Section 4.2. Feed flow control and feed nozzle performance results are given in Section 4.3. Results of glass sampler performance, glass pour pressure control, extent of off-gas line cadmium deposits and WVDP off-gas line cleaner performance are presented in Sections 4.4 through 4.7, respectively. Off-gas system performance and characterization results are presented in Sections 4.8 through 4.11.

4.1 LFCM Processing Results

A primary objective of the LFCM-8 campaign was to establish nominal and maximum processing rates for the NCAW melter feed. LFCM-8 is the first HWVP pilot-scale test in a melter having lid heating. Before selecting the DWPF melter as the reference melter for the HWVP, testing had been conducted in pilot-scale melters without lid heating. This section presents the results of assessing the processing characteristics of the melter feed in the LFCM.

4.1.1 Process Rate and Conditions

Process rate is determined by establishing melter parameters within set ranges and then achieving a steady-state feeding rate. Feed rate is increased until the cold cap coverage over the glass surface reaches approximately 75%. Cold cap coverage is then allowed to vary between 75% and 90% for nominal processing. Coverages of 90% to 95% are maintained when maximum production rates are being established. Feed rate adjustments are made when the cold cap coverage is outside of the control limits for a period of 2 or more hours. However, feed rate changes are made at the discretion of the shift leader. Therefore, a feed rate change may occur more quickly if it appears that cold cap coverage has rapidly exceeded 90% and is approaching or reaches 100%. The operational parameters for the LFCM under which LFCM-8 was conducted are shown in Table 4.1.

Feed to the LFCM began April 17, 1993 at 1350 h. Following several feed interruptions discussed in Section 3.5 a steady feed rate of approximately 45 L/h was established after one day. The feed rates for LFCM-8A and LFCM-8B are shown in Figures 4.1 and 4.2. The feed rate was increased over the next several days up to a maximum feed rate of 80 L/h. The feed rate could not be maintained, however, because the bulk glass temperature ranged between 1175°C and 1225°C during much of this time. The failure of thermocouples in the glass and the thermowell itself made it difficult to monitor the glass temperatures precisely during this period. When the glass thermocouples and thermowell were replaced, the electrode power was reduced to return the bulk glass temperature to within the 1125°C to 1175°C operating range. With the reduction in temperature, the LFCM could no longer maintain an 80 L/h process rate, and the feed rate was reduced to between 50 L/h and 60 L/h. This rate was maintained for the remainder of LFCM-8A and was continued throughout LFCM-8B. Table 4.2 summarizes key variables related to the LFCM processing rate. Plots of cold cap coverage, average bulk glass temperature, electrode power, average plenum temperature, and plenum power are presented in Figures 4.3 through 4.14.

Table 4.1. LFCM Operating Parameters

Parameter	Operation Set Point or Range
Cold Cap Coverage	75% to 90% (Nominal), 90% to 95% (Maximum)
Average Bulk Glass Temperature	1150°C ± 25°C
Plenum Heater Pipe Temperature	950°C ± 25°C
Plenum Space Temperature	750°C ± 50°C
Plenum Pressure	-7 in. WC ± 2 in. WC
Electrode Temperature	≤ 1000°C
Discharge Overflow Temperature	1075°C ± 25°C

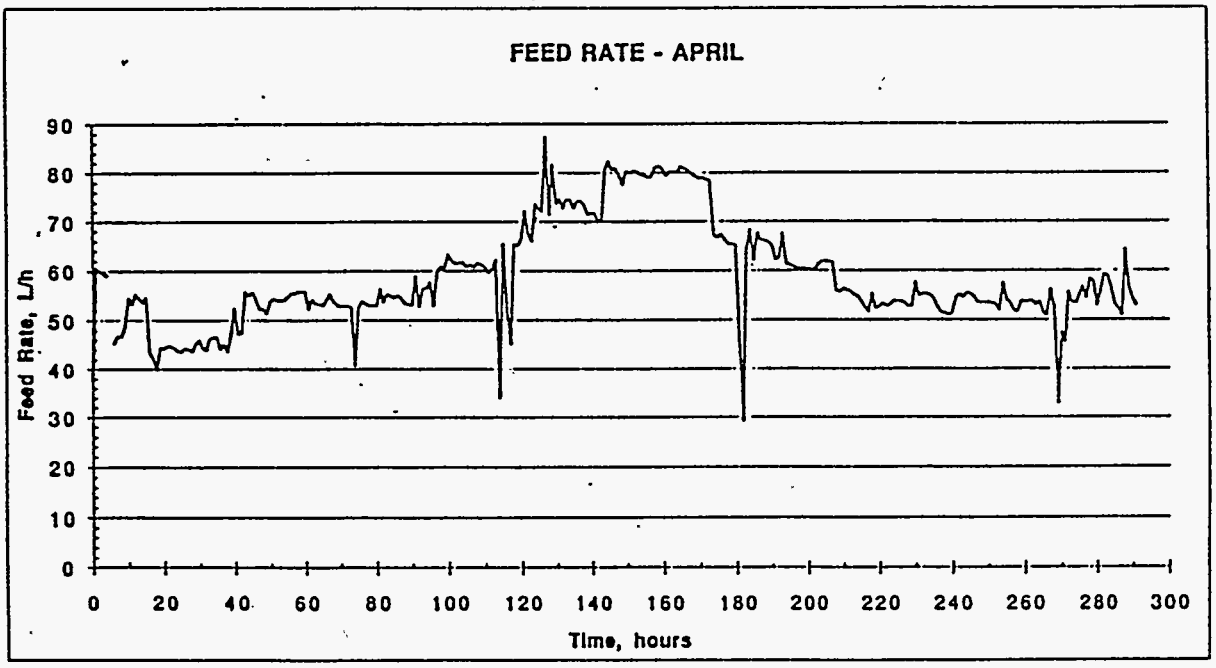

Figure 4.1. LFCM Feed Rate During LFCM-8A

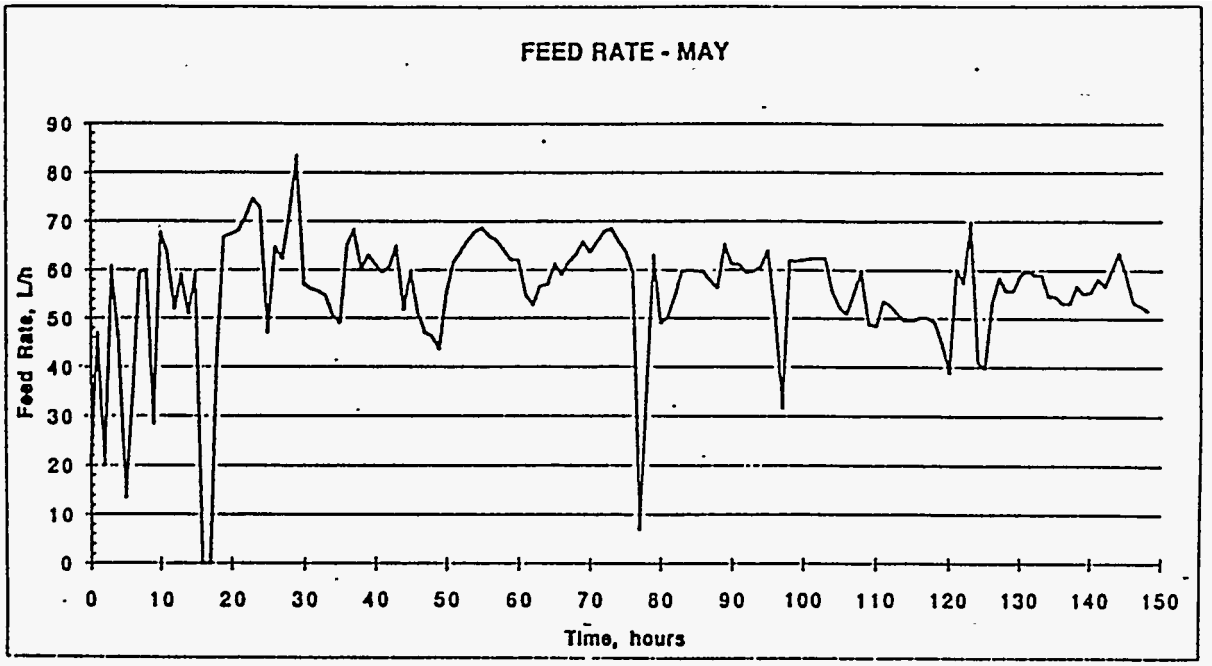

Figure 4.2. LFCM Feed Rate During LFCM-8B

Table 4.2. Summary of LFCM-8 Feed Processing Parameters

Variable	Mean Value	Median Value	Standard Deviation
LFCM-8A Feed Rate, L/h	59	55	11
LFCM-8B Feed Rate, L/h	56	59	13
LFCM-8A Cold Cap Coverage, %	88	90	12
LFCM-8B Cold Cap Coverage, %	89	95	14
LFCM-8A Ave. Bulk Glass Temperature, °C	1166	1164	13
LFCM-8B Ave. Bulk Glass Temperature, °C	1158	1158	16
LFCM-8A Electrode Pwr, kW	70.4	66.9	9.2
LFCM-8B Electrode Pwr, kW	64.5	63.2	4.1
LFCM-8A Ave. Plenum Temperature, °C	653	649	35
LFCM-8B Ave. Plenum Temperature, °C	652	649	37
LFCM-8A Plenum Pwr, kW	70.3	70.6	1.9
LFCM-8B Plenum Pwr, kW	67.3	68.8	3.6

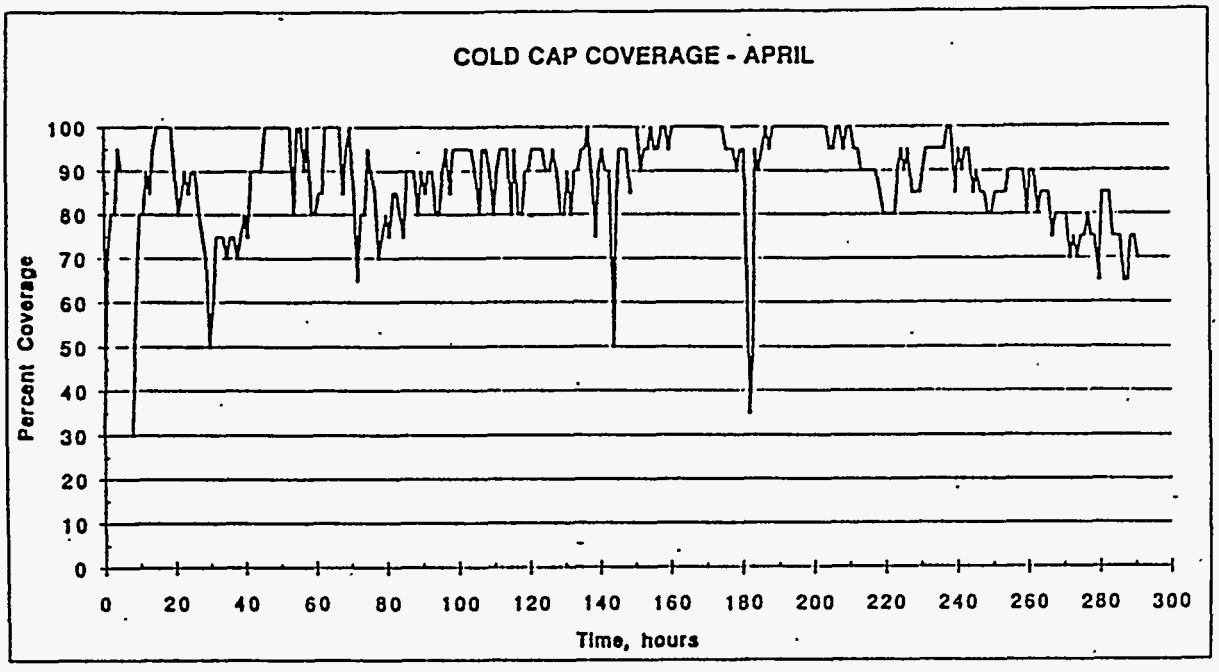

Figure 4.3. Cold Cap Coverage During LFCM-8A

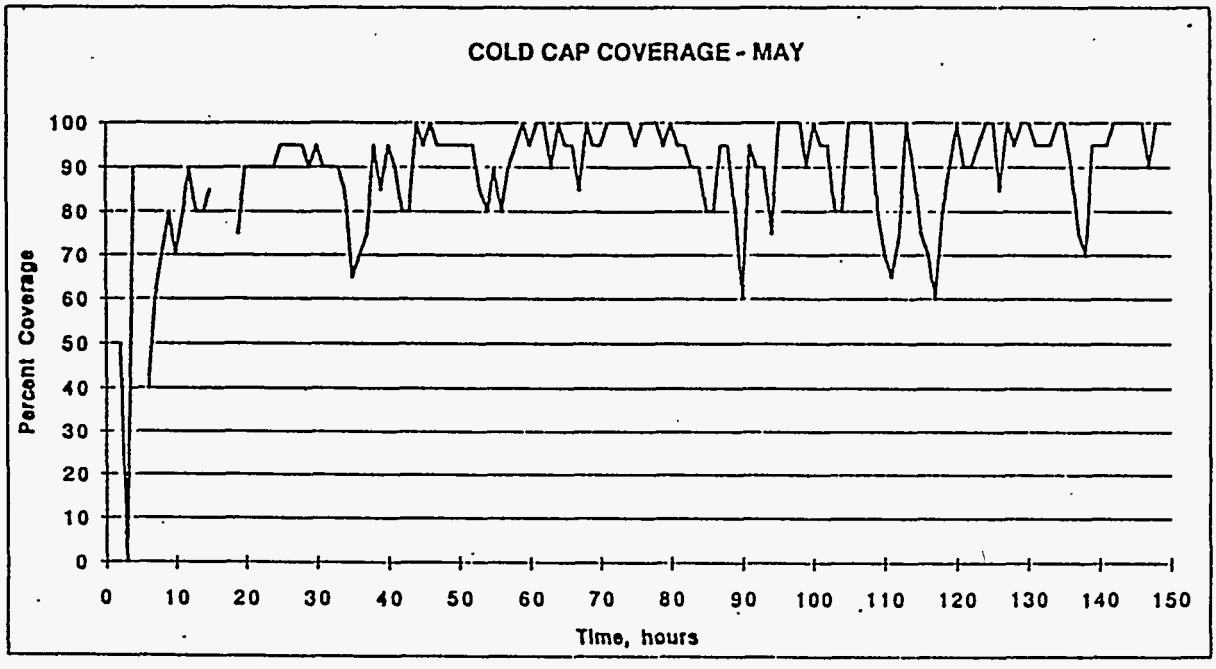

Figure 4.4. Cold Cap Coverage During LFCM-8B

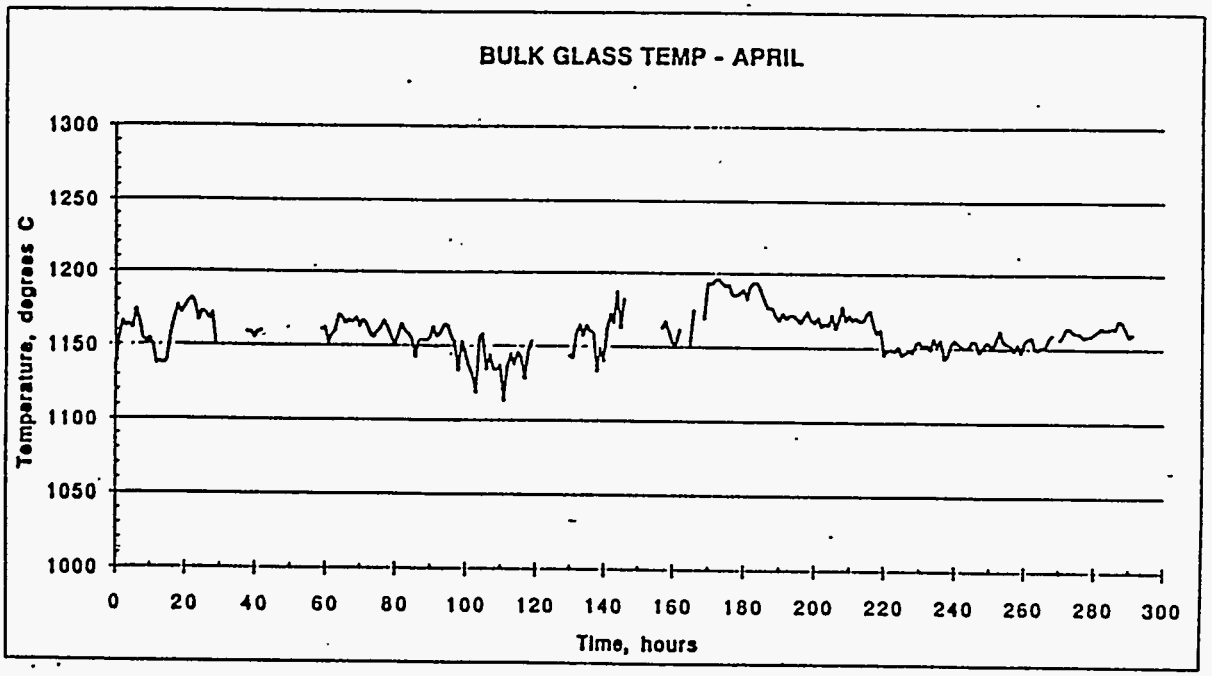

Figure 4.5. Bulk Glass Temperature During LFCM-8A

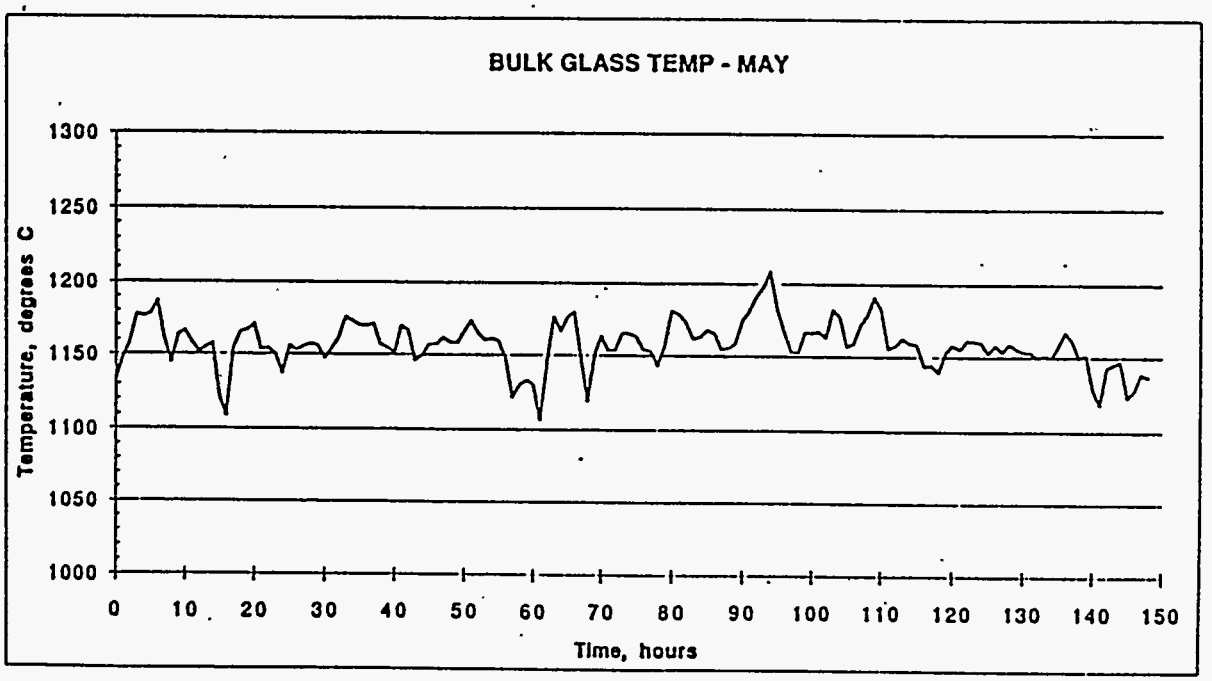

Figure 4.6. Bulk Glass Temperature During LFCM-8B

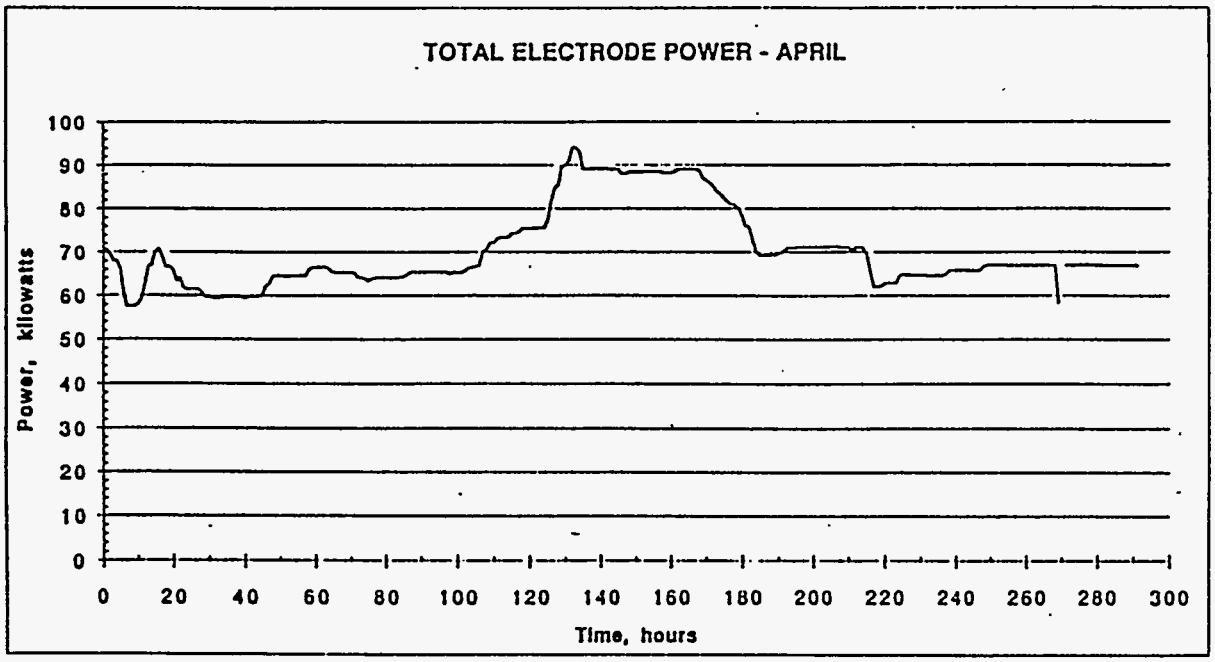

Figure 4.7. Total Electrode Power During LFCM-8A

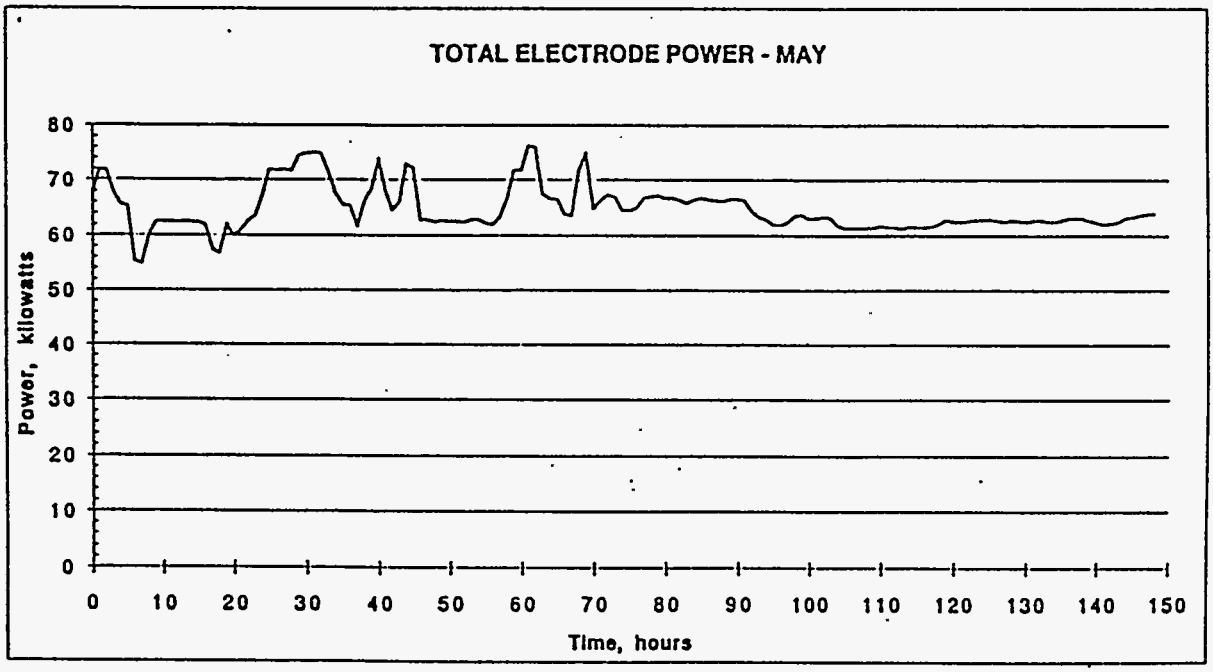

Figure 4.8. Total Electrode Power During LFCM-8B

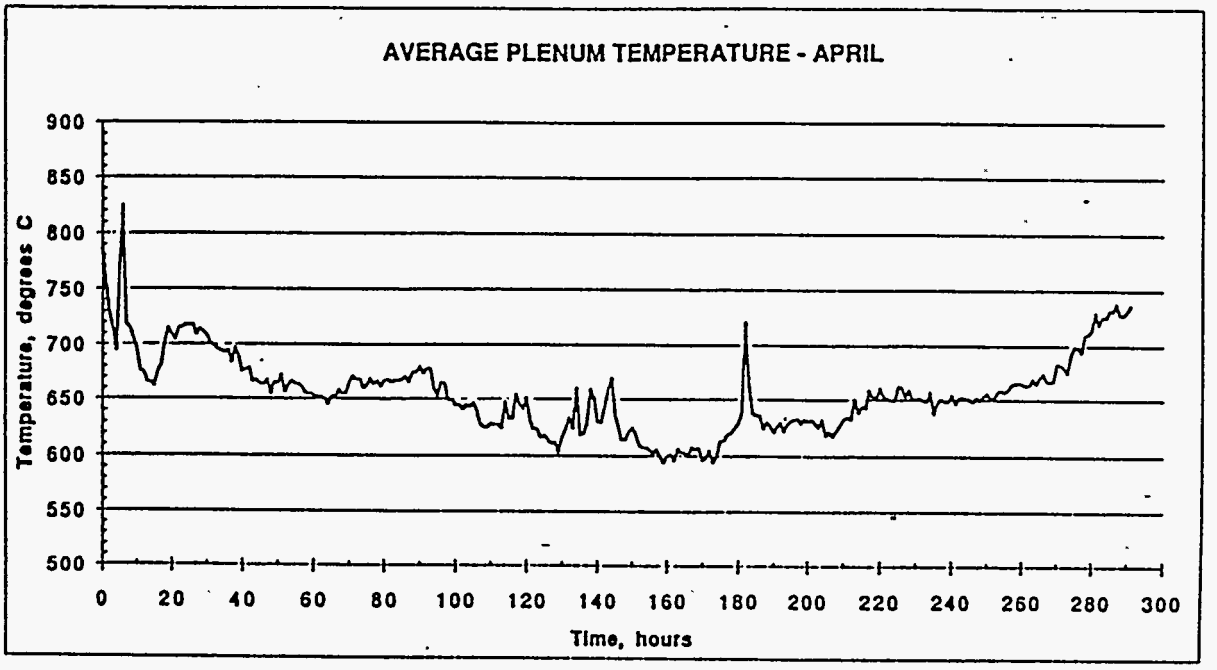

Figure 4.9. Average Plenum Temperature During LFCM-8A

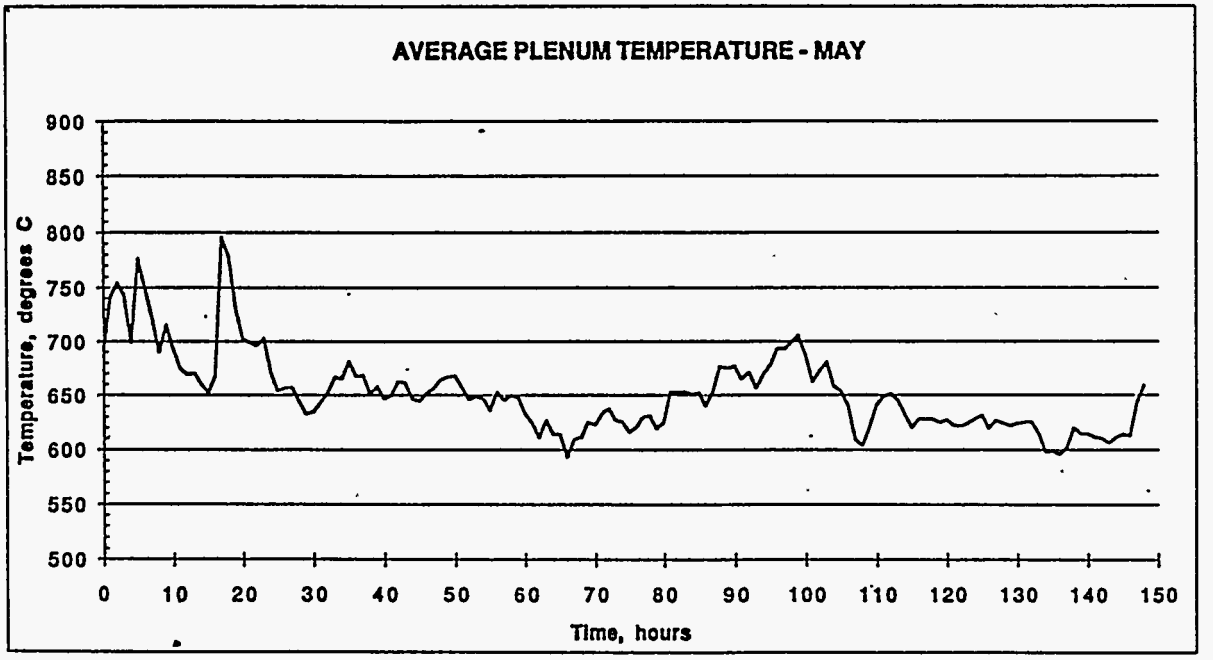

Figure 4.10. Average Plenum Temperature During LFCM-8B

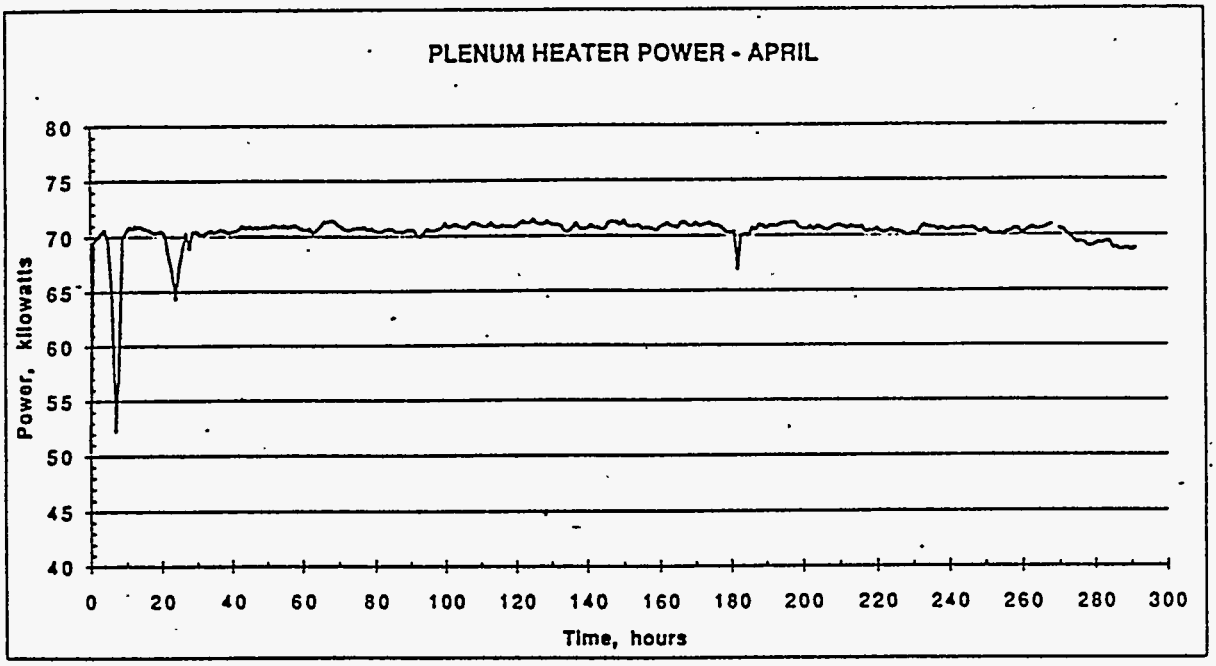

Figure 4.11. Total Plenum Heater Power During LFCM-8A

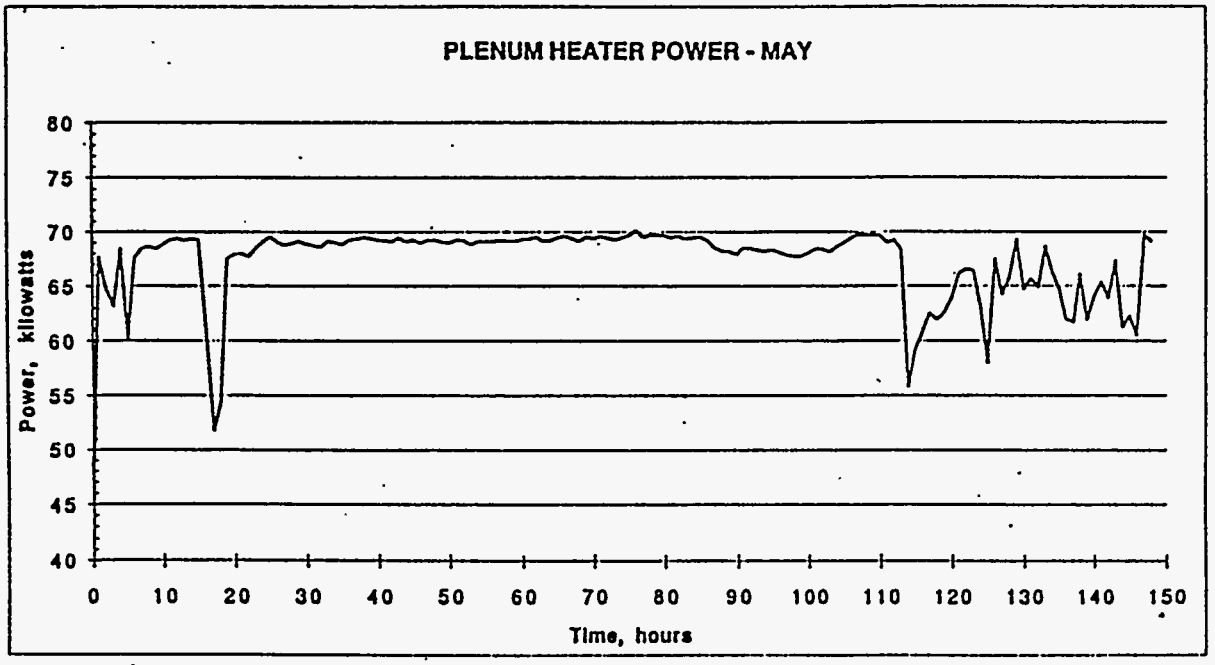

Figure 4.12. Total Plenum Heater Power During LFCM-8B

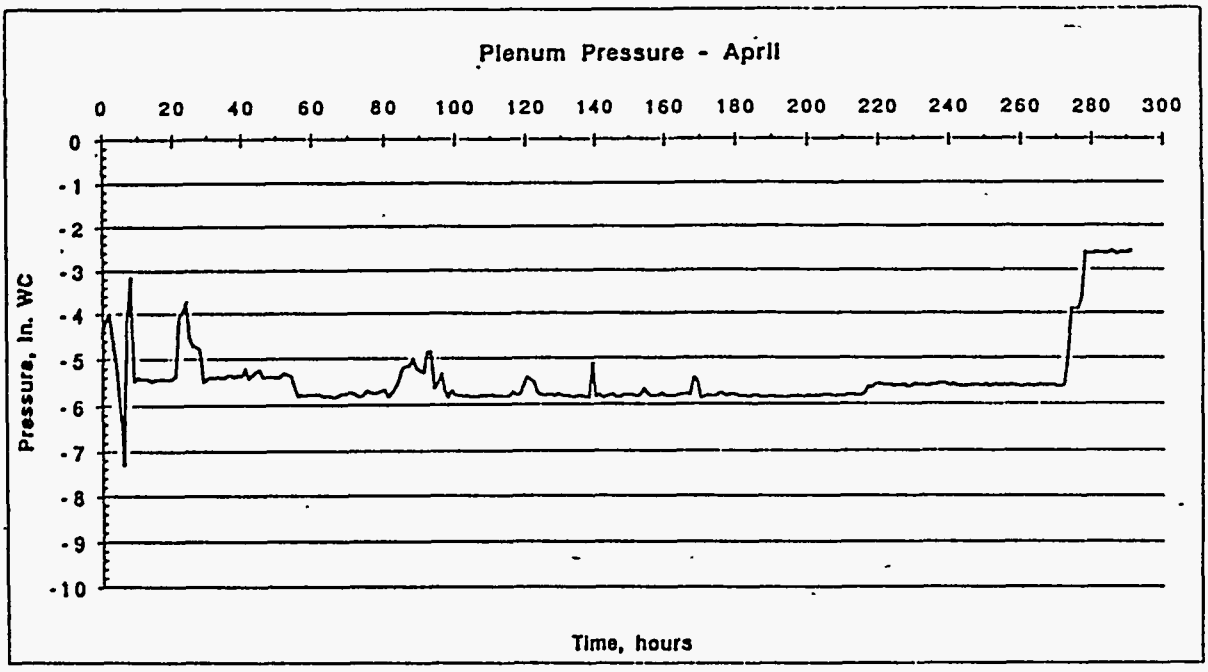

Figure 4.13. Plenum Pressure During LFCM-8A

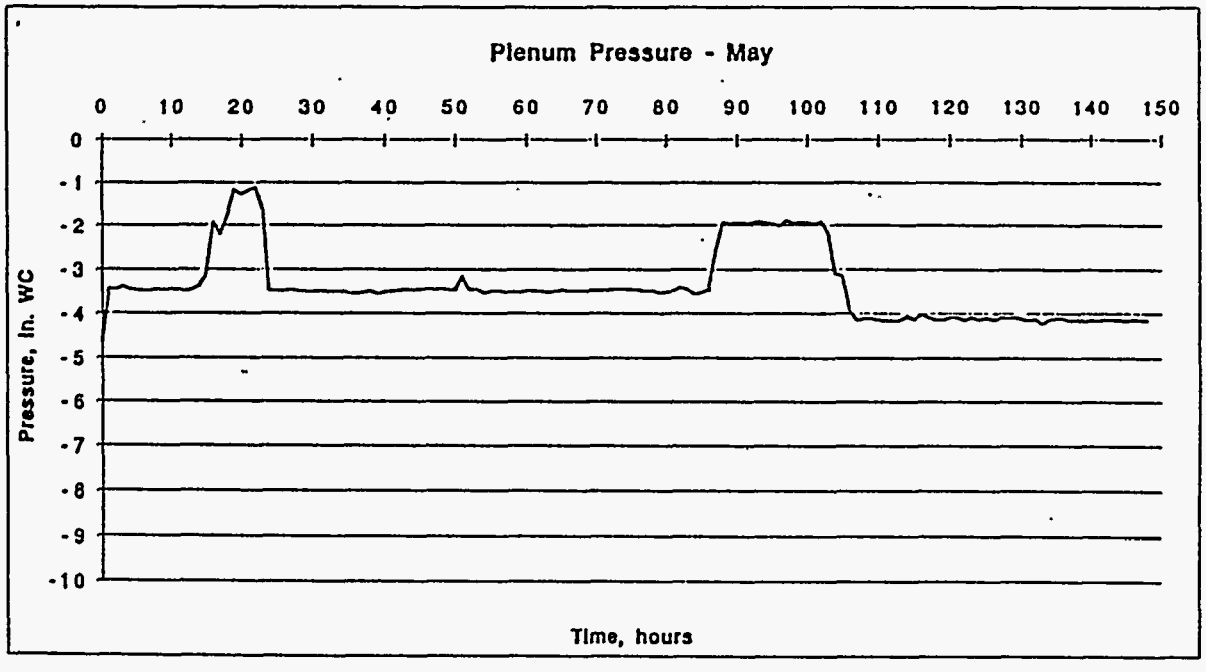

Figure 4.14: Plenum Pressure During LFCM-8B

4.1.2 Melter Process Rate

The target process rate of the LFCM, based on glass surface area and the HWVP reference rate of 200 L/h-feed or 100 kg/h-glass, is 84 L/h of feed. At a feed oxide loading of 500 g/L, the glass production rate should be 42 kg/h. LFCM-8 achieved average feed rates of 59 L/h during LFCM-8A and 56 L/h during LFCM-8B. The average feed oxide loading for each segment was 460 g/L and 413 g/L, respectively. Therefore, glass production rates of 27 kg/h and 23 kg/h, respectively, were achieved. As a result, slurry and glass production rates were only 70% and 64% of HWVP target values. The reason for this significant shortfall is thought to be due to the processability of the HWVP simulated feed and/or frit compositions. This consideration is based on the previous experience of engineering-scale melter tests processing this same feed. Most convincing are the results obtained by Grünewald et al. (1993) in the Engineering-Scale Melter (ESM). The ESM is a 10th-scale melter (based on glass surface area). During a two-month period, 16,840 liters of melter feed were processed. Process rates of 12 to 15 L/h were achieved, compared to a design rate of 20 L/h. This translates into process rates 60 to 75% of target. These values are in good agreement with the LFCM-8 results. Previous testing under HWVP in engineering-scale and pilot-scale melters established that reasonably good agreement (e.g., 75 to 90%) was achieved between engineering-scale and pilot-scale melters (Perez and Nakaoka, 1986)[(a)].

Previous PHTD testing in the PNL pilot-scale ceramic melter (PSCM) demonstrated nominal process rates between 62 to 56 L/h•m^2. These results were achieved with the previous NCAW and frit compositions. Although these campaigns were performed without lid-heat boosting they matched the LFCM-8 results. During engineering-scale tests and before PSCM testing, simulated HWVP NCAW was evaluated using the high-bay ceramic melter (HBCM) (Nakaoka and Perez, 1986). This melter had a 0.25 m^2 glass surface area and 20% of the glass holdup that the KfK melter possessed. However, it did not have lid heaters. These tests were performed to compare feeds containing frit and feeds containing unreacted chemicals comprising 2/3 of the glass formers (on an oxide basis). The use of HW39 frit resulted in nominal and maximum process rates of 11 and 14 L/h•m^2, respectively. The use of unreacted glass formers and frit resulted in nominal and maximum process rates of 8 and 9 L/h•m^2, respectively. This 25 to 35% drop in process rate is significant in that it was due only to a change in feed chemical type.

Certainly, process rates in excess of those experienced in past campaigns were expected. The significant shortfall in achieving these rates is widely considered to be due to the poor melting characteristics of the cold cap. Visual observations of the cold cap during LFCM-8 indicated that the thickness of the cold cap was as high as three inches along the perimeter of the cold cap. The cold cap material was also described as rigid and had a hardened or baked appearance. Slurry coverage over the cold cap rarely exceeded 25%. This is quite different from past experiences using lid-heat boosting when nearly complete slurry coverage was possible. Given the slow melt rate of the cold cap into the glass; it is possible that the high plenum temperatures and poor slurry coverage only exacerbated the situation. Without the slurry pool to "protect" the solids from the high temperatures and radiant heat flux reactions of the cold cap material could proceed in the upper regions of the cold cap. This could have

---

(a) Nakaoka, R. K., J. M. Perez, Jr., 1986. *Hanford Waste Vitrification Plant Nonradioactive Liquid-Fed Ceramic Melter Testing for Fiscal Year 1986.* RHO-RE-CR-17 P. Prepared for Rockwell Hanford Operations by Pacific Northwest Laboratory, Richland, Washington.

resulted in the trapping of decomposition gases or the early production and loss of molten alkali salts required to flux the refractory components. In fact, cold cap probing conducted at the end of the campaign determined that a considerable amount of slurry existed underneath the solid top layer of the cold cap. These conditions could certainly result in a cold cap with poor melting properties.

During a short period of LFCM-8A, the bulk glass temperature was allowed to increase to between 1200 and 1250°C. Slurry feeding rates were able to increase up to about 80 L/h. This 45% increase in feed rate supports the argument that the cold cap melt rate into the glass contributes significantly in limiting the process rate. When the glass temperature was returned to the proper range of 1150 ± 25°C, the feed rate had to be returned to previous levels.

Freeman[(a)] (1994) applied an energy balance approach to predicting the melt rate of a cold cap in slurry-fed glass melters. This work included measuring several properties of the dried feed. He determined that a minima exists for the thermal conductivity of the feed between 300 and 500°C. At this temperature range the thermal conductivity decreases from 1 W/m•K to 0.2 W/m•K. It is quite conceivable that the temperature range of the upper cold cap crust was at this temperature due to lid heater use. As a result, the effective transfer of heat from the lid heaters into the cold cap would be severely impeded. Freeman used the energy balance methodology in conjunction with known LFCM-8 processing values and measured feed properties to estimate slurry processing rates under varying conditions. This analysis determined that the model predicted higher processing rates than were obtained. It was further determined that a key parameter, slurry pool coverage, greatly affected the model's result. Upon changing slurry pool coverage from the visual observation of 20 to 30% to the 80 to 90% estimated at the end of the campaign during probing activities, the model prediction was accurate to within 20%. Further demonstration of Freeman's model and approach should be performed with different feed slurries to validate the model. However, used in its present form it does support the LFCM-8 process measurement and visual observations that the melter feed composition has properties that resulted in poor melting "efficiency."

Supporting this comparison to a limited extent are the results obtained by Hutson (1993). Testing at the Savannah River Site's Integrated DWPF Melter System (IDMS) preceded the ESM and LFCM tests. Directed primarily at feed preparation objectives, some data was obtained from the melter operation. The IDMS test was the first HWVP test to process the melter feed composed of FY 1991 reference neutralized current acid waste (NCAW) feed and FY 1991 frit. Poor pumping and feeding characteristics of the melter feed resulted in numerous feed line plugs forming. Pressure drops in the recirculation feed loop exceeded the ability of the system to maintain a consistent feed rate to the melter. As a result, stable feeding rates could not be maintained over the long periods (i.e., > 1 day) usually required to establish production rates. However, over shorter periods IDMS operation did establish production rates equivalent to the plant target of 40 kg/h•m^2 (8 lb./h•ft.^{2}).

4.1.3 Plenum Heater Operation

The LFCM lid heaters provided a maximum of 70 kW of power during the campaign. This was equivalent to the power provided by the electrodes (see Table 4.2). The nearly 50% split in power, characteristic of expected plant operation, was not achieved intentionally. Rather, the rate at which

---

(a) Freeman, C. J. 1994. *Melt Rate Predictions for Slurry-Fed Glass Melters*. PVTD Milestone PHTD-C93-04.15K, Pacific Northwest Laboratory, Richland, Washington.

heat could be transmitted through the cold cap from the glass limited the power output of the electrodes. Had the cold cap heat transfer been higher, higher feeding rates and higher electrode power rates may have been possible. The plenum heaters were run at maximum power. Head space restrictions prevented any additional heaters from being installed during the LFCM refurbishment in FY 1990. Average plenum temperatures of approximately 650°C were achieved. These were 50°C below the minimum target temperature of the plant melter. The maximum operating temperature of the DWPF plenum heater pipes is 950°C. Heater pipe temperatures in the LFCM ranged between 800°C and 950°C. One lid heater thermocouple consistently indicated a heater pipe temperature of 1,000 to 1,050°C during LFCM-8B.

The benefit of plenum heating to boost HWVP production rates cannot be effectively evaluated with the data available. A direct comparison of processing results with previous HWVP tests, such as Pilot-Scale Ceramic Melter (PSCM-23), also cannot be performed. This is because of the processing characteristics of the current melter feed. Specific evaluation of the effect of plenum heaters had been planned for LFCM-8, but because of testing priorities, this objective was not performed.

Typically, when a melter is performing at optimum conditions--that is, with a full cold cap--the slurry pool covers 50 to 80% of the cold cap. At such conditions, a significant fraction of plenum heater power output would be expected to directly increase the evaporation rate of water from the slurry. Modeling work performed by Eyler (Elliott et al. 1989)[a] estimated that the effect of plenum heaters could increase the solids melting rate by up to 50%. Unfortunately, insufficient experimental data exists to verify this modeling analysis. Elliott et al. (1989) also compiled a data base of 44 melter campaigns performed at PNL, West Valley, and Savannah River. The data contained comparative campaigns when the same flowsheet was evaluated with and without lid heat boosting. A 1981 test in the LFCM processing Savannah River feed containing frit 131 and treated with formic acid achieved a 100% increase in process rate when lid heaters were used. Conversely, a 1982 test in the PSCM processing Savannah River feed containing frit 165 and treated with formic acid showed essentially no improvement in production rate when plenum heaters were used. These two data points strongly suggest that cold cap melting is not dependent solely on thermal flux conditions. Slurry, rheology, evaporation rate, heat transfer reaction kinetics, and mass transfer should all be considered to be potentially significant. As such, vitrification flowsheets can not be designed based solely on either laboratory studies to optimize glass properties or engineering studies to blend streams. A key consideration has to be achieving a flowsheet that can be efficiently processed. Based on LFCM-8 results and observations for the present flowsheet, slurry rheology and/or melting kinetics may be the primary variables that dictate processing rate. Because of this fact, the evaporation rate of water from the slurry is not necessarily rate-limiting.

(a) Elliott, M. L., C. C. Chapman, L. L. Eyler, and D. D. Yasuda. 1989. *Preliminary Studies of Vitrification Rate Enhancement*. Internal HLWPO Letter Report, Pacific Northwest Laboratory, Richland; Washington.

4.2 Melter Sample Analyses

Daily samples of feed slurry, glass, and SBS condensate were obtained for post-test analyses. In addition to the daily samples, samples of glass, cold cap, off-gas line deposits, and off-gas stream samples were obtained. Results of off-gas stream sample analyses are reported separately in Sections 4.9, 4.10, and 4.11.

Melter Feed Physical Characterization. Melter feed samples were analyzed to determine density, oxide loading, weight percent solids, and water loading. These values are presented in Table 4.3. Oxide loading was determined by direct measurement and estimated from ICP analytical results. Melter feed samples were taken twice each day during the campaign. Samples selected for the analysis were taken from the morning (8 a.m.) sample set. LFCM-8A is represented by samples 2b through 156, inclusively. Samples numbered 169 through 229 were taken during LFCM-8B. With the exception of the second sample, No. 9a, the measurement results are quite explainable.

Table 4.3. Melter Feed Analytical Results for Density, Oxide Loading, Weight Percent Solids, and Water Loading

Run Day	Sample No.	Density, g/mL	Oxide Loading (ICP), g/L	Oxide Loading (Direct), g/L	Wt. Percent Solids	Water Loading, ml/L
1	2b	1.32	484	478	42.8	755
2	9a	1.24	446	445	42.4	714
3	21a	1.32	467	470	42.1	764
4	35	1.35	479	474	42.7	774
5	48	1.31	471	462	41.2	770
6	62	1.30	460	456	41.6	759
7	77	1.33	471	471	41.9	773
8	89	1.34	454	463	41.0	791
9	104	1.30	459	447	41.3	763
10	117	1.33	483	478	42.4	766
11	131	1.33	470	467	41.6	777
12	143	1.32	466	460	41.5	772
13	156	1.33	469	418	41.6	777
14	169	1.31	460	445	40.1	785
15	177	1.27	387	385	37.6	792
16	195	1.27	379	410	38.3	784
17	202	1.29	383	399	38.2	797
18	215	1.28	416	420	38.8	783
19	229	1.31	419	419	37.9	814
Average		1.31	449	446	40.8	774

The feed slurry was initially diluted to an oxide value of approximately 480 g/L to assure that it could be properly agitated and pumped. In the first days of the campaign, the prototypic sampler introduced approximately 20 gallons of water with each sampling operation. This was caused by the significant amount of water required to prime the pump at the beginning of the operation and to flush water used at the end of the cycle. As a result, the oxide loading was further reduced to between 455 g/L and 460 g/L. To prevent any further dilution, the sampler pump was left running continuously. Between LFCM-8A and LFCM-8B the feed was transferred from the SIPT tank HB-15 into HB-13. This occurred because the liquid level in HB-15 was approaching the minimum operating level at the end of LFCM-8A. Line flush water that followed the transfer resulted in the feed oxide level being diluted to approximately 400 g/L. Throughout the campaign, the slurry oxide concentration averaged about 450 g/L. The weight percent solids and water loading in the slurry averaged 41 wt.% and 774 ml/L, respectively.

Daily slurry, glass, and SBS samples were analyzed for cation and anion composition. ICP-AES analyses have been reported in weight percent oxides and ppm, depending on the sample preparation method used. Hydroxide fusions were used on samples if a sufficient amount of sample was obtained (e.g., feed and glass samples). The fusion dissolves the entire sample. If an insufficient quantity of solids existed, as is the case for SBS condensate samples, the sample was dissolved in dilute HCl. This method does not pull all constituents into the solution, especially the more refractory constituents. As a result, these components should be expected to be under reported.

The feed composition was prepared to the reference target composition given in Table 4.4. The feed oxides consisted of 28% NCAW plant feed, 3.4% internal plant recycle waste stream, and 68.6% frit. The cation analytical results for the feed, glass, and SBS condensate are presented in Tables 4.5, 4.6, and 4.7, respectively. Anion analyses of feed samples are presented in Tables 4.8 and 4.9.

The glass and feed compositions throughout the campaign were close to the target values and fairly constant with some exceptions. The glass that was present at the start of the campaign, and which was used to start up the LFCM, was based on the major oxides in the HWVP HW39-4 composition. The rate of turnover of the tank can be determined by mapping the concentration of cadmium in the discharge glass (see Figure 4.15). Cadmium was not a constituent of the startup glass. The approach of the cadmium concentration in the glass to that in the feed is reached after seven days of operation. The shape of the curve is characteristic of a well-mixed tank, indicating that the three-electrode, slope-walled LFCM exhibited good mixing characteristics.

In comparing the glass and feed analyses to each other and to the target composition, several comments should be made. Table 4.10 compares the average feed and glass oxides to the target composition. An average glass composition was estimated by taking only the glass samples analyzed after seven days (i.e., LFCM-8 sample No. 93) of operation. The feed and glass are compared to the target by taking a ratio of the target values to feed and glass, as well as comparing the feed to the glass (last column of Table 4.10). A value below unity for the ratios of the target to the feed and glass indicate that the sample concentration exceeded the target value. The major oxides have been highlighted in Table 4.10. For the major oxides, feed preparation strives to achieve a composition that is within five relative percent. For the minor oxides, present at concentrations of one percent or less, accuracies will vary between 5 and 20 relative percent. Looking first at the feed results, the non-frit oxides, aluminum, cadmium, iron, manganese, neodymium, sodium, and zirconium are within 7% of the target with the exception of sodium and zirconium. The low zirconium concentration was due to the vendor-supplied slurry being low in zirconium. Additional zirconium was added to the slurry at PNL;

Table 4.4. Reference Melter Feed and Glass Composition (Wt. % oxide)

Oxide	Plant Feed Oxide Conc. (%)	Recycle Feed Oxide Conc. (%)	Frit Oxide Conc. (%)	Total (%)
Ag_2O	0.03			0.03
Al_2O_3	2.60	0.14		2.74
B_2O_3	2E-3		14.03	14.03
BaO	0.05			0.05
CaO	0.23	0.01		0.24
CdO	0.87	0.11		0.98
CeO_2	0.18			0.18
Cl	0.08			0.08
Cr_2O_3	0.07			0.07
Cs_2O	0.17			0.17
CuO	0.07			0.07
F	0.03			0.03
Fe_2O_3	8.12	0.04		8.16
GeO_2	4E-5			4E-5
K_2O	0.06	0.01		0.07
La_2O_3	0.19			0.19
LiO_2	5.00		5.00	5.00
MgO	0.10	0.01		0.11
MnO_2	0.61	0.03		0.64
MoO_3	0.16			0.16
Na_2O	6.15	1.45		7.60
Nb_2O_3	3E-3			3E-3
Nd_2O_3	1.00			1.00
NiO	0.66			0.66
P_2O_5	0.25	0.11		0.36
PbO_2	0.20			0.20
Pr_2O_3	0.04			0.04
Rb_2O_3	0.02			0.02
Sb_2O_3	2E-3			2E-3
SeO_2	5E-3			5E-3
SiO_2	1.15	1.49	49.57	52.21
Sm_2O_3	0.02			0.02
SnO	3E-3			3E-3
SO_3	0.19			0.19
SrO	0.03			0.03
Ta_2O_5	1E-3			1E-3
TeO_2	0.03			0.03
TiO_2	0.19	4E-3		0.19
Y_2O_3	0.02			0.02
ZnO	0.10			0.10
ZrO_2	4.35			4.35
Totals	28.00	3.4	68.6	100.00

Table 4.5. Feed Sample Cation Analyses By ICP-AES, (Wt.% oxide)

Sample No.:	2b	9a	21a	35	48	62	77	89	104	117	131	143	156	169	177	195	202	215	229
Run Day :	1	2	3	4	5	6	7	8	9	10	11	12	13	14	15	16	17	18	19
Ag2O	0.02	0.02	0.02	0.02	0.02	0.02	0.02	0.01	0.02	0.02	0.01	0.02	0.02	0.02	0.02	0.01	0.01	0.02	0.01
Al2O3	2.85	2.85	2.84	2.88	2.82	2.79	2.87	2.66	2.88	2.77	2.79	2.89	2.76	2.74	2.82	2.82	2.81	2.82	2.81
B2O3	12.37	12.50	12.51	12.66	12.49	12.27	10.96	10.56	11.14	11.73	12.35	10.51	12.13	11.82	10.87	10.99	10.71	12.02	12.58
BaO	0.06	0.06	0.06	0.06	0.06	0.06	0.06	0.06	0.06	0.06	0.06	0.06	0.06	0.06	0.06	0.06	0.06	0.06	0.06
Bi2O3	0.00	0.00	0.00	0.00	0.00	0.00	0.00	0.00	0.00	0.00	0.00	0.01	0.00	0.00	0.00	0.00	0.01	0.00	0.00
CaO	0.31	0.31	0.30	0.31	0.30	0.30	0.31	0.28	0.31	0.30	0.29	0.30	0.29	0.29	0.32	0.30	0.29	0.32	0.31
CdO	1.05	1.05	1.05	1.05	1.04	1.02	1.04	0.96	1.04	1.03	1.04	1.05	1.02	1.01	1.02	1.02	1.02	1.04	1.03
CeO2	0.18	0.18	0.18	0.17	0.18	0.18	0.17	0.14	0.18	0.17	0.16	0.17	0.19	0.17	0.18	0.13	0.16	0.19	0.18
Co2O3	0.01	0.01	0.01	0.01	0.01	0.01	0.01	0.01	0.01	0.01	0.02	0.02	0.01	0.02	0.02	0.02	0.02	0.02	0.02
Cr2O3	0.10	0.10	0.10	0.10	0.10	0.10	0.10	0.09	0.10	0.10	0.10	0.10	0.10	0.10	0.10	0.10	0.10	0.10	0.10
CuO	0.08	0.08	0.08	0.08	0.08	0.08	0.08	0.07	0.08	0.08	0.08	0.08	0.08	0.07	0.08	0.08	0.08	0.08	0.08
Dy2O3	0.01	0.01	0.01	0.01	0.01	0.01	0.01	0.01	0.01	0.01	0.01	0.01	0.01	0.01	0.01	0.01	0.01	0.01	0.01
Eu2O3	0.00	0.00	0.00	0.00	0.00	0.00	0.00	0.00	0.01	0.00	0.01	0.01	0.00	0.00	0.00	0.01	0.01	0.01	0.01
Fe2O3	8.52	8.49	8.46	8.60	8.40	8.33	8.54	7.85	8.48	8.23	8.28	8.60	8.25	8.04	8.21	8.20	8.16	8.31	8.30
K2O	0.91	0.88	0.92	0.70	1.19	1.08	1.10	1.16	1.90	1.18	1.92	2.12	1.70	1.59	1.52	1.51	2.08	2.09	1.86
La2O3	0.22	0.22	0.22	0.23	0.22	0.22	0.22	0.20	0.22	0.22	0.22	0.22	0.22	0.22	0.22	0.22	0.22	0.22	0.22
Li2O	4.71	4.74	4.77	4.84	4.71	4.70	4.78	4.58	4.86	4.71	4.66	4.77	4.61	4.48	4.66	4.63	4.57	4.56	4.58
MgO	0.26	0.25	0.26	0.25	0.26	0.25	0.26	0.24	0.26	0.26	0.28	0.28	0.27	0.26	0.25	0.26	0.27	0.27	0.27
MnO	0.70	0.70	0.69	0.70	0.69	0.68	0.70	0.65	0.71	0.68	0.68	0.70	0.67	0.66	0.69	0.69	0.68	0.69	0.69
MoO3	0.18	0.18	0.18	0.18	0.18	0.18	0.18	0.17	0.18	0.18	0.18	0.18	0.18	0.17	0.17	0.18	0.18	0.18	0.18
Na2O	6.73	6.86	6.86	6.71	6.53	6.86	5.80	5.74	5.75	6.52	6.68	5.30	6.51	6.63	5.33	5.69	5.73	6.55	6.94
Nd2O3	1.02	1.03	1.02	1.03	1.00	1.01	1.02	0.94	1.02	0.99	1.00	1.03	0.99	0.98	0.99	1.00	1.00	1.00	1.00
NiO	0.66	0.66	0.66	0.68	0.67	0.66	0.68	0.63	0.66	0.66	0.68	0.69	0.66	0.64	0.66	0.63	0.64	0.65	0.65
P2O5	0.47	0.48	0.47	0.48	0.46	0.46	0.49	0.45	0.49	0.48	0.46	0.49	0.46	0.45	0.48	0.49	0.48	0.48	0.49
PbO	0.24	0.24	0.23	0.24	0.24	0.23	0.24	0.22	0.24	0.23	0.25	0.25	0.24	0.23	0.24	0.24	0.24	0.24	0.25
SO3	0.28	0.26	0.27	0.27	0.26	0.26	0.28	0.26	0.29	0.27	0.28	0.29	0.27	0.27	0.27	0.33	0.29	0.29	0.28
SiO2	53.54	53.37	53.38	53.28	53.70	51.87	53.68	55.81	54.42	54.81	53.30	53.39	51.91	52.67	53.55	52.98	52.76	53.28	52.60
SrO	0.04	0.04	0.04	0.04	0.04	0.04	0.04	0.04	0.04	0.04	0.04	0.04	0.04	0.04	0.04	0.04	0.04	0.04	0.04
TeO2	0.07	0.07	0.06	0.06	0.07	0.07	0.07	0.06	0.06	0.07	0.08	0.08	0.07	0.07	0.06	0.06	0.07	0.08	0.07
TiO2	0.24	0.24	0.24	0.24	0.24	0.23	0.24	0.22	0.24	0.23	0.23	0.24	0.23	0.23	0.23	0.23	0.23	0.23	0.23
VO2	0.00	0.00	-0.01	-0.01	0.00	1.42	1.43	1.39	0.00	0.00	0.01	1.43	1.43	1.43	1.64	1.67	1.68	0.00	0.01
Y2O3	0.03	0.03	0.03	0.03	0.03	1.12	1.12	1.09	0.03	0.03	0.03	1.12	1.12	1.12	1.28	1.31	1.31	0.03	0.03
ZnO	0.11	0.11	0.11	0.12	0.11	1.14	1.14	1.11	0.12	0.11	0.11	1.19	1.15	1.15	1.30	1.33	1.33	0.11	0.11
ZrO2	4.03	3.97	3.97	3.98	3.89	2.35	2.36	2.30	4.15	3.80	3.69	2.36	2.36	2.36	2.70	2.76242		4.03	4.02

Table 4.6. Glass Sample Cation Analyses By ICP-AES (Wt.% oxide)

Sample No.:	1	11	23	38	51	66	79	93	107	121	135	148	165	171	180	192	205	220	227	245
Run Day:	1	2	3	4	5	6	7	8	9	10	11	12	13	14	15	16	17	18	19	20
Ag2O	0.00	0.00	0.00	0.01	0.01	0.01	0.01	0.01	0.02	0.02	0.02	0.01	0.02	0.02	0.01	0.01	0.02	0.01	0.02	0.01
Al2O3	4.15	3.92	3.81	3.68	3.41	3.42	3.36	3.32	3.41	3.14	3.24	3.34	3.88	3.09	3.06	2.97	3.05	3.16	2.94	2.98
B2O3	10.27	11.29	11.58	12.15	12.35	12.44	12.56	12.41	12.13	12.02	12.75	12.81	12.58	12.59	12.57	12.33	12.24	12.66	12.16	12.45
BaO	0.26	0.19	0.15	0.12	0.09	0.08	0.07	0.07	0.07	0.06	0.36	0.07	0.06	0.06	0.06	0.06	0.06	0.06	0.06	0.06
Bi2O3	0.00	0.00	0.00	0.00	0.00	0.00	0.04	0.00	0.06	0.06	0.00	0.00	0.00	0.04	0.05	0.05	0.05	0.00	0.06	0.06
CaO	0.90	0.70	0.60	0.58	0.40	0.38	0.36	0.36	0.38	0.36	0.33	0.31	0.33	0.33	0.32	0.33	0.32	0.33	0.32	0.32
CdO	0.06	0.41	0.59	0.76	0.89	0.96	1.01	1.03	1.01	1.01	1.04	1.05	1.03	1.03	1.02	1.01	1.01	1.03	1.00	1.02
CeO2	0.02	0.09	0.12	0.06	0.17	0.17	0.15	0.18	0.20	0.22	0.21	0.17	0.22	0.20	0.15	0.20	0.20	0.17	0.21	0.20
Co2O3	0.04	0.03	0.02	0.02	0.02	0.02	0.02	0.02	0.02	0.02	0.01	0.01	0.01	0.02	0.02	0.02	0.02	0.02	0.02	0.02
Cr2O3	0.38	0.30	0.27	0.21	0.16	0.15	0.14	0.13	0.14	0.12	0.12	0.12	0.21	0.12	0.12	0.11	0.11	0.11	0.11	0.11
CuO	0.17	0.14	0.12	0.11	0.10	0.09	0.09	0.09	0.09	0.09	0.09	0.09	0.08	0.08	0.09	0.08	0.08	0.08	0.08	0.08
Dy2O3	0.01	0.01	0.01	0.01	0.01	0.01	0.01	0.01	0.02	0.02	0.01	0.01	0.01	0.01	0.01	0.01	0.01	0.01	0.01	0.01
Eu2O3	0.00	0.00	0.00	0.00	0.01	0.00	0.01	0.01	0.01	0.01	0.01	0.01	0.01	0.01	0.01	0.01	0.00	0.01	0.01	0.01
Fe2O3	6.73	7.54	7.79	8.25	8.39	8.57	8.71	8.73	8.48	8.39	8.77	8.66	8.53	8.50	8.38	8.22	8.10	8.31	8.04	8.19
K2O	0.39	0.00	0.49	0.51	0.80	0.94	0.81	1.44	1.23	1.94	1.57	2.09	1.95	1.06	1.58	1.81	1.82	0.98	2.60	1.68
La2O3	1.66	1.17	0.88	0.64	0.45	0.36	0.30	0.26	0.26	0.24	0.25	0.25	0.23	0.23	0.23	0.23	0.22	0.22	0.22	0.22
Li2O	3.66	4.19	4.32	4.60	4.68	4.76	4.81	4.75	4.61	4.53	4.92	4.95	4.83	4.86	4.81	4.69	4.64	4.79	4.57	4.73
MgO	0.87	0.65	0.54	0.43	0.38	0.33	0.31	0.33	0.37	0.35	0.28	0.28	0.29	0.29	0.30	0.31	0.30	0.27	0.32	0.30
MnO	0.37	0.50	0.56	0.63	0.66	0.69	0.71	0.71	0.70	0.69	0.71	0.71	0.70	0.70	0.69	0.68	0.67	0.69	0.67	0.68
MoO3	0.26	0.24	0.22	0.21	0.20	0.20	0.20	0.20	0.19	0.19	0.19	0.19	0.18	0.18	0.18	0.18	0.18	0.18	0.18	0.18
Na2O	10.24	9.32	9.32	7.95	8.28	8.09	8.45	8.85	10.72	10.77	7.25	6.53	7.15	8.34	7.74	8.24	8.56	7.28	8.57	8.16
Nd2O3	0.69	0.83	0.89	0.98	1.02	1.04	1.08	1.09	1.09	1.07	1.08	1.10	1.06	1.06	1.05	1.03	1.03	1.04	1.02	1.04
NiO	0.64	0.66	0.64	0.70	0.69	0.68	0.70	0.68	0.68	0.65	0.67	0.68	0.63	0.64	0.65	0.63	0.64	0.64	0.63	0.64
P2O5	0.57	0.53	0.52	0.52	0.50	0.50	0.50	0.52	0.52	0.50	0.48	0.48	0.47	0.44	0.46	0.46	0.45	0.46	0.45	0.46
PbO	0.00	0.10	0.14	0.18	0.22	0.23	0.24	0.26	0.28	0.28	0.24	0.25	0.25	0.25	0.25	0.25	0.26	0.24	0.26	0.25
SO3	0.28	0.26	0.26	0.26	0.26	0.27	0.27	0.27	0.28	0.29	0.26	0.26	0.26	0.25	0.26	0.25	0.25	0.25	0.26	0.25
SiO2	53.10	52.64	51.60	51.98	51.43	51.01	50.54	49.59	48.59	48.52	50.53	50.89	50.27	50.92	51.40	51.37	51.41	52.49	50.90	51.71
SrO	0.03	0.03	0.03	0.04	0.04	0.04	0.04	0.04	0.04	0.04	0.04	0.04	0.04	0.04	0.04	0.04	0.04	0.04	0.04	0.04
TeO2	0.00	0.00	0.00	0.00	0.06	0.06	0.07	0.08	0.09	0.09	0.06	0.08	0.07	0.07	0.08	0.08	0.09	0.06	0.08	0.08
TiO2	0.16	0.19	0.21	0.22	0.23	0.24	0.25	0.25	0.24	0.24	0.25	0.25	0.24	0.24	0.24	0.24	0.24	0.24	0.23	0.24
VO2	0.00	0.00	0.00	0.00	0.00	0.01	0.01	0.02	0.02	0.02	0.00	0.00	0.00	0.01	0.01	0.01	0.02	0.00	0.02	0.01
Y2O3	0.01	0.02	0.02	0.02	0.03	0.02	0.03	0.03	0.03	0.03	0.03	0.03	0.03	0.03	0.03	0.03	0.03	0.03	0.03	0.03
ZnO	0.41	0.31	0.25	0.20	0.16	0.14	0.13	0.13	0.12	0.12	0.12	0.12	0.12	0.12	0.12	0.11	0.11	0.11	0.11	0.11
ZrO2	3.66	3.87	4.00	3.91	3.88	4.05	4.00	4.10	3.91	3.91	4.10	4.12	4.21	4.15	3.99	3.93	3.78	3.98	3.83	3.67

Table 4.7. SBS Condensate Sample Cation Analyses By ICP-AES (Micrograms/liter)

Sample No.: No	7	19	33	46	60	74	87	102	115	130	141	154	175	185	198	211	225	237
Run Day :	2	3	4	5	6	7	8	9	10	11	12	13	14	15	16	17	18	19
Ag	-0.01	-0.01	-0.01	-0.01	0.09	0.03	0.27	0.09	0.06	0.08	0.42	0.94	-0.05	0.22	0.16	0.21	0.44	0.50
Al	3.57	9.55	14.57	17.06	22.16	26.86	39.37	39.83	41.01	45.75	48.28	55.50	50.56	47.48	43.46	37.35	36.91	41.78
B	41.24	110.74	191.92	241.2	331.8	435.60	664.20	722.40	755.00	856.30	907.10	1018.00	821.00	728.60	660.20	601.50	592.40	655.80
Ba	0.24	0.47	0.38	0.45	0.62	0.65	0.79	0.59	0.56	0.54	0.58	0.66	0.51	0.67	0.67	0.60	0.63	0.72
Bi	-0.12	-0.12	-0.12	0.15	0.17	0.26	0.38	0.37	-0.6	-0.6	-0.6	0.66	0.66	-0.6	-0.6	-0.6	-0.6	-0.6
Ca	35.22	40.66	40.92	36.9	37.52	37.32	45.48	39.83	37.00	37.27	36.18	38.25	44.08	35.20	27.79	21.40	18.56	17.41
Cd	1.62	5.81	10.93	15.05	21.72	30.30	51.65	58.80	62.61	70.16	73.25	80.89	66.44	60.66	55.96	50.53	48.44	54.79
Ce	0.11	0.81	1.60	2.04	2.81	3.64	5.58	5.74	6.07	6.71	7.14	8.04	7.43	6.89	6.22	5.39	5.06	5.78
Co	-0.02	-0.02	0.03	0.04	0.06	0.08	0.14	0.16	0.17	0.19	0.23	0.28	0.37	0.31	0.27	0.22	0.19	0.22
Cr	0.55	1.11	1.83	2.32	3.36	4.56	8.13	9.54	11.17	13.89	16.40	20.67	35.39	28.42	22.55	18.40	16.32	16.50
Cu	0.16	0.47	0.77	0.93	1.23	1.58	2.43	2.52	2.60	2.88	3.01	3.35	3.19	3.03	2.80	2.48	2.39	2.66
Dy	-0.01	-0.01	0.03	0.04	0.06	0.08	0.13	0.13	0.14	0.15	0.17	0.20	0.18	0.17	0.14	0.11	0.10	0.13
Eu	-0.01	0.01	0.03	0.03	0.05	0.06	0.09	0.10	0.10	0.11	0.12	0.14	0.13	0.12	0.11	0.09	0.09	0.10
Fe	0.49	3.20	14.48	22.18	34.3	46.92	86.70	92.88	101.20	121.30	139.60	180.00	225.60	195.70	167.60	138.50	132.20	147.20
La	0.46	1.54	2.52	3.09	4.07	5.07	7.48	7.55	7.72	8.53	8.80	9.81	8.61	8.00	7.38	6.42	6.11	6.81
Li	4.12	12.40	20.44	26.22	36.42	47.76	71.16	74.70	77.36	86.99	90.22	101.40	90.26	85.72	80.82	73.52	72.36	81.72
Mg	8.70	10.14	10.28	9.31	9.60	9.69	11.99	10.69	10.08	10.30	10.33	11.09	14.77	12.03	9.65	7.54	6.54	6.69
Mn	0.30	0.86	1.61	2.21	3.25	4.51	7.79	8.31	8.88	10.20	11.10	13.31	13.72	12.12	10.76	9.31	8.90	10.14
Mo	0.65	0.50	1.46	1.91	2.60	3.53	5.75	6.32	6.34	7.19	7.83	9.31	7.65	6.26	5.17	4.19	4.10	4.72
Na	98.78	139.18	166.78	173.62	205.8	240.00	338.52	333.66	336.10	360.80	373.80	412.40	344.40	309.30	273.20	236.20	220.50	246.30
Nd	1.21	4.97	8.75	11.08	15.05	19.36	29.38	30.21	31.34	35.01	36.39	40.79	36.56	34.55	32.44	28.42	27.25	30.63
Ni	0.32	0.81	1.58	2.24	3.44	4.86	9.13	10.38	11.73	14.45	17.11	23.50	39.60	32.10	25.82	21.05	19.13	20.04
P	11.04	10.48	6.71	6.39	6.51	7.20	12.21	10.27	12.49	12.08	15.96	17.19	14.37	12.03	12.48	10.35	10.16	10.38
Pb	-0.16	0.26	0.92	1.47	2.33	3.27	5.46	5.66	6.05	6.64	7.12	8.01	6.26	6.02	5.63	5.06	4.91	5.60
S	18.52	38.52	71.14	88.76	122.16	170.92	285.12	322.26	334.50	373.30	388.30	422.40	324.90	276.10	237.50	205.00	186.00	201.40
Si	22.86	57.44	95.86	113.14	134.18	151.92	186.36	185.46	184.40	190.60	200.20	212.10	144.30	145.70	146.50	137.70	139.90	158.70
Sn	-0.16	-0.16	-0.16	-0.16	-0.16	-0.16	-0.48	-0.48	-0.8	-0.8	-0.8	-0.8	-0.8	-0.8	-0.8	-0.8	-0.8	-0.8
Sr	0.24	0.40	0.52	0.58	0.71	0.86	1.25	1.25	1.27	1.40	1.43	1.58	1.45	1.35	1.25	1.08	1.03	1.14
Te	-0.12	0.17	0.39	0.54	0.89	1.36	2.94	3.50	3.42	3.82	4.51	5.90	3.89	3.36	2.93	2.52	2.72	3.26
Ti	-0.01	0.02	0.10	0.15	0.21	0.29	0.45	0.47	0.46	0.52	0.58	0.73	0.58	0.44	0.33	0.21	0.24	0.33
V	-0.02	-0.02	-0.02	-0.02	-0.02	0.02	-0.06	-0.06	-0.1	-0.1	-0.1	0.13	0.20	0.15	0.10	-0.1	-0.1	-0.1
Y	0.03	0.13	0.22	0.28	0.37	0.48	0.72	0.74	0.77	0.85	0.88	0.99	0.87	0.82	0.76	0.67	0.64	0.72
Zn	0.90	1.66	2.24	2.49	2.95	3.42	4.91	4.83	4.92	5.15	5.29	5.78	5.11	4.65	4.24	3.60	3.46	3.63
Zr	0.80	6.84	18.64	25.00	34.76	48.18	77.04	82.98	86.52	98.48	103.7	118.60	103.00	92.94	84.16	71.01	67.33	78.51
Totals =	252.18	459.25	687.66	806.86	1041.3	1310.6	1963	2072.2	2142	2381.64	2516	2822.6	2416	2151.1	1929	1700.6	1635	1814.3

Table 4.8. Feed Sample Anion Analyses by Ion Chromatography, (ppm)

Run Day	Sample No.	Chloride, Cl	Nitrite, NO_2	Nitrate, NO_3	Phosphate, PO_4	Sulphate, SO_4	Oxalate, $(COOH)_2$	Formate, (HCOO)
1	2b	505	991	19,500	801	845	1,050	31,900
2	9a	568	1,030	19,200	916	902	1,170	31,600
3	21a	560	1,030	19,700	895	929	1,200	32,000
4	35	550	1,000	20,600	NM	915	1,270	34,100
5	48	550	1,030	20,100	877	919	1,270	32,600
6	62	503	1,020	20,200	801	880	1,200	33,100
7	77	528	961	20,100	837	901	1,220	32,400
8	89	582	996	20,600	977	962	1,310	33,900
9	104	597	1,090	20,000	976	997	1,290	32,700
10	117	544	1,020	19,900	853	920	1,220	32,400
11	131	573	1,030	19,800	967	965	1,290	32,100
12	143	616	1,040	20,500	1,040	1,020	1,350	34,000
13	156	581	1,040	19,800	1,110	959	1,280	32,500
14	169	539	1,170	18,800	928	974	1,290	30,300
15	177	550	1,030	17,700	979	905	1,270	29,000
16	195	527	916	18,000	897	887	1,230	28,900
17	202	560	936	18,100	1,040	920	1,250	29,400
18	215	560	938	17,400	922	885	1,230	28,500
19	229	595	934	17,500	1,060	964	1,270	28,800
Average		557	1,011	19,300	938	929	1,240	31,600

Table 4.9. Comparison of Measured Anion Values in Feed Samples to Reference Values Prior to Formic Acid Reactions, (μg/g-oxide)

Anion	Chlorine	Nitrate	Phosphate	Sulfate	Oxalate
Reference	849	36,500	4,831	2,267	4,250
Avg. in Feed	1,642	57,000	2,762	2,737	3,670

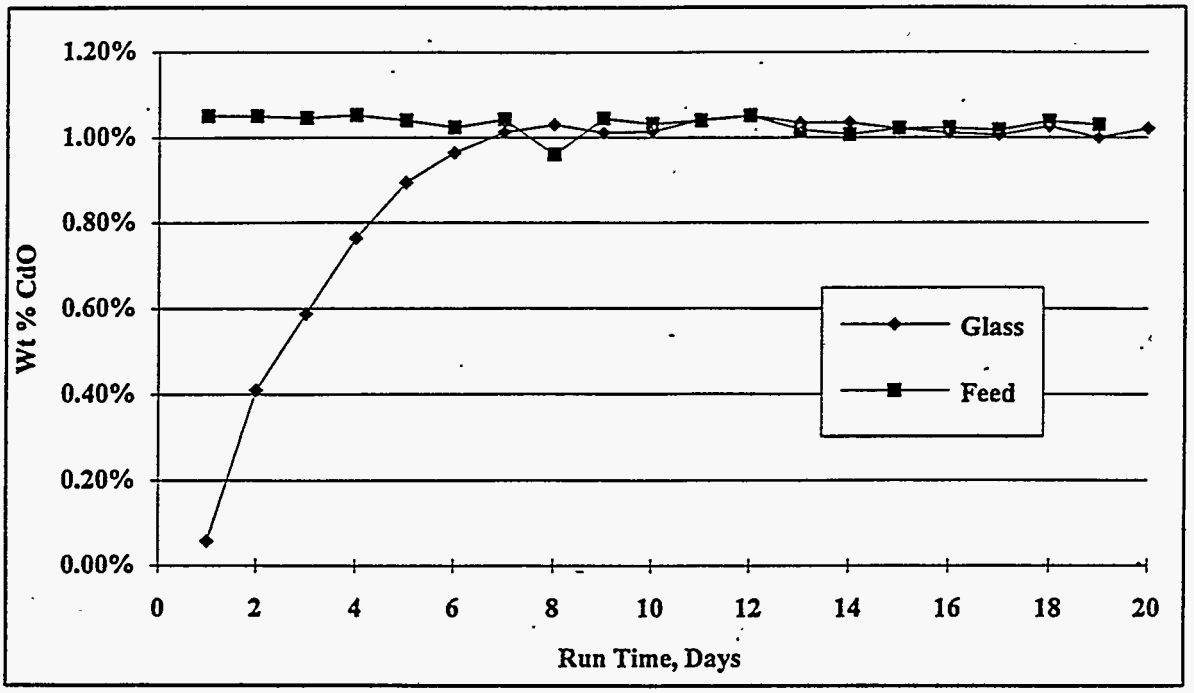

Figure 4.15. Approach of the LFCM to a Steady-State Composition Based on CdO Values

however, the relative concentration of zirconium was still low. The zirconium that was added to the slurry as a shim chemical was added as an oxide. Refractory-fired zirconium is extremely difficult to dissolve into the fusion. It is quite possible that some undissolved solids persisted after the fusion and were accounted for in the analyses. As a glass, however, the zirconium would be partly "fused" as part of the borosilicate glass matrix and more easily dissolved during the sample fusion. The sodium concentration was similarly low in the feed relative to the reference target value. The sodium concentration will be primarily dictated by the amount of sodium nitrite and nitrate added to the feed during SIPT operations.

Comparing the sodium level in the glass to the sodium level in the feed, the sodium in the feed is below the target while the sodium value in the glass is above the target. There is no explanation for the difference in sodium values relative to the target. Sodium analyses are sometimes more difficult on the ICP-AES because only one of the two samples can be analyzed, i.e., the KOH fusion sample. Also, fluctuations in ICP-AES plasma power can lead to more difficulty in separating out the sodium diffraction lines from interference lines.

The frit oxides all exceeded their target values with the exception of silica. The frit composition, as analyzed by the vendor and Hutson (1993), are shown in Table 4.11. When received from the supplier, American Porcelain and Enamel Co., their analyses reported that only the boron oxide concentration was outside the specification—19.6 wt.% versus the minimum allowable of 19.95 wt.%. Following consultation of the composition differences with P. R. Hrma, the frit was determined to be acceptable for our use. WSRC analysis showed silica to exceed the specification range. Also, based on which of their multiple analyses WSRC staff selected for each oxide, the total oxides exceeded 100%

Table 4.10. Comparison of Average Feed and Glass Analyses to the Reference

Oxide	Reference	Feed	Ratio Target/Feed	Glass	Ratio Target/Glass	Ratio Feed/Glass
Ag_2O	0.03	0.02	1.72	0.02	1.79	1.04
Al_2O_3	2.74	2.81	0.97	3.23	0.85	0.87
B_2O_3	14.03	11.74	1.19	12.45	1.13	0.94
BaO	0.05	0.06	0.84	0.09	0.57	0.68
Bi_2O_3	NA[a]	2E-03	NA	0.03	NA	0.06
CaO	0.24	0.30	0.79	0.34	0.71	0.90
CdO	0.98	1.03	0.95	1.02	0.96	1.01
CeO_2	0.18	0.17	1.06	0.19	0.94	0.89
Cl	0.08	0.16	0.50	NM	NA	NA
Co_2O_3	NA	0.01	NA	0.02	NA	0.80
Cr_2O_3	0.07	0.10	0.72	0.13	0.54	0.76
Cs_2O	0.17	0.15	1.13	0.14	1.21	1.07
CuO	0.07	0.08	0.89	0.09	0.82	0.93
Dy_2O_3	NA	0.01	NA	0.01	NA	0.72
Eu_2O_3	NA	5E-03	NA	0.01	NA	0.89
F	0.03	NM[b]	NA	NM	NA	NA
Fe_2O_3	8.16	8.33	0.98	8.45	0.97	0.99
GeO_2	4E-05	NM	NA	NM	NA	NA
K_2O	0.07	1.44	0.05	1.61	0.04	0.90
La_2O_3	0.19	0.22	0.87	0.24	0.79	0.90
Li_2O	5.00	4.68	1.07	4.75	1.05	0.98
MgO	0.11	0.26	0.42	0.31	0.36	0.84
MnO	0.64	0.69	0.93	0.70	0.92	0.99
MoO_3	0.16	0.18	0.90	0.19	0.86	0.96
Na_2O	7.60	6.30	1.21	8.34	0.91	0.76
Nb_2O_3	3E-03	NM	NA	NM	NA	NA
Nd_2O_3	1.00	1.00	1.00	1.06	0.94	0.95
NiO	0.66	0.66	1.00	0.66	1.01	1.00
P_2O_5	0.36	0.47	0.76	0.48	0.76	1.00
PbO	0.20	0.24	0.84	0.25	0.79	0.94
Pr_2O_3	0.04	NM	NA	NM	NA	NA
Rb_2O_3	0.02	NM	NA	NM	NA	NA
Sb_2O_3	2E-03	NM	NA	NM	NA	NA
SeO_2	0.01	NM	NA	NM	NA	NA
SiO_2	52.21	53.38	0.985	0.57	1.03	1.06
Sm_2O_3	0.02	NM	NA	NM	NA	NA
SnO	3E-03	NM	NA	NM	NA	NA
SO_3	0.19	0.28	0.69	0.26	0.72	1.05
SrO	0.03	0.04	0.78	0.04	0.75	0.96
Ta_2O_5	1E-03	NM	NA	NM	NA	NA
TeO_2	0.03	0.07	0.44	0.08	0.39	0.87
TiO_2	0.19	0.23	0.81	0.24	0.79	0.97
VO_2	NA	0.71	NA	0.01	NA	60.63
Y_2O_3	0.02	0.57	0.03	0.03	0.74	21.05
ZnO	0.10	0.63	0.16	0.12	0.84	5.31
ZrO_2	4.35	3.26	1.34	4.00	1.09	0.81

(a) Not Applicable
(b) Not Measured

Table 4.11. LFCM-8 Frit Composition, Wt.% Oxides

Oxide	Specified	Vendor's Analysis	WSRC Analysis	WSRC Corrected
SiO_2	72.26 ± 1.0	72.5	74.550	73.135
B_2O_3	20.45 ± 0.5	19.6	20.292	18.902
LiO_2	7.29 ± 0.5	7.13	7.619	6.972
Impurities	<2%	0.77	-2.461	0.991

by 2.461 wt.%. Following their normal procedures, WSRC applied correction factors to the ICP analyses, the results of which are shown in the last column of Table 4.11. Based on the corrected values, boron oxide is below the specification range, while silica oxide is within the specification. Of the three analyses, the "WSRC Corrected" value for boron oxide came closest to the values measured in the feed and glass samples.

Cesium Analyses. Cesium concentration was determined for selected feed and glass samples. Cesium concentration was determined by Atomic Absorption Spectroscopy (AA). The measured values are presented in Table 4.12. The average of the need analysis indicates the cesium oxide in the feed achieved 87% of the target value of 0.17 wt.%. The average feed value and the average of the last five glass samples (when the glass stream had reached a "steady-state" composition); agree to within 3%. As will be discussed in section 4.10, very little cesium was detected to have been lost to the off-gas stream. Based on an estimated DF of 128, less than 1% of the cesium in the melter feed entered the off-gas stream.

Glass Redox Analyses. A determination of ferrous oxide to total iron ratio was made for the daily glass samples. These are presented in Table 4.13. The lower limit of the analysis is on the order of 0.005. Therefore, based on the values obtained, reliable redox measurements were recorded after the third day of operation. It is interesting to note that between run days number 13 and 14, ten days of idling occurred. However, there is no indication of significant change in glass redox state. It could be concluded, therefore, that there is little convection in the glass during idling that would allow the glass tank to come to equilibrium with the plenum space.

Cold Cap Sample Analyses. Cold cap samples were retrieved from the LFCM at two different periods of the campaign. Cold cap material was extracted from the melter when the glass thermowell was replaced on April 24 and at the conclusion of the campaign on May 16. The samples were subsequently analyzed by optical microscopy and chemical analysis. The analyses are reported in detail by Kim and Hrma (1993).[a] Only a summary of the analyses is presented in this report.

(a) Kim, D. and P. R. Hrma. 1993. *PNL HWVP Technology Development Project Melting Rate Test Approach.* Internal HWVP Letter Report: PHTD-C93-03.01G, Pacific Northwest Laboratory, Richland, Washington.

Table 4.12. Results of Cesium Oxide Analyses by Atomic Absorption Spectroscopy

Feed Spl No.	Target	2b	35	77	117	156	195	229
Run Day No.		1	4	7	10	13	16	19
Wt.% Cs_2O	0.17	0.137	0.149	0.146	0.141	0.154	0.150	0.160
Glass Spl No.	1	38	79	121	148	171	205	227
Run Day No.	1	4	7	10	12	14	17	19
Wt.% Cs_2O	0.027	0.094	0.114	0.135	0.133	0.152	0.149	0.150

Table 4.13. Results of Ferrous-to-Total-Iron Determination of the Glass

Sample No.	Run Day No.	Ferrous: Total Iron
1	1	0.002
11	2	0.001
23	3	0.002
38	4	0.012
52	5	0.012
66	6	0.015
79	7	0.02
93	8	0.027
107	9	0.017
121	10	0.014
135	11	0.012
148	12	0.013
165	13	0.033
171	14	0.033
180	15	0.019
192	16	0.031
205	17	0.029
220	18	0.029
227	19	0.029
245	20	0.027

Two distinct types of cold cap samples were obtained from the melter. When the failed thermowell was extracted from the melter, a porous pumice-like material (LFCM-8 samples #160 and #161) was adhered to it. At the end of the campaign a more representative cold cap sample, containing unreacted feed, partly-reacted feed, and glassy phase (LFCM-8 sample #166) was obtained. In contrast, the pumice material consisted of porous dried feed without any noticeable unreacted feed material.

Optical Microscopy Results. Thin sections were prepared from Sample #166, mounted in a polymer resin and observed with an optical microscope under reflected and transmitted light. This cold cap sample was deformed during retrieval from the melter and did not retain the original geometry of the cold cap in the melter. The boundary between the cold cap and molten glass appeared to be reasonably well preserved only in a small portion of the sample. The thickness of the cold cap was approximately 1.1 cm. This cold cap would have been thicker in the melter than observed in the sample because it is likely that the upper part of the cold cap, which consisted mainly of unreacted dry feeds, was very loose and, thus, was lost during sample retrieval and thin section preparation.

In the upper zone of the cold cap the frit particles were observed to be dispersed throughout the continuous phase of waste components. From the relatively homogeneous microstructure of this zone, it seemed that no significant reaction took place in the feeds in the upper zone of the cold cap. Sharp edges of the frit particles were also observed to be present. This was unexpected because most of the frit particles were expected to have dissolved to some degree during the time it was suspended in the feed slurry. As the feed progressed down into the cold cap, frit particles were distributed similarly to frit in the upper zone of the cold cap, but the particles were closer to each other. Also, most of the sharp edges observed disappeared. The distinction between frit particles and the waste region was not as clear as in the upper zone.

In the lower zone of the cold cap the original frit particles and glassy phase formed by the reactions were no longer distinguishable. The glassy phase appeared interconnected to form a larger continuous phase. It is not clear whether this was a result of sintering of frit particles or borate glass formed from the reactions. However, most isolated frit particles were separated by thin layers of undissolved particle clusters. At the glass interface the boundary area between cold cap and molten glass was dominated by bubbles. Large bubbles mixed with small bubbles occupied most of the cold cap part, and the glass phase and unreacted particle clusters were confined to films separating bubbles. In the glass side, the reflected light micrograph showed continuous phase with a few small bubbles. The transmitted light micrograph delineated the cluster of the undissolved waste components in a horizontal streak, which suggested the melt flowed in this direction. Surprisingly, the transition from the cold cap to the glass was abrupt. From these observations, it seems that the cold cap did not smoothly transform to glass. Rather, a part of the cold cap at the bottom—which consisted of glass, undissolved particle clusters, and bubbles—periodically detached from the cold cap and was swept away by the melt flow while the bubbles rose to the cold cap-glass boundary.

The cold cap micrographs were compared with those from gradient furnace (GF) heat-treated samples for an hour for feeds with fiscal year 1991 (FY 1991) frit. Furnace samples melted at 620°C were found to be similar to the lower zone of the LFCM-8 cold cap. An exception was that the GF samples had a more interconnected glass phase. GF feed samples melted at 650°C were also similar but showed a larger continuous glass area.

Chemical Analysis. One of the proposed phenomena that could account for the lower melting rate of the feed with FY 1991 frit was demixing of the slurry. The lithia borate content of the FY 1991 frit could be leached into the solution. As the solution dried in the melter, the salt content could be segregated from the refractory material in the cold cap. This refractory material, composed of silica-rich frit particles and dried refractory waste components, could result in poor melting behavior. Chemical analyses of porous "pumice" material (Samples #160 and #161) were performed to see if it was depleted of Li and B. The sample of "pumice" material used in this study was attached to the thermocouple well and may not be representative of either the slurry feed above the cold cap or the material at

the upper part of the cold cap. A lump of cold cap sample containing unreacted feed, partly reacted feed, and glassy phase (Sample #166) was also analyzed for comparison. During sample preparation from #166, an attempt was made to take the material mainly from the cold cap region at the cold cap-glass boundary area, although it was not possible to entirely eliminate material from other parts of the cold cap and glass phase attached to the cold cap. The results from ICP and flame AA analyses of these cold cap samples are shown in Table 4.14. Table 4.14 also includes the ICP analysis results of LFCM-8 slurry feed before melting for comparison.

The detection limits of some minor elements from the different fusion methods used for the ICP analyses of the slurry sample and the cold cap samples were slightly different. The as-analyzed elemental concentrations are shown in Table 4.14(A), and the concentrations normalized to the subtotal of the elements that were detected in both slurry feed sample and cold cap samples are in Table 4.14(B). The balance of the elemental compositions in Table 4.14(A) would consist mainly of oxygen in the cold cap samples, and oxygen, water, and anions (nitrate, formate, etc.) in the slurry feed. The very similar results were obtained from two different fusion methods (methods 1 and 2; see Table 4.14) for the slurry feed, and also from Samples #160 and #161, which indicate good reproducibility of these analyses. For the four major elements of the feed, the differences between Sample #166 and the average of Samples #160 and #161 are summarized in Table 4.15. The ratio of the sum of B, Li, and Na concentrations to Si concentration is also included. Table 4.15 shows that the concentration of the slurry feed was very similar to that of cold cap Samples #160 and #161 within analytical error. When Sample #166 was compared with Samples #160 and #161, it had lower B, Li, and Na but higher Si concentrations. These results may suggest that demixing occurred in the lower part of cold cap. The possibility of demixing in the upper part of the cold cap or in the slurry feed above the cold cap was neither confirmed nor disproved. The fractional difference between the average concentration from Samples #160 and #161 and the concentration of Sample #166 in Table 4.15 indicates that the key component responsible for demixing was Na. It must be noted that Na was present as a waste component in the feed while B, Li, and Si were the frit components (e.g., 98 wt.% of SiO2 in the feed was from the frit). These frit components did not show a significant level of demixing. This indicates that demixing occurs mainly within waste components and that the effect of frit composition on demixing is minor.

4.3 Feed Flow Control and Feed Nozzle Performance

The prototypic feed nozzle (see Figure 3.7) and feed line described in Section 3.3.1 were used during LFCM-8. Data taken to assess the performance of the nozzle and SIPT feed system control were:

- feed nozzle cooling water flow rate
- feed nozzle cooling water exit temperature
- cooling water header temperature
- feed line pressure
- inspection of the feed nozzle after testing had been concluded.

Table 4.14. Chemical Analysis Results of LFCM-8 Feeds and Cold Cap Samples

(A) Element Composition						(B) Normalized Element Composition*					
	Slurry Feed		Cold Cap Sample				Slurry Feed		Cold Cap Sample		
(wt.%)	Method 1	Method 2	#160	#161	#166	(wt.%)	Method 1	Method 2	#160	#161	#166
Ag	0.01	0.02				Ag					
Al	0.51	0.48	1.38	1.41	1.49	Al	2.96	2.78	2.77	2.75	2.91
B	1.78	1.85	5.05	5.21	4.82	B	10.32	10.72	10.12	10.18	9.40
Ba	0.02	0.02	0.05	0.06	0.05	Ba	0.12	0.12	0.11	0.11	0.11
Ca	0.12	0.16	0.25	0.27	0.26	Ca	0.70	0.93	0.49	0.54	0.51
Cd	0.32	0.30	1.19	1.19	1.22	Cd	1.86	1.74	2.39	2.32	2.38
Ce			0.17	0.17	0.17	Ce					
Co	0.00	0.00				Co					
Cr	0.02	0.02	0.05	0.05	0.05	Cr	0.12	0.12	0.10	0.10	0.11
Cs			0.18	0.18	0.17	Cs					
Cu	0.02	0.02				Cu					
Fe	1.95	1.83	5.94	6.24	6.01	Fe	11.31	10.60	11.91	12.19	11.72
K	0.00	0.00				K					
La			0.19	0.20	0.19	La					
Li	0.91	1.06	2.69	2.60	2.37	Li	5.28	6.14	5.39	5.08	4.62
Mg	0.03	0.03	0.05	0.05	0.06	Mg	0.17	0.17	0.11	0.11	0.12
Mn	0.15	0.14	0.38	0.40	0.40	Mn	0.87	0.81	0.76	0.78	0.77
Mo	0.04	0.04				Mo					
Na	1.93	1.93	5.78	6.00	4.52	Na	11.19	11.18	11.59	11.72	8.82
Nd			0.97	1.02	0.97	Nd					
Ni	0.17	0.17	0.48	0.52	0.50	Ni	0.99	0.98	0.97	1.01	0.98
P	0.06	0.06				P					
Pb	0.06	0.06	0.18	0.20	0.19	Pb	0.35	0.35	0.36	0.38	0.36
Si	8.27	8.21	23.40	23.90	26.30	Si	47.97	47.57	46.91	46.68	51.30
Sr	0.01	0.01				Sr					
Ti	0.05	0.04				Ti					
Zn	0.03	0.03				Zn					
Zr	1.00	1.00	3.01	3.11	3.02	Zr	5.80	5.79	6.03	6.07	5.89
Total	17.46	17.48	51.39	52.76	52.77	Total	100.00	100.00	100.00	100.00	100.00
Subtotal*	17.24	17.26	49.89	51.20	51.27						

* Normalized to the subtotal of the elements that were detected in both slurry feed sample and cold cap samples.

Table 4.15. Comparison of Concentrations of Four Major Components in Table 4.14

Element (ratio)	Average in Slurry feed (wt.%)	Average from #160 and #161 (wt.%)	Average from #166 (wt.%)	Fractional Difference[a] (%)
B	10.52	10.15	9.40	-7.4
Li	5.71	5.24	4.62	-11.7
Na	11.19	11.65	8.82	-24.3
Si	47.77	46.79	51.30	+9.6
(B+Li+Na)/Si	0.574	0.578	0.445	-22.9

(a) The fractional difference (ΔC or Δr) between the average concentration or ratio from Samples #160 and #161 (C1 or r1) and the concentration or ratio of Sample #166 (C2 or r2) is defined as $\Delta C = 100*(C2 - C/C1$ or $\Delta r = 100*(r2-r1)$.

The test plan stated that the water cooling rates were to be limited between 2 to 4 gpm (8 to 15 Lpm) and/or cooling water temperature differential of 2 to 10°C. Because of feed nozzle cooling water discharge line limitations, the maximum cooling rate achieved was 2.8 gpm (10.6 Lpm). Since the cooling water temperature differential did not exceed 10°C until the water cooling rate was lowered to 1.9 gpm, the following water cooling rates were evaluated: 2.8, 1.9, 1.5, and 1 gpm, equivalent to 10.6, 7.2, 5.7, 3.8, and 1.9 Lpm (see Figure 4.16).

There were 8 flushing sequences during the span of the testing. One occurred during the first 2.8 gpm feed nozzle cooling water period, two during the 1.9 gpm feed nozzle cooling water period, two during the 1.5 gpm feed nozzle cooling water period, none during the 1 gpm feed nozzle cooling water period, and three during the final 1.9 gpm feed nozzle cooling water period. There is no reason to conclude that the frequency of feed nozzle flushing was related to the reduction/increase in feed nozzle cooling water flow rate within the ranges evaluated. Feed line flushing was initiated whenever the feed rate to the melter appeared to be dropping. Water flushes were performed by direction 0.5 gpm water into the feed line for one minute. The 3-way valve was then switched to direct 0.5 gpm of water back through the strainer for one minute. The flushes resulted in about 7 line volumes of flush water through the feed line at 3.4 ft./sec. The backflushes through the strainer resulted in about 22 line volumes of flush water at a velocity of 1 ft./sec. During LFCM-8B, feed was transferred to Tank 60 via Tank HB-13, and a small diaphragm pump was used to meter feed to the melter. It is not unusual to experience a high number of line pluggages when a new system is first started. It is during the first days that small stones, foreign objects, and bits of dried feed are "screened" from the system.

The change in cooling water exit temperature is shown in Figure 4.16. Inlet temperature was constant at 4°C. The maximum exit temperature was 27°C and occurred when a 1 gpm cooling water rate was tested. This resulted in a maximum temperature differential between inlet and outlet conditions of 13°C. There was no observable change in slurry behavior as it entered the LFCM.

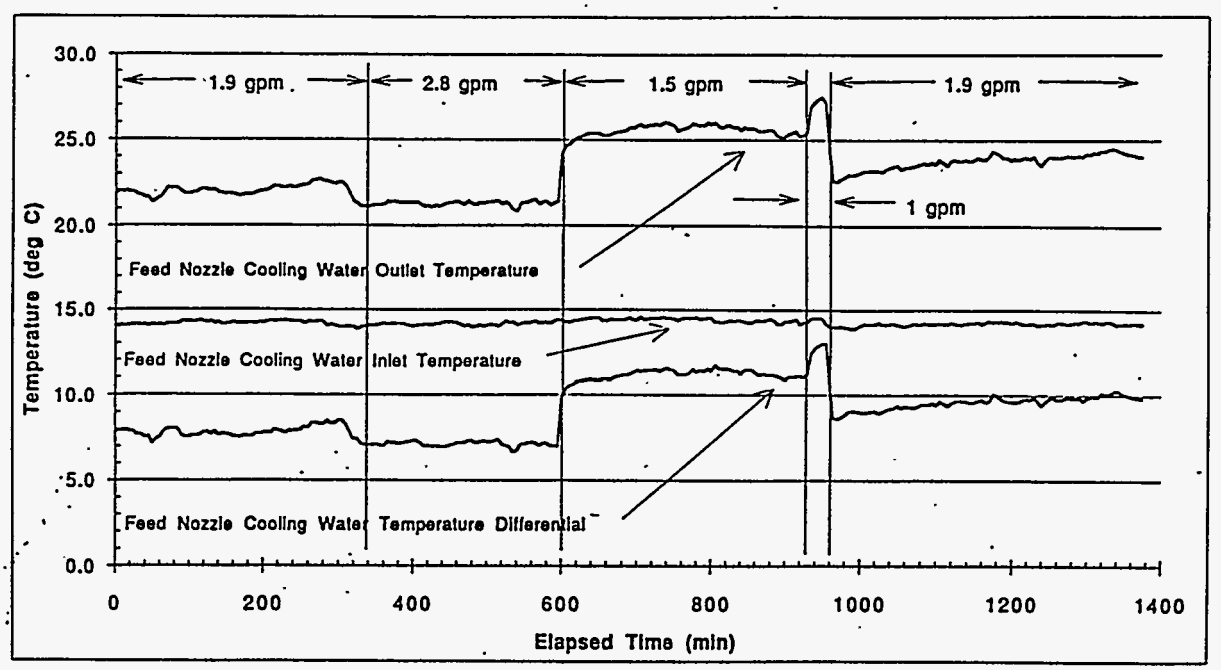

Figure 4.16. Feed Nozzle Cooling Water Temperature Versus Water Rate

During both segments of LFCM-8, feed material accumulated on the exposed surface of the feed nozzle. This buildup caused bridging between the feed nozzle and the cold cap on at least one occasion. Attempts were made to break the bridge with extended flushing and by lowering the glass level. It is possible that the bridging action could have prevented the flow of feed to the melter or caused a pressurization of the melt cavity if the buildup were allowed to continue. When the feed nozzle was pulled from the melter, it was noted that the heat from the plenum heaters had vitrified the surface of the buildup on the feed nozzle (see Figure 4.17). The glazing, coupled with the hot external surface of the feed nozzle, prevented the buildup from sloughing off.

The effect of feed rate on feed line pressure was also measured during LFCM-8. Figures 4.18 and 4.19 display the feed rate and line pressure readings. The 3-way valve back-pressure measurement was taken between the in-line strainer and the 3-way valve. The feed nozzle back pressure measurement is taken immediately after the flow meter (see Figure 3.6). Data was reviewed at the maximum feed rate attained, 80 L/h, and during a period of low feed rates, 45 L/h. The change in feed nozzle pressure, in response to an increase in feed rate, was 20 in. WC. There was little or no change in the pressure transducer reading immediately after the 3-way valve.

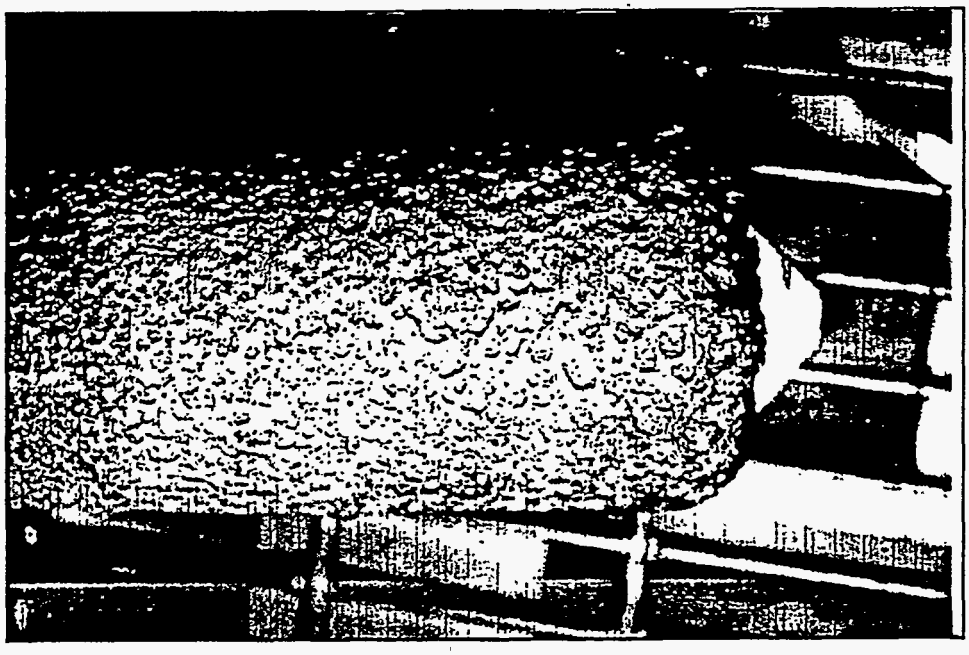

Figure 4.17. Feed Nozzle and Heavy Deposits of Feed Material Adhered to Outer Surface

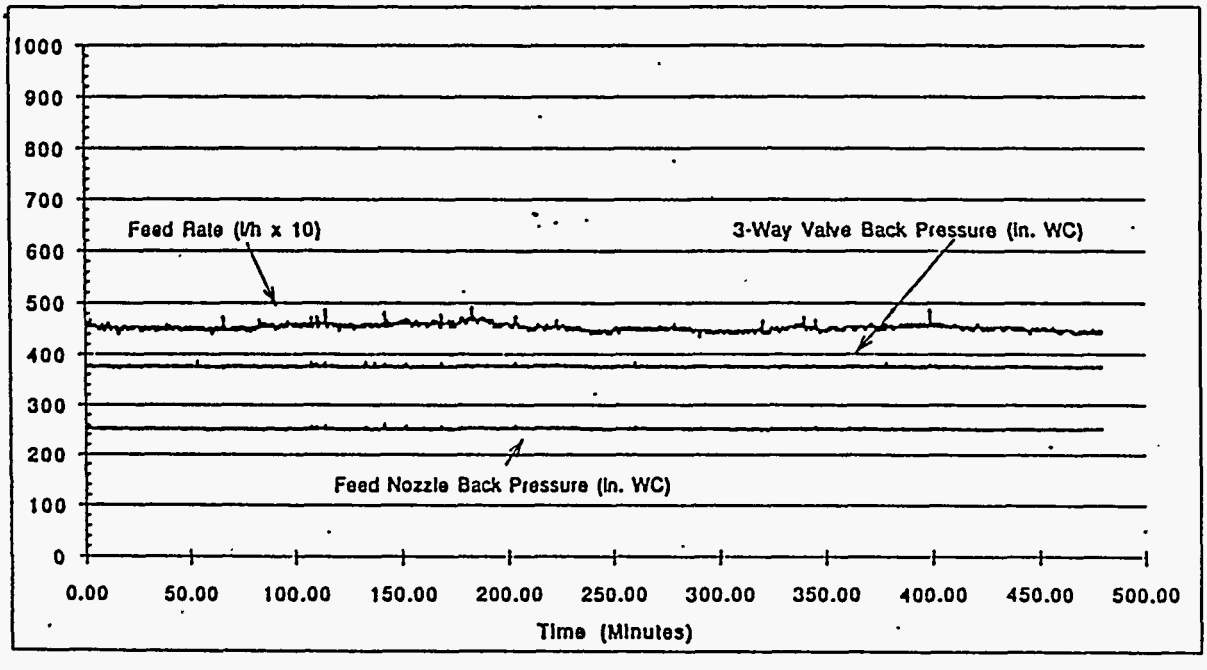

Figure 4.18. Feed Line Pressure At 45 L/h Slurry Feed Rate

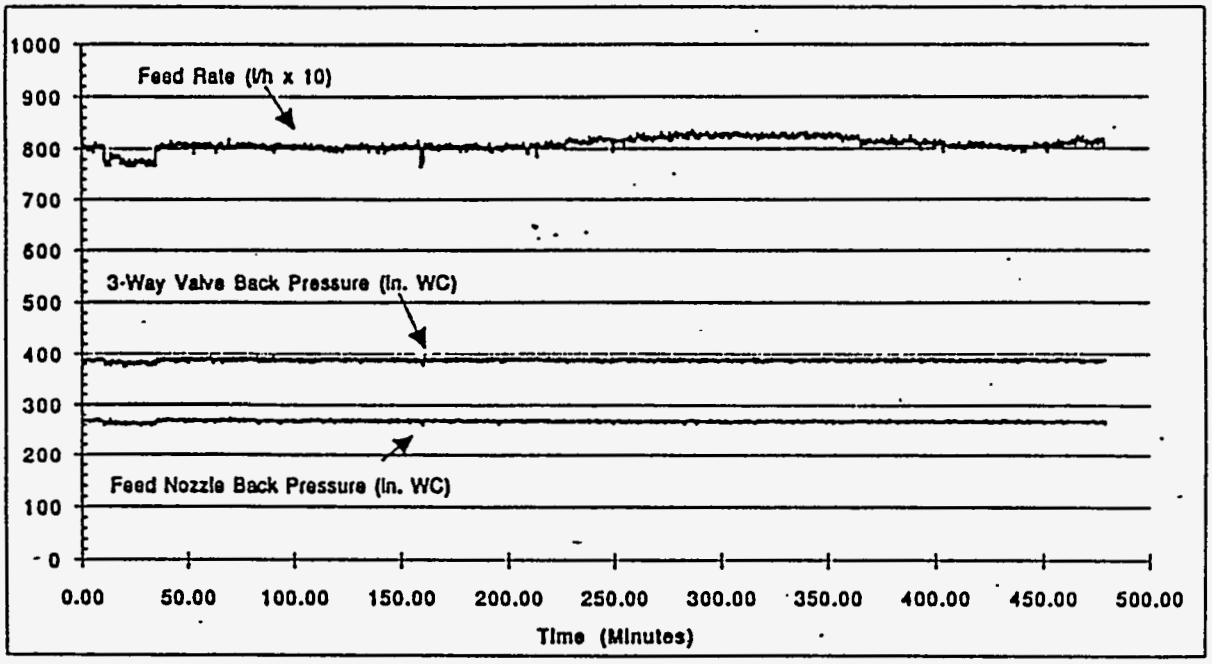

Figure 4.19. Feed Line Pressure At 80 L/h Slurry Feed Rate

4.4 DWPF Canister Throat Protector/Sampler Performance

The prototypic DWPF throat protector and glass sampler was installed 39 in. from the discharge trough pour tip. This distance is identical to the plant melter design. The device is shown in Figure 4.20. Testing was intended to determine the effects of fill time, overflow temperature, and glass pour rate on sampler performance. The data obtained would be used to recommend the optimum operating parameters for plant operation. The effect of the sampler on the glass pour stream was also to be observed to identify any undesirable effects, such as glass stringing or the glass stream being deflected onto the throat protector. In plant operation, the sample cup would be pushed into the glass stream by an operator using a manipulator. After a prescribed period, the cup would be retracted back into the throat protector. The sampler cup is constructed of stainless steel. It was expected that after repetitive use, exposure to the 1150°C glass would ultimately lead to the glass bonding to the cup. Four tests were completed before glass bonding required the cessation of testing. The results of the test are compiled in Table 4.16.

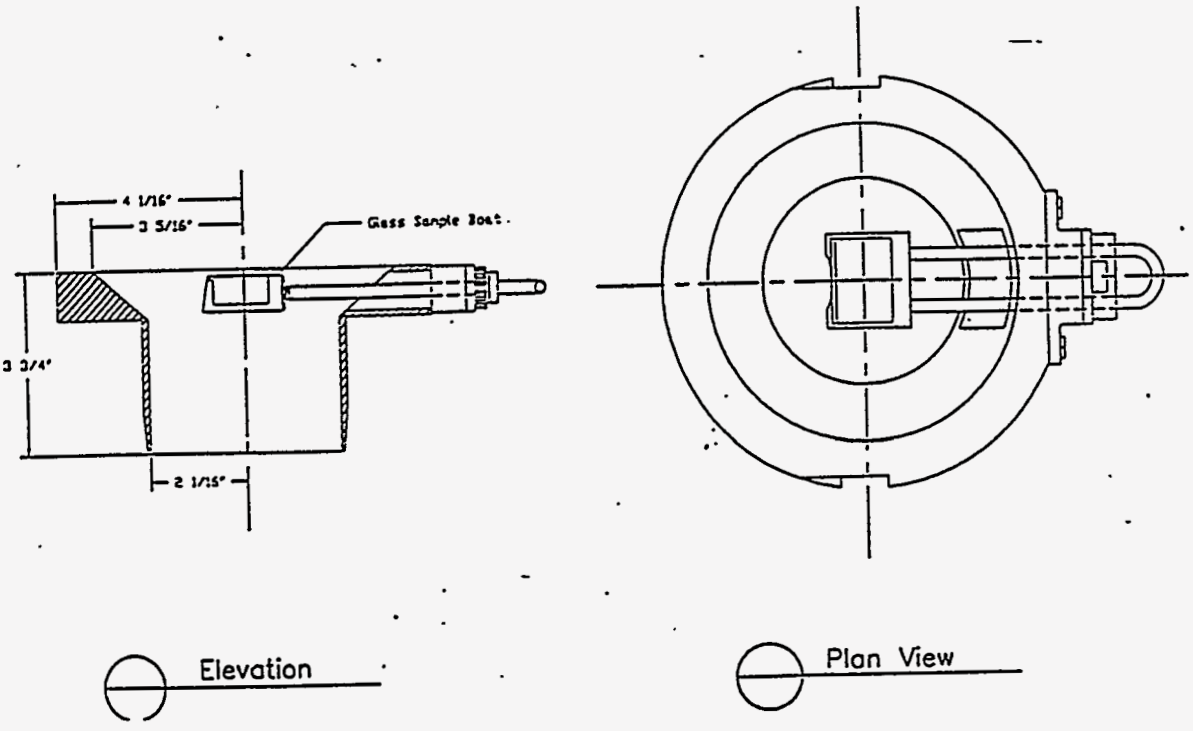

Figure 4.20. DWPF/HWVP Prototypic Glass Sampler

Table 4.16. DWPF Glass Sampler Test Results

Test No.	Overflow Temp., °C	Glass Pour Rate, kg/h	Cup Fill Time, sec.	Overflow Time, sec.	Sample Cup Percent Filled
1	1,088	93 to 107	1.5	0	50 to 75
2	1,088	93 to 107	3	0	75
3	1,088	100 to 110	5	5	100
4	1,125	100 to 120	2	2	100

The glass pour rate was adjusted to achieve a rate as close to the reference rate of 100 kg/h as was possible with the LFCM system. Based on canister weigh scale observations, glass pour rates of 90 to 120 kg/h were achieved. Fill time was varied to test the sampler when the cup was not completely filled and also when it was allowed to fill completely and overflow. Allowing the cup to remain in the glass stream for a protracted time is not considered necessary for obtaining a representative sample. However, it might occur if the operator has difficulty retracting the cup. Also, in the event that the cup becomes stuck under the stream, it is important to determine that the canister-filling operation will not be compromised while corrective actions are being initiated. For the first three tests, the melter discharge section temperature was held at 1088°C. The final test was conducted with the discharge section temperature raised to 1125°C. This was done because the glass did not completely

drain from the cup on the previous test. Increasing the discharge section temperature would slow the cooling rate of the glass. This would help maintain a higher glass viscosity and better draining properties.

With fill times of 1.5 and 3 seconds, the first two tests resulted in partially filled cups that could be pulled back into the throat protector. Glass pour stream deflection was minimal, which meant that the glass pour stream did not contact the throat protector. The short fill time prevented the cup from becoming very hot. That is, the glass sample cooled quickly and did not bond to the cup surfaces. The third and fourth tests were performed by allowing the glass to overflow the cup. In the third test, the cup was filled after 5 seconds and glass was then allowed to overflow the cup for 5 seconds. When removed from the glass stream the cup was moved about mid-distance between the pour stream and the flange. This was done to allow any glass still dripping from the cup to do so before the cup was pulled into the flange.

Overfilling the cup resulted in the cup becoming very hot, and the glass adhered to the cup. It was possible, once the sample cup was removed from the assembly, to physically remove essentially all of the glass sample from the cup. When the glass overflowed from the cup, it formed a single pour stream in the side of the weir that was cut into the side of the cup. When the cup was pulled out of the pour stream, the glass in the cup cooled quickly enough that the glass level did not recede to the weir level. It is estimated that the glass remained 1/8 to 1/16 in. above the wall of the cup. This prevented the cup from being retracted completely into the throat protector flange as designed. Test four results were very similar to the third test, the exception being that the glass could not be removed from the cup. No significant impact was observed when the discharge section was operated at the elevated temperature.

The following conclusions can be drawn from the sampler tests. The insertion of the cup into the pour stream caused very little deflection of the glass stream at prototypic pouring rates. When filled to overflowing, the pour stream entering the canister was stable and formed a single stream. Therefore, canister filling should not be compromised should the cup become stuck during the sampling operation. Retraction of the cup into the flange after sampling is important to remove it as a possible obstruction should the pour stream become unstable for any reason. When filled to overflowing, the cup can not be retracted back into the flange. Glass does not completely drain down to the weir level in the cup. Redesign of the flange and cup to allow greater clearance between the flange and cup top is necessary to assure that the cup can be retracted properly. The sample cup is affixed to two stainless steel rods that extend through the flange. Difficulty was experienced in smoothly sliding the cup back and forth. A certain amount of side-to-side action was required to move the cup. It is expected that an operator using a manipulator will have similar or greater difficulty in assuring that even pressure is applied to both rods. It is recommended that consideration be given to either using a fixed hydraulic push arm that can be attached to the sampler rod assembly or replacing the twin rods with a single rod. The single rod can be designed to include flat edges along the sides to assure that the horizontal orientation of the cup is maintained.

4.5 Differential Pressure Glass Pour Control System Performance

The LFCM was rebuilt in FY 1990 to allow differential pressure glass pouring to be performed. The LFCM arrangement is shown in Figure 3.12. Glass was transferred into the receiving canister by drawing the overflow pressure down relative to the melter pressure. The negative pressure was provided by a line connecting the LFCM overflow to the SBS. To provide for some scrubbing of the gas from the overflow, the line in the SBS was submerged in the condensate. Submergences of between 10 and 15 inches were planned. However, due to SBS operation at the lower overflow point and a wrong measurement during fabrication of the submergence line, the actual submergence varied between 4 and 8 inches.

Glass was discharged into the West Valley Demonstration Project (WVDP) canisters using both batch pour and continuous pour methods. To initiate a pour, the ball valve isolating the SBS from the overflow was opened. This was followed by initiating control air into the vent line by way of a rotometer. The differential pressure between the melter and the discharge section was adjusted to between 5 in. and 15 in. WC. This was sufficient to initiate glass pouring. Glass pouring would begin within 15 to 60 seconds of initiating the pour. The pour stream became fully developed within 5 to 10 seconds and remained steady. The lack of pour stream movement indicated that there was little or no air inleakage into the discharge section or pour pipe. An uncalibrated magnahelic gauge indicated the differential pressure between the melter and discharge section (i.e., Category 3 indication only calibration). The dynamic action of the SBS pressure resulted in a movement of the indicated pressure of between ± 3 in. WC. However, there was no observed instability in the glass stream. Control air flow into the vacuum line was indicated by a standard rotameter (i.e., Category 3 indication only calibration). During batch pouring operations the amount of control air ranged between 500 scfh and 200 scfh based on rotameter readings. During continuous pouring operations the control air rate was approximately 200 scfh. Batch pour glass pour rates varied throughout the campaign. The target rate was 250 kg/h; however, rates typically ranged between 160 kg/h and 180 kg/h. During continuous pouring operations, glass production rates were approximately 20 to 40 kg/h. At the end of a filling operation, the transfer was terminated by turning off the control air followed by closing the ball valve that isolated the SBS from the overflow. Within minutes the pour stream stopped, followed by several minutes of glass dripping into the canister.

4.6 Off-Gas Line Deposits

Fluor Detailed Design Data Need 3.9a identified the requirement to quantify the amount of cadmium depositing in the off-gas line between the LFCM and the SBS. The issue of cadmium volatility was raised due to the limited data on cadmium volatility in HLW vitrification. A summary of the evaluation is provided here. Complete details are reported in Perez et al. (1993).

Before the start of LFCM-8, the off-gas line sections were removed and inspected. Any pre-existing deposits were removed from the lines prior to reinstallation of the lines. The off-gas line between the LFCM and SBS is shown in Figure 4.21. The line between the film cooler spool piece and SBS is 4-in., 304-Schedule 40 stainless steel. The pipe has a length of 28.6 ft. and a cross-section area of 0.0884 ft^2. Following the LFCM-8 campaign, the lines were again removed and solid deposits were sampled and the quantity of deposits estimated. The extent of solids deposits was visually assessed, and samples of deposits were obtained from the flange joint areas of the off-gas line jumper (see

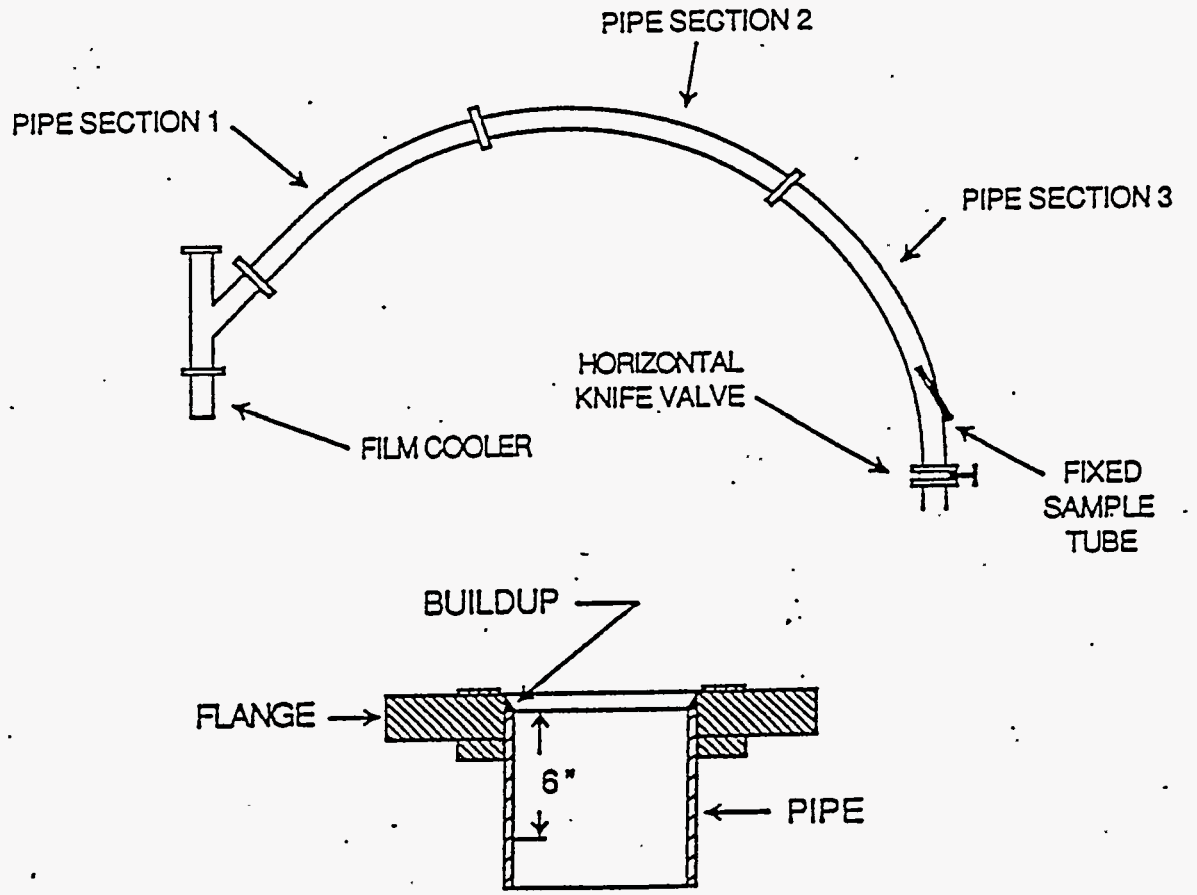

Figure 4.21. Off-Gas Line Jumper and Sample Locations

Figure 4.21). Data analyzed as part of this work included chemical analysis of feed, glass, line deposits, in-line off-gas stream, and SBS condensate samples. Process data included melter feeding and glass production rates, off-gas flow rate, and plenum and off-gas stream temperatures.

The off-gas line deposits were very minimal. At the entrance to the off-gas line jumper it was estimated that a 0.04-in.-thick deposit coated the inside pipe surface. Approximately six feet past this point, at the next flanged joint, the thickness was less than 0.04 but could not be quantified. Twelve feet past the entrance, the deposits were too small to sample; i.e., only a very thin coating or film existed. Cadmium concentrations in the line samples varied approximately 15% to 80% above its value in the feed on an oxide basis. This was also the case for most of the other minor feed constituents. Therefore, there does not appear to be any preferential accumulation of cadmium oxide in the off-gas line. Assuming that the deposits decrease linearly down the first twelve feet of line, from 0.04 in. to zero, a volume of 0.02 $ft.^3$ of deposits would exist. With a roughly measured density of solids samples of approximately 70 $lb./ft.^3$, a quantity of solids weighing 1.4 lb. could have accumulated in the off-gas line during LFCM-8.

Two off-gas stream samples were taken during LFCM-8 on 4/29/93 and 5/12/93. Cadmium concentrations of 1.31 and 1.08 μgr per standard liter per hour, respectively, were measured. Process and feed data necessary to calculate a cadmium mass balance, and the resulting values, are given in Table 4.17. The rate of release from the melter, as indicated by the decontamination factor of about 350, is similar to those that have been established for the semivolatiles for sodium and potassium (Goles et al. 1990). Based on these measurements and analyses of the off-gas line deposits, cadmium accumulation should not be expected to pose a unique problem. Based on the process and analytical data it was also possible to calculate the fraction of CdO in the off-gas stream that deposited in the off-gas line. It was estimated that 1.4 lb. of solids accumulated in the line.

The average concentration of CdO in the off-gas line deposits was 1.42 wt.%. This gives a mass quantity of 0.02 lb. CdO (9 gr) in the line. From Table 4.17, cadmium emission rates from the melter of 0.736 g/hr and 0.554 g/hr were measured during LFCM-8A and LFCM-8B, respectively. Run lengths were 286 hr and 147 hr, respectively. From this data an estimated 292 g of cadmium (334 g CdO) escaped the LFCM in the off-gas stream. The fraction of CdO exiting the LFCM that deposited in the off-gas line is, therefore, (9 gr/334 gr) x 100% = 2.7%.

4.7 WVDP Off-Gas Line Cleaner Performance

The WVNS off-gas line cleaner (OLC) shown in Figure 4.22 was installed and operated during LFCM-8. The objective of the testing was to obtain relevant operational experience with the device during an actual vitrification operation. Testing results and post-test inspections are summarized below. Complete details are provided in the technical letter report prepared and transmitted to WVNS under the PNL West Valley Support Program (Buchmiller et al. 1993).

Table 4.17. Estimate of Cadmium Loss to Melter Off Gas

Variable	April 29, 1993	May 12, 1993
Average Feed Rate	56.7 L/h	59.1 L/h
Slurry Oxide Loading	469 g/L	395 g/L
CdO Concentration in Feed	0.0102 g CdO/ g-oxide	0.0102 g CdO/ g-oxide
Off-Gas Flow Rate	9,431 slpm	8,553 slpm
Cd Concentration in Off Gas	1.31 μg/slphr	1.08 μg/slphr
Calculated g Cd Processed/hr	237.4 g Cd/hr	208.4 g Cd/hr
Calculated g Cd in Off Gas/hr	0.736 g Cd/hr	0.554 g Cd/hr
Calculated Decon. Factor (DF)	323	376

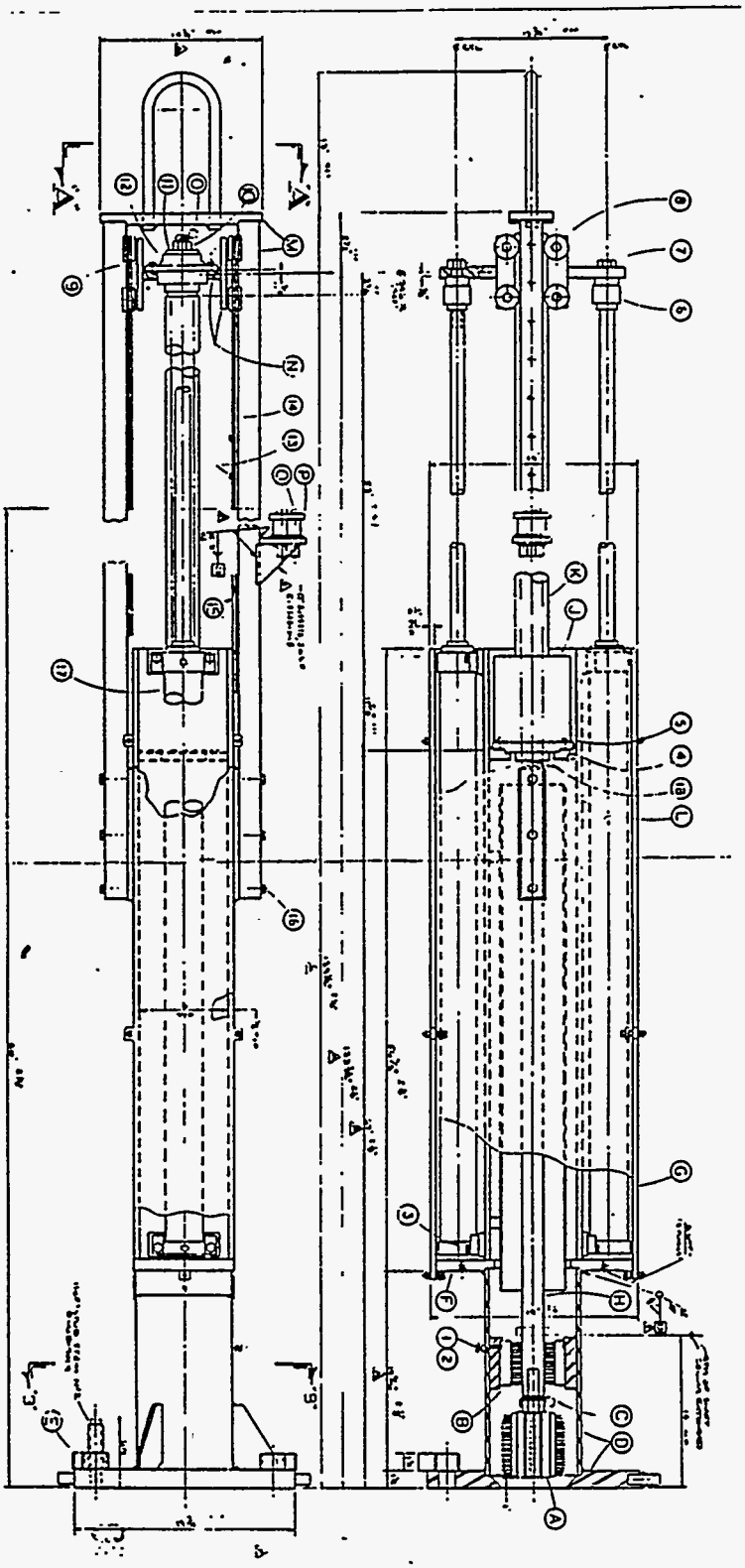

Figure 4.22. West Valley Nuclear Services Off-Gas Line Cleaner

LFCM-8 Operation. The OLC is a pneumatically driven clearing device that rotates an Inconel-690® brush down into the film cooler and off-gas jumper. Where air is applied for the down stroke, the threaded shaft is rotated through a roll nut. This rotates the brush through its full range of vertical travel. To retrack the brush air is applied to the opposite side of the cylinders. During LFCM-8A the OLC was operated every hour for a total of 281 cycles. No operational problems were experienced during this time. In most instances, the roll nut shaft would travel the full length just by the turning of the 3-way valve used for raising the cleaner to the vent position. Toward the end of LFCM-8A, the roll nut shaft would stop 12 to 18 in. before completion of full travel. However, the travel could be completed by the turning of the 3-way valve used to lower the cleaner to the down position. Once the cleaner was in the up position, the Bimba stop blocks were used to keep the brush from lowering, and then the three-way valve for raising the cleaner was placed in the vent position. On the 11th day of LFCM-8, and following discussions with Mr. Hardip Dhingra, it was decided that between operation cycles the 3-way valve used to raise the cleaner would be left in the up position and the lock mechanism would not be used. This was the anticipated operating mode at West Valley. The air cylinders used to raise the cleaner were left pressurized during the week of downtime before LFCM-8B.

When LFCM-8B was started, the OLC operated for the first 24 hours in a way similar to its prior operation. However, after the first day the OLC began to work sporadically. The roll nut shaft would alternately 1) travel 8 to 12 in. downward; 2) travel the full length downward except for the last 12 to 18 in.; 3) travel the full length downward; and/or 4) not travel at all. In total, 29 cycles were achieved during the second segment of LFCM-8. This resulted in a total of 310 cycles during LFCM-8. After observing that the molybdenum (moly) lube had worn away unevenly on the first 6 to 8 in. of the roll nut shaft, it was initially believed that either the tolerance between the roll nut and the roll nut shaft was too close or the lubricant was being scraped off and depositing inside the roll nut. A detailed inspection of the OLC was conducted following LFCM-8 to determine the cause or causes of the failure.

Temperature History. Plenum, off-gas and OLC temperatures were continuously monitored by the LFCM computer data acquisition system. The results are presented in Figures 4.23a and 4.23b, covering LFCM-8A and LFCM-8B, respectively. Both segments have similar process conditions. The plenum temperature averaged between 600°C and 700°C. Temperatures of off gas flowing into the SBS were close to 300°C during the entire campaign. A conscious effort to lower inleakage into the LFCM by reducing the melter plenum vacuum led to an increase in off-gas temperature during the second segment of the run. The OLC temperature shown was measured approximately 20 in. above the OLC mounting flange. Average temperatures of between 30°C and 40°C were predominant for both segments. The upper thermocouple essentially monitored ambient room conditions, which were 5°C to 10°C lower then the other thermocouple. The film cooler, the spool piece adaptor, and the OLC flange were covered by a blanket insulation to protect operating staff. As a result, heat loss from the metal components was minimized. Based on these results it is quite convincing that the OLC components, except for the brush, will not experience excessively high temperatures.

Post-Test Inspection. Upon removal of the device from the LFCM it was discovered that the brush attachment had come free from the OLC and had dropped into the melter. The reason for the brush coming free was the failure of an Inconel cotter pin that held the brush to the shaft. The brush was subsequently recovered from the LFCM. The film cooler was free of any significant buildup. However, since we can not be sure when the brush was lost, it is not possible to attribute this to the OLC at this time.

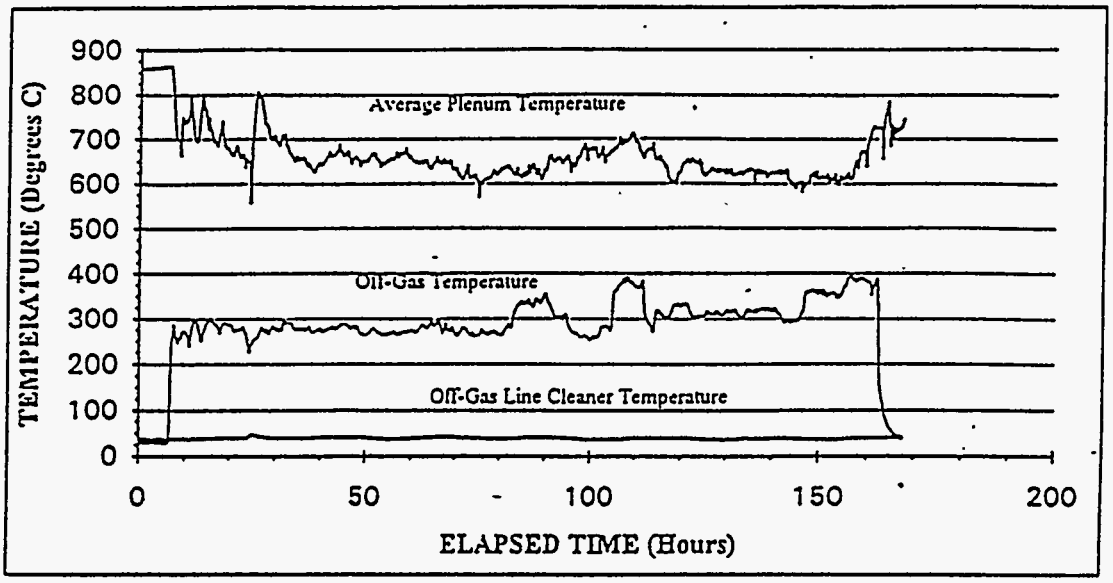

Figure 4.23a. OLC Process Temperatures During LFCM-8A

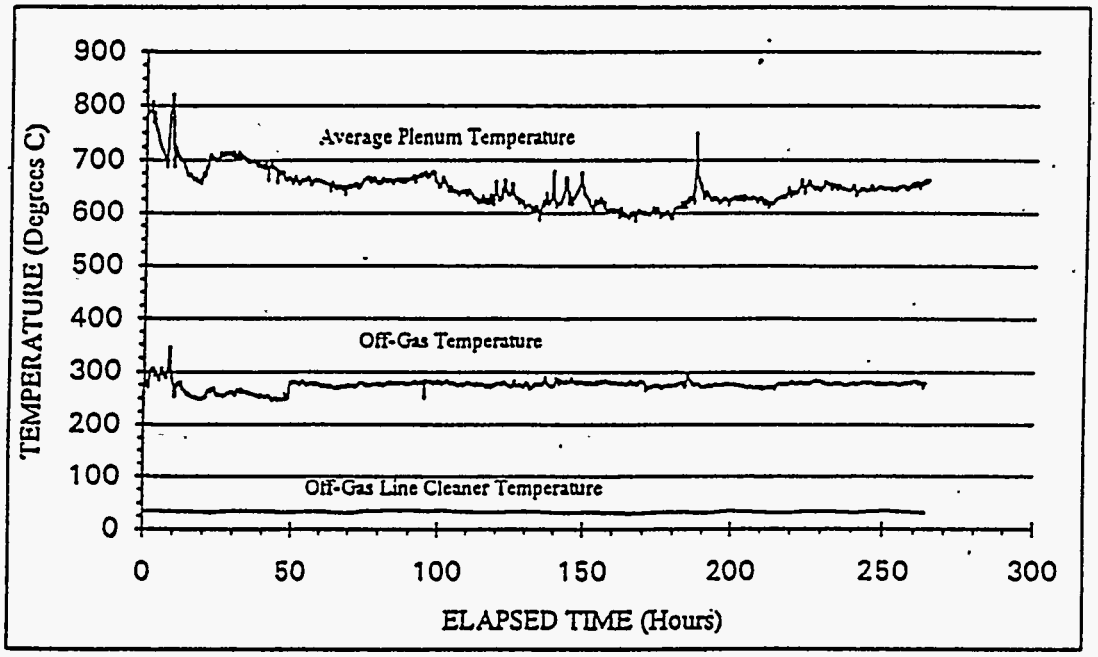

Figure 4.23b. OLC Process Temperatures During LFCM-8B

The failure of the OLC to operate was due to the shaft coming out of alignment. Several cap screws, which secured different parts of the device, had come loose during operation. This allowed the system to come out of tolerance. Also, the base plate on which the shaft's roll nut was secured was found to be warped. It was not observed to be warped at the beginning of testing. Therefore, it is presumed to have occurred as a result of testing. A list of recommended repairs was generated based on the post-test inspection. Following concurrence with WVNS the repairs were made. Subsequent testing (100 operating cycles) verified that the OLC's operation was returned to proper working order.

4.8 Off-Gas Equipment Operation (Process Data)

In this section, the operational characteristics of each component in the LFCM off-gas system are examined. Flow rates, pressure drops and other selected data will be presented for the film cooler, off-gas jumper, SBS, chevron demister, heat exchanger, and HEMF. Obtaining this information was not a primary objective of LFCM-8 and therefore will not be discussed in detail. Pressure drop, circulation rates, and other operating characteristics were determined for the SBS prior to LFCM-8 and are presented elsewhere (Whyatt et al. 1992, and Anderson et al. 1993). Equipment performance data (filtration and scrubbing efficiencies) are presented in Section 4.9. As was discussed in Section 4.1, LFCM-8 consisted of two separate segments separated by a period of melter idling. The first segment (from 4/17/93 to 4/29/93) is referred to as LFCM-8A. The second segment (from 5/10/93 to 5/16/93) is referred to as LFCM-8B. Values reported here as typical are averages for April 26, 1993. On that day, most process variables were relatively steady throughout the day and the flows were close to nominal.

4.8.1 Gas Flow Rates During LFCM-8

Flows through the off-gas system during the run were made up of the film cooler air injection flow rate, control air injection flow rate, melter source gas flow rate, and melter in leakage. Flow through the system was measured at two locations--before entering the SBS (Off-Gas Flow) and at the end of the off-gas line past the HEMF and the downstream air injection location (Final Flow). The flow of gas leaving the SBS (SBS Exit Flow) was determined by subtracting the downstream air injection flow rate from the final flow rate. All three flows are expressed in standard volumetric flow (scfm) in Figures 4.24 (LFCM-8A) and 4.25 (LFCM-8B). Flows are also shown in actual volumetric flow rate (acfm) in Figures 4.26 (LFCM-8A) and 4.27 (LFCM-8B). The off-gas and SBS exit flows remained relatively steady throughout LFCM-8A, while the final flow rate varied because of changes in downstream control air injection flow rate. During the LFCM-8B, all flow rates varied due to changes in film cooler air injection flow rates as well as control air injection flow rates.

4.8.2 Film Cooler

The purpose of the film cooler, which was described in Section 3.3, is to cool the melter exhaust stream below the softening point of glass (~400°C) and to maintain the off-gas velocity above 60 ft./sec. to minimize off-gas deposits. The film cooler was operated throughout the melter run. The film cooler supply air was maintained at flows between 125 and 140 scfm during the majority of LFCM-8, resulting in gas temperatures in the off-gas jumper of approximately 275°C. The resulting gas velocity in the off-gas jumper was approximately 130 ft./sec. During the last three days of the run,

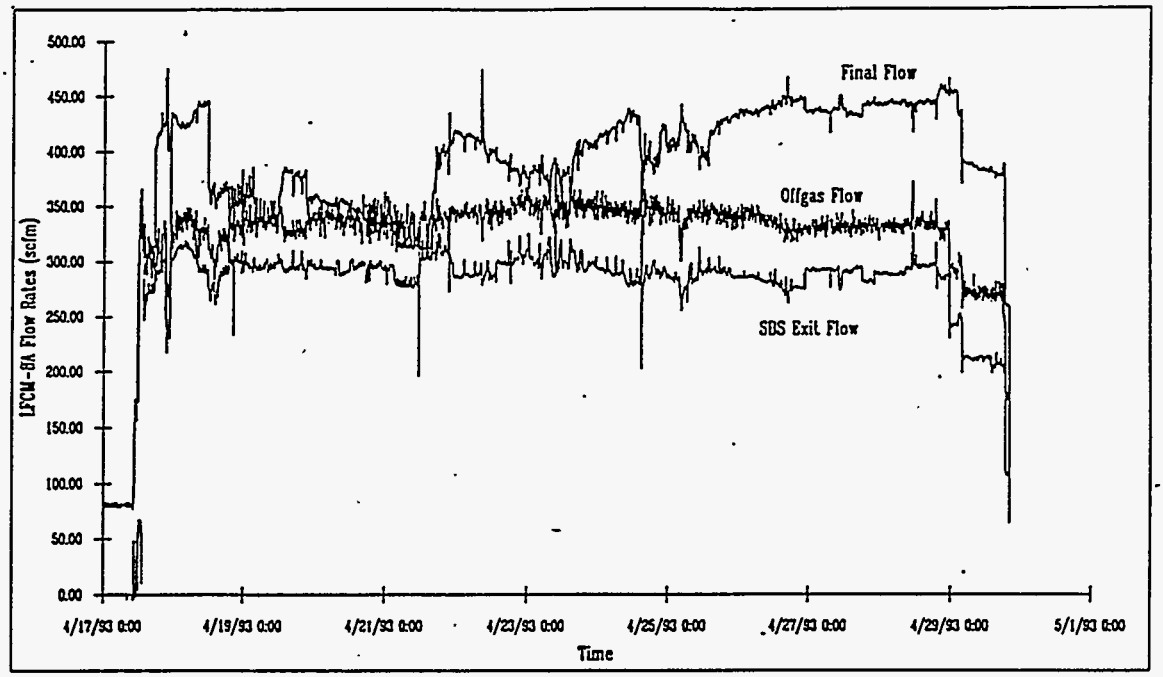

Figure 4.24. Off-Gas Jumper, SBS Exit and Final Flow Rates During LFCM-8A (acfm)

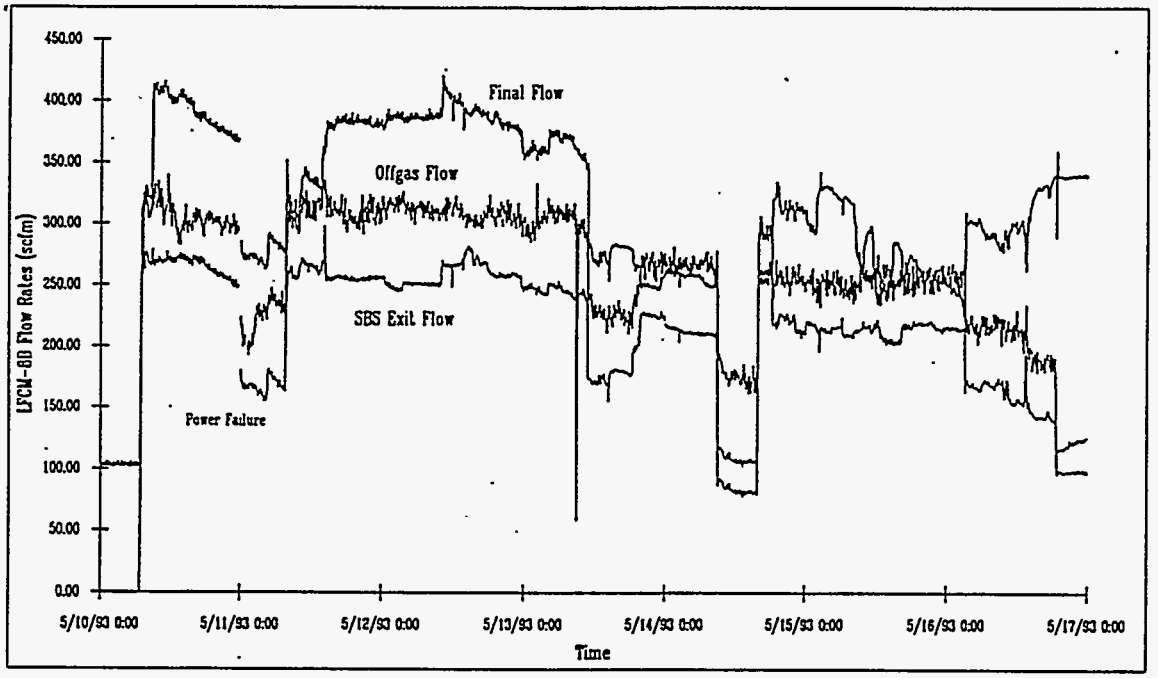

Figure 4.25. Off-Gas Jumper, SBS Exit and Final Flow Rates During LFCM-8B (acfm)

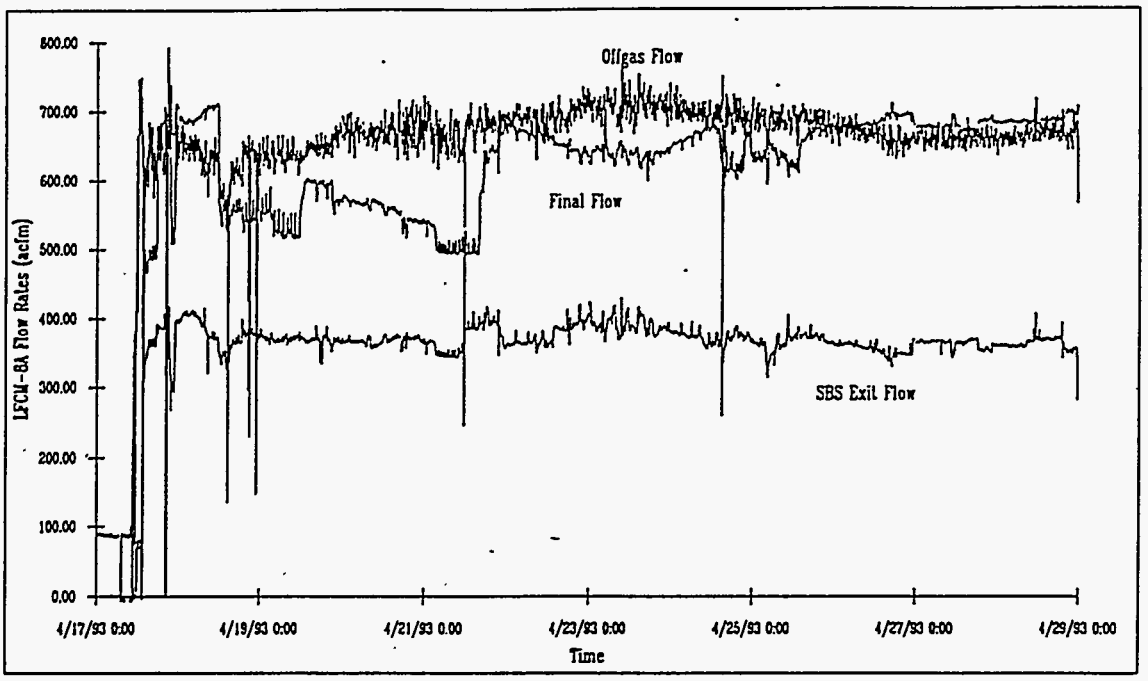

Figure 4.26. Off-Gas Jumper, SBS Exit and Final Flow Rates During LFCM-8A (acfm)

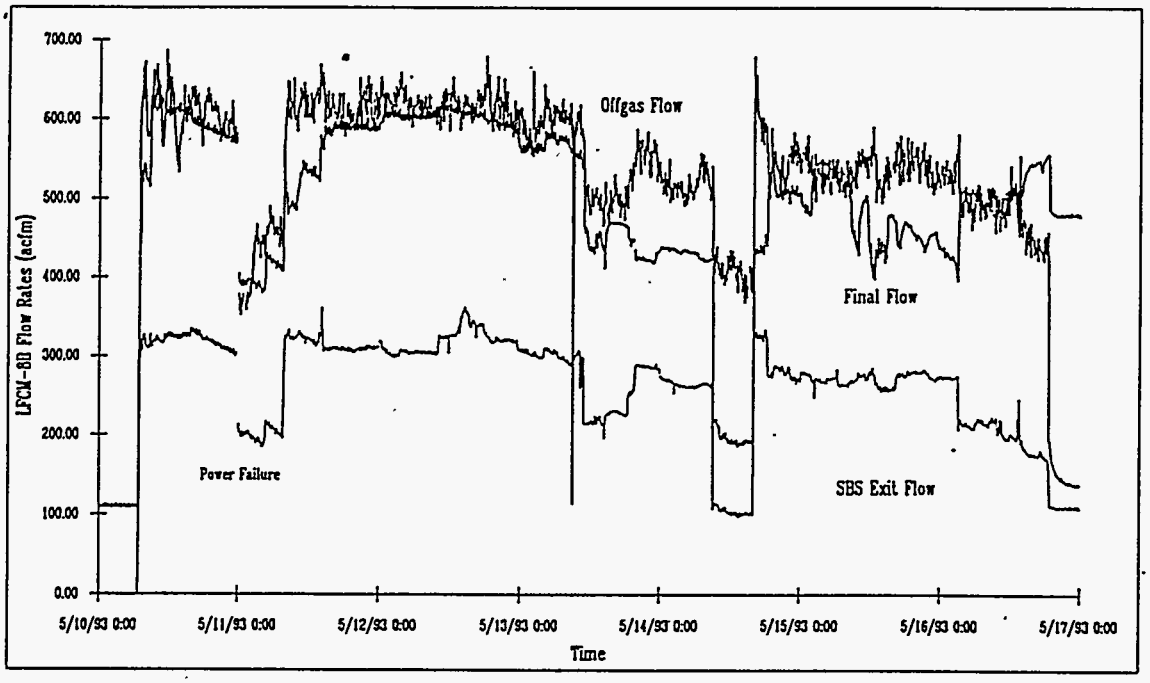

Figure 4.27. Off-Gas Jumper, SBS Exit and Final Flow Rates During LFCM-8B (acfm)

the flow rate was decreased to approximately 50 scfm, resulting in gas temperatures in the off-gas jumper of approximately 340°C and a gas velocity in the off-gas jumper of 80 ft/sec. Typical film cooler operational parameters are shown in Table 4.18. Pressure drop data for the film cooler and the off-gas jumper are shown in Figure 4.28 for a representative day during LFCM-8 (4/26/93). The average film cooler pressure drop was 2.5 in. WC for flows through the film cooler of approximately 325-350 scfm (approximately 650-700 acfm). Pressure oscillations in the off-gas line, caused by the SBS, cause the actual film cooler pressure drop to vary ±1-2 in. WC. These oscillations will be discussed further in the next section. The average film cooler pressure drop was determined to be 2.1 in. WC during testing prior to LFCM-8 (Whyatt, et al. 1992) with a total flow through the film cooler of 296 scfm, including 170 scfm air supplied to the film cooler. However, the previous testing was done with a film cooler that had been installed for a long period of time during melter idling and was badly corroded. The film cooler used during LFCM-8 was new, but appears to exhibit a pressure drop similar to that of the old film cooler under nominal flows used in LFCM-8. Film cooler pressure drop was not determined as a function of gas flow rate through the film cooler.

4.8.3 Submerged Bed Scrubber (SBS)

The purpose of the SBS, which was discussed in Section 3.3, is to quench the hot melter off gas and to capture the larger particulate. The SBS was operated in a condensing mode throughout LFCM-8, although the overflow drainage rate was not directly measured. Typical operational parameters are shown in Table 4.19. The pressure drop of the SBS is primarily determined by the liquid submergence of the off-gas downcomer pipe below the liquid level.

The SBS pressure drop is shown in Figure 4.29 for a representative day during LFCM-8 (4/26/93), and is maintained near 30 in. WC.

The submergence of the downcomer pipe is 32 in.; however, some liquid is lost due to splashing into the overflow drain. The superficial velocity was maintained near the nominal design velocity of 52 fpm throughout most of LFCM-8A. The superficial velocity is defined as the actual gas flow rate (including humidity) at SBS exit conditions divided by the cross-sectional area of the bed. During LFCM-8B the SBS superficial velocity dropped as low as 28 fpm at times due to changes in leakage caused by operating the melter at a lower vacuum, and because of changes in film cooler air injection flow rate.

Table 4.18. Typical Film Cooler Process Data During LFCM-8

Parameter	Typical Operating Value
Air Injection Flow Rate (scfm)	140
Average Pressure Drop (in. WC)	2.5
Line Velocity at Film Cooler Exit (ft/sec)	130

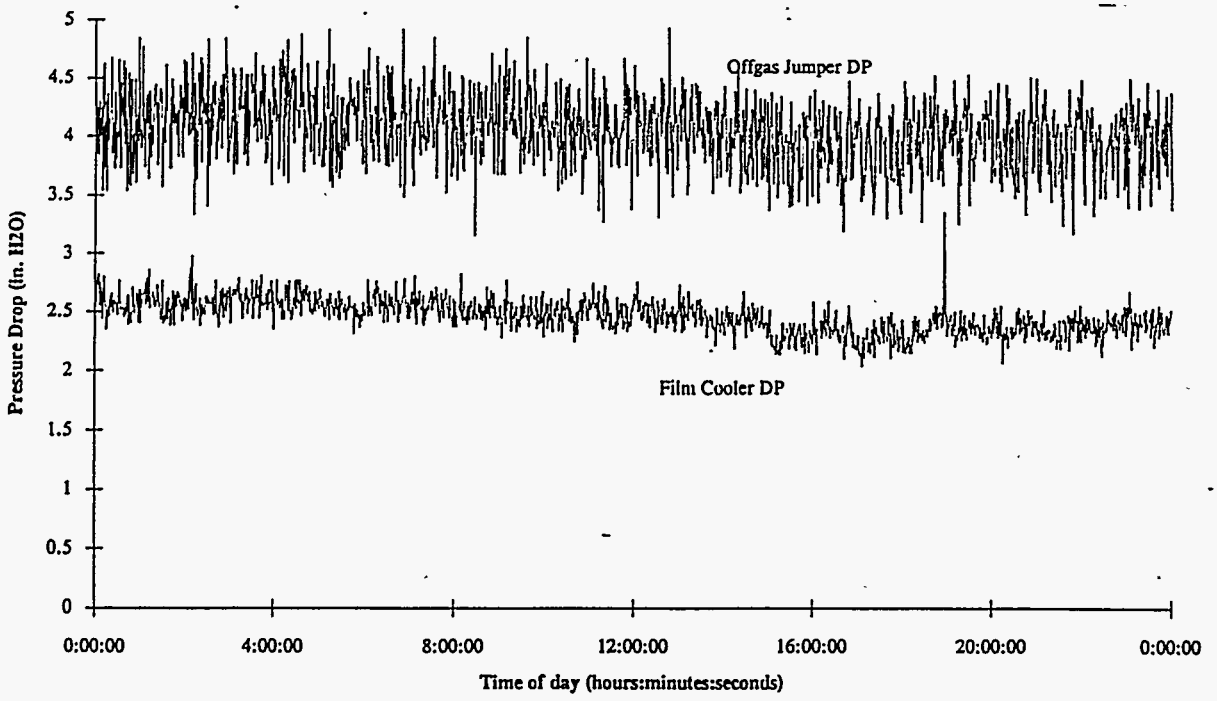

Figure 4.28. Film Cooler and Off-Gas Jumper Pressure Drops for a Representative 24-hour Period (4/26/93). Data are 1-minute averages of samples taken every 2 seconds.

Table 4.19. Typical SBS Process Data During LFCM-8

Operational Parameter	Typical Value
SBS Bed Temperature (°C)	47
Pressure Drop (in. WC)	30
Gas Inlet Temperature (°C)	275
Gas Outlet Temperature (°C)	45
Outlet Pressure (psia)	13.0
Exit Flow Rate, including humidity (scfm)	282
Superficial Velocity[(a)] (fpm)	52

(a) Evaluated at SBS exit conditions including humidity; bed area = 6.8 ft^2.

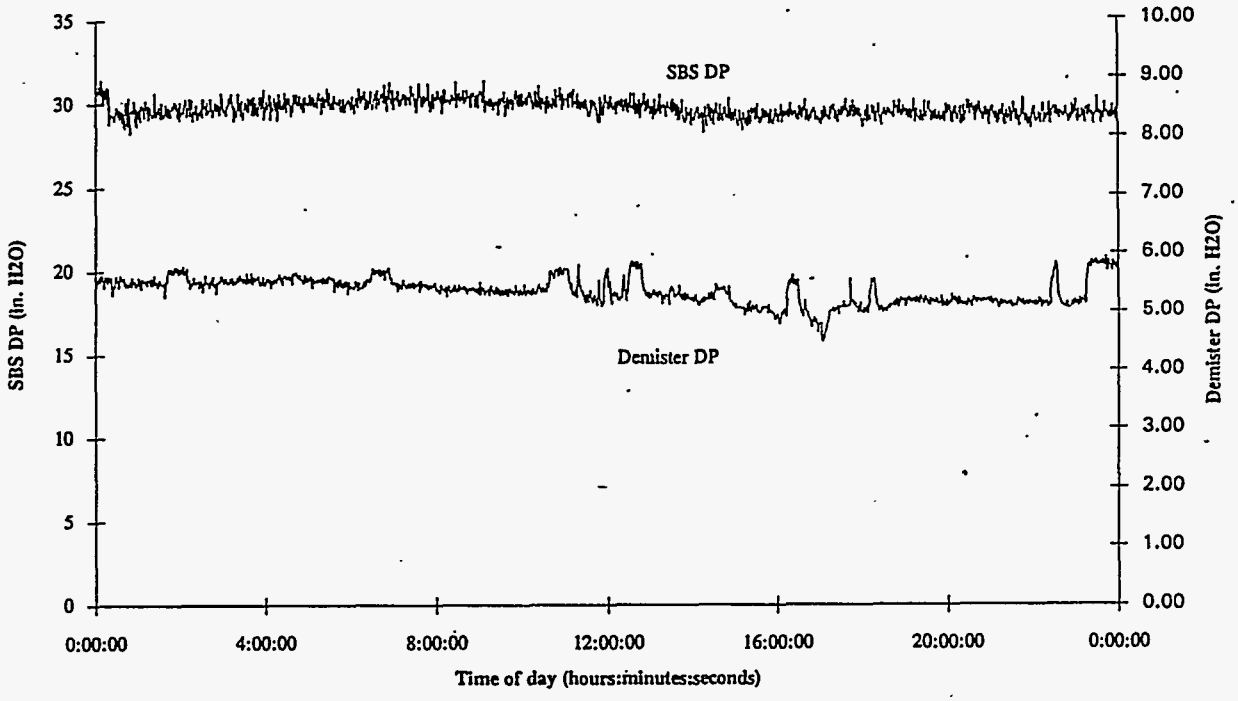

Figure 4.29. SBS and Demister Pressure Drop for a Representative 24-hour Period (April 26, 1993). Data are 1-minute averages of samples taken every 2 seconds.

Oscillations in pressure in the SBS were observed during LFCM-8. These oscillations have been seen before in the LFCM SBS and have been documented (Whyatt et al. 1993). Similar oscillations have also been seen in a submerged gravel scrubber (Owen and Postma 1981). Tests done on the PSCM SBS subsequent to LFCM-8 showed similar behavior. For the operating conditions present during the run, the oscillations exhibited a frequency of 2.7 Hz, and a magnitude of 2.5 in. WC (peak-to-peak). This phenomena is known to be affected by changes in liquid level and the associated upstream piping configuration. The effect of these variables upon SBS pressure drop oscillations was not studied during LFCM-8.

After the conclusion of LFCM-8, the SBS was drained and the lid was removed to examine the interior of the SBS for any solids buildup or corrosion. The welds that connect the sections of wire mesh screen above the bed had failed and a gap had been created between the sections of screen. The Intalox® saddle packing was apparently fluidized and entrained through this gap, leaving the bed entirely devoid of packing by the conclusion of the run. It is not possible to determine the exact time at which this occurred. As discussed earlier, the SBS pressure drop is basically a function of the submergence, and did not show any significant change throughout the run that can be attributed to the loss of packing. Exit gas temperatures also were not affected. Observations by LFCM personnel through the SBS viewport were used to narrow down the period of time the packing loss most likely occurred; it appears that it occurred some time during LFCM-8B. The overall operation of the SBS was not noticeably affected. The impacts on off-gas scrubbing efficiency will be discussed in Section 4.9.

4.8.4 Koch Chevron Demister

The purpose of the chevron demister, which was discussed in Section 3.3, is to remove a fraction of the liquid entrainment from the SBS exhaust before the gas passes through the HEME. The demister is considered part of the SBS for purposes of gas scrubbing efficiencies, etc. The demister itself was not studied during LFCM-8, although pressure drop data was recorded at certain intervals. Demister pressure drop was then calculated for the entire run based on a pressure drop-flow relationship determined earlier during steam and air testing and using the recorded data. This calculated pressure drop data is presented along with the SBS pressure drop data in Figure 4.29.

4.8.5 High Efficiency Mist Eliminator (HEME)

The HEME (discussed in Section 3.3) removes essentially all aerosol particles larger than one micron, and a fraction of submicron particles, from the gas stream before it enters the final stage of filtration (HEPA or HEMF). To accomplish the HEMF test objectives, it was necessary to load the HEMF more quickly than would be possible while operating the HEME. Therefore, the HEME was bypassed for most of the campaign. However, the off gas was routed through the HEME between April 24, 1993 and April 29, 1993. Aerosol scrubbing efficiency was determined for the HEME for this time period, and pressure drop data was recorded. The pressure drop ranged between approximately 6-9 in. WC while the HEME was in operation, but no definite increase was seen with time. The flow through the HEME during this time was essentially equal to the SBS exit flow discussed earlier.

4.8.6 Heat Exchanger

The heat exchanger was used to preheat the gas exiting the SBS and HEME to above its dew point before final filtration in the HEMF. Although the HEMF can be operated wet without damage if necessary, the intention was to obtain pressure drop information during high particulate loading without interference from moisture.

The heat exchanger was operated throughout the run. Typical operational parameters are shown in Table 4.20. The temperature of the gas entering the heat exchanger ranged from 40°C to 45°C, while exit temperatures ranged from 75°C to 100°C. The steam flow necessary to achieve the temperature increase was not measured. The pressure drop across the heat exchanger is shown in Figures 4.30 (LFCM-8A) and 4.31 (LFCM-8B).

Table 4.20. Typical Heat Exchanger Process Data During LFCM-8

Operational Parameter	Typical Value
Flow Rate through Heat Exchanger (scfm)	282
Inlet Temperature (°C)	45
Outlet Temperature (°C)	75
Pressure Drop (in. WC)	13.5

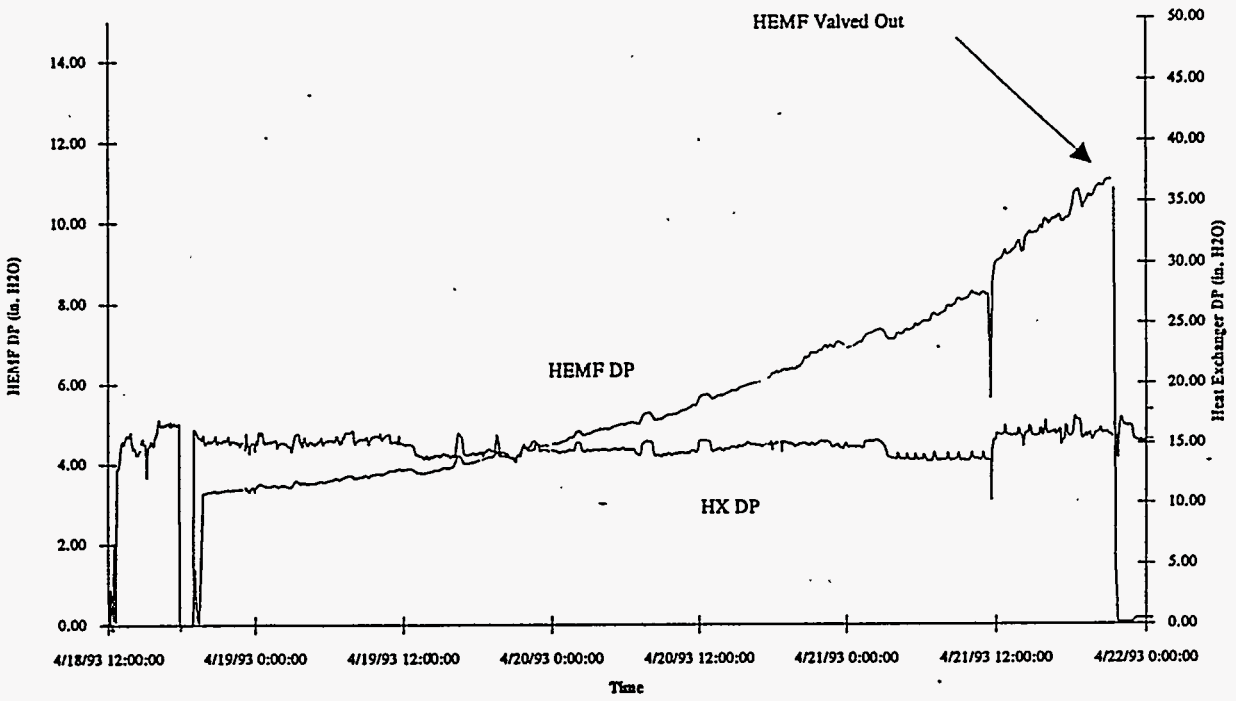

Figure 4.30. Heat Exchanger and HEMF Filter Pressure Drop During LFCM-8A. Data are 10-minute averages of samples taken every 2 seconds.

4.8.7 High Efficiency Metal Fiber (HEMF) Filter

The HEMF filter, which was described in Section 3.3, was installed before the LFCM-8 run, and had not previously been used in any melter testing. The HEMF filter takes the place of two HEPA filters in series as the final filtration to remove submicron aerosols. The advantage of an HEMF filter over a HEPA filter is that is does not require filter changeouts, but only periodic cleaning, which can be done remotely. Unlike a HEPA filter, moisture will not damage the filter. The HEMF was used during portions of LFCM-8 to obtain information on pressure drop and filtration efficiency. The HEME was bypassed during the run so that the HEMF could be loaded with particulate quickly to observe the increase in pressure drop with time. A mass DF for the HEME of $\geq$400 would be expected based on experience during PSCM-23. Thus, the loading of the metal filter would proceed at $<$1/400th of the rate observed with the HEME bypassed. Loading the filter was also recommended so that a filter cleaning procedure could be tested after the conclusion of LFCM-8.

The pressure drop for the HEMF is shown along with that for the heat exchanger in Figure 4.30 for LFCM-8A and in Figure 4.31 for LFCM-8B. The HEMF was operated for the first four days of the melter run. An increase in pressure drop from 3 in. WC to 11 in. WC was seen before the HEMF was valved out on the fourth day. Aerosol sampling equipment for the HEMF was not operating correctly at this time, so on April 29, 1993 the melter run was halted until the aerosol analyzer could be repaired. When LFCM-8B was begun on May 10, 1993, the HEMF pressure drop had fallen back

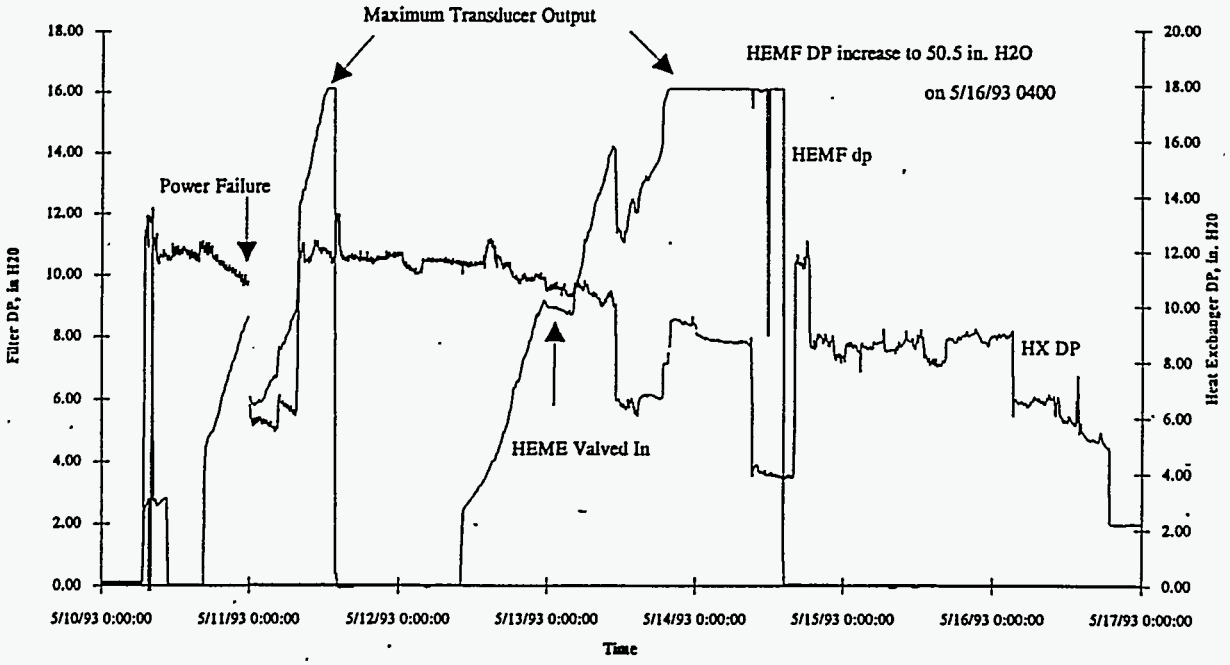

Figure 4.31. Heat Exchanger and HEMF Filter Pressure Drop During LFCM-8B. Data are 10-minute averages of samples taken every 2 seconds.

down to 2.5 in. WC. This was followed by an increase over the next day and a half up to 16 in. WC, which is the maximum pressure transducer output. The HEMF was again valved out, this time for approximately one day. Again, when flow was routed through the filter, it showed a clean (2.5 in. WC) pressure drop. The pressure drop increased during the last four days, except for a brief period (May 13, 1993) when the HEME was valved in. During the time the HEME was used, the majority of particulate was filtered out of the gas entering the HEMF; therefore, no pressure drop increase occurred. After valving out the HEME, the pressure drop continued to increase throughout the run, and reached a value of 50.5 in. WC at the conclusion of LFCM-8B.

The restoration of a clean pressure drop after the filter had been valved out is believed to be due to two possible causes. The first is that without the HEME operating, droplets of water were able to enter the filter, causing the increase in pressure drop. When the filter was valved out, the moisture was redistributed on the filter elements, resulting in a clean pressure drop when flow was re-routed through the HEMF filter. The second possible cause is that although the filter elements were becoming plugged with particulate, the valving sequence used to valve out the HEMF created a brief period of backflow, which knocked the particulate off the filter elements. It is not likely that the first possibility occurred alone. A combination of these two effects is probable. At the conclusion of LFCM-8B, a flow of dry air was maintained through the filter to determine whether or not moisture was responsible for any of the increase in pressure drop. It is clear that the pressure drop, at least at the end of the run, was due entirely to particulate, since the pressure drop did not decrease with time.

After LFCM-8, the filter was removed from the off gas line and disassembled for examination. The filter elements were visibly loaded with yellowish-white particulate. The loading was not evenly distributed between filter elements or between different areas within a single filter element. There were areas that appeared much cleaner than the overall element. This may have been caused by certain areas becoming wet due to mist droplets and therefore not being used for filtration. These areas were a very small fraction of the overall surface area of the filter elements. The appearance of the filter elements was documented with photographs. No significant amount of particulate was found anywhere in the housing. Areas near the welds in the housing, especially in the upper bonnet, exhibited some surface rust. These areas were also documented with photographs. After inspection, the filter elements were replaced in the housing and the filter was reassembled and installed back into the off-gas line.

After re-assembly, a procedure to clean the HEMF filter was tested to determine its effectiveness in restoring the clean pressure drop. This procedure involved filling the filter housing with water, in which the elements were soaked for approximately 30 minutes. Pressurized air was then introduced into the top of the housing, causing a pulse of flow in the direction opposite normal flow. This pulse removed the particulate from the filter elements. The water and removed particulate were then drained from the filter housing. The detailed procedure is provided in Appendix I. The flush was performed once, followed by measurement of pressure drop. The procedure was effective in restoring the pressure drop to its initial value of 2.5 in. WC from the post-run value of 50.5 in. WC for a gas flowrate of approximately 525 acfm.

4.9 Off-Gas Equipment Performance

Melter off gas was analyzed nearly continuously during LFCM-8. Production rates and concentrations of the non-condensible gases were determined and are discussed in this section.

4.9.1 Production and Concentration of Noncondensible Gases

Molar production rates for the major noncondensible gases produced from vitrification were determined. These gases are CO_2, NO_x (NO and NO_2), and H_2. The molar production of these gases for a representative day (4/26/93) during LFCM-8 is shown in Figure 4.32 along with the melter feed rate. The levels of NO, NO_2, and H_2 remained relatively constant, while the CO_2 levels appear to vary considerably. Because the CO_2 levels of the diluted sample were so close to the detection limit of the analyzer (approximately 0.5%), the readings were very sensitive to variables such as temperature.

Therefore, the CO_2 readings drift considerably more than the readings for the other gases. Variations in all the gas production rates occur due to cold cap dynamics, changes in melter plenum temperature and pressure, and possible feed inhomogeneities. Molar gas production graphs for each day of LFCM-8 are shown in Appendix J. Analysis was attempted for other gases that may be present in the melter exhaust (CO, N_2O, NH_3, and CH_4). However, these gases are present in concentrations too low to be accurately quantified.

The concentration in the off gas, rather than the molar production, is of interest for certain gases, especially for the explosive gases H_2 and CO. The concentration range of measured gases (sampled after the HEMF filter) is shown in Table 4.21.

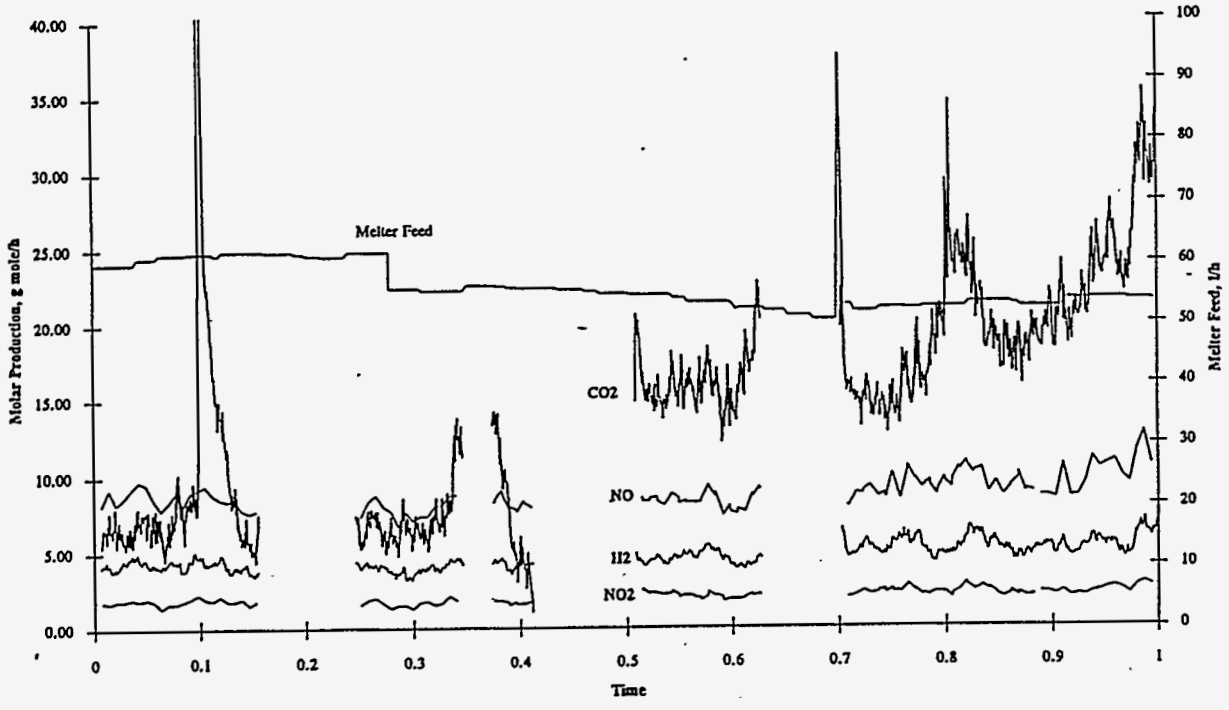

Figure 4.32. Molar Gas Production Rates of H_2, CO_2, NO, and NO_2 for a Representative 24-Hour-Period During LFCM-8 (4/26/93). Melter feed rates are shown for reference.

The concentrations of H_2 and CO are well below their respective LELs of 4.65% and 15.5%. The concentration ranges shown in Table 4.21 were measured at the end of the off-gas line (past the HEMF filter but before the downstream control air injection). Assuming a final flow rate of 310 scfm and a melter inleakage flow of 50 scfm for a plenum vacuum of 4 in. WC, the concentration ratio between the melter plenum and the sample point is 6.2 (steam present in the melter plenum is neglected). Also assuming that gases in the melter plenum are perfectly mixed and use the highest recorded concentration of gas during LFCM-8, the concentrations of H_2 and CO in the melter plenum are calculated to be 1.3% and 0.6%, respectively. These concentrations are well below the LEL. However, localized concentrations in cold cap gas bubbles or in the gas near the cold cap surface could possibly exceed the LEL.

Table 4.21. Concentration Range for Noncondensible Gases

Gas	Concentration Range
CO_2	0 - 4.9%[a]
CO	< 0.1%
NO_x	0 - 0.2%
NO	0 - 0.2%
H_2	0 - 0.2%
N_2O	< 0.1%
CH_4	< 0.2%

(a) High value believed to be in error as discussed in text. Actual CO_2 concentration probably did not exceed approximately 1.5 to 2.0%.

A mass spectrometer was used to qualitatively detect the presence of gases with atomic masses less than 50. These samples were also taken at the end of the off-gas line. A representative set of spectra are shown in Figures 4.33 through 4.35. These spectra are taken at three progressively higher sensitivities (indicated by the amplifier gain setting used). The peak heights indicate relative molar concentrations of gas. The majority of peaks were identified, as shown in the figures. Small peaks that have not been identified occur at atomic masses of 41 and 42.

4.9.2 Nitrogen Balance

Nitrogen is present in the melter feed as nitrate or nitrite ions, which decompose as the slurry is heated. This nitrogen leaves the melter as NO, NO_2, or other nitrogen-containing gases. The amount of nitrogen leaving the melter as NO_x only accounts for approximately 65% of the nitrogen present in the feed. It is clear, therefore, that other gases, possibly ammonia, N_2, or N_2O_4, accounts for the remainder of the nitrogen. However, this could not be confirmed during LFCM-8. Similar results were seen during PSCM-23, where approximately 75% of the nitrogen in the feed could be accounted for. The NH_3 analyzer used during LFCM-8 was subject to interference from other gases, which prevented accurate quantification of NH_3 concentration.

4.9.3 Hydrogen Production Versus Temperature

As shown earlier, the hydrogen concentration in the off-gas system ranges from 0 to 0.2% throughout the melter run. The concentration centered around 0.1% the majority of the time. The hydrogen is believed to be produced by the reaction of CO with H_2O as follows:

$$CO + H_2O \rightarrow CO_2 + H_2 \qquad (4.1)$$

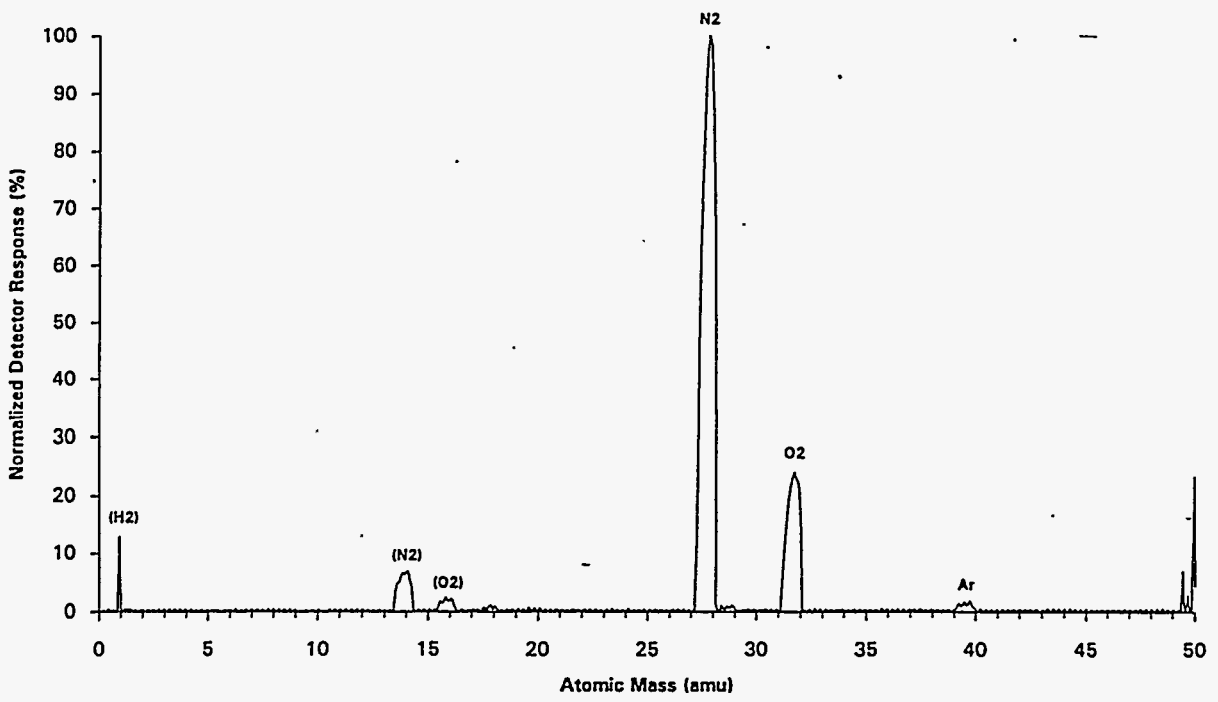

Figure 4.33. Mass Spectrometer Analog Scan (Current = 1.0E-07 amps). Identified Gases are labeled. Gases in Parentheses Indicate a Minor Peak of the Gas.

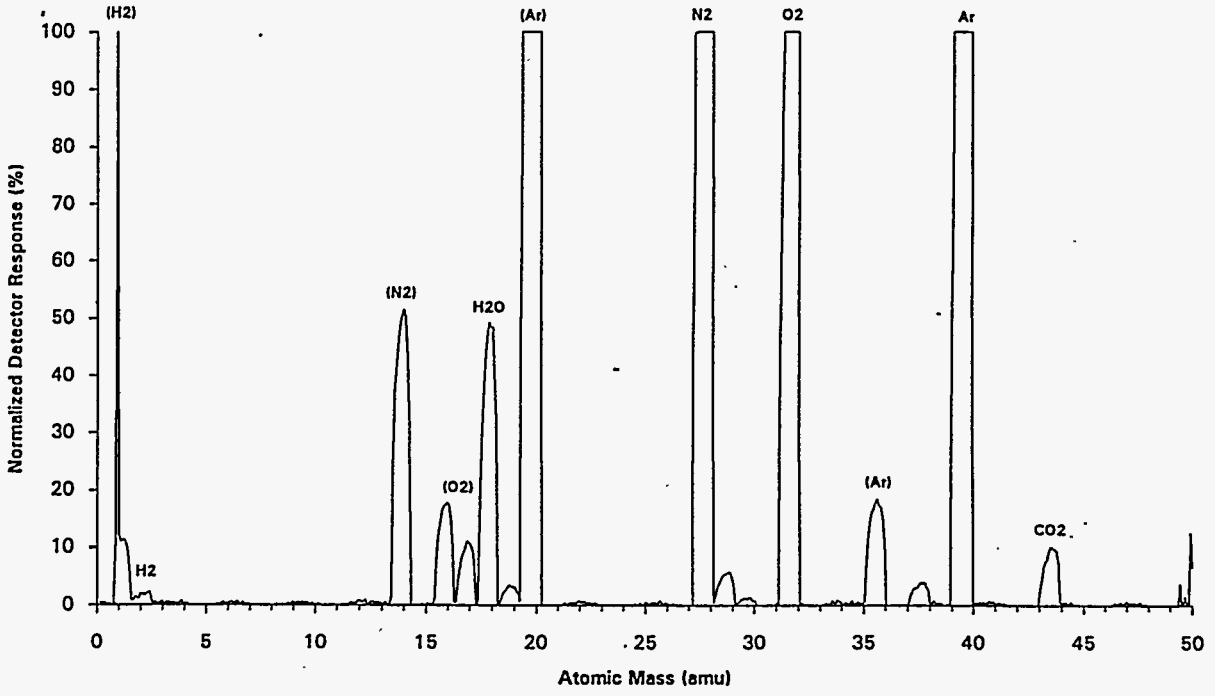

Figure 4.34. Mass Spectrometer Analog Scan (Current = 1.0E-09 amps). Identified gases are labeled. Gases in parentheses indicate a minor peak of the gas..

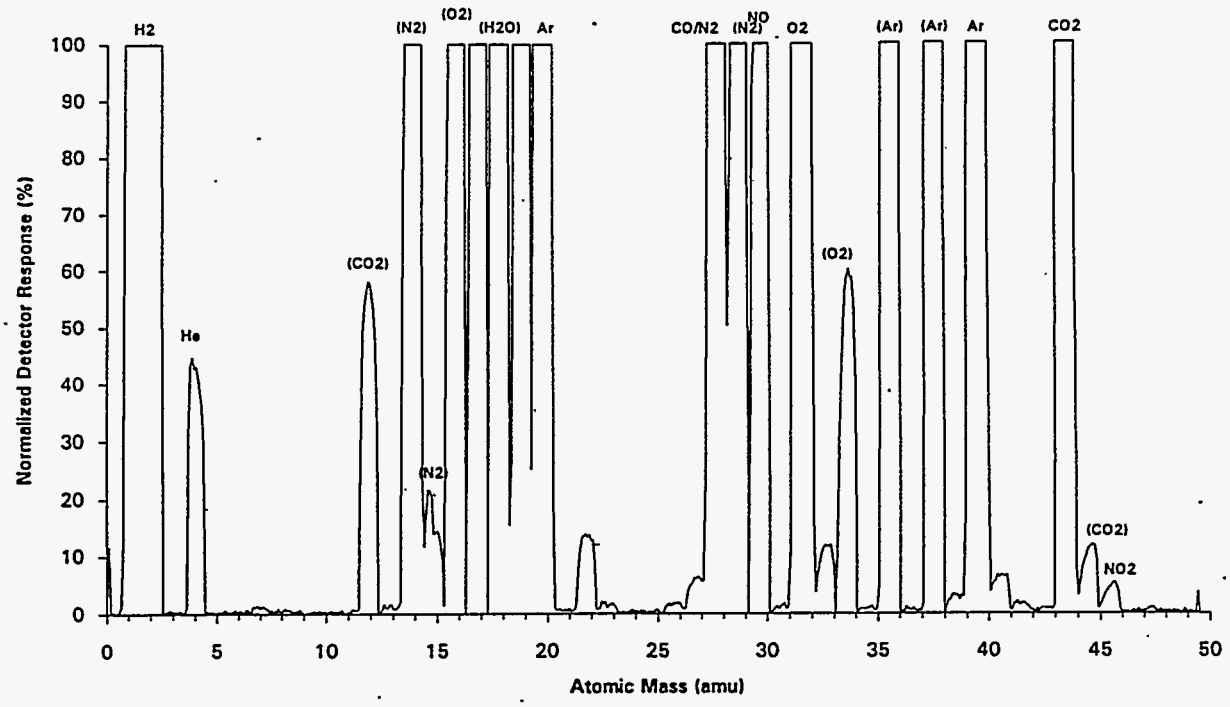

Figure 4.35. Mass Spectrometer Analog Scan (Current = 1.0E-11 amps). Identified gases are labeled. Gases in parentheses indicate a minor peak of the gas.

The CO results from the decomposition of formic acid or formates present in the feed. Although CO levels were below the detection limit of the CO analyzer, if the detection limit for CO is assumed and the above reaction proceeds quantitatively, this could account for the levels of the H_2 observed. However, it has not been proven that this reaction accounts for all of the H_2 generated in the melter. Plenum temperature was seen to affect the concentration of H_2 leaving the melter. The concentration of hydrogen decreased with increasing temperature, as shown in Figure 4.36. The amount of hydrogen leaving the melter is very likely a function of the melter feed rate. To normalize changes in feed rate, hydrogen production is expressed as (mol H_2/L feed). There is a significant spread in the data, so that an exact relationship cannot be determined; however, the relative trend is clear.

There are several possible reasons for the decrease in hydrogen leaving the melter at increased temperatures. These include increased burning of hydrogen at higher temperatures, and a decrease with temperature of the CO - water reaction. The kinetics of these reactions were not examined as part of LFCM-8. However, it can be seen that the use of plenum heaters to increase melter plenum temperature is effective in decreasing H_2 concentration in the melter plenum and off-gas system. It is important to remember that the reported plenum temperature is biased high because of the effect of radiant heat transfer to the thermocouples located in the plenum. The actual temperature of the gas in the plenum is lower than the reported plenum temperature indicates.

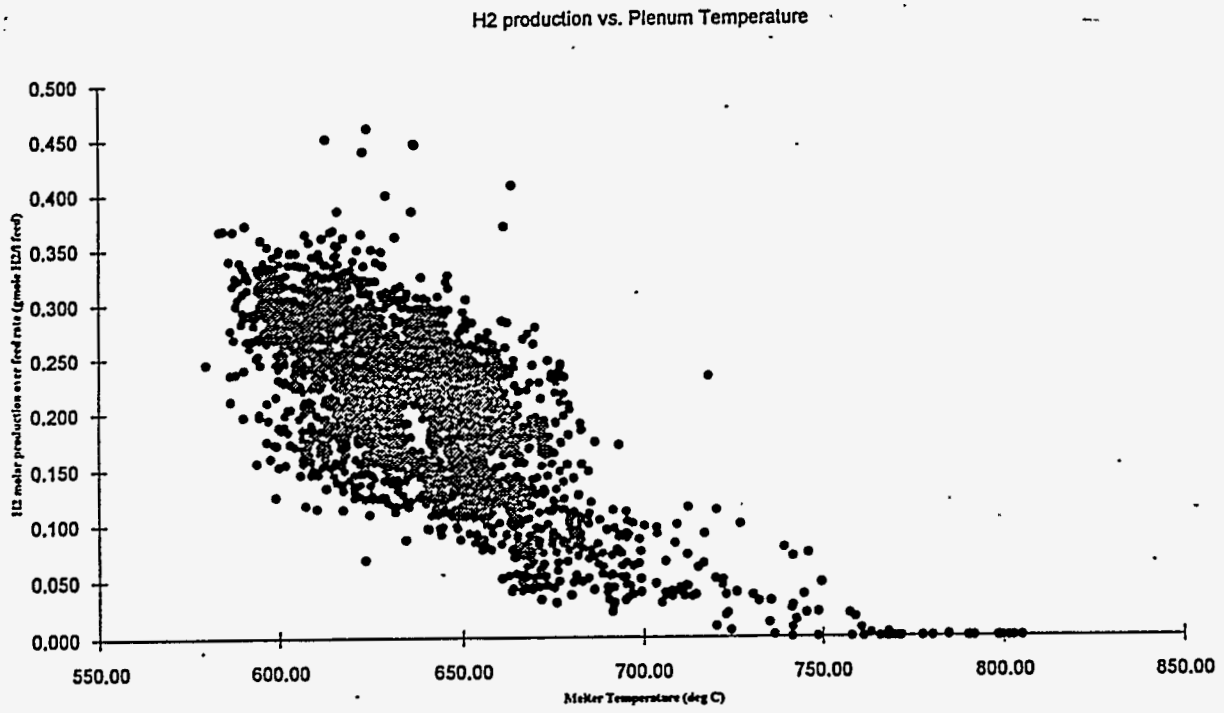

Figure 4.36. Normalized Hydrogen Production Versus Plenum Temperature. Data Points are for 10-Minute Averages.

4.9.4 NO_x Removal in the SBS

The LFCM offgas equipment was not designed to remove NO_x; however, a small amount of NO_x is expected to be scrubbed out by the SBS. the amount will depend primarily on the condensation rate in the SBS and the SBs solution properties, but it is not expected to exceed a few percent for normal melter operating conditions without chemical additions to the SBS solution.

Melter off gas was sampled to determine the extent of NO_x removal in the SBS and to determine the NO:NO_2 ratio at each location. Samples were taken before and after the SBS and after the HEMF filter. Because the HEME was not normally operated during LFCM-8, no samples were taken after the HEME. The gas analysis results did not show any removal of NO_x in the SBS. However, it is known that a small amount of NO_x was removed in the SBS because the scrub solution contained nitrates and nitrates resulting from scrubbing of NO_x. Ion chromatography analyses of the SBS solution for NO_3– and NO_2– showed the amount of NO_x scrubbed to be insignificant (less than 1). This was to be expected, as the SBS operated at a pH of approximately 1, and there is little driving force for NO_x removal.

The NO:NO_2 ratio remained relatively constant at each location throughout the melter run. The ratio at each location is shown in Table 4.22; these ratios were determined for the sampled gas entering the NO_x analyzer. Some conversion of NO to NO_2 would have taken place between the actual sampling point and the analyzer, so the measurement is lower than that at the actual sampling point in the off-gas line.

Table 4.22. $NO:NO_2$ Ratio in the Off-Gas System During LFCM-8

Location	$NO:NO_2$
Before SBS	6.8
After SBS	5.9
After HEMF	5.3

A small amount of NO was oxidized to NO_2 as the gas progressed down the off-gas line, but the majority of NO_x continues to be present as NO. This was also a clear indication that scrubbing of NO_x in the SBS was not occurring. Because NO_2 is much more easily scrubbed in an aqueous solution than NO, the amount of NO_2 would be expected to decrease across the SBS if it were being scrubbed. However, the opposite trend was occurring, indicating very little NO_2 removal.

4.10 Decontamination Factors for Melter and Off-Gas Equipment

The melter effluent was characterized not only for non-condensibles, but also with respect to condensed-phase (aerosol) concentrations and compositions. Overall aerosol decontamination factors were determined for the melter, SBS, HEME, and HEMF. Where possible, elemental DFs were determined, and size distributions and compositions were determined for the effluent gases. Except where otherwise noted, diameters listed are aerodynamic diameters, which equal the diameter of a particle of unit density (1g/cm3) with the same terminal velocity due to gravity as the particle under consideration.

4.10.1 Melter Aerosol Emissions

A portion of the feed entering the melter was not incorporated into the glass, but exits the melter with the off-gas stream. This is caused either by entrainment of small particles of feed from the surface of the boiling slurry, or by volatilization of materials from the melt. The melter source term for aerosols is shown in Table 4.23 for various 2- to 8-hour sampling periods. Relevant feed and off-gas information is also presented. The average aerosol emission rate for LFCM-8 was 0.36 g/min. Increases in aerosol emissions were seen to accompany increases in melter feed rate.

The size breakdown of the aerosols in the melter effluent (by mass) is shown in Table 4.24. Tests indicated as series-01 through series-11 used the sampling point at the end of the bend in the off-gas line. The remaining tests used a sampling point located a few inches above the SBS lid. The change in sampling location was made because the sampling port in the off-gas line where the nozzle was inserted had been installed incorrectly, and it was not possible to obtain data at the outside of the bend in the pipe. These measurements could be made at the new sampling location. For both sampling locations, the majority of the mass consisted of particles greater than 23 μm in diameter or particles smaller than 1.6 μm in diameter. The cutpoints used here differ from those used during PSCM-23, where cutpoints of 16 μm, 6 μm, and 1 μm were used. During PSCM-23, 30 wt.% of the melter effluent existed as particles greater than 16 μm, and 46 wt.% existed as submicron particles.

Table 4.23. Aerosol Emissions from Melter

Series	Sampling Date and Time	Feed Rate (L/hr)	Oxide Loading (g/L)	Air Flow (scfm)	Offgas Solids (g/min.)
SER-01[a]	4/18 1049-1447	44.4	445	246	0.52
SER-02[a]	4/19 1620-1926	54.2	470	264	0.57
SER-03	4/20 1550-2348	52.8	474	274	0.37
SER-04	4/21 1218-2019	59.3	462	267	0.40
SER-06	4/23 1455-2102	80.0	471	263	0.66
SER-07	4/24 1110-1238	81.1	463	252	0.55
SER-08	4/25 1030-1255	65.9	447	260	0.31
SER-11[b]	4/28 1405-1654	52.3	460	262	0.22
SER-13	4/29 1555-1712	55.1	418	185	0.25
SER-15	5/11 1452-1657	56.1	385	237	0.36
SER-16[c]	5/11 1810-2016	51.3	385	236	0.37
SER-17[b]	5/11 2115-2319	63.5	385	236	0.44
SER-18	5/12 1420-1619	68.2	410	240	0.29
SER-20	5/14 1002-1542	62.5	420	72	0.16

(a) Non-isokinetic sample (sampling flow decreased to approximately 50% of isokinetic during duration of sample) - not included in average.
(b) Sample taken from inside of bend in off-gas line.
(c) Sample taken from outside of bend in off-gas line.

The NO:NO_2 ratio remained relatively constant at each location throughout the melter run. The ratio at each location is shown in Table 4.22. These ratios were determined for the sampled gas entering the NO_x analyzer. Some conversion of NO to NO_2 would have taken place between the actual sampling point and the analyzer, so the measured ratio is lower than that at the actual sampling point in the off-gas line.

To determine the uniformity of aerosol concentration within the off-gas line, samples were taken at locations approximately 1/2 in. from the inside and outside walls of the pipe. These results are also shown in Tables 4.23 and 4.24. The results did not show any significant difference in aerosol concentration or size distribution between the inside, outside, and center of the pipe. This suggests that the samples taken from the center of the pipe were representative of the entire cross-section of pipe.

One long-term sample was taken during melter idling as well. During idling, the majority of particles were less than 1.6 μm. This was expected, since the major source of particulate during idling was expected to be condensation of volatiles. A small percentage of larger particles (>23 μm) was detected.

Table 4.24. Size Distribution of Melter Effluent Aerosols

Series	Sampling Date and Time	>23 μm[a] (wt.%)	>8.2 μm[a] (wt.%)	>1.6 μm[a] (wt.%)	<1.6 μm (wt.%)
SER-01[b]	4/18 1049-1447	78	5	0	17
SER-02[b]	4/19 1620-1926	82	0	0	18
SER-03	4/20 1550-2348	71	1	5	23
SER-04	4/21 1218-2019	60	1	7	31
SER-05	4/22 1522-1728	61	3	10	25
SER-06	4/23 1455-2102	44	1	11	44
SER-07	4/24 1110-1238	36	0	16	49
SER-08	4/25 1030-1255	39	3	7	52
SER-11[c]	4/28 1405-1654	41	4	9	46
SER-13	4/29 1555-1712	42	2	15	41
SER-14[d]	4/29 2009	3	0	1	96
SER-15	5/11 1452-1657	24	1	21	54
SER-16[e]	5/11 1810-2016	29	3	26	41
SER-17[c]	5/11 2115-2319	35	10	28	27
SER-18	5/12 1420-1619	26	14	29	31
SER-20	5/14 1002-1542	30	2	25	44
Average		40	4	17	40

(a) Cutpoint diameter to next greater cutpoint diameter.
(b) Non-isokinetic sample, not included in average.
(c) Sample taken from inside of bend in off-gas line.
(d) Melter idling, not included in average.
(e) Sample taken from outside of bend in off-gas line.

The elemental composition of the melter effluent has also been broken down into size fractions. These are shown in Table 4.25. The values shown result from an average of four samples. Of the elements analyzed for, the elements with the highest percentages existing as particles <1.6 μm are Ag, Cl, Cs, S, Se, and Te. With the exception of Ag, these elements are potentially volatile. Condensation of these volatile species into small particles accounts for their predominance in the smallest size fraction.

Elemental breakdowns of off-gas effluents need to be considered only semi-quantitative. The amount of sample obtained in most cases was not sufficient to ensure accurate analytical results. In addition, the samples could not be analyzed for B, K, Li, Na, or Mg by X-ray fluorescence (XRF) and, therefore, the data does not exist to determine the quantities or size distributions of these elements.

Table 4.25. Size Distribution of Melter Effluent by Element

Series	>23 μm (wt.%)	>8.2 μm (wt.%)	>1.6 μm (wt.%)	<1.6 μm (wt.%)
Ag	5	1	4	90
Al	35	4	12	49
Ba	37	0.0	6	57
Ca	46	4	34	16
Cd	10	1	8	81
Ce	33	4	23	39
Cl	2	0.3	1	96
Cr	4	28	0.0	68
Cs	3	0	2	94
Cu	27	2	16	54
F	15	1	5	79
Fe	52	9	32	7
I	1	1	1	1
Mn	56	5	33	6
Mo	9	2	7	81
Nb	53	0	9	39
Nd	57	2	41	1
Ni	48	11	30	11
P	12	0	6	82
Pb	22	1	12	66
Rb	8	1	6	86
S	2	0.2	1	97
Sb	49	4	10	37
Se	5	1	5	89
Si	40	1	7	52
Sn	1	1	1	1
Sr	51	3	31	15
Te	2	1	6	92
Zn	49	3	30	18
Zr	55	3	35	7

Certain species are evolved from the melter primarily as gases, rather than as condensed-phase aerosols. These are Cl, F, I, P, and S. Although these elements exist as gaseous species in the melter exhaust, these species may condense further on in the off gas lines or scrubbers. The presence of these elements in gases was determined by analysis of the NaOH scrub solutions after the filter in the off gas sample train as was described in Section 3.2. The percentages of these elements present in the melter off gas as gases are shown in Table 4.26. The exact species or distributions of species for these elements was not determined during LFCM-8; the results indicate only that the element is present as a gaseous species.

Table 4.26. Gaseous Melter Effluent Losses

Element	Element Losses from Melter Due to Gaseous Escape (%)				
	Ser-05	Ser-07	Ser-13	Ser-18	Average
Cl	83	81	82	91	84
F	97	88	91	97	93
I	100	100	100	100	100
P	97	72	85	50	76
S	77	84	82	87	82

Elemental and total mass melter decontamination factors are shown in Table 4.27. Total DFs are reported (including gases and condensed-phase aerosols). The elemental DFs reported are for the average of four sets of samples that were analyzed for composition. The total mass DF was determined from the average of 8 samples. The average mass DF (based on mass of metal oxides) is 1300. This value is consistent with the average melter DF of 1500 for PSCM-23. However, the variation in melter DFs from sample to sample was much smaller during PSCM-23 than during LFCM-8. Also, even though overall processing was more steady during PSCM-23 than during LFCM-8, the LFCM-8 aerosol sampling tests were run during relatively steady periods. Therefore, the reported melter DF of 1300 may be optimistic if applied to the entire LFCM-8 run.

The elements of primary interest during LFCM-8 (those listed in the objectives) were Cd, Pb, Te, Se, Sn, Sb, and I. Fairly good agreement was obtained among the four series for melter DFs for these elements. The DFs for these elements are lower than the overall mass DF for the melter. However, as stated before, many of these elements are potentially volatile. In the case of iodine, essentially all the iodine entering the melter in the feed is exhausted to the off-gas line.

With the exception of Nb, the elemental DFs are all lower than the overall mass DF (based on oxides) of 1300. This is because the elemental DFs were determined from analytical results, while the overall mass DF was determined from filter weights before and after sampling. Measurement uncertainties exist for both of these methods, primarily for the analytical results, because of the relatively small amount of sample available. As stated before, results for B, K, Li, Na, and Mg could not be obtained. Based on PSCM-23 results, the individual melter DFs for these elements should be equal to or greater than the average melter DF, with the exception of Na, which may be lower by a factor of five.

4.10.2 Submerged Bed Scrubber (SBS) Performance

The SBS is the first piece of filtration equipment in the melter off-gas system. The primary purpose of the SBS is to quench the hot melter off gas and capture a majority of the larger particulate. The SBS is not specifically designed to scrub gas-phase effluents, although this does occur to a small extent. The aerosol capture performance of the SBS was determined by drawing samples isokinetically

Table 4.27. Melter Decontamination Factors

	Melter Decontamination Factor (DF)				
Element	Ser-05	Ser-07	Ser-13	Ser-18	Average
Ag	59	51	67	61	60
Al	500	346	351	80	319
Ba	944	531	682	430	647
Ca	623	651	1038	465	694
Cd	260	195	339	205	250
Ce	813	736	569	386	626
Cl	3	2	6	4	4
Cr	188	378	528	176	317
Cs	109	75	148	181	128
Cu	453	526	737	450	541
F	3	2	8	2	4
Fe	698	813	969	478	739
I	1	1	1	1	1
Mn	693	882	999	537	778
Mo	160	145	299	181	196
Nb	2460	2645	2523	1344	2243
Nd	832	1008	1076	599	879
Ni	623	824	994	445	722
Pb	504	463	587	417	493
P	12	49	35	122	54
Rb	243	192	338	395	292
Sb	152	568	51	87	214
Se	3	3	4	6	4
Si	738	1158	844	795	884
Sn	1631	322	746	897	899
S	7	7	15	10	10
Sr	656	850	924	516	736
Te	23	13	42	29	27
Zn	398	518	472	171	390
Zr	792	862	961	552	792
Total	--	--	--	--	1300

from the off-gas lines before and after the SBS and determining total mass, size distributions, and compositions for each sample. The chevron demister is included as part of the SBS for the purposes of determining aerosol capture and gas-scrubbing efficiency. No separate data was taken during LFCM-8 for the demister.

The size breakdown of SBS effluent is shown in Table 4.28. These results are an average of 11 separate samples. By comparison with Table 4.24, it is clear that the size distribution of aerosols leaving the SBS is more highly concentrated in the smaller particles than in the stream entering the SBS. Approximately 86% of the mass exiting the SBS consists of particles with aerodynamic diameters of <1 micron.

The SBS decontamination factors for individual elements and total mass (on an oxide basis) are shown in Table 4.29. Total DFs are reported (including gases and condensed-phase aerosols). The elemental DFs were determined from the average of four separate samples, which were analyzed for composition. The total mass DF was determined from the average of 8 separate samples.

The overall mass DF of 5.0 compares well with the SBS DF for PSCM-23 of 7.4. The mass DFs during LFCM-8 ranged from 2.0 to 6.9. However, there was no identifiable correlation between length of time into the melter run and SBS DF. As was discussed in Section 4.8, the SBS packing was blown out of the bed at some point during the run because of a faulty weld in the top screen. This likely occurred during LFCM-8B. The last samples of SBS effluent were taken on May 14, 1993, two days before the end of the melter run. Assuming the packing was lost before this time, there was no detectable effect on SBS DF due to the absence of packing. In this case, the distribution plate and/or turbulence of the bubbling gas were sufficient for quenching and scrubbing the off gas. However, because of the uncertainty in the time of the packing loss, definitive tests would need to be conducted without SBS packing to confirm this.

The lack of significant change in SBS DF with time also suggests that the aerosols in the SBS effluent were primarily due to breakthrough rather than entrainment of the SBS solution. If entrainment of the solution contributed significantly to the downstream solids loading, the SBS DF would have been expected to decrease noticeably with buildup of material in the SBS. These results agreed with earlier calculations, which indicated that entrainment of SBS solution did not contribute to a significant portion of solids loading downstream of the SBS during normal melter feeding conditions (Anderson et al. 1993).

The elemental DFs were highest for Al, Fe, Nd, and Zr. These elements were more highly concentrated in the larger-size fraction of particles leaving the melter, and were scrubbed more efficiently than the smaller particles. Determining DFs for Cd, Pb, Te, Se, Sn, Sb, and I were of primary importance for LFCM-8. The SBS DF for iodine was found to be one; in other words, within measurement accuracy, no iodine was scrubbed out in the SBS. The other elements of interest showed average DFs ranging between 2 and 10, with the exception of one high value for Sn. Most of these elements are present in the melter effluent mainly as submicron particles, and are therefore inefficiently scrubbed in the SBS. As mentioned earlier, many of the samples were not sufficient for XRF analysis and, therefore, the elemental DFs can only be considered to be semi-quantitative because the accuracy of the values is not known.

Table 4.28. Size Distribution of SBS Effluent

Size (μm)	19.6	11.7-19.6	4.7-11.7	2.8-4.7	1.8-2.8	1.0-1.8	0.5-1.0	<0.5
Wt %	2.8	2.8	1.8	2.1	4.1	3.9	10.1	72.4

Table 4.29. SBS Decontamination Factors

Element	SBS Decontamination Factor (DF)				
	Ser-05	Ser-07	Ser-13	Ser-18	Average
Ag	2	2	3	3	3
Al	516	796	5	12	332
Ba	128	2	2	3	34
Ca	53	12	55	18	34
Cd	3	3	4	4	4
Ce	103	2	4	4	28
Cl	15	18	9	3	11
Cr	6	4	3	9	6
Cs	2	2	2	2	2
Cu	8	6	9	13	9
F	235	292	22	38	147
Fe	919	314	391	2458	1020
I	1	1	1	1	1
Mn	49	81	55	126	78
Mo	3	3	5	4	4
Nb	2	2	3	5	3
Nd	786	419	647	95	487
Ni	9	20	15	53	24
Pb	5	7	10	8	7
P	4	3	4	1	3
Rb	3	3	3	3	3
Sb	1	17	2	2	5
Se	3	3	4	3	3
Si	6	5	4	4	5
Sn	7	121	2	3	33
S	11	10	7	6	9
Sr	17	13	16	14	15
Te	2	3	5	3	3
Zn	3	21	47	5	19
Zr	1566	994	1419	1383	1340
Total	–	–	–	–	5.0[(a)]

(a) Based on total mass.

Cation and anion concentrations in the SBS over the duration of LFCM-8 are shown in Figures 4.37 and 4.38. Concentrations of ions increased sharply during the first several days of LFCM-8 and leveled off or dropped during the last few days of the run. The pH in the SBS solution showed a corresponding sharp decrease during the first few days of the run before attaining an approximately steady value of 1.4 for the last five days of LFCM-8. The leveling off and drop in ion concentrations

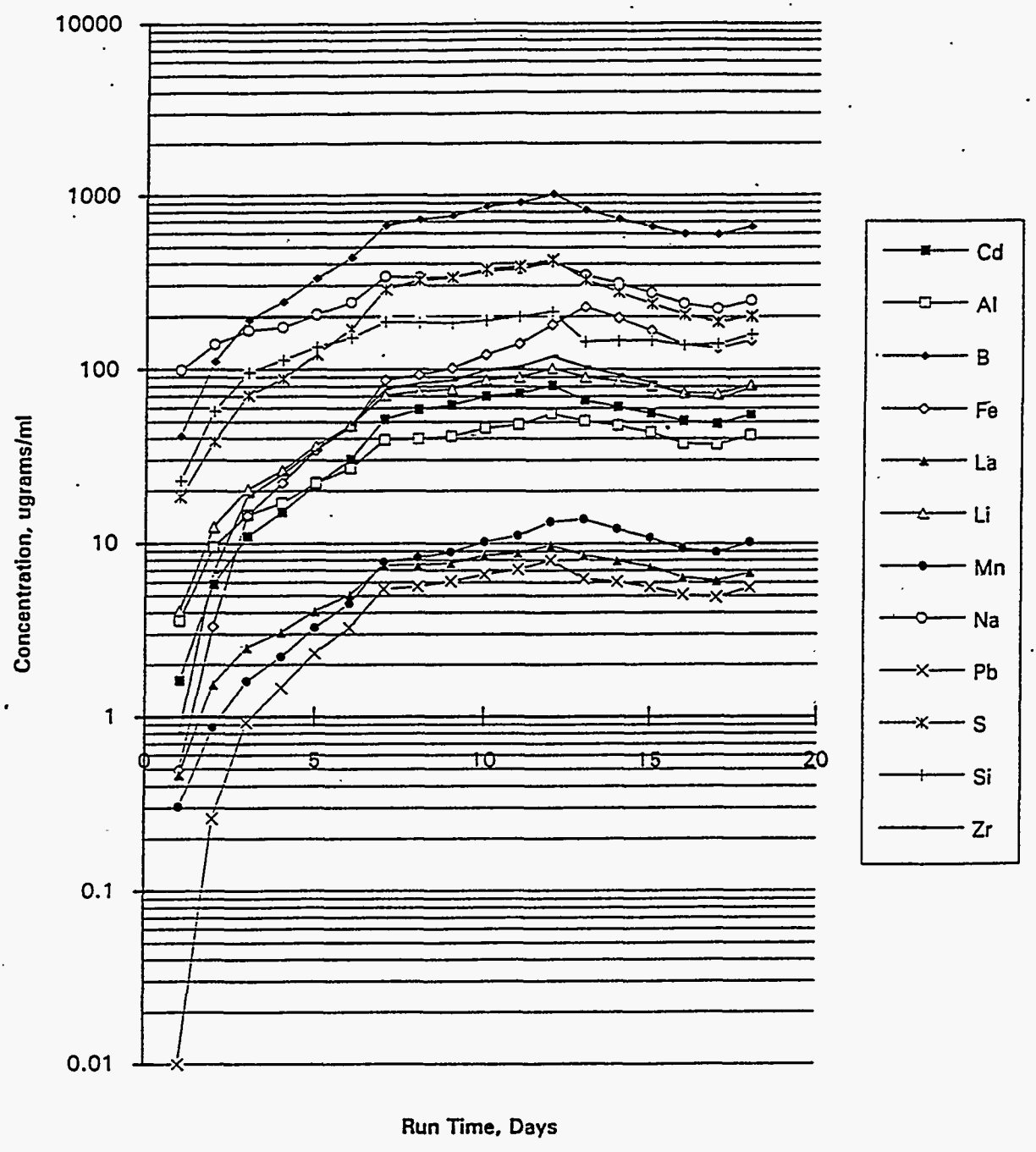

Figure 4.37. Submerged Bed Scrubber Anion Concentrations

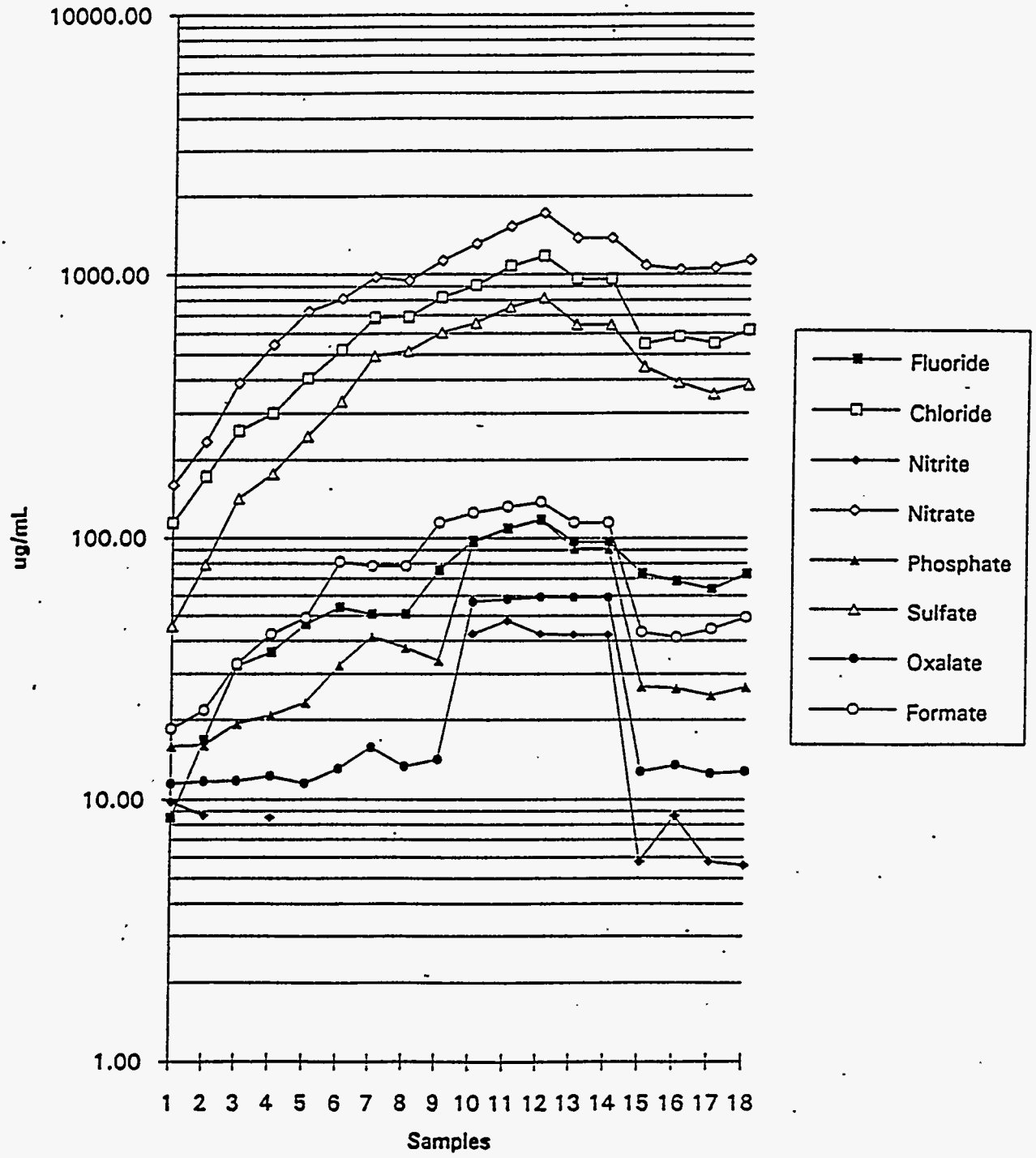

Figure 4.38. Submerged Bed Scrubber Cation Concentrations

stream entering the HEME during PSCM-23; however, PSCM data is not available to confirm this. In addition, lower flow rates through the SBS and demister during PSCM-23 may have led to lower re-entrainment of water droplets. Higher re-entrainment from the SBS during LFCM-8 may have caused the lower HEME DF.

4.10.4 HEME Performance Measured by Electrical Aerosol Analyzer (EAA)

As described in Section 3.3, the EAA was used to characterize the performance of the HEME. EAA measurements were made difficult by the fact that the aerosol source from the SBS may vary over the 2 minutes required to obtain a size distribution. Figure 4.39 provides an illustration of the variability in the total current over time. The figure shows the total electrometer current measured twice over 5 minute intervals and one period of 10 minutes over which the concentration is tracked. Because the EAA measures the total electrometer current and then measures differences as the voltage is increased, changes in the total aerosol concentration interfere with determination of the smallest aerosol particles. Because of this, the majority of measurements were started with channel 3, in effect collecting all particles in the 0.0035-to 0.019-micron size range into channel 3. In addition, the uncertainty in channel 3 is greater than in higher channels because of this drift in total signal strength.

Diluter Operation. The TSI model 3302 diluters were set at the specified pressure drops associated with the capillary installed to achieve the desired dilution. The dilution ratio of each diluter was qualitatively verified by sampling room air with the EAA with and without passing through the diluter. Additional measurements were made with post-HEME offgas. The verifications are qualitative because the stability of the source cannot be assured. Measurements indicated that the diluters were operating properly.

Characterization of Aerosols from SBS. On May 14, 1993 between 10:55 and 11:10 a series of 6 consecutive measurements of size distribution were obtained from the port in front of the HEMF with the HEME in the bypass position. The results of these measurements are consistent with other measurements where fewer measurements were made. Figure 4.40 shows the size distribution based on numbers of particles/cm^3 of off gas in each particle size range. The particle size ranges (identified as channels on the x-axis) represent approximately evenly spaced particle size ranges on a log scale, although the actual cut points are defined during the calibration of the instrument. The same information is provided in the form of a volume distribution in Figure 4.41. This distribution would more closely represent a characterization of the mass of aerosol that passes through the HEME.

Characterization of HEME DF. The best EAA data collected for determination of HEME DF was collected on May 12, 1993 between 13:29 and 13:46. First, a series of three consecutive measurements were made of the SBS exit concentration with the off gas bypassing the HEME. Then the off gas was rerouted through the HEME and an additional three measurements were made downstream of the HEME. The measurements taken upstream and downstream of the HEME are separated by approximately 10 min., which was required to reroute the off gas through the HEME. These data are preferred for determination of the HEME DF because the data upstream and downstream of the HEME were taken within a period of 17 min. during which the melter system was relatively steady. This makes a steady melter aerosol source more likely. Additional measurements are included in summary Tables 4.30 (HEME bypassed) and 4.31 (HEME effluent) although only the six measurements on May 12, 1993 are used for the HEME DF calculation.

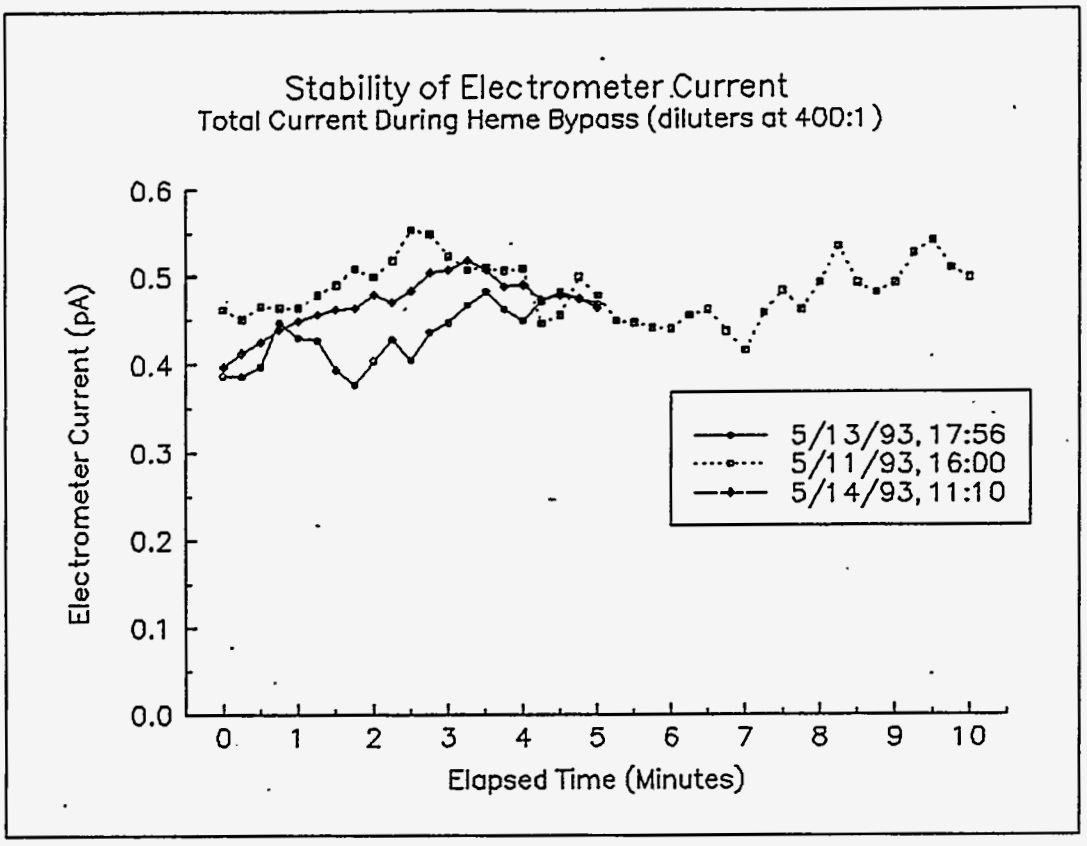

Figure 4.39. Variability in EAA Electrometer Current Over Time. Figure shows the EAA electrometer current produced over time while the off gas is configured to bypass the HEME and the aerosol sample is being withdrawn downstream of the heat exchanger at the HEMF inlet.

The distribution of the particle size on a volume basis while the off gas was bypassing the HEME is shown in Figure 4.42. The data shown here is the average of the 3 consecutive measurements and would indicate the mass distribution by size range if density were not size-dependent. The average of the final two measurements made after the HEME was valved in is shown in Figure 4.43. Based on the results of these measurements, a mass DF for the HEME is estimated to be 317. The mass DF estimated on the basis of the single filter sample taken behind the HEME was 107. This was less than observed during PSCM-23 where a DF of 1400 was observed (although DF values as low as 340 were also recorded during PSCM-23). The observed reduction in the HEME DF is likely related to the off gas flow rate through the HEME. During PSCM-23, the flow ranted 110 to 170 SCFM while during LFCM-8, offgas flows were 275 SCFM during the EAA HEME DF measurements and in the range of 250 to 350 SCFM during most of the test.

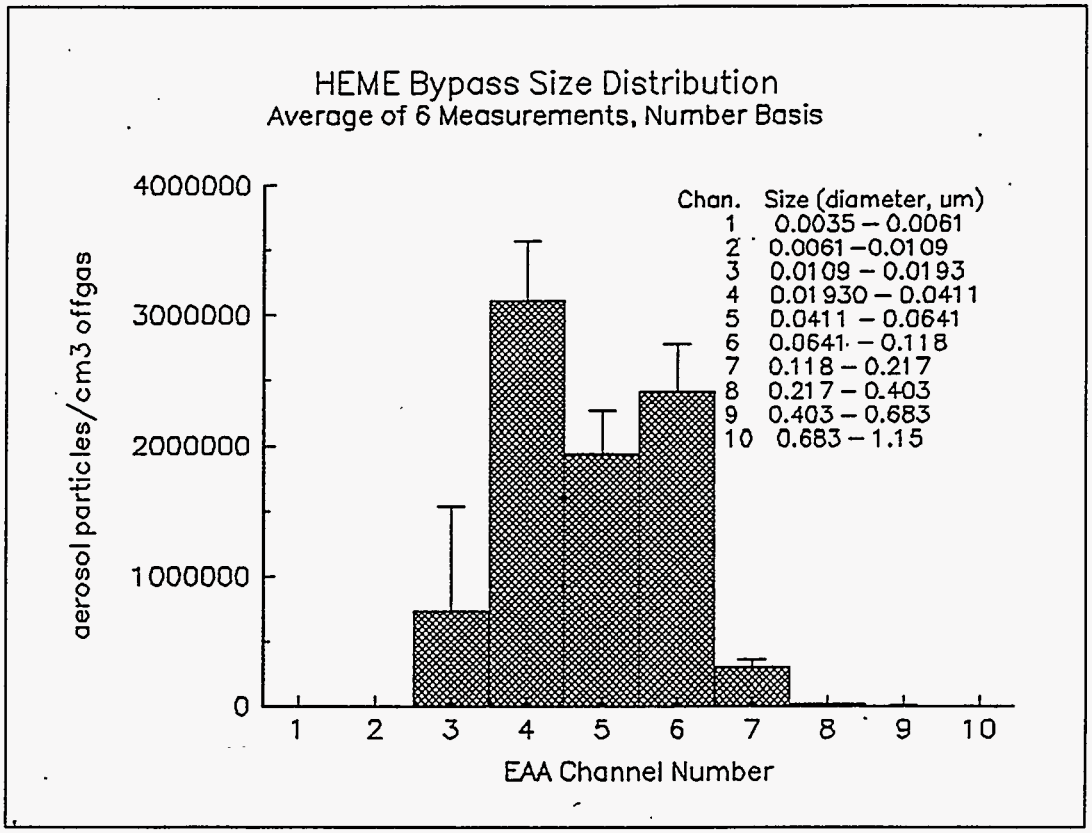

Figure 4.40. Particle Number Distribution From SBS During HEME Bypass. Measured downstream of heat exchanger at HEMF inlet.

Characterization of HEME DF. The best EAA data collected for determination of HEME DF was collected on May 12, 1993 between 13:29 and 13:46. First, a series of three consecutive measurements were made of the SBS exit concentration with the off gas bypassing the HEME. Then the off gas was rerouted through the HEME and an additional three measurements were made downstream of the HEME. The measurements taken upstream and downstream of the HEME are separated by approximately 10 min., which was required to reroute the off gas through the HEME. These data are preferred for determination of the HEME DF because the data upstream and downstream of the HEME were taken within a period of 17 min. during which the melter system was relatively steady. This makes a steady melter aerosol source more likely. Additional measurements are included in summary Tables 4.30 (HEME bypassed) and 4.31 (HEME effluent) although only the six measurements on May 12, 1993 are used for the HEME DF calculation.

The distribution of the particle size on a volume basis while the off gas was bypassing the HEME is shown in Figure 4.42. The data shown here is the average of the 3 consecutive measurements and would indicate the mass distribution by size range if density were not size-dependent. The average of the final two measurements made after the HEME was valved in is shown in Figure 4.43. Based on

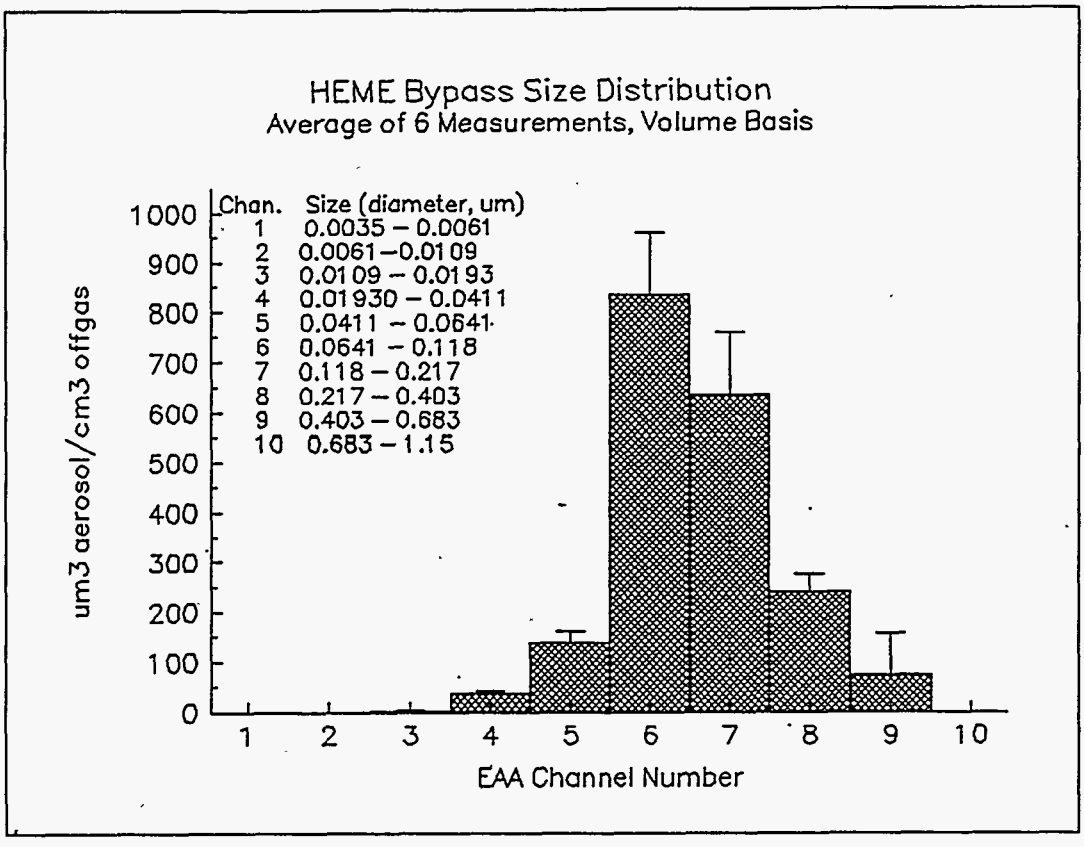

Figure 4.41. Particle Volume Distribution From SBS During HEME Bypass. Measured downstream of heat exchanger at HEMF inlet.

the results of these measurements, a mass DF for the HEME is estimated to be 317. The mass DF estimated on the basis of the single filter sample taken behind the HEME was 107. This was less than observed during PSCM-23 where a DF of 1400 was observed (although DF values as low as 340 were also recorded during PSCM-23). The observed reduction in the HEME DF is likely related to the off gas flow rate through the HEME. During PSCM-23, the flow ranted 110 to 170 SCFM while during LFCM-8, offgas flows were 275 SCFM during the EAA HEME DF measurements and in the range of 250 to 350 SCFM during most of the test.

Comparison of EAA Results to Filter and Impactor Samples

Post-HEME. The total volume indicated by the EAA aerosol size (volume) distributions (such as in Figure 4.44) can be compared to the single filter sample collected over a period of approximately 48 hours from behind the HEME. If the aerosol mass collected in the filter sample is extrapolated to the volume indicated by the average of all EAA post-HEME analyses, the implied aerosol density is 14.5 g/cm^3. This is greater than the expected density of the aerosols (the specific gravity of amorphous SiO_2 would be 2.2, and even very heavy aerosols such as PbO would only have a specific gravity of

Table 4.30. Particle Size Distribution on Volume Basis During HEME Bypass

Sample Date (1993)	5/10	5/10	5/12	5/12	5/12	5/12	5/13	5/13
Sample Time	11:45	14:10	~12:00[b]	13:29	13:31	13:33	17:47	17:49
Off-Gas Flow (SCFM)	271	270	264.8	268.4	274.2	268.8	179	178
HEMF Exit Temp (°C)	77	78	78	80	80	80	84	84
Melter Feed Rate (l/hr)	66	51	63	65	65	65	50	50
Melter Inleakage (SCFM)	101	116	124	122	127	123	102	101
Mean Particle Diameters (μm)	$\mu m^3/cm^3$							
1. 0.0035 - 0.0061	0.95[a]	0.95[a]	0	0	0	0	0	0
2. 0.0061 - 0.0109	1.88[a]	0	0	0	0	0	0	0
3. 0.0109 - 0.0193	0	0	2.11	0.42	0	0	3.66	0
4. 0.0193 - 0.0411	54.07	38.30	37.40	51.37	29.7	64.9	56.32	26.1
5. 0.0411 - 0.0641	203.8	156.8	108.2	169.3	192.8	189.7	203.8	192.8
6. 0.0641 - 0.118	1107	805.1	618.9	709.5	1042	910.8	976.2	1062
7. 0.118 - 0.217	572.0	572.0	457.6	495.8	673.7	572.0	673.7	686.4
8. 0.217 - 0.403	200.6	200.6	160.5	80.3	200.6	160.5	240.8	160.5
9. 0.403 - 0.683	0	0	0	0	0	0	0	0
10. 0.683 - 1.15	0	0	0	0	0	0	0	0
Total $\mu m^3/cm^3$	2140	1774	1385	1507	2139	1908	2155	2128

Table 4.30. (contd)

Sample Date (1993)	5/13	5/13	5/14	5/14	5/14	5/14	5/14	5/14
Sample Time	17:51	17:53	10:54	10:57	11:00	11:02	11:05	11:08
Off-Gas Flow (SCFM)	177	179	85	86	85	82	88	88
HEMF Exit Temp (°C)	84	84	82	82	82	82	82	82
Melter Feed Rate (l/hr)	51	51	62	62	62	62	62	62
Melter Inleakage (SCFM)	103	104	25	25	22	20	26	27
Mean Particle Diameters (μm)	um^3/cm^3							
1. 0.0035 - 0.0061	0	0	0	0	0	0	0	0
2. 0.0061 - 0.0109	0	0	0	0	0	0	0	0
3. 0.0109 - 0.0193	1.69	2.67	0.84	0	2.67	0.70	2.82	0
4. 0.0193 - 0.0411	36.5	42.4	38.3	27.0	35.6	41.5	41.5	35.2
5. 0.0411 - 0.0641	163.1	117.6	123.9	138.0	97.2	155.2	150.5	156.8
6. 0.0641 - 0.118	910.8	855.4	764.8	920.8	749.7	759.8	744.7	1052
7. 0.118 - 0.217	572.0	597.5	584.7	737.3	610.2	495.8	559.3	826.3
8. 0.217 - 0.403	80.3	160.5	240.8	280.9	240.8	200.6	200.6	280.9
9. 0.403 - 0.683	0	0	0	0	0	149.1	149.1	149.1
10. 0.683 - 1.15	0	0	0	0	0	0	0	0
Total $\mu m^3/cm^3$	1764	1776	1753	2104	1736	1803	1849	2500

(a) Data for channels one and two are not reliable due to drift in total electrometer current.
(b) Time is estimated, possibly in error $\pm$15 minutes.

Table 4.31. Post-HEME Size Distribution on Volume Basis

Sample Date	5/11/93	5/11/93	5/11/93	5/12/93	5/12/93	5/12/93
Sample Time	15:30[a]	15:35[a]	15:40[a]	13:42	13:44	13:46
Off-Gas Flow (SCFM)	255	260	256	261	264	264
HEMP Exit Temp (°C)	89	89	89	80	80	81
Melter Feed Rate (l/hr)	57	57	56	67	67	67
Melter Inleakage (SCFM)	107	110	109	111	113	113
Mean Particle Diameter (μm)	$\mu m^3/cm^3$					
1. 0.0035 - 0.0061	0	0	0.0002[b]	0	0	0
2. 0.0061 - 0.0109	0	0.004[b]	0.0023[b]	0	0	0
3. 0.0109 - 0.0193	0	0.002	0.0004	0	0.013	0
4. 0.0193 - 0.0411	0.023	0.026	0.0665	0.048	0.079	0.019
5. 0.0411 - 0.0641	0.314	0.259	0.231	0.466	0.365	0.392
6. 0.0641 - 0.118	3.522	3.145	2.84	3.56	3.01	3.18
7. 0.118 - 0.217	2.542	2.860	2.77	02.01	1.88	1.88
8. 0.217 - 0.403	0	1.003	0.803	0.201	0.301	0.301
9. 0.403 - 0.683	0	0	0.746	0	0	0
10. 0.683 - 1.15	0	0	0	0	0	0
Total ($\mu m^3/cm^3$)	6.40	7.30	7.46	6.28	5.64	5.77

(a) Estimated time, ±20 min.
(b) Results in channels 1 and 2 are unreliable due to drift in total electrometer current.

4.10.5 High Efficiency Metal Fiber (HEMF) Filter Performance

The EAA, described previously in Section 3.2.2, was also used to characterize the performance of the HEMF filter. A schematic of the experimental sampling configuration for the EAA was shown previously in Figure 3.4.

Early Difficulties. No results were obtained in the first half of LFCM-8. During initial operation, the wire filament of the charger assembly burned out and shorted against the screen in the charger assembly. A new charger assembly was procured and installed in the instrument. It was then discovered that the shorting of the filament when it burned out had caused damage to the electrical circuitry of the instrument. Another analyzer of the same model was located on site and parts were borrowed from that instrument to allow repair. The additional damaged parts included the electrometer operational amplifiers (J310) and operational amplifiers U2 and U4 (refer to circuit diagram in manual). Once the repairs were completed, the device again began operating normally.

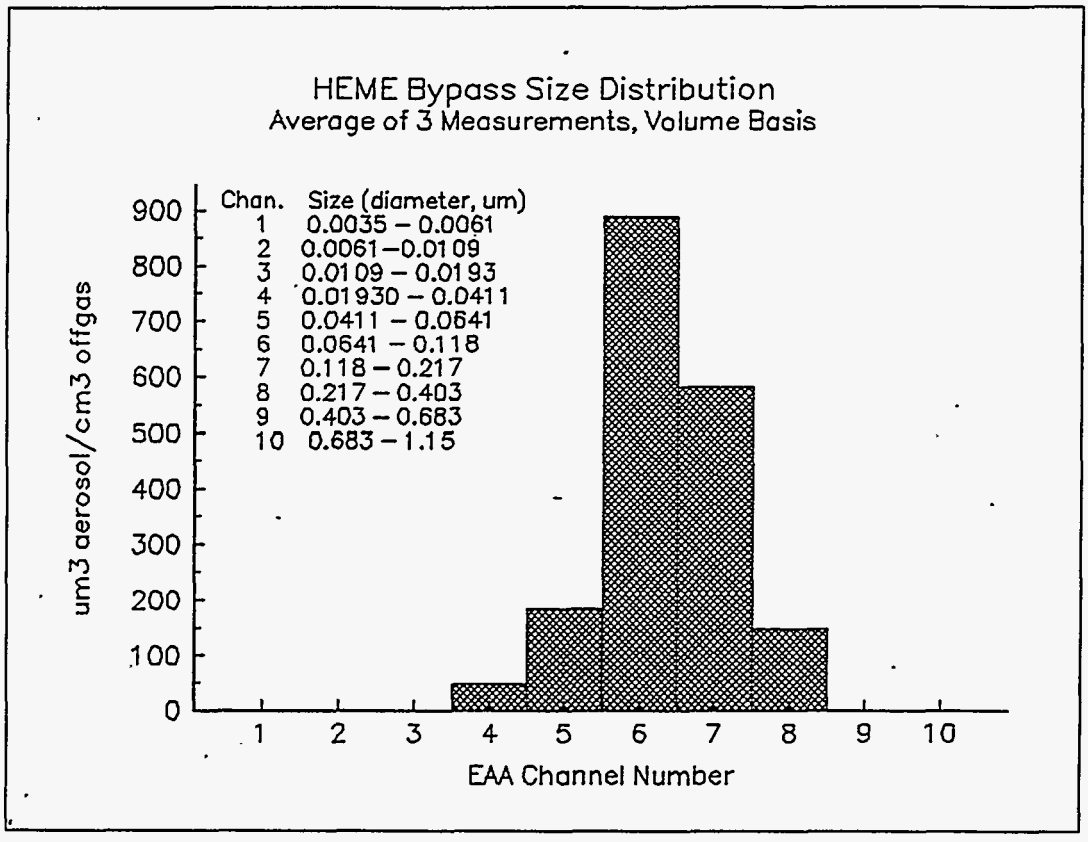

Figure 4.42. Size Distribution During HEME Bypass (Volume Basis)

9.5). However, this is considered reasonably good agreement. It should be noted that the EAA samples and the single filter sample do not overlap in time and that the post-SBS concentration may vary by a factor of four depending on the sample time selected during the run.

Results. The HEMF filter was extremely efficient and the concentration downstream of the filter was always below the detection limit of the electrical aerosol analyzer. Therefore, there is no downstream particle size distribution information and all DF results are presented as "greater-than" values and depend upon the strength of the aerosol source entering the filter. To calculate the DF value, it was assumed that a 0.001 pA change in current could have been detected as the voltage was stepped through the series of voltages on the collector rod. The sensitivity used to determine the DF corresponded to the 0.087 μm particle size. This cut point was selected because it is close to the 0.1 μm particle size used in the DF specification of the filter and because the off gas upstream of the filter contained a large number of particles in this size range. This detection limit should be considered approxi mate. In addition, the DF is calculated for all of the aerosol sizes in the source to the filter to improve the detection limit. However, the filter specification is intended to apply at 0.1 μm. Table 4.32 provides the results of all valid measurements of the DF across the filter. Results are provided both on the

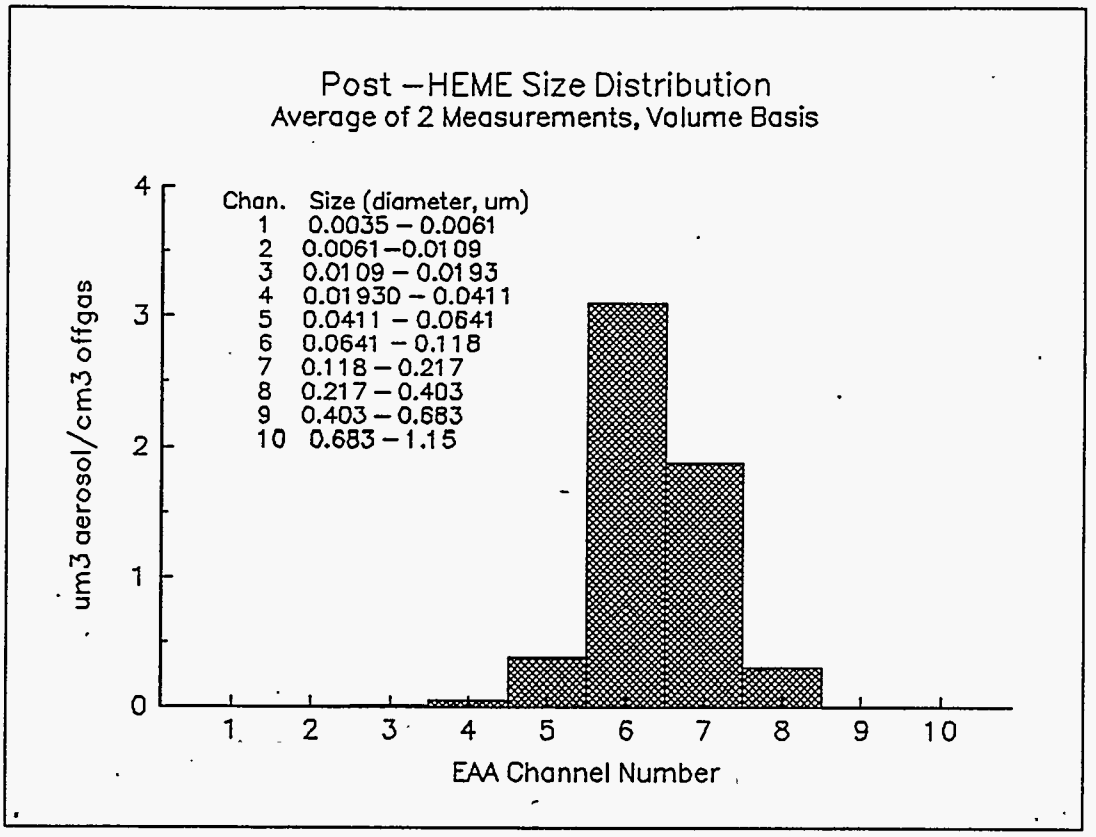

Figure 4.43. Size Distribution With HEME In Line (Volume Basis)

bases of both particle number and particle volume (which would correspond to a mass DF). As a comparison, the performance requirement placed on the filter is a DF of $1x10^5$ (1e-5 penetration) at 0.1 μm corresponding to two HEPA filters in series with a 1000 DF in the first and a 100 DF in the second. Based on the available data, all measurements exceeded a 10^5 DF when the entire particle size range is considered. Table 4.32 provides the volume basis DF using only the particles detected in the 0.0641 to 0.118 μm (log-mean 0.087μm) size range. These are also all minimum DF values due to the lack of detection downstream of the filter. However, all of the values are less than 10^5 DF.

In summary, the results indicate that the filter exceeded the 10^5 DF when evaluated using the full particle size distribution obtained while bypassing the HEME. For particles having approximately 0.1 μm diameter the results are not conclusive that this performance criteria was met because of the detection limit. However, there was every indication that the filter was functioning properly from a particle removal standpoint. Measurements of HEMF DF in the 0.064 - 0.118 μm size range varied from $>4.9 \times 10^4$ to $>8.8 \times 10^4$. In no case were aerosol particles detected downstream of the HEMF. To obtain a measured value downstream of the HEMF, which demonstrates the 10^5 DF at

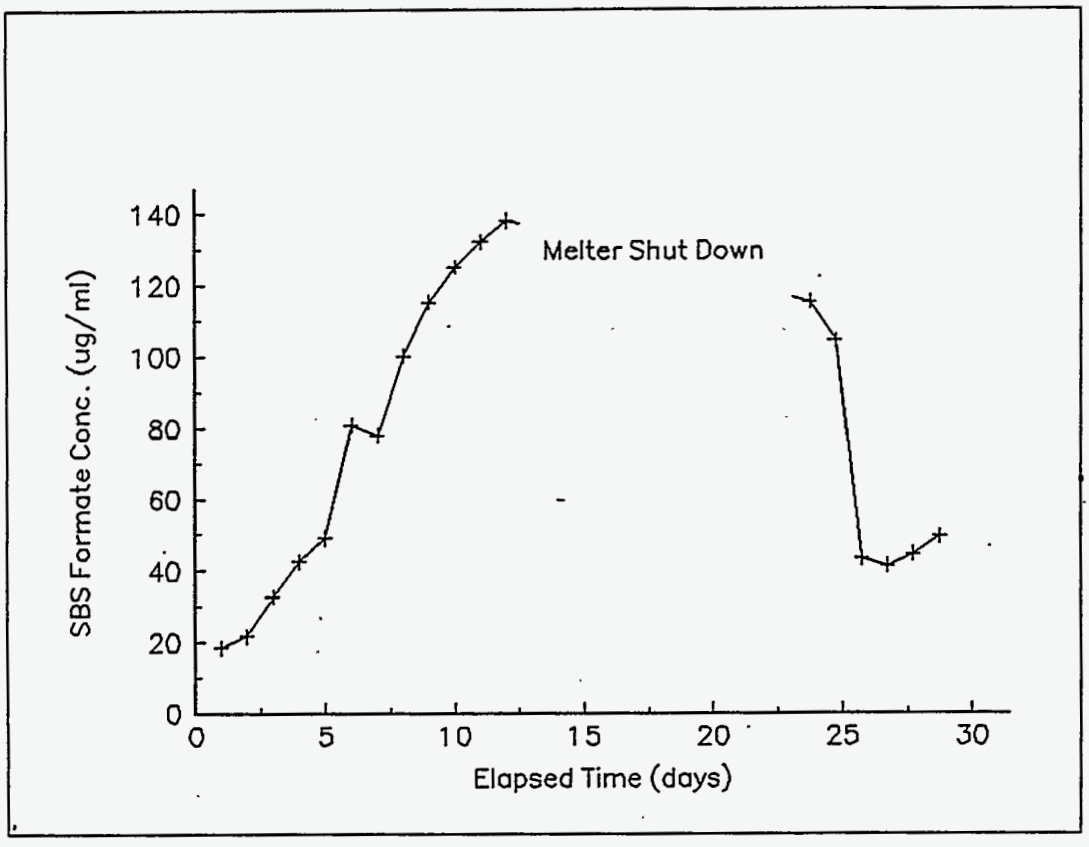

Figure 4.44. Formate Concentration in the SBS During LFCM-8

0.1 μm, requires either a more concentrated aerosol source or a more sensitive measurement device. To make such a measurement successful with the same instrument would require a more concentrated aerosol source.

4.11 Organic Destruction and Removal Efficiency (DRE)

The method used for determining organic destruction and removal efficiency (DRE) for the melter and off-gas system was described in Section 3.2.2. The DRE was determined for formic acid (or formate ion) as a preliminary indication of the DRE for organics in general. The destruction of formate was determined to be at least 99.8% efficient. The DRE result has been downgraded due to unexplained discrepancy in the results of analysis of SBS scrub solution samples and condensate samples and may actually be higher.

Table 4.32. DF Measurements of HEMF Filter

Measurement		Total Distribution DF (≥)		DF for 0.064 μm - 0.118 μm Particles (≥) (Volume Basis)	HEMF Process Conditions		
Date	Time	Number Basis	Volume Basis		Exit Temperature (°C)	Flow rate (SCFM)	HEMF Pressure Drop (in. WC)
5/10	11:45	9.9×10^5	1.7×10^5	8.8×10^4	77	271	~2.5[a]
5/10	14:10	7.3×10^5	1.4×10^5	6.4×10^4	78	270	~2.5[a]
5/12	~12:00	2.2×10^5	1.1×10^5	4.9×10^4	78	265	2.85
5/12	13:29	2.6×10^5	1.2×10^5	5.7×10^4	80	268	3.33
5/12	13:31	2.4×10^5	1.7×10^5	8.3×10^4	80	274	3.41
5/12	13:33	3.1×10^5	1.5×10^5	7.2×10^4	80	269	3.34
5/13	17:47	3.6×10^5	1.7×10^5	7.7×10^4	84	179	13.8
5/13	17:49	2.3×10^5	1.7×10^5	8.5×10^4	84	178	13.8
5/13	17:56	2.6×10^5	1.4×10^5	7.2×10^4	84	177	13.8
5/13	17:53	2.7×10^5	1.4×10^5	6.7×10^4	84	179	13.8
5/14	10:54	2.2×10^5	1.4×10^5	6.1×10^4	82	85	~16.2[a]
5/14	10:57	2.0×10^5	1.7×10^5	7.4×10^4	82	86	~16.2[a]
5/14	11:00	2.4×10^5	1.4×10^5	6.1×10^4	82	85	~16.2[a]
5/14	11:02	2.4×10^5	1.4×10^5	5.9×10^4	82	82	~16.2[a]
5/14	11:05	2.7×10^5	1.5×10^5	6.0×10^4	82	88	~16.2[a]
5/14	11:08	2.4×10^5	2.0×10^5	8.4×10^4	82	88	~16.2[a]

(a) Approximate ΔP Determined from Difference of Absolute Pressure Measurements on Either Side of HEMF Filter. Time of pressure measurement does not match time of aerosol measurement.

The DRE was determined by the following equation:

$$DRE = \frac{m_i - m_f}{m_i} \quad (4.2)$$

where: m_i = the amount (μg) of formate entering the melter over the sample period
m_f = the amount (μg) of formate contained in the off gas entering the submerged bed scrubber (SBS), if examining destruction in the melter, or exiting the SBS or HEME for overall DRE over the sample period.

The amount of formate entering the melter, m_i, was calculated by multiplying the average melter feed rate over the sampling period by the formate ion concentration in the melter feed and the sample duration. The formate concentration in the melter feed was determined from a daily analysis of a melter feed sample. The formate concentration in the melter feed varied from 36.5 g/L to 45.5 g/L over the testing period. The formate concentration in the feed was determined using ion chromatography. The amount of formate leaving the melter system was determined from the composition of condensate samples taken after the SBS and after the HEME.

To determine the DRE from a condensate sample, the sample gas was assumed to be saturated, leaving the condenser at 15°C. This temperature was not measured. However, it was consistent with mass values measured for condensate and weight gain on desiccant columns following the condenser. The calculation was not sensitive to this temperature, changing only about 15% as the condenser exit temperature assumption was changed from 0°C to 25°C. From an IC analysis of the condensate for formate and an equilibrium calculation of the condenser exit gas, the ratio of formate to water in the off-gas line could be determined. Then, from the flow rate in the off-gas line and an assumption of saturation at the SBS exit, the total flow of formate out of the system was determined. For samples taken before the SBS, the water content in the line was taken as equivalent to the moisture in the feed provided to the melter over the sample period. The resulting calculated quantity of formate in the off-gas line was then compared to the formate fed to the melter as described above.

A summary of melter destruction results calculated based on samples taken upstream of the SBS is provided below. The percent destruction values neglect formate aerosol particles that may have been collected on the filter, since the amount was below the analytical detection limit. Some amount of formate may have existed in aerosol form and because it was below detection limits was not included in the DRE results. In addition, formate deposited in the off-gas line upstream of the sample point was not included in these values, although this contribution would be small.

Sample	Destruction (%)
4/28, series 11	99.959
4/28, series 12	99.963
5/11, series 15	99.945
5/11, series 17	99.964
5/13, series 19	99.939

Average = 99.954 % Destruction

Additional information on destruction can be obtained from the increase in SBS formate concentration over the first 12 days of the test, and the off-gas deposits observed at the conclusion of the melter test. Based on these pieces of information, the destruction of formate in the melter was $\leq$ 99.956%. This was very consistent with the average value obtained above, and indicated that a significant fraction of the formate was being scrubbed in the SBS during this period. The concentration of the SBS over time is shown in Figure 4.44. The concentration increased fairly steadily over the first 12 days until LFCM-8A was halted. The reason for the drop in concentration after LFCM-8B started is not known. However, lower air rates through the SBS during LFCM-8B, compared to LFCM-8A, would have resulted in additional water accumulation in the SBS. This would have led to a dilution in the anion concentrations measured in the SBS. A summary of DREs calculated based on condensate samples taken downstream of the SBS is provided below.

Sample	DRE (%)
4/27, post-HEME	99.950
4/27, post-HEME	99.939
5/13, post-SBS (series 19)	99.987
5/14, post-SBS (series 20)	99.995
Average = 99.968 % DRE	

The results indicate that the destruction in the melter was roughly 99.95%. The variability in the SBS formate concentration made estimation of downstream formate removal and subsequent DRE values questionable. If the SBS was increasing or decreasing in concentration, the downstream formate concentrations would be expected to be significantly affected. It is expected that the average DRE would almost equal the melter destruction efficiency. It may be a very small amount larger because of formate lost to the overflow from the SBS.

There are a couple of interesting points in the data. The largest DRE for formic acid (99.995% on May 14) was obtained when the off-gas flow conditions through the melter and SBS were minimized; i.e., melter inleakage was reduced. This had the effect of maximizing residence time of the off gases in the melter. The melter plenum pressure average was -1.9 in. WC, and the inleakage was estimated to be 21 SCFM. The higher measured DRE may be the result of actual higher destruction under these conditions.

A second point to note is that the all formate concentrations measured in the condensate samples (9 samples total) taken from the off-gas line were significantly lower in formate than those measured in the SBS solution. Based on the pure component vapor pressures and a Henry's Law Constant assumption, the condensate would be expected to be slightly enriched in formic acid compared to the SBS concentration. The result was examined in more detail by reanalysis of three of the off-gas condensate samples using a different analyst and IC equipment. The results from the reanalysis were higher than the initial analysis, but still lower than the SBS solution. A summary of the analysis results for the three reanalyzed samples is provided in Table 4.33.

Table 4.33. Comparison of Condensate Analysis and Reanalysis to SBS Scrub Solution Analysis

Associated Aerosol Sample Number	SBS Scrub Solution Analysis (μg/mL)	Post-SBS Offgas Condensate Analysis[a] (μg/mL)	Reanalysis of Post-SBS Off-gas Condensate Samples (μg/mL)
3-100-cond-03	Avg of 5 = 110	28.5	40
2-19-cond-01	41.3	10.4	21
2-20-cond-01	44.6	9.0	14.9

(a) Due to interference from fluoride, these results were obtained from a conservative manual splitting of peaks to avoid overstating the DRE. For the samples shown, concentrations were increased 10 to 20% over the result obtained from the computer split valves.

Unfortunately, the disagreement between initial and subsequent analysis results could not be resolved so it is not known which of the two condensate analyses is the better value. It is possible that some of the discrepancy between condensate and SBS scrub solution is related to analytical error. However, there are other possible factors as well.

There are several factors that make this sampling activity difficult. First, formic acid is known to react with NO_2 in acidic solutions to form CO_2 and HNO_2. Although the NO to NO_2 ratio in the off-gas line was more than 4:1, this still represents an excess of NO_2 with respect to the small formic acid concentration. There is a potential for some reaction occurring in either the off gas or the condensate sample. If the formic acid is consumed in the off gas, then it is appropriate to consider the loss as contributing to the overall DRE of the system. If reaction of formic acid were to occur in the condensate during sampling, this might contribute to lower concentrations in the condensate taken downstream of the SBS.

A second factor that complicates the analysis of the sampling operation is data which indicates that dilute formic acid solutions do not obey Henry's Law Constant. Data generated by Wiemers (1988) provided the vapor pressure over dilute formic acid solutions containing 0.54 and 0.99 wt.% formic acid at 10% and 50°C. The concentrations are higher than exist in the condensate, but the temperatures approximately correspond to the SBS and sampling condenser temperatures. In any case, it is the best available vapor pressure information over dilute formic acid solutions. The experimental results from Wiemers (1988) are repeated below in Table 4.34 with a comparison to what is predicted using a Henry's Law Constant assumption. As can be seen, Henry's Law Constant predicted vapor pressures may be in error by a factor of 2 to 5. In addition, this information would suggest an explanation for the lower downstream condensate samples, because the vapor pressure over the SBS solution would thus be predicted to be lower by a factor of 2 to 5. One piece of potentially conflicting data is the similarly low measurements made on condensate samples obtained from the SBS inlet. It is possible that these measurements could be low due to a gas phase reaction caused by the greater time at off-gas temperatures in the sampling train, or possibly due to some entrained aerosol formate (although formate on the filter was below detection).

Table 4.34. Deviation of Dilute Formic Acid solution from Henry's Law Constant Behavior (Reproduced from Wiemers 1988)

Temperature (°C)	HCOOH in Water (Wt.%)	HCOOH Content over solution[a] (ppm)	Predicted HCOOH assuming Henry's Law[b] (ppm)
10	0.54	11	57.5
10	0.99	17	105.5
50	0.54	66	369.2
50	0.99	267	677.2

(a) Data taken from Wiemers, 1988.
(b) For pure component vapor pressure data see Coolidge 1930.

A third potential factor complicating the analysis of the sampling is the possibility that the formic acid may form a dimer in the gas phase. If this occurs, the mass of formic acid in the gas phase is increased while the pressure is not. This phenomenon is discussed in detail by Coolidge (1928). However, by extrapolation of data from Coolidge, formation of significant quantities of the dimer in the gas phase is not expected due to the low concentrations existing in the melter off-gas system.

A possible explanation of the observed data is that the condensate samples taken downstream from the SBS are lower in formate due to the non-ideal vapor pressure relationship for formic acid. On the other hand, the samples taken upstream of the SBS may be lower in formate than the SBS due either to formate carried over from the melter in aerosol form or due to reaction in the sampling equipment due to the longer time at elevated temperature in the sampler than in the off-gas line. Analytical difficulties may be contributing to either of these observations and force some qualification of the data. Therefore, the estimate of melter destruction (and DRE) has been decreased from a calculated value of 99.95% to 99.80%, representing a factor of 4 greater formate penetration of the system than was measured. It is possible that higher DREs were achieved, but this is difficult to prove with the data available.

5.0 References

Coolidge, A. S. 1928. *The Vapor Density and Some Other Properties of Formic Acid.* Journal of the American Chemical Society, Vol. 50.

Coolidge, A. S. 1930. *The Vapor Pressure and Heat of Fusion and Vaporization of Formic Acid.* Journal of the American Chemical Society, Vol. 52.

Goles, R. W., and R. K. Nakaoka, principal investigators. 1990. *Hanford Waste Vitrification Project Pilot-Scale Ceramic Melter Test 23.* PNL-7142, Pacific Northwest Laboratory, Richland, Washington.

Hutson, N. D. 1993. *Integrated DWPF Melter System (IDMS) Campaign Report: Hanford Waste Vitrification Plant (HWVP) Process Demonstration (U).* WSRC-TR-92-0403, Rev. 2, Westinghouse Savannah River Company, Aiken, South Carolina.

May, T. H. 1992. *Hanford Waste Vitrification Plant Melter Testing Definition.* WHC-SD-HWV-ES-042, Westinghouse Hanford Company, Richland, Washington.

Nakaoka, R. K., and J. M. Perez Jr. 1986. *Hanford Waste Vitrification Plant Nonradioactive Liquid-Fed Ceramic Melter Testing for Fiscal Year 1986.* RHO-RE-CR-17 P. Prepared for Rockwell Hanford Operations by Pacific Northwest Laboratory, Richland, Washington.

Owen, R. K., and A. K. Postma. 1981. "Development of a Passive Self Cleaning Scrubber for Containment Venting Applications." CONF-801030, In *Proceedings of the 16th DOE Nuclear Air Cleaning Conference*, U.S. Department of Energy, Washington, D.C.

Perez, J. M., Jr., and R. K. Nakaoka. 1986. "Vitrification Testing of Simulated High-Level Radioactive Waste at Hanford." In *Proceedings of the Symposium on Waste Management '86*, Tucson, Arizona, Ed. R. G. Post, M. E. Wacks, Vol. II. pp. 495-505.

Wiemers, K. D. 1988. *Formic Acid Vapor Phase Concentrations Over Dilute Aqueous Solutions at the Proposed HWVP Condenser Operating Temperatures* Milestone HWVP-88-V110203A.

APPENDIX A Measuring & Testing Equipment Control Listing

TRANSMITTED TO RECORD CENTER

QA Plan WTC-006
Task 1.2.2.04.15
File Cat. 74.3.8.1
Page 1 of 3

Liquid Fed Ceramic Melter - MTE Control Listing

LINE ITEM #	CONTROL NO.	MATE DESCRIPTION	LOCATION	CALIBRATION INTERVAL	CUSTODIAN	CALIBRATING AGENCY	CATEGORY	REMARKS
1	1660	Pressure XDCR	EDL 102, 324 Bldg, Mod 17, Pos. 2	12 Months	LD Anderson	PNL	1	Off-Gas Flow Rate DP
2	698	Pressure XDCR	EDL 102, 324 Bldg, Mod 17, Pos. 4	12 Months	LD Anderson	PNL	1	Final Off Gas Flow Rate DP
3	1694	Pressure XDCR	EDL 102, 324 Bldg, Mod 17, Pos. 1	12 Months	LD Anderson	PNL	1	Compressed Air Flow Rate DP
4	700	Pressure XDCR	EDL 102, 324 Bldg, Mod 17, Pos. 6	12 Months	LD Anderson	PNL	1	Air Injection Flow Rate (Blower) DP
5	1080	Pressure XDCR	EDL 102, 324 Bldg, Mod 3	12 Months	LD Anderson	PNL	1	Air Injection Flow Rate (Melter) DP
6	1593	Pressure XDCR	EDL 102, 324 Bldg, Mod 11	12 Months	LD Anderson	PNL	1	Melter Plenum Pressure
7	1046	Pressure XDCR	EDL 102, 324 Bldg, Mod 3	12 Months	LD Anderson	PNL	1	Film Cooler DP
8	703	Pressure XDCR	EDL 102, 324 Bldg, Mod 17, Pos. 3	12 Months	LD Anderson	PNL	1	Film Cooler to SBS DP
9	1238	Pressure XDCR	EDL 102, 324 Bldg, Mod 17, Pos. 5	12 Months	LD Anderson	PNL	1	SBS DP
10	1079	Pressure XDCR	EDL 102, 324 Bldg, Mod 3	12 Months	LD Anderson	PNL	1	HEME DP
11	697	Pressure XDCR	EDL 102, 324 Bldg, Mod 17, Pos. 9	12 Months	LD Anderson	PNL	1	Off Gas Vacuum @ DOV
12	695	Pressure XDCR	EDL 102, 324 Bldg, Mod 3	12 Months	LD Anderson	PNL	1	Melter Plenum to Discharge DP
13	1081	Pressure XDCR	EDL 102, 324 Bldg, Mod 3	12 Month	LD Anderson	PNL	1	Demister DP
14	1041	Pressure XDCR	EDL 102, 324 Bldg, Mod 3	N/A	LD Anderson	PNL	3	SBS SpG
15	1082	Pressure XDCR	EDL 102, 324 Bldg, Mod 3	N/A	LD Anderson	PNL	3	SBS W.F.
16	702	Pressure XDCR	EDL 102, 324 Bldg, Mod 17, Pos. 8	12 Months	LD Anderson	PNL	1	Compressed Air Pressure
17	699	Pressure XDCR	EDL 102, 324 Bldg, Mod 3	12 Months	LD Anderson	PNL	1	Control Air Injection Pressure (Melter)
18	701	Pressure XDCR	EDL 102, 324 Bldg, Mod 3	12 Months	LD Anderson	PNL	1	Control Air Injection Pressure (Blower)
19	1662	Pressure XDCR	EDL 102, 324 Bldg, Mod 3	12 Months	LD Anderson	PNL	1	Heat Exchanger DP
20	1661	Pressure XDCR	EDL 102, 324 Bldg, Mod 3	12 Months	LD Anderson	PNL	1	HEMF DP
21	1765	Pressure XDCR	EDL 102, 324 Bldg, Mod 17, Pos. 10	N/A	LD Anderson	PNL	3	Off-Gas Flow Rate DP (alt)
22	1764	Pressure XDCR	EDL 102, 324 Bldg, Mod 17, Pos. 13	N/A	LD Anderson	PNL	3	Final Off-Gas Flow Rate DP (alt)
23	CNTRL-4	Controller	EDL 102, 324 Bldg, Mod 13	N/A	WC Buchmiller	N/A	3	Air Injection Valve Control Signal
24	CNTRL-5	Controller	EDL 102, 324 Bldg, Mod 13	N/A	WC Buchmiller	N/A	3	Downstream Control Valve Signal
25	1671	Interface Module	EDL 102, 324 Bldg, Mod 11	12 Months	WC Buchmiller	PNL	1	West Elec. Volt, Amp, kW
26	1171	Interface Module	EDL 102, 324 Bldg, Mod 11	12 Months	WC Buchmiller	PNL	1	Bottom Elec. Volt, Amp, kW
27	1670	Interface Module	EDL 102, 324 Bldg, Mod 11	12 Months	WC Buchmiller	PNL	1	East Elec. Volt, Amp, kW
28	1672	Interface Module	EDL 102, 324 Bldg, Mod 11	N/A	WC Buchmiller	PNL	3	Primary Elec. Volt, Amp, kW
29	1169	Interface Module	EDL 102, 324 Bldg, Mod 13	12 Months	WC Buchmiller	PNL	1	Discharge Heater, Zn 1 Volt, Amp, kW
30	1170	Interface Module	EDL 102, 324 Bldg, Mod 13	12 Months	WC Buchmiller	PNL	1	Discharge Heater, Zn 2 Volt, Amp, kW
31	835	Interface Module	EDL 102, 324 Bldg, Mod 13	12 Months	WC Buchmiller	PNL	1	Plenum Heater Volt, Amp, kW
32	ELEC_WT1	Type K Thermocouple	EDL 102, 324 Bldg, Mod 11	N/A	WC Buchmiller	N/A	3	Electrode West (Top #1)
33	ELEC_WT2	Type K Thermocouple	EDL 102, 324 Bldg, Mod 11	N/A	WC Buchmiller	N/A	3	Electrode West (Top #2)
34	ELEC_WB1	Type K Thermocouple	EDL 102, 324 Bldg, Mod 11	N/A	WC Buchmiller	N/A	3	Electrode West (Bot #1)
35	ELEC_WB2	Type K Thermocouple	EDL 102, 324 Bldg, Mod 11	N/A	WC Buchmiller	N/A	3	Electrode West (Bot #2)
36	ELEC_ET1	Type K Thermocouple	EDL 102, 324 Bldg, Mod 11	N/A	WC Buchmiller	N/A	3	Electrode East (Top #1)
37	ELEC_ET2	Type K Thermocouple	EDL 102, 324 Bldg, Mod 11	N/A	WC Buchmiller	N/A	3	Electrode East (Top #2)
38	ELEC_EB1	Type K Thermocouple	EDL 102, 324 Bldg, Mod 11	N/A	WC Buchmiller	N/A	3	Electrode East (Bot #1)
39	ELEC_EB2	Type K Thermocouple	EDL 102, 324 Bldg, Mod 11	N/A	WC Buchmiller	N/A	3	Electrode East (Bot #2)
40	ELEC_B1	Type K Thermocouple	EDL 102, 324 Bldg, Mod 11	N/A	WC Buchmiller	N/A	3	Electrode Bottom (#1)
41	ELEC_B2	Type K Thermocouple	EDL 102, 324 Bldg, Mod 11	N/A	WC Buchmiller	N/A	3	Electrode Bottom (#2)
42	PLNHTR11	Type K Thermocouple	EDL 102, 324 Bldg, Mod 11	N/A	WC Buchmiller	N/A	3	Plenum Heater (#1-1)
43	PLNHTR12	Type K Thermocouple	EDL 102, 324 Bldg, Mod 11	N/A	WC Buchmiller	N/A	3	Plenum Heater (#1-2)
44	CANTEMP1	Type K Thermocouple	EDL 102, 324 Bldg, Mod 11	12 Months	WC Buchmiller	N/A	1	Can Temperature
45	CANTEMP2	Type K Thermocouple	EDL 102, 324 Bldg, Mod 11	12 Months	WC Buchmiller	N/A	1	Can Temperature
46	PLNHTR21	Type K Thermocouple	EDL 102, 324 Bldg, Mod 11	N/A	WC Buchmiller	N/A	3	Plenum Heater (#2-1)
47	PLNHTR22	Type K Thermocouple	EDL 102, 324 Bldg, Mod 11	N/A	WC Buchmiller	N/A	3	Plenum Heater (#2-2)

Liquid Fed Ceramic Melter - MTE Control Listing

LINE ITEM #	CONTROL NO.	MATE DESCRIPTION	LOCATION	CALIBRATION INTERVAL	CUSTODIAN	CALIBRATING AGENCY	CATEGORY	REMARKS
48	REAMER1	Type K Thermocouple	EDL 102, 324 Bldg, Mod 11	N/A	WC Buchmiller	N/A	3	Offgas reamer
49	REAMER2	Type K Thermocouple	EDL 102, 324 Bldg, Mod 11	N/A	WC Buchmiller	N/A	3	Offgas reamer
50	PLNHTR31	Type K Thermocouple	EDL 102, 324 Bldg, Mod 11	N/A	WC Buchmiller	N/A	3	Plenum Heater (#3-1)
51	PLNHTR32	Type K Thermocouple	EDL 102, 324 Bldg, Mod 11	N/A	WC Buchmiller	N/A	3	Plenum Heater (#3-2)
52	PLNHTR41	Type K Thermocouple	EDL 102, 324 Bldg, Mod 11	N/A	WC Buchmiller	N/A	3	Plenum Heater (#4-1)
53	PLNHTR42	Type K Thermocouple	EDL 102, 324 Bldg, Mod 11	N/A	WC Buchmiller	N/A	3	Plenum Heater (#4-2)
54	PLN34	Type K Thermocouple	EDL 102, 324 Bldg, Mod 11	12 Months	WC Buchmiller	N/A	1	Melter Plenum (34")
55	PLN43	Type K Thermocouple	EDL 102, 324 Bldg, Mod 11	12 Months	WC Buchmiller	N/A	1	Melter Plenum (43")
56	PLN54	Type K Thermocouple	EDL 102, 324 Bldg, Mod 11	12 Months	WC Buchmiller	N/A	1	Melter Plenum (54")
57	DIS_HTR_4	Type K Thermocouple	EDL 102, 324 Bldg, Mod 11	12 Months	WC Buchmiller	N/A	1	Discharge Heater Section (Trough 40")
58	SBS_OGIN	Type K Thermocouple	EDL 102, 324 Bldg, Mod 3	12 Months	WC Buchmiller	N/A	1	SBS: Off Gas In
59	SBS_NZLP	Type K Thermocouple	EDL 102, 324 Bldg, Mod 3	N/A	WC Buchmiller	N/A	3	SBS: Nozzle P (52")
60	SBS_NZLRT	Type K Thermocouple	EDL 102, 324 Bldg, Mod 3	N/A	WC Buchmiller	N/A	3	SBS: Nozzle R (Top) (36")
61	SBS_NZLRB	Type K Thermocouple	EDL 102, 324 Bldg, Mod 3	N/A	WC Buchmiller	N/A	3	SBS: Nozzle R (Bot) (48")
62	SBS_NZLST	Type K Thermocouple	EDL 102, 324 Bldg, Mod 3	N/A	WC Buchmiller	N/A	3	SBS: Nozzle S (Top) (12")
63	SBS_NZLSB	Type K Thermocouple	EDL 102, 324 Bldg, Mod 3	N/A	WC Buchmiller	N/A	3	SBS: Nozzle S (Bot) (36")
64	SBS_NZLTT	Type K Thermocouple	EDL 102, 324 Bldg, Mod 3	N/A	WC Buchmiller	N/A	3	SBS: Nozzle T (Top) (36")
65	SBS_NZLTB	Type K Thermocouple	EDL 102, 324 Bldg, Mod 3	N/A	WC Buchmiller	N/A	3	SBS: Nozzle T (Bot) (48")
66	SBS_NZLET	Type K Thermocouple	EDL 102, 324 Bldg, Mod 3	N/A	WC Buchmiller	N/A	3	SBS: Nozzle E (Top) (36")
67	SBS_NZLEB	Type K Thermocouple	EDL 102, 324 Bldg, Mod 3	N/A	WC Buchmiller	N/A	3	SBS: Nozzle E (Bot) (72")
68	SBS_OUT	Type K Thermocouple	EDL 102, 324 Bldg, Mod 3	12 Months	WC Buchmiller	N/A	1	Off Gas Line Temp: Pre-HEME
69	HEME_OUT	Type K Thermocouple	EDL 102, 324 Bldg, Mod 3	12 Months	WC Buchmiller	N/A	1	Off-Gas Line Temp: Pre-HX
70	OG_POST	Type K Thermocouple	EDL 102, 324 Bldg, Mod 3	12 Months	WC Buchmiller	N/A	1	Off-Gas Line Temp: Post-HX
71	OG_FIN	Type K Thermocouple	EDL 102, 324 Bldg, Mod 3	12 Months	WC Buchmiller	N/A	1	Off Gas Line Temp: Final Flow Rate
72	MLTR_G04	Type K Thermocouple	EDL 102, 324 Bldg, Mod 11	12 Months	WC Buchmiller	N/A	1	Melter: Glass (4")
73	MLTR_G06	Type K Thermocouple	EDL 102, 324 Bldg, Mod 11	12 Months	WC Buchmiller	N/A	1	Melter: Glass (6")
74	MLTR_G08	Type K Thermocouple	EDL 102, 324 Bldg, Mod 11	12 Months	WC Buchmiller	N/A	1	Melter: Glass (8")
75	MLTR_G11	Type K Thermocouple	EDL 102, 324 Bldg, Mod 11	12 Months	WC Buchmiller	N/A	1	Melter: Glass (11")
76	MLTR_G14	Type K Thermocouple	EDL 102, 324 Bldg, Mod 11	12 Months	WC Buchmiller	N/A	1	Melter: Glass (14")
77	MLTR_G17	Type K Thermocouple	EDL 102, 324 Bldg, Mod 11	12 Months	WC Buchmiller	N/A	1	Melter: Glass (17")
78	MLTR_G19	Type K Thermocouple	EDL 102, 324 Bldg, Mod 11	12 Months	WC Buchmiller	N/A	1	Melter: Glass (19")
79	MLTR_G21	Type K Thermocouple	EDL 102, 324 Bldg, Mod 11	12 Months	WC Buchmiller	N/A	1	Melter: Glass (21")
80	SBS_CWTR	Type J Thermocouple	EDL 102, 324 Bldg, Mod 3	12 Months	WC Buchmiller	N/A	1	SBS: Cooling Water Out
81	FEED_NZ1	Type J Thermocouple	EDL 102, 324 Bldg, Mezzanine	12 Months	WC Buchmiller	N/A	1	Feed Nozzle Cooling Water In
82	FEED_NZ2	Type J Thermocouple	EDL 102, 324 Bldg, Mezzanine	12 Months	WC Buchmiller	N/A	1	Feed Nozzle Cooling Water Out
83	FC_AR_T	Type J Thermocouple	EDL 102, 324 Bldg, Mezzanine	12 Months	WC Buchmiller	N/A	1	Film Cooler Air In
84	AIN_T_M	Type J Thermocouple	EDL 102, 324 Bldg, Mod 3	12 Months	WC Buchmiller	N/A	1	Air Injection (Melter)
85	AIN_T_B	Type J Thermocouple	EDL 102, 324 Bldg, Mod17	12 Months	WC Buchmiller	N/A	1	Air Injection (Blower)
86	BI-1	Type J Thermocouple	EDL 102, 324 Bldg, Mod 3	12 Months	GA Whyatt	User	2	SBS Bed Temperatures
87	BI-2	Type J Thermocouple	EDL 102, 324 Bldg, Mod 3	12 Months	GA Whyatt	User	2	SBS Bed Temperatures
88	BI-3	Type J Thermocouple	EDL 102, 324 Bldg, Mod 3	12 Months	GA Whyatt	User	2	SBS Bed Temperatures
89	BC-1	Type J Thermocouple	EDL 102, 324 Bldg, Mod 3	12 Months	GA Whyatt	User	2	SBS Bed Temperatures
90	BC-2	Type J Thermocouple	EDL 102, 324 Bldg, Mod 3	12 Months	GA Whyatt	User	2	SBS Bed Temperatures
91	BC-3	Type J Thermocouple	EDL 102, 324 Bldg, Mod 3	12 Months	GA Whyatt	User	2	SBS Bed Temperatures
92	BO-1	Type J Thermocouple	EDL 102, 324 Bldg, Mod 3	12 Months	GA Whyatt	User	2	SBS Bed Temperatures
93	BO-2	Type J Thermocouple	EDL 102, 324 Bldg, Mod 3	12 Months	GA Whyatt	User	2	SBS Bed Temperatures
94	BO-3	Type J Thermocouple	EDL 102, 324 Bldg, Mod 3	12 Months	GA Whyatt	User	2	SBS Bed Temperatures

Liquid Fed Ceramic Melter - MTE Control Listing

LINE ITEM #	CONTROL NO.	MATE DESCRIPTION	LOCATION	CALIBRATION INTERVAL	CUSTODIAN	CALIBRATING AGENCY	CATEGORY	REMARKS
95	MI-1	Type J Thermocouple	EDL 102, 324 Bldg, Mod 3	12 Months	GA Whyatt	User	2	SBS Bed Temperatures
96	MI-2	Type J Thermocouple	EDL 102, 324 Bldg, Mod 3	12 Months	GA Whyatt	User	2	SBS Bed Temperatures
97	MI-3	Type J Thermocouple	EDL 102, 324 Bldg, Mod 3	12 Months	GA Whyatt	User	2	SBS Bed Temperatures
98	MC-1	Type J Thermocouple	EDL 102, 324 Bldg, Mod 3	12 Months	GA Whyatt	User	2	SBS Bed Temperatures
99	MC-2	Type J Thermocouple	EDL 102, 324 Bldg, Mod 3	12 Months	GA Whyatt	User	2	SBS Bed Temperatures
100	MC-3	Type J Thermocouple	EDL 102, 324 Bldg, Mod 3	12 Months	GA Whyatt	User	2	SBS Bed Temperatures
101	MO-1	Type J Thermocouple	EDL 102, 324 Bldg, Mod 3	12 Months	GA Whyatt	User	2	SBS Bed Temperatures
102	MO-2	Type J Thermocouple	EDL 102, 324 Bldg, Mod 3	12 Months	GA Whyatt	User	2	SBS Bed Temperatures
103	MO-3	Type J Thermocouple	EDL 102, 324 Bldg, Mod 3	12 Months	GA Whyatt	User	2	SBS Bed Temperatures
104	TI-1	Type J Thermocouple	EDL 102, 324 Bldg, Mod 3	12 Months	GA Whyatt	User	2	SBS Bed Temperatures
105	TI 2	Type J Thermocouple	EDL 102, 324 Bldg, Mod 3	12 Months	GA Whyatt	User	2	SBS Bed Temperatures
106	TI-3	Type J Thermocouple	EDL 102, 324 Bldg, Mod 3	12 Months	GA Whyatt	User	2	SBS Bed Temperatures
107	TC-1	Type J Thermocouple	EDL 102, 324 Bldg, Mod 3	12 Months	GA Whyatt	User	2	SBS Bed Temperatures
108	TC-2	Type J Thermocouple	EDL 102, 324 Bldg, Mod 3	12 Months	GA Whyatt	User	2	SBS Bed Temperatures
109	TC-3	Type J Thermocouple	EDL 102, 324 Bldg, Mod 3	12 Months	GA Whyatt	User	2	SBS Bed Temperatures
110	TO-1	Type J Thermocouple	EDL 102, 324 Bldg, Mod 3	12 Months	GA Whyatt	User	2	SBS Bed Temperatures
111	TO-2	Type J Thermocouple	EDL 102, 324 Bldg, Mod 3	12 Months	GA Whyatt	User	2	SBS Bed Temperatures
112	TO-3	Type J Thermocouple	EDL 102, 324 Bldg, Mod 3	12 Months	GA Whyatt	User	2	SBS Bed Temperatures
113	C-IN	RTD	EDL 102, 324 Bldg, Mod 3	12 Months	GA Whyatt	User	2	SBS
114	C-OUT	RTD	EDL 102, 324 Bldg, Mod 3	12 Months	GA Whyatt	User	2	SBS
115	528	EA 3-Pen Recorder	EDL 102, 324 Bldg, Mod 13	12 Months	WC Buchmiller	PNL	1	Recorder TPR-1
116	1659	EA 3-Pen Recorder	EDL 102, 324 Bldg, Mod 13	12 Months	WC Buchmiller	PNL	1	Recorder TPR-2
117	1512	EA 3-Pen Recorder	EDL 102, 324 Bldg, Mod 13	12 Months	WC Buchmiller	PNL	1	Recorder TPR-3
118	1513	EA 3-Pen Recorder	EDL 102, 324 Bldg, Mod 13	12 Months	WC Buchmiller	PNL	1	Recorder TPR-4
119	1600	EA 3-Pen Recorder	EDL 102, 324 Bldg, Mod 13	12 Months	WC Buchmiller	PNL	1	Recorder TPR-5
120	1601	EA 3-Pen Recorder	EDL 102, 324 Bldg, Mod 13	12 Months	WC Buchmiller	PNL	1	Recorder TPR 6
121	1515	EA 3-Pen Recorder	EDL 102, 324 Bldg, Mod 13	12 Months	WC Buchmiller	PNL	1	Recorder TPR-7
122	1514	EA 3-Pen Recorder	EDL 102, 324 Bldg, Mod 13	12 Months	WC Buchmiller	PNL	1	Recorder TPR-8
123	460	Fluke Data Logger	EDL 102, 324 Bldg, Mod 13	N/A	WC Buchmiller	PNL	3	
124	WA71950	Validyne Display	EDL 102, 324 Bldg, Mod 13	N/A	GA Whyatt	PNL	3	
125	[illegible] 422927	Water Rotameter	EDL 102, 324 Bldg, Mod 11	12 Months	WC Buchmiller	Dunlin	1	Feed Nozzle Coolant Flow
126	WR-1	Water Rotameter	EDL 102, 324 Bldg, Mod 11	N/A	WC Buchmiller	PNL	3	Electrode XFMR Coolant
127	WR 2	Water Rotameter	EDL 102, 324 Bldg, Mod 11	N/A	WC Buchmiller	PNL	3	Feed Nozzle Flush
128	WR-3	Water Rotameter	EDL 102, 324 Bldg, Mod 11	N/A	WC Buchmiller	PNL	3	South Wall Cooling Jacket
129	WR 4	Water Rotameter	EDL 102, 324 Bldg, Mod 11	N/A	WC Buchmiller	PNL	3	West Wall Cooling Jacket
130	WR 5	Water Rotameter	EDL 102, 324 Bldg, Mod 11	N/A	WC Buchmiller	PNL	3	East Wall Cooling Jacket
131	WR 6	Water Rotameter	EDL 102, 324 Bldg, Mod 11	N/A	WC Buchmiller	PNL	3	North Wall Cooling Jacket
132	WR-7	Water Rotameter	EDL 102, 324 Bldg, Mod 11	N/A	WC Buchmiller	PNL	3	Bottom Electrode Coolant
133	AR-1	Air Rotameter	EDL 102, 324 Bldg, Mod 11	N/A	WC Buchmiller	PNL	3	Floor Cooling Jacket
134	AR 2	Air Rotameter	EDL 102, 324 Bldg, Mod 11	N/A	WC Buchmiller	PNL	3	Glass Discharge Rate Control
135	MAG-1	Magnehelic	EDL 102, 324 Bldg, Mod 11	N/A	WC Buchmiller	PNL	3	Discharge/Plenum D.P.
136	PGAGE-1	Pressure Gage	EDL 102, 324 Bldg, Mod 11	N/A	WC Buchmiller	PNL	3	Feed Nozzle Flush Water Pressure

Prepared by: WC Buchmiller 3/22/93 Task Leader: [signature] 3/22/93

Signature / Date Signature / Date

A.3

APPENDIX B Staff Training Record

LFCM-8 CAMPAIGN STAFF TRAINING RECORD

Please print name and date in left column. Initial each column documenting that you have completed each item.

NAME & DATE	Test Plan	LFCM SOP	POG SOP	AOG SOP	LFCM-1	LFCM-2	LFCM-3	LFCM-4	LFCM-5	LFCM-6	LFCM-7	LFCM-8

LFCM-8 CAMPAIGN STAFF TRAINING RECORD

Please print name and date in left column. Initial each column documenting that you have completed each item.

NAME & DATE	LFCM-9	Attended Pre-Run Meeting	Attended Pre-Run Training	Fork-Lift Trained (yes/no)	Crane Trained (yes/no)	

APPENDIX C Operational Readiness Checklists

PRE-RUN ACTIVITIES

The following items will be completed prior to the LFCM-8 Test:

		Approval	Date
1.	All required feed analyses are completed and the slurry is acceptable for use.	_____	_____
2.	The Pre-Run Training Briefings have been conducted.	_____	_____
3.	The Pre-Run meeting was conducted.	_____	_____
4.	All operating personnel have completed the necessary review of operating documentation and are capable of the required duties (documentation is in Test File).	_____	_____
5.	A shift schedule has been completed and lead assignments have been made (documentation is in Test File).	_____	_____
6.	The LFCM and POG Operational Readiness Checklists have been completed (documentation is in Test File).	_____	_____
7.	All necessary procedures are approved.	_____	_____
8.	The melter floor has been probed and two samples of the glass melt were obtained prior to start up.	_____	_____

LFCM-8
LFCM OPERATIONAL READINESS CHECKLIST

NOTE: This is a permanent record, please be accurate and legible.

Initials	Date	
		A. Glass Receiving
_____	_____	1. _____ 24" dia. by 10' tall canisters are available and located in the 324 Building yard.
_____	_____	2. _____ discharge view port windows are on hand.
_____	_____	3. _____ view port fiberfrax gaskets are on hand.
_____	_____	4. The initial glass receiving canister is on the platform scale and connected to the melter.
_____	_____	5. The discharge view port window, gaskets and window retainer are in place, and the retainer bolts run free.
_____	_____	6. The platform scale is calibrated and operable.
_____	_____	7. The canister/discharge connecting device is in place and operable.

Initials	Date	
_____	_____	8. _____ complete canister overpacks are on hand.
_____	_____	9. The canister number and tare weight have been recorded on the "Canister Log."
_____	_____	10. The discharge knife valve is operable.
_____	_____	11. The differential pour dip leg is properly adjusted and piped to the melter discharge. The differential pour air bleed system is operable.
_____	_____	12. Use of the forklift has been cleared and slings/chokers/shackles are available for removing canisters.

B. Melter

_____	_____	1. _____ view port windows are on hand.
_____	_____	2. _____ view port window fiberfrax gaskets are on hand.
_____	_____	3. The view port knife valves are operable.
_____	_____	4. _____ graphite glass sampler boats are on hand.

Initials	Date	
_____	_____	5. The sample boat handle with a boat in place is on hand.
_____	_____	6. _____ sample containers for glass samples are on hand.
_____	_____	7. Pens for labeling sample containers are on hand.
_____	_____	8. The electrode power control system is operable and properly adjusted.
_____	_____	9. The vacuum control system is operable and properly adjusted.
_____	_____	10. The plenum heater temperature control system is operable and properly adjusted.
_____	_____	11. The discharge trough temperature control system is operable and properly adjusted.
_____	_____	12. The closed loop cooling system has been valved into the melter cooling water supply header.
_____	_____	13. All of the melter air and cooling water circuits are operable and properly adjusted.
_____	_____	14. New calibrated TC bundles for the glass, plenum, and discharge have been installed.

Initials	Date	
		C. Feed System
_____	_____	1. _____ L of feed suitable for use is on hand.
_____	_____	2. The main feed system is operational.
_____	_____	3. The backup feed pumps are in place and operational.
_____	_____	4. The main and backup feed rate indicators are operational and feed rate can be monitored on the DAS.
_____	_____	5. _____ sample bottles and lids for feed samples are on hand.
_____	_____	6. Labeling pens for sample bottles are on hand.
_____	_____	7. The melter feed nozzle is in place and cooling water is turned on; no cooling water leaks are apparent.
_____	_____	8. The dip rod necessary to measure the volume of feed in tank 60 is on hand.
		D. Off-Gas System
_____	_____	1. POG ORC is complete.

Initials	Date	
_____	_____	2. Tank 20 is available and contains a minimum of 10 in. of water.
_____	_____	3. The SBS has been filled to its operating level.
_____	_____	4. The SBS liquid sample port is functional.
_____	_____	5. The SBS cooling coils are valved into the closed loop cooling system and adjusted to _____ gpm.
_____	_____	6. The SBS _____upper and/or _____ lower overflow valve(s) are open and connected to tank 20.
_____	_____	7. The HEPA overflow valve is open and connected to tank 20.
_____	_____	8. The HEMF overflow valve is open and connected to tank 20.
_____	_____	9. The Chevron Demister overflow valve is open and connected to tank 20.
_____	_____	10. The off-gas jumper has been cleaned and reinstalled.
_____	_____	11. POG Butterfly valve controller is functional in both auto and manual modes. Controller is set to manual mode with 100% controller output (closed).

Initials	Date	
_____	_____	12. POG air injection valve controller is functional in both auto and manual modes. Controller is set to auto mode with 0% controller output (closed).
_____	_____	13. Total POG system in-leakage has been determined, is acceptable and value entered in appropriate log book. To determine in-leakage at idling conditions: a. valve out film cooler air b. using butterfly valve controller, set melter plenum pressure to - 7 in. WC c. read off-gas flow rate, this is the total POG system in-leakage.
_____	_____	14. The HEMF has been installed.
_____	_____	15. Film cooler air is valved to the system and can be controlled with the manual control valve.
_____	_____	16. Off-gas sampling trains are set up and equipment is calibrated.

E. Safety Equipment

_____	_____	1. _____ face shields are on hand.

Initials	Date		
_____	_____	2.	_____ pair of shoulder-length heat resistant gloves are on hand.
_____	_____	3.	_____ pair leather gloves are on hand.
_____	_____	4.	_____ pair of gauntlet-length heat resistant gloves are on hand.
_____	_____	5.	_____ heat-resistant bib aprons are on hand.
_____	_____	6.	_____ ceramic fiber blanket pads are on hand.
_____	_____	7.	A water hose that can reach the area under the melter is connected to a hose bib, is available for use, and is operable.
_____	_____	8.	A grounding wire is on hand for grounding the melter tank dip samplers or probes, the airlift lance, and the discharge sampler fork.
_____	_____	9.	_____ heat resistant hoods are on hand.
_____	_____	10.	_____ pair of heat resistant knee pads are on hand.
_____	_____	11.	_____ pair of heat resistant shoe covers are on hand.

Initials	Date	
_____	_____	12. _____ feet of yellow safety rope is on hand.

F. General

_____	_____	1. The melter emergency vent system is operational and has been tested. It vents @ _____ H_2O pressure, and resets @ _____ H_2O pressure.
_____	_____	2. The LFCM system over temp alarms have been set to: _____°C Plenum Htr. _____°C Discharge Htr. _____°C Electrodes
_____	_____	3. All recorders have sufficient chart paper to record the entire experiment and have been calibrated.
_____	_____	4. All data sheets have been prepared and sufficient copies are on hand to record the entire experiment.
_____	_____	5. Critical system temperature sensors, as identified by the current run plan, are functional and in calibration.
_____	_____	6. Critical system differential pressure transducers, as identified by the current run plan are functional and in calibration. The following checks have been performed:

Initials	Date	
		a. sensor lines to all pressure transducers are clear of obstructions. b. equalization valves are closed. c. tightness of all fittings have been checked.
_____	_____	7. All recorders used for critical system data are functional and in calibration.
_____	_____	8. The Data Acquisition System has been configured and retrieval of critical data has been verified.
_____	_____	9. Data Transfer disks and printer paper are available and on hand.
_____	_____	10. All crafts items have been completed.
_____	_____	11. The run plan has been written and approved.
_____	_____	12. The Run Book has been prepared and approved.
_____	_____	13 Pre-run activities as listed on the Pre-Run Activities list are complete.
_____	_____	14. The MT&E file is complete and current.

Initials	Date	
_____	_____	15. Copies of all SOPs and Procedures that apply to LFCM operations are in the control room.
_____	_____	16. Emergency phone numbers are posted or on file in the control room.
_____	_____	17. The off-shift crafts supervisor call list is posted or on file in the control room.

VI. PROCEDURE

POG OPERATIONAL READINESS CHECKLIST[a*]

Date Completed	Initials		
_____	____	1.	Verify that the POG blower is running; if not see note b* below before continuing.
_____	____	2.	AOG blower available as backup.
_____	____	3.	Most recent service tunnel POG blower PM checkup on (date) _____ with _____ checkup intervals.
_____	____	4.	Vacuum at POG blower inlet is ___ in WC.
_____	____	5.	Check AOG/POG operations logbook to see if POG services are in use; contact appropriate staff.
_____	____	6.	Verify that hazardous emissions will not be processed through POG piping.
_____	____	7.	Place an experiment in progress sign on the POG start/stop switch.
_____	____	8.	Document your equipment use of POG services in the AOG/POG operations logbook.
_____	____	9.	Remove experiment in progress sign upon completion of your experiment.
_____	____	10.	Note experiment completion in AOG/POG operations logbook.

a* This document is intended as an aid and not as a permanent record. Your entry into the AOG/POG operations logbook implies completion of the above steps 1 - 8.

b* Only the AOG/POG equipment custodian or designee may start the POG blower.

APPENDIX D Daily Activities Schedule & Log

LFCM-8/HWVP-16 ACTIVITIES SCHEDULE AND LOG REV. 1

Page ____ of ___

TIME (HRS)	STATUS SHEET 1	STATUS SHEET #2	Feed Sample	SBS Liquid Sample	TK60 LEVEL SS#5	Glass Sample CP/AR	GLASXFR DS #1 AS-REQD	TK13 TRANSFR SSs#4&6
1:00	X				X			
2:00	X	X						
3:00	X				X			
4:00	X	X		X		CP		
5:00	X				X			
6:00	X	X						
7:00	X				X			
8:00	X	X	X					
9:00	X				X			
10:00	X	X		X		CP		
11:00	X				X			
12:00	X	X						
13:00	X				X			
14:00	X	X						
15:00	X				X			
16:00	X	X		X		CP		
17:00	X				X			
18:00	X	X						
19:00	X				X			
20:00	X	X	X					
21:00	X				X			
22:00	X	X		X		CP		
23:00	X				X			
24:00	X	X						

CP/AR = CP means sample if continuously pouring. Otherwise after each Batch Pour

Note: Place Initials in Box When Task is Completed.

APPENDIX E Data & Status Sheets

DATA SHEET 1

	BY:							
	DATE:							
	CAN #:							
	START TIME:							
	END TIME:							
DESCRIPTION:	UNITS							
WT, START OF POUR	KG							
DISCHARGE INJECTION AIR	SCFH							
PLENUM/DISCHARGE D.P.	IN. W.C.							
DISCHARGE AIR PRESSURE	PSIG							
WT, END OF POUR	KG							
KG OF GLASS POURED	KG							
ELAPSED TIME	MIN							

	BY:							
	DATE:							
	CAN #:							
	START TIME:							
	END TIME:							
DESCRIPTION:	UNITS							
WT, START OF POUR	KG							
DISCHARGE INJECTION AIR	SCFH							
PLENUM/DISCHARGE D.P.	IN. W.C.							
DISCHARGE AIR PRESSURE	PSIG							
WT, END OF POUR	KG							
KG OF GLASS POURED	KG							
ELAPSED TIME	MIN							

Reviewed by: _____ Date: _____ Page _____ of _____

DATA SHEET #2
Sample Log

REVIEWED BY: _____ DATE: _____ PAGE____ OF ____

SAMPLE NO.	DATE	TIME	BY	SOURCE/COMMENTS

	BY:						
	DATE:						
	TIME:						
DESCRIPTION:	UNITS						
RELATIVE HUMIDITY	%						
FEED TOTALIZER	LITERS						
REAMER OPERATION	NA						
COLD CAP COVERAGE	%						
SLURRY POOL COVERAGE	%						
VENTING ACTION	NA						
COLD CAP RIGIDITY	NA						
COLD CAP THICKNESS	INCHES						
XFMR COOLANT	GPM						
WATER HEADER PRESSURE	PSIG						
FEED NOZZLE COOLANT	GPM						
ELECTRODE FINGER COOLANT	GPM						
FLOOR COOLANT	SCFM						
SOUTH WALL COOLANT	GPM						
WEST WALL COOLANT	GPM						
EAST WALL COOLANT	%						
NORTH WALL COOLANT	%						
DISCHARGE VALVE	O / C						
OVER TEMP ALARMS	Y / N						
TRANS COOLING LOSS ALARM	Y / N						
CANISTER WEIGHT	KG						
POURING	Y / N						
DISCHARGE VACUUM VALVE	O / C						
BUTTERFLY VALVE POSITION	0-90-						
SBS COOLANT FLOW	GPM						
HEME AIR FLOW	SCFM						
HEME AIR PRESSURE	PSIG						
HEME WATER FLOW	GPH						
HEME WATER PRESSURE	PSIG						
SBS DRAIN VALVE	O / C						

	BY:						
	DATE:						
	TIME:						
DESCRIPTION:	UNITS						
MLT_PLNP	IN WC						
SBS_OGIN	DEGC						
SBS_OUT	DEGC						
SBS_CWTR	DEGC						
OG_FR	SCFH						
OG_POST	DEGC						
OGVACDOV	IN WC						
HEMF_DP	IN WC						
HEME_DP	IN WC						
DEM_DP	IN WC						
SBS_DP	IN WC						
FIN_FR	SCFH						
FEEDTK60	L/H						
FEEDSIPT	L/H						
E_ELEC_O	OHMS						
E_ELEC_K	KW						
AMPS_BOT	AMPS						
W_ELEC_K	KW						
W_ELEC_O	OHMS						
TOTELEKW	KW						
BULKGLAS	DEGC						
ELEC_WT2	DEGC						
ELEC_ET2	DEGC						
ELEC_B1	DEGC						
PLN_PWR	KW						
PLNHTR11	DEGC						
PLN54	DEGC						
TOTDISKW	KW						
DIS_HTR4	DEGC						
MLT-D_DP	IN WC						

Reviewed by:_____ Date:_____ Page____of____

	BY:						
	DATE:						
	TIME:						
DESCRIPTION:	UNITS						
CLOSE UPPER SBS DRAIN VALVE *1	O/C						
CLOSE LOWER SBS DRAIN VALVE *2	O/C						
OPEN HEMF DRAIN VALVE	O/C						
WAIT 5 MINUTES	NA						
CLOSE HEMF DRAIN VALVE	O/C						
OPEN UPPER SBS DRAIN VALVE *1	O/C						
OPEN LOWER SBS DRAIN VALVE *2	O/C						
DEMISTER DRAIN	O/C						
HEME DRAIN	O/C						
*1 ONLY IF THE UPPER SBS VALVE WAS OPEN DURING ROUTINE OPERATIONS							
*2 ONLY IF THE LOWER SBS VALVE WAS OPEN DURING ROUTINE OPERATIONS							

	BY:						
	DATE:						
	TIME:						
DESCRIPTION:	UNITS						
CLOSE UPPER SBS DRAIN VALVE *1	O/C						
CLOSE LOWER SBS DRAIN VALVE *2	O/C						
OPEN HEMF DRAIN VALVE	O/C						
WAIT 5 MINUTES	NA						
CLOSE HEMF DRAIN VALVE	O/C						
OPEN UPPER SBS DRAIN VALVE *1	O/C						
OPEN LOWER SBS DRAIN VALVE *2	O/C						
DEMISTER DRAIN	O/C						
HEME DRAIN	O/C						
*1 ONLY IF THE UPPER SBS VALVE WAS OPEN DURING ROUTINE OPERATIONS							
*2 ONLY IF THE LOWER SBS VALVE WAS OPEN DURING ROUTINE OPERATIONS							

Reviewed by: _____ Date: _____ Page _____ of _____

STATUS SHEET 4 (TANK 60 XFER) PAGE ____ OF ____

START TIME	BY	BEG TANK DIP	BEG VOLUME	END TIME	FIN TANK DIP	FIN VOLUME	LITERS

REVIEWED BY: _____ DATE: _____

STATUS SHEET 5 (TANK 60 FEED RATE) PAGE ____ OF ____

TIME	BY	TANK DIP	VOLUME	LITERS	FEED RATE (CALC)	FEED RATE (COMP)

REVIEWED BY: _____ DATE: _____

STATUS SHEET 6 (TANK HB13 FEED XFER) PAGE ____ OF ____

START TIME	BY	BEG TANK WT	END TIME	END TANK WT	WT XFER'D	TOTAL WT XFER'D

REVIEWED BY: _____ DATE: _____

APPENDIX F Formic Acid Sampling Procedure

1 Summary of Method

A known volume of air is drawn through two glass tubes containing Chromosorb 103 to trap formic acid vapors. The formic acid is desorbed from the Chromosorb 103 with high purity water. These samples are injected into a gradient eluent stream consisting of 40mM NaOH/5% MeOH and passed through an ion suppressor, guard column and separator column. The formate ion is then measured by an electrolytic conductivity detector. These samples will be identified in this procedure as vapor samples.

Condensation from the in-line cold trap will be weighed and an aliquot sampled, labeled, filtered and diluted with high purity water to the appropriate concentration. These samples will be analyzed with the same method as the vapor samples. These samples will be identified in this procedure as condensate samples.

The formate ion is identified on the basis of retention time by comparison to standards. The amount of formate ion formation of formic acid in water, is by comparison to standards prepared with sodium formate. Concentration of the samples are quantified by area response using a standard curve to convert area to concentration.

A separate test to determine the desorption efficiency is performed by spiking a sample tube with a formic acid solution and comparing the desorption efficiency with prepared standards.

2 Applicability

This procedure is intended for use by personnel familiar with the operation of the ion chromatograph and experience with basic lab techniques. Training is required for all staff prior to utilizing this procedure. Training will be documented in the project laboratory record book and documented by the task leader.

This procedure is primarily for the analysis of the formate anion; other anions including chloride, nitrate, nitrite and sulfate can also be analyzed. Sample dilutions can be varied according to the concentrations of the stock samples or to resolve interference difficulties.

3 Analysis Precautions

Formate ion detection limit is estimated to be 1 μg/ml standard. Samples of high concentrations (above 30 μg/ml) should be diluted to accommodate the standards range of 1 to 30 μg/ml.

Breakthrough:
Sample breakthrough can occur at high effluent concentrations or with overly long sample times. A second sample tube run in series with the first is used to determine sample breakthrough. Breakthrough should be measured with every sample in order to determine total vapor concentration.

Interferences:

Any substance that has a retention time coinciding with that of formate anion will interfere and corrupt the data. High concentrations of other closely eluting ions may interfere with resolution of the formate ion. Sample dilutions or a change in the eluent gradient program may overcome this problem. Frequently samples containing late eluting anions will require a longer run time to prevent sample overlap.

Sample Handling and Identification:

All samples must have a recorded identification number corresponding to a BNW# laboratory notebook and page number. Samples should be recorded in the notebook with any unique sample characteristics including: time of sampling, sample locale and personal identification.

APPENDIX G Off-Gas System Sample & Measurement Locations

HWVP - LFCM POG ELEMENT DESCRIPTION

ELEMENT NO.	SIZE	M&TE NO.	ELEMENT DESCRIPTION
A1	1/8" Swagelok	83	Film Cooler Air In Temp
A2	1/8" Swagelok	84	Air Injection In (Melter) Temp
A3	1/8" Swagelok	58	SBS: Off Gas In Temp
A4	1/8" Swagelok	68	SBS: Out Temp
A5	1/8" Swagelok	69	HEME Out Temp
A6	1/8" Swagelok	70	Post Heat Exchanger Temp
A7	1/8" Swagelok	71	Final Off Gas Temp
A8	1/8" Swagelok	85	Air Injection In (Final) Temp
B1	3/8" Swagelok	6	Melter Plenum Vacuum
B2	3/8" Swagelok	7	Film Cooler Dp
B3	3/8" Swagelok	16	Film Cooler Air Pressure
B4	3/8" Swagelok	17	Air Injection (melter) Pressure
B5	1/4" Pipe Coupling	8	Film Cooler to SBS Dp
B6	3/8" Swagelok	9	SBS Dp
B7	3/8" Swagelok	10	HEME Dp (Hi)
B8	3/8" Swagelok	10,19	HEME Dp (Low)
B9	3/8" Swagelok	19	Heat Exchanger Dp (Hi)
B10	3/8" Swagelok	19,20	Heat Exchanger Dp (Low)
B11	3/8" Swagelok	20	HEMF Dp (Low)
B12	3/8" Swagelok	11	Off Gas Vacuum (Final)
B13	3/8" Swagelok	18	Air Injection (Final) Pressure
C1	3/8" Swagelok	1	Off Gas Flow Rate @ Melter
C2	3/8" Swagelok	3	Film Cooler Air Flow Rate
C3	3/8" Swagelok	5	Air Injection (Melter) Flow Rate
C4	3/8" Swagelok	4	Air Injection (Final) Flow Rate
C5	3/8" Swagelok	2	Off Gas Flow Rate @ Final
D1	1" Pipe Coupling	N/A	Off Gas Sample - Pre SBS
D2	1" Pipe Coupling	N/A	Spare Sample Port
D3	1-1/4" Pipe Coupling	N/A	Post SBS & HEME Sample Port
D4	1-1/4" Pipe Coupling	N/A	Pre-HEMF Sample Port
D5	1-1/4" Pipe Coupling	N/A	Post-HEMF Sample Port
D6	1-1/2" Pipe Coupling	N/A	Final Off Gas Sample Port
E1	4"	N/A	Knife Valve, Manual
E2	4"	N/A	Knife Valve, Manual
E3	4"	N/A	Knife Valve, Manual
E4	4"	N/A	Knife Valve, Manual
E5	3"	N/A	Butterfly Valve, Motor Control

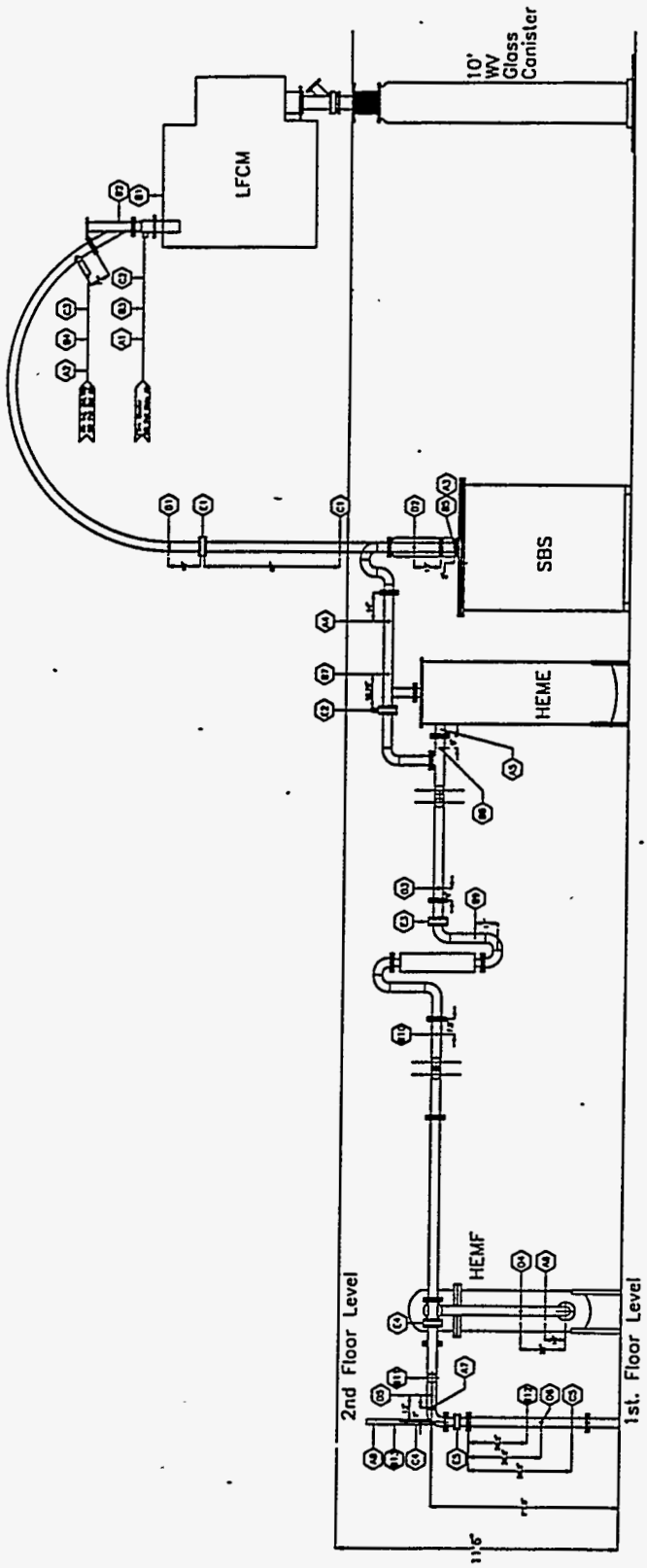
10' WV Glass Canister
LFCM
SBS
HEME
HEMF
2nd Floor Level
1st. Floor Level

G.2

APPENDIX H Sample Log

SAMPLE	DATE	TIME	BY	SOURCE/COMMENTS
1	4/16/93	1100	WCB	Glass from melt cavity
2	4/17/93	0928	SDH	Two 125 ml SIPT samples (2a & 2b)
3	4/17/93	2200	TC	1 SBS Sample
4	4/17/93	2248	TC	End of JJH batch pour-sample glass
5	4/18/93	0140	JMP	Tk 15 Feed sample
6	4/18/93	0140	JMP	Tk 15 Feed Sample
7	4/18/93	0400	JMP	SBS Condensate Sample
8	4/18/93	0800	MLE	End of 2nd bathe pour-sample glass
9	4/18/93	0828	JJH	Tk 15 Feed Sample (9a & 9b)
10	4/18/93	1000	MLE	SBS Sample
11	4/18/93	1350	JJH	Batch Pour-sample glass
12	4/18/93	1600	MLE	SBS Sample
13	4/18/93	1905	TC	Batch Pour end run sample (glass)
14	4/18/93	2000	JMP	Tk 15 Feed Sample
15	4/18/93	2000	JMP	Tk 15 Feed Sample
16	4/18/93	2205	TC	SBS Sample
17	4/19/93	0040	TC	Glass Sample End of Batch Pour
18	4/19/93	0334	TC	Glass Sample End of Batch Pour
19	4/19/93	0400	TC	SBS Sample
20	4/19/93	0750	JJH	Glass Sample
21	4/19/93	0805	JJH	Feed Sample (21a & 21b)
22	4/19/93	1000	MLE	SBS Sample
23	4/19/93	1120	JJH	Glass Sample
24	4/19/93	1600	MLE	SBS Sample
25	4/19/93	1635	JJH	Glass Sample
26	4/19/93	1940		Glass Sample
27	4/19/93	2000	JMP	Feed Sample
28	4/19/93	2000	JMP	Feed Sampl e
29	4/19/93	2000	JMP	1 L feed sample
30	4/19/93	2200	TC	SBS Sampl e
31	4/19/93	2250	TC	Glass Sample
32	4/20/93	0215	TC	Glass Sample
33	4/20/93	0400	JMP	SBS condensate sample
34	4/20/93	0720	KEE	Glass Sample
35	4/20/93	0825	KEE	Feed Sample
36	4/20/93	0825	KEE	Feed Sample
37	4/20/93	1012	KEE	SBS Condensate Sample
38	4/20/93	1204	KEE	Glass Sample
39	4/20/93	1612	KEE	SBS condensate sample
40	4/20/93	1804	GAW	Glass Sample
41	4/20/93	2015	GAW	Feed Sample
42	4/20/93	2150	GAW	Glass Sample
43	4/20/93	2208	GAW	SBS Sampl e
44	4/21/93	0115	GAW	Feed Sample

SAMPLE	DATE	TIME	BY	SOURCE/COMMENTS
45	4/21/93	0138	GAW	Glass Sample
46	4/21/93	0410	GAW	SBS Sample
47	4/21/93	0613	KEE	Glass Sample
48	4/21/93	0800	MFC	Feed Sample
49	4/21/93	0800	MFC	Feed Sample
50	4/21/93	0956	KEE	SBS Sample
51	4/21/93	1017	KEE	Melt Sample
52	4/21/93	1420	KEE	Melt Sample
53	4/21/93	1605	KEE	SBS Sample
54	4/21/93	1825	GAW	Glass Melt Sample
55	4/21/93	2008	GAW	Feed Sample
56	4/21/93	2008	GAW	Feed Sample
57	4/21/93	2206	GAW	SBS Sample
58	4/21/93	2240	GAW	Glass Samples
59	4/22/93	0234	GAW	Glass Samples
60	4/22/93	0400	GAW	SBS Samples
61	4/22/93	0611	KEE	Glass Samples
62	4/22/93	0851	KEE	Feed Samples
63	4/22/93	0851	KEE	Feed Samples
64	4/22/93	1000	MFC	SBS Liquid Sample
65	4/22/93	1021	KEE	Melt Sample
66	4/22/93	1337	KEE	Melt Sample
67	4/22/93	1613	KEE	SBS Sample
68	4/22/93	1734	KEE	Melt Sample
69	4/22/93	1955	GAW	Feed Sample
70	4/22/93	1955	GAW	Feed Sample
71	4/22/93	2115	GAW	Glass Sample
72	4/22/93	2210	GAW	SBS Sample
73	4/23/93	0024	GAW	Glass Sample
74	4/23/93	0404	GAW	SBS Sample
75	4123/93	0409	GAW	Glass Sample
76	4/23/93	0735	JJH	Glass Sample
77	4/23/93	0800	JJH	Tk-15 Feed Sample
78	4/23/93	1010	JJH	SBS Sample
79	4/23/93	1145	JJH	Glass Sample
80	4/23/93	1455	JJH	Glass Sample
81	4/23/93	1745	JJH	SBS Sample
82	4/23/93	1834	DAL	Glass Samples
83	4/23/93	2057	DAL	Feed Samples
84	4/23/93	2252	DAL	SBS Samples
85	4/23/93	2330	DAL	Glass Samples
86	4/24/93	0326	DAL	Glass Sample
87	4/24/93	0400	TC	SBS Samples
88	4/24/93	0730	KFW	Glass Sample

SAMPLE	DATE	TIME	BY	SOURCE/COMMENTS
89	4/24/93	0815	KFW	Feed Sample
90	4/24/93	0825	KFW	Glass Sample
91	4/24/93	1132	KFW	Glass Sample
92	4/24/93	1355	KFW	SBS Sample
93	4/24/93	1354	JJH	Glass Sample
94	4/24/93	1620	JJH	SBS Sample
95	4/24/93	1620	JJH	Glass Sample
96	4/24/93	1920	DAL	Glass Sample
97	4/24/93	2020	TC	Feed Sample
98	4/24/93	2020	TC	Feed Sample
99	4l24/93	2205	DAL	SBS Sample
100	4/24/93	2307	DAL	Glass Sample
101	4/25/93	0240	DAL	Glass Sample
102	4/25/93	0403	DAL	SBS Sample
103	4/25/93	0746	JJH	Glass Sample
104	4/25/93	0800	JJH	Tank-15 feed Sample
105	4/25/93	1000	KFW	SBS Sample
106	4/25/93	1104	KFW	Glass Sample
107	4/25/93	1400	JJH	Glass Samples
108	4/25/93	1600	JJH	SBS Samples
109	4/25/93	1730	KFW	Glass Sample
110	4/25/93	2000	TC	Feed Sample
111	4/25/93	2000	TC	Feed Sample Duplicate
112	4/25/93	2110	DAL	Glass Sample
113	4/25/93	2205	T C	SBS Sample
114	4/26/93	0209	DAL	Glass Sample
115	4/26/93	0400	TC	Feed Sample
116	4/26/93	0647	KEE	Glass Sample
117	4/26/93	0811	SH	Duplicate Feed Sample
118	4/26/93	0811	SH	SBS Sample
119	4/26/93	1013	KEE	Glass Sample
120	4/26/93	1055	RAL	Glass Sample
121	4/26/93	1448	KEE	Glass Sample
122	4/26/93	1613	KEE	SBS Sample
123	4/26/93	1817	GAW	Glass Sample
124	4/26/93	2008	GAW	Feed Sample
125	4/26/93	2008	GAW	Feed Sample
126	4/26/93	2203	GAW	SBS Sample
127	4/26/93	2233	GAW	Glass Sample
128	4/27/93	0010	GAW	Glass Sample
129	4/27/93	0404	GAW	Glass Sample
130	4/27/93	0410	GAW	SBS Sample
131	4/27/93	0810	RAL	Feed Sample
132	4/27/93	0810	RAL	Feed Sample

SAMPLE	DATE	TIME	BY	SOURCE/COMMENTS
133	4/27/93	1007	KEE	SBS Sampl e
134	4/27/93	1018	KEE	Melt/Glass Sample
135	4/27/93	1503	KEE	Melt/Glass Sample
136	4/27/93	1505	KEE	SBS Sample
137	4/27/93	2010	GAW	Feed Sample
138	4/27/93	2010	GAW	Feed Sample
139	4/27/93	2210	GAW	SBS Sampl e
140	4/27/93	2250	GAW	Glass Sample
141	4/28/93	0400	GAW	SBS Sample
142	4/28/93	0408	GAW	Glass Sample
143	4/28/93	0813	KEE	Feed Sample
144	4/28/93	0813	KEE	Feed Sample
145	4/28/93	1023	RAM	Glass Sample
146	4/28/93	1027	RAM	SBS Sample
147	4/28/93	1554	KEE	SBS Sample
148	4/28/93	1625	RAL	Glass Sample
149	4/28/93	2000	GAW	Feed Sample
150	4/28/93	2000	GAW	Feed Sample
151	4/28/93	2200	GAW	Glass Sample
152	4/28/93	2205	GAW	SBS Sample
153	4/29/93	0410	GAW	Glass Sample
154	4/29/93	0411	GAW	SBS Sample
155	4/29/93	0828	KEE	Feed Sample
156	4/29/93	0828	KEE	Feed Sample
157	4/29/93	1018	KEE	SBS Sample
158	4/29/93	1015	RAL	Glass Sample
159	4/29/93	1529	RAL	Glass Sample
160	4/24/93	1450	JMP	Cold Cap Sample (near glass)
161	4/24/93	1450	JMP	Cold Cap Sample (near glass)
162	4/24/93	1450	JMP	Cold Cap Sample (near glass)
163	4/24/93	1450	JMP	Cold Cap Sample (near Slurry)
163	4/29/93	1620	RAL	SBS Sample
164	4/29/93	1840	GAW	SBS Sample
165	4/29/93	1845	GAW	Glass Sample
166	4/29/93	2000	WCB	Cold Cap Sample
167	5/5/93	1100	JMP	Thermosyphon bottoms sample
168	5/10/93	0905	KEE	Feed (Tk-60)
169	5/10/93	0905	KEE	Feed (Tk-60)
170	5/10/93	0908	KEE	SBS Liquid
171	5/10/93	1242	WCB	Glass Sample
172	5/10/93	2010	GAW	Feed (Tk-60)
173	5/10/93	2010	GAW	Feed (Tk-60)
174	5/10/93	2205	GAW	Glass Sample
175	5/10/93	2211	GAW	SBS Liquid Sample

SAMPLE	DATE	TIME	BY	SOURCE/COMMENTS
176	5/11/93	0521	GAW	Glass Sample
177	5/11/93	0803	GJS	Feed Sample
178	5/11/93	0803	GJS	Feed Sample
179	5/11/93	1000	GJS	SBS Sample
180	5/11/93	1000	RAL	Glass Sample
181	5/11/93	1600	DRJ	SBS Sample
182	5/11/93	1600	DRJ	Glass Sample
183	5/11/93	2010	GAW	Feed Sample
184	5/11/93	2010	GAW	Feed Sample
185	5/11/93	2204	GAW	SBS Sample
186	5/11/93	2205	GAW	Glass Sample
187	5/12/93	0400	GAW	SBS Sample
188	5/12/93	0430	GAW	Glass Sample
189	5/12/93	0800	GJS	Feed (Tk-60)
190	5/12/93	0800	GJS	Feed (Tk-60)
191	5/12/93	1000	WCB	SBS Sample
192	5/12/93	1000	RAL	Glass Sample
193	5/12/93	1500	GJS	SBS Sample
194	5/12/93	1500	GJS	Glass Sample
195	5/12/93	2000	GAW	Feed
196	5/12/93	2000	GAW	Feed
197	5/12/93	2020	GAW	Glass Sample
198	5/12/93	2200	GAW	SBS Sample
199	5/12/93	2208	GAW	Glass Sample
200	5/13/93	0245	GAW	Glass Sample
201	5/13/93	0404	GAW	SBS Sample
202	5/13/93	0805	JJH	Feed Sample
203	5/13/93	0805	JJH	Feed Sample
204	5/13/93	1008	JJH	SBS Sample
205	5/13/93	1001	JJH	Glass Sample
206	5/13/93	1500	JJH	Glass Sample
207	5/13/93	1615	JJH	SBS Scrub Solution
208	5/13/93	2010	GAW	Feed Sample
209	5/13/93	2010	GAW	Feed Sample
210	5/13/93	2200	GAW	Glass Sample
211	5/13/93	2210	GAW	SBS Sample
212	5/14/93	0400	GAW	Glass Sample
213	5/14/93	0408	GAW	SBS Sample
214	5/14/93	0820	CJF	Feed Sample
215	5/14/93	0820	CJF	Feed Sample
216	5/14/93	0830	JJH	Thermosyphon Bottoms Sample
217	5/14/93	0830	JJH	Thermosyphon Bottoms Sample
218	5/14/93	0830	JJH	Thermosyphon Bottoms Sample
219	5/14/93	1000	JJH	SBS Solution Sample

SAMPLE	DATE	TIME	BY	SOURCE/COMMENTS
220	5/14/93	1017	JJH	Glass Sample
221	5/14/93	1600	JJH	SBS Solution Sample
222	5/14/93	1610	JJH	Glass Sample
223	5/14/93	2000	GAW	Feed Sample
224	5/14/93	2000	GAW	Feed Sample
225	5/14/93	2205	GAW	SBS Sample
226	5/14/93	2210	GAW	Glass Sample
227	5/15/93	0404	GAW	Glass Sample
228	5/15/93	0408	GAW	SBS Sample
229	5/15/93	0800	JJH	Feed Sample
230	5/15/93	1000	JJH	SBS Sample
231	5/15/93	1205	GAW	Glass Sample
232	5/15/93	1600	JJH	SBS Sample
233	5/15/93	1840	GAW	Feed Sample of final transfer for Tk-13
234	5/15/93	1844	GAW	Glass Sample
235	5/15/93	2008	GAW	Feed Sample
236	5/15/93	2008	GAW	Feed Sample
237	5/15/93	2200	GAW	SBS Sample
238	5/15/93	2204	GAW	Glass Sample
239	5/16/93	0305	GAW	Glass Sample
240	5/16/93	0404	GAW	SBS Sample
241	5/16/93	0807	JJH	Feed Sample
242	5/16/93	1000	JJH	SBS Sample
243	5/16/93	1030	JJH	DWPF Glass sampler
244	5/16/93	1030	JJH	DWPF Glass sampler
245	5/16/93	1030	JJH	DWPF Glass sampler
246	5/16/93	1030	JJH	DWPF Glass sampler
247	5/16/93		JJH	Glass Sample

APPENDIX I HEMF Filter Washing & Flushing Procedure

TITLE: High Efficiency Metal Fiber (HEMF) Filter Cleaning

1.0 Applicability

The objective of this procedure is to ensure the proper cleaning of the high efficiency metal fiber (HEMF) filter in the Liquid-Fed Ceramic Melter (LFCM) off-gas system. After the filter has been loaded with particulate, this flushing procedure is used to clean the filter elements, by providing a pulse of water flow in the direction opposite the normal flow. A drawing of the HEMF is shown in Figure 1. The filter may be flushed when the pressure drop becomes excessive during melter operation or any time it is desired to remove all particulate loading from the filter.

2.0 Definitions

HEMF - High Efficiency Metal Fiber filter
LFCM - Liquid Fed Ceramic Melter
Tank 20 - Tank to which HEMF drain is connected (located in tank pit)

3.0 Responsible Staff

Operator - Engineer or technician performing the flushing procedure

4.0 Safety

The particulate loaded on the filter elements consists mainly of submicron particles that have passed through the submerged bed

CONCURRENCE	DATE	APPROVAL TASK LEADER	DATE
Greg Whyatt	8/10/93	[signature]	8/10/93
PREPARED BY	DATE	QUALITY SYSTEM & REPORTING DEPARTMENT	DATE
L.D. Anderson	8/10/93	B.L. Hanlon	8-10-93
BUILDING MANAGER	DATE	SAFETY	DATE
J.E. [illegible]	8/10/93	Glenn R. Hoeen	8/10/93

scrubber (SBS) and possibly the high efficiency mist eliminator (HEME). The particulate contains various oxides and salts and must be treated as hazardous material. However, because the elements are contained inside the filter housing, no contact with the hazardous material is expected during the water flush. However, should any water leak from the vessel during the flush, the operator shall wear rubber gloves when cleaning up any spill and dispose of the wastes according to the Waste Technology Center Environmental Safety & Health (ES&H) Plan. The filter is located in EDL-102, therefore a hard hat and safety goggles will be worn at all times.

5.0 HEMF Flushing Procedure

This procedure is based on the procedure provided by Pall Advanced Separations Systems. Valves referred to in this procedure are shown in Figure 2. All observations shall be recorded in a Laboratory Record Book.

5.1 Pre-flushing Procedure

1. Cover the floor underneath the HEMF filter with plastic liner in case any flush water leaks from the housing. The plastic should extend outwards far enough to cover the floor underneath the gas inlet and outlet flanges.
2. Check calibration of air receiver pressure gauge, and record results in a Laboratory Record Book.
3. Disconnect poly tubing to pressure taps and plug the taps.

CONCURRENCE N/A	DATE	APPROVAL TASK LEADER N/A	DATE
PREPARED BY N/A	DATE	QUALITY SYSTEM & REPORTING DEPARTMENT N/A	DATE
BUILDING MANAGER N/A	DATE	SAFETY N/A	DATE

4. If the flush is to occur during melter operation, open the HEMF bypass valve to allow uninterrupted flow of the melter off-gas. Install teflon blanks at the offgas inlet and outlet of the filter. Check these flanges and others on the filter housing for tightness, and tighten if necessary. The bolts holding the tubesheet assembly between the bottom housing and the bonnet should have previously been tightened properly during filter assembly, and should not need any adjustment, however, this should be verified.
5. Tank 20 shall be sufficiently emptied to assure the capacity exists for all liquid that will be drained during the flushing procedure (<150 gallons). The level can be determined from the weight factor pressure gauge attached to the tank lid. If the flush is to occur during melter off-gas system operation, leave enough liquid in Tank 20 so that the drain from the SBS is sufficiently diplegged.
6. Disconnect the upper vent line past where it joins with the lower vent line, and drain the line into a bucket or provide some other means to detect flow.
7. Assure that valves V1, V3, V4, V5, V6, and V8 are closed.

5.2 Flushing Procedure

1. Open V5, V3, and V6. Note the time and the water flow rate into the filter housing as indicated by the flowmeter in the water supply line, in order to estimate the volume of water. Close V5 when water is at the standpipe level just above the element medium, as detected by water entering the flowmeter. This requires approximately 85 gallons of water.

2. Continue water flow and close V6 and V3 when water flows from the upper vent line. Put the collected liquid in a capped, labeled, container.
3. Soak the elements in water for 20 - 30 minutes.
4. Open V9 to pressurize air receiver to 30 psig as indicated by the pressure gauge on the air receiver. Close V9.
5. If the flush is to occur during melter off-gas system operation, the valves to the SBS overflow drains should be closed at this time.
6. Open V4 quickly to achieve backflow and immediately open V8.
7. Leave V8 open to discharge water to Tank 20. Open V3 after the liquid has begun draining. If desired, the flush solution can be sampled at this time through the sample port in the drain line. However, a more homogeneous, representative sample can be obtained as described below in 5.3.4.

5.3 Post-flushing Procedure

1. After draining is complete, allow the filter to dry by closing V8, and V4. Remove the teflon blanks, open V1 and close the HEMF bypass valve. Open the butterfly valve downstream of the HEMF to establish flow through the filter (per SOP No. 57 Rev. 4).
2. If there is little or no flow through the filter because of a water film on the element, allow time for the water to be removed by the suction in the line downstream from the HEMF.
3. Re-connect the poly lines to the HEMF pressure taps. Check the pressure drop across the filter to determine the effectiveness of the flushing procedure. Use a portable pressure indicator initially to check inlet and outlet pressures to assure the pressure drop is in the correct range

for the transducer used in the LFCM data acquisition system. Continue to monitor the pressure drop over several days as additional drying of the elements may occur.

4. To sample the flush solution, agitate the soluti in Tank 20, then remove a sample through the drain. To sample in this way, Tank 20 will need to have been rinsed before the flushing occurs. This sampling method is not practical during melter operation.
5. Pump the flush solution from Tank 20 to the thermosyphon per SOP No. 53.

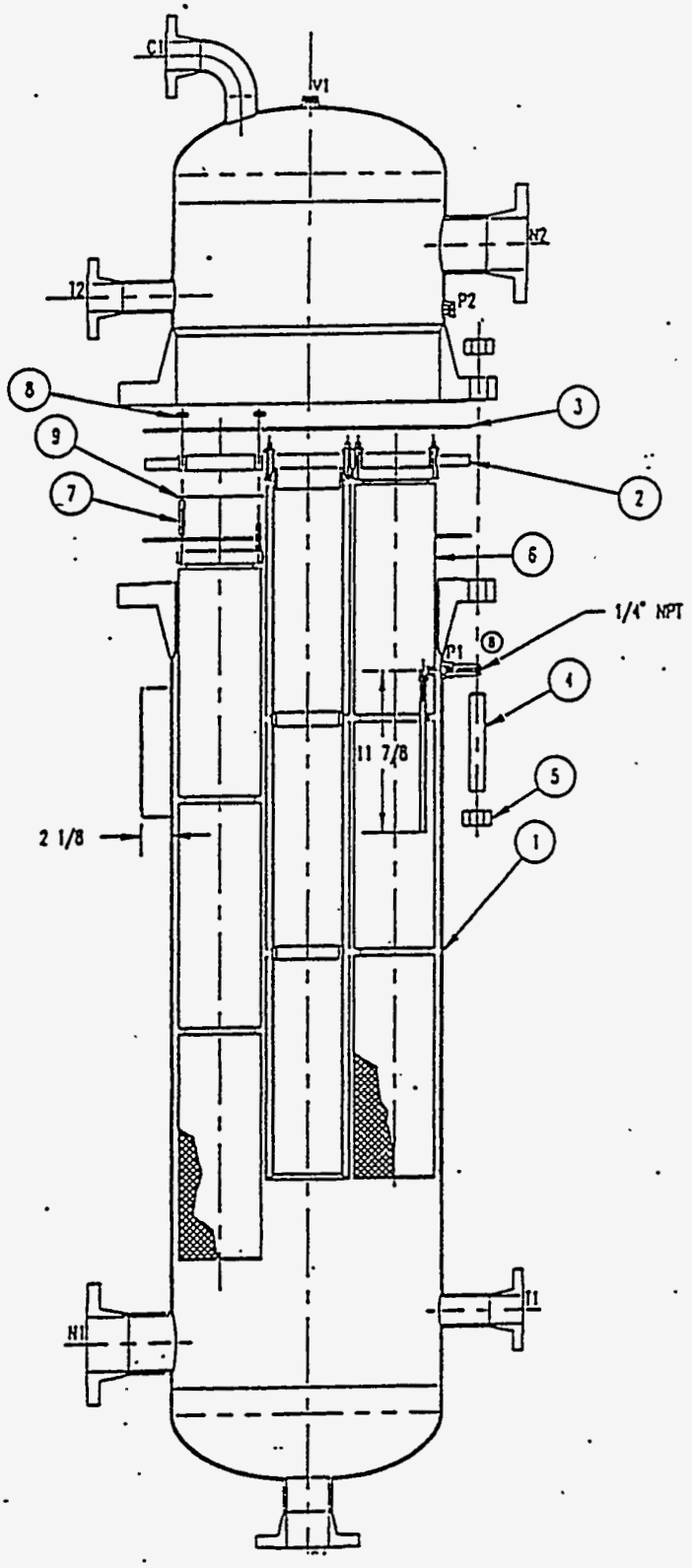

Figure 1. Schematic of HEMF

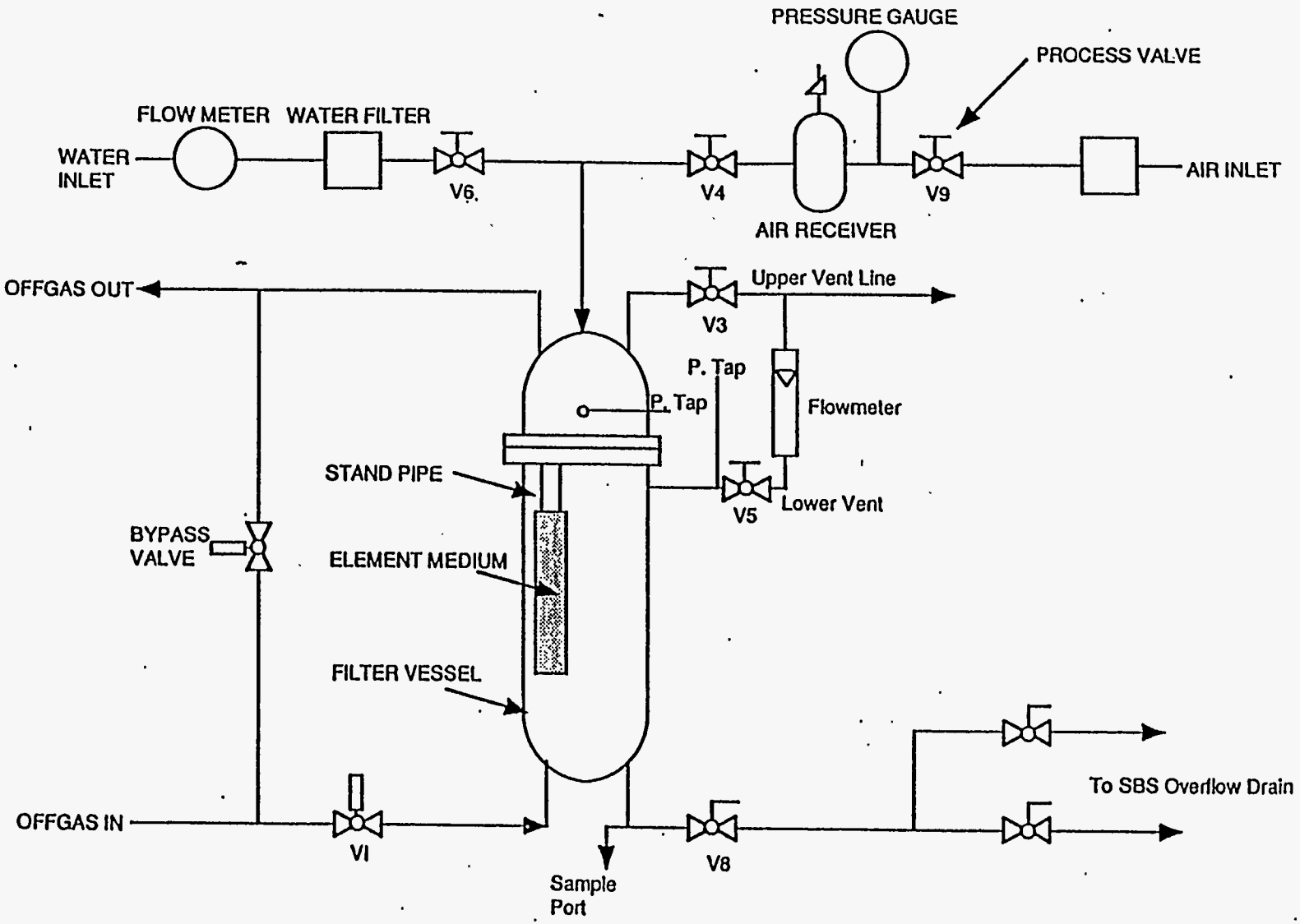

Figure 2. Backwash Flow Schematic

APPENDIX J Daily Plots of Noncondensible Gas Production Rates

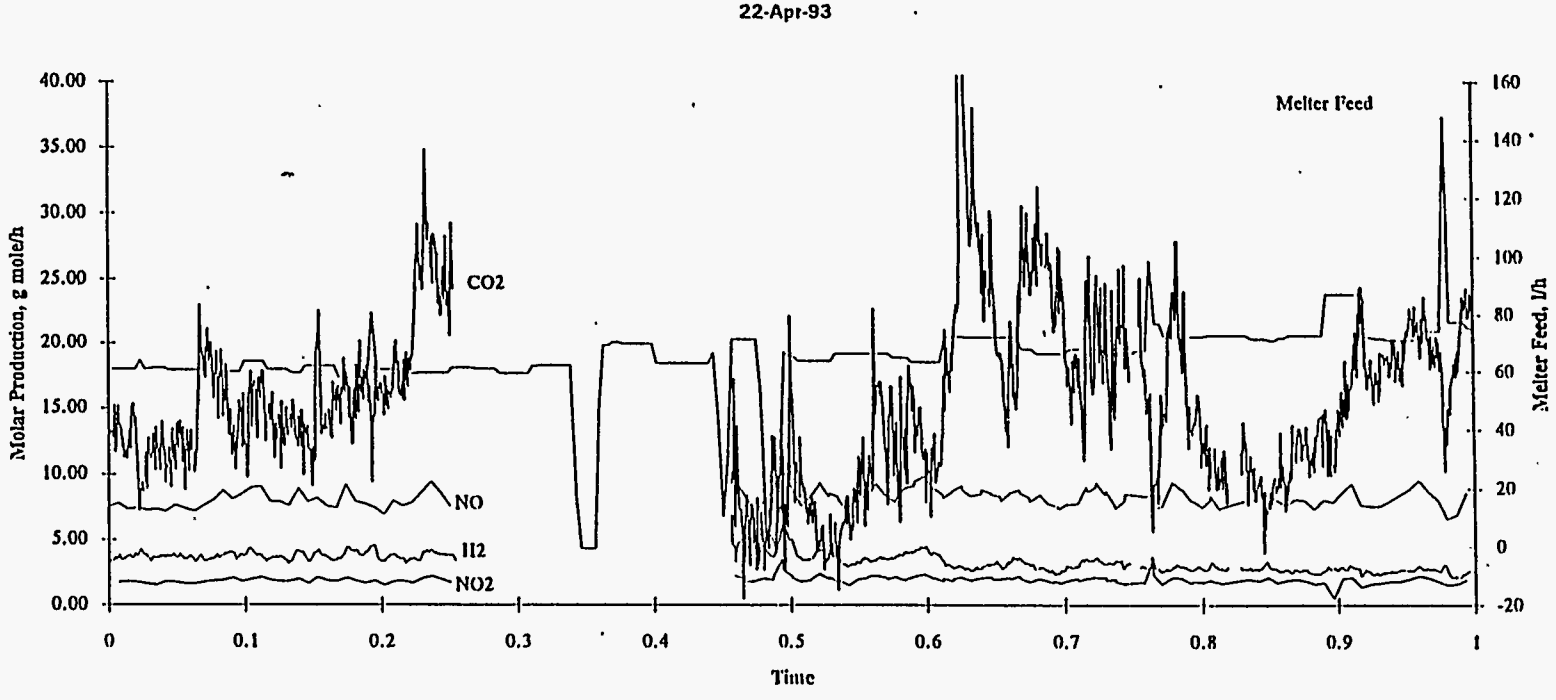
22-Apr-93
Molar Production, g mole/h
Melter Feed, l/h
Time
CO2
NO
H2
NO2
Melter Feed
40.00
35.00
30.00
25.00
20.00
15.00
10.00
5.00
0.00
160
140
120
100
80
60
40
20
0
-20
0
0.1
0.2
0.3
0.4
0.5
0.6
0.7
0.8
0.9
1

APR23GAS.XLC

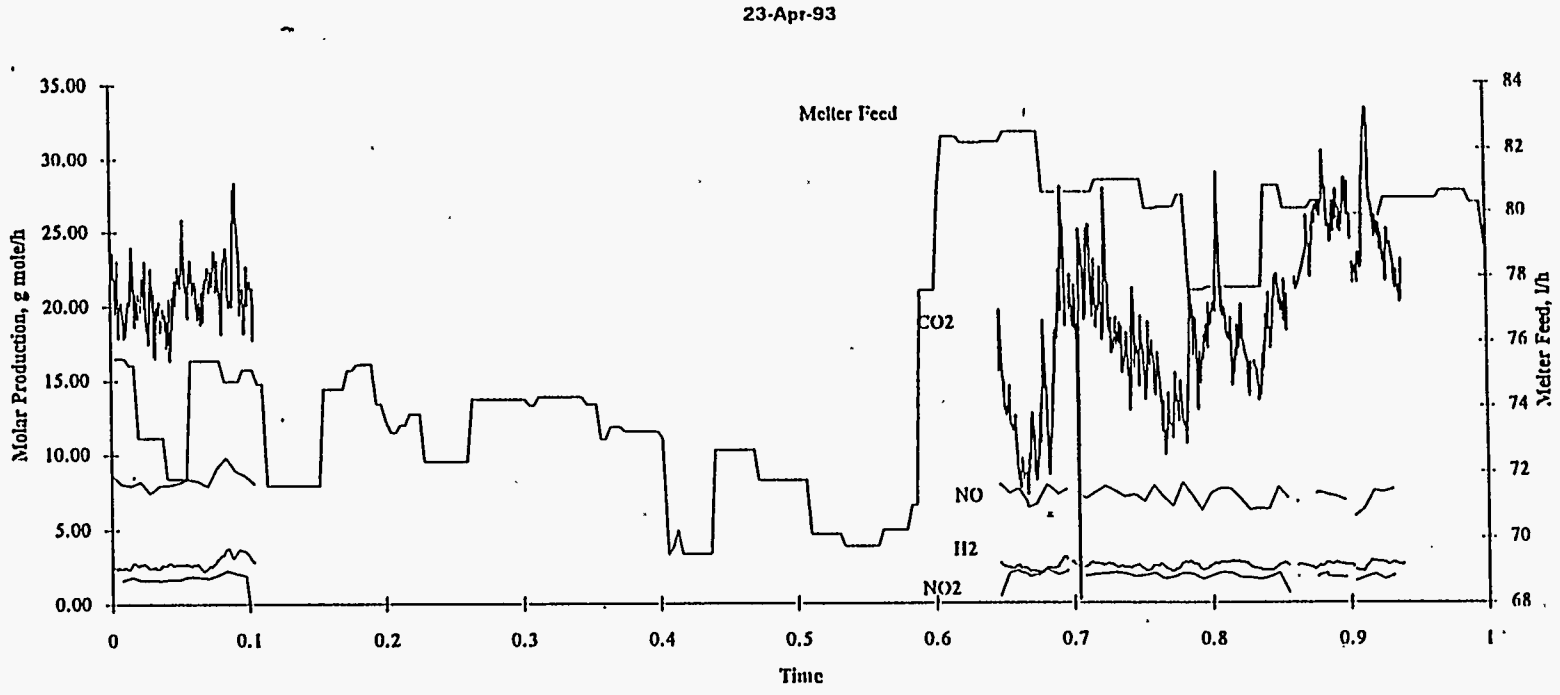

J.2

APR24GAS.XLC

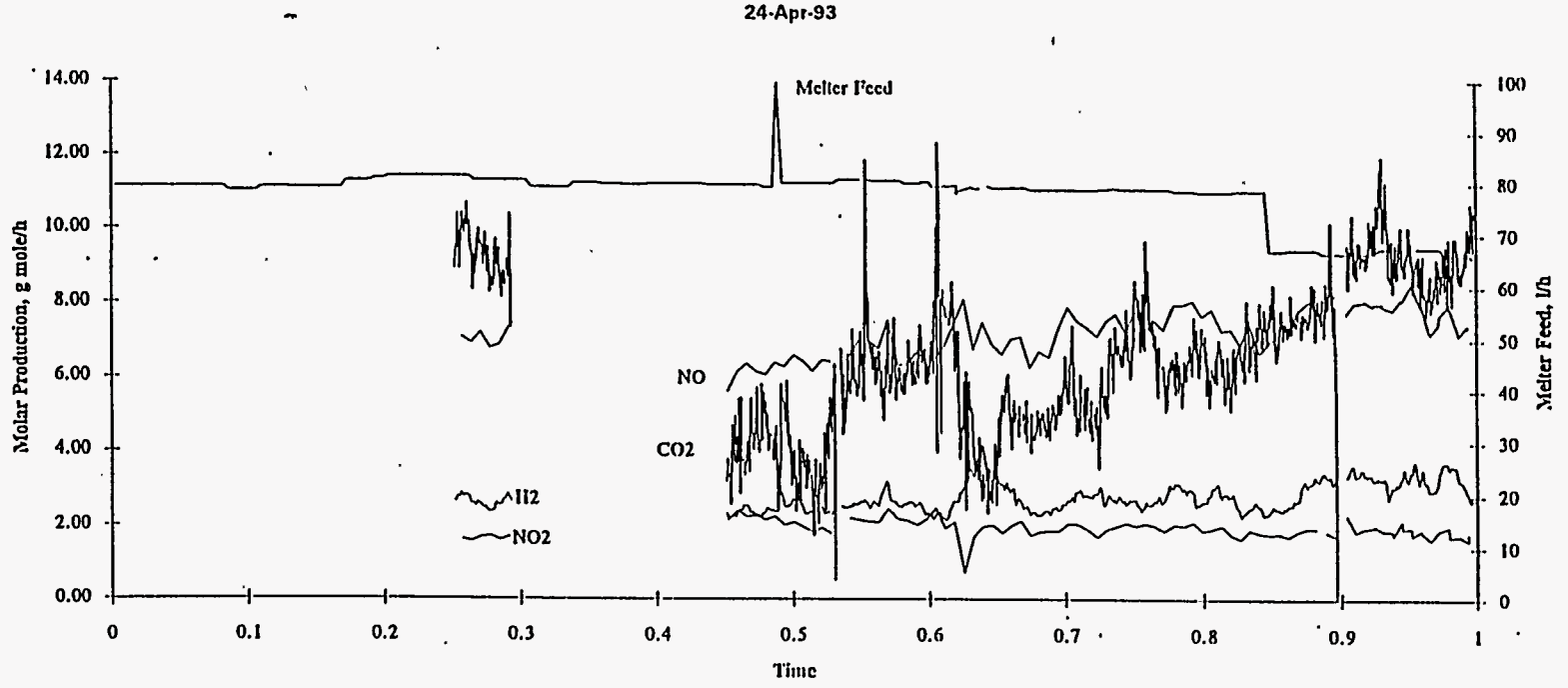

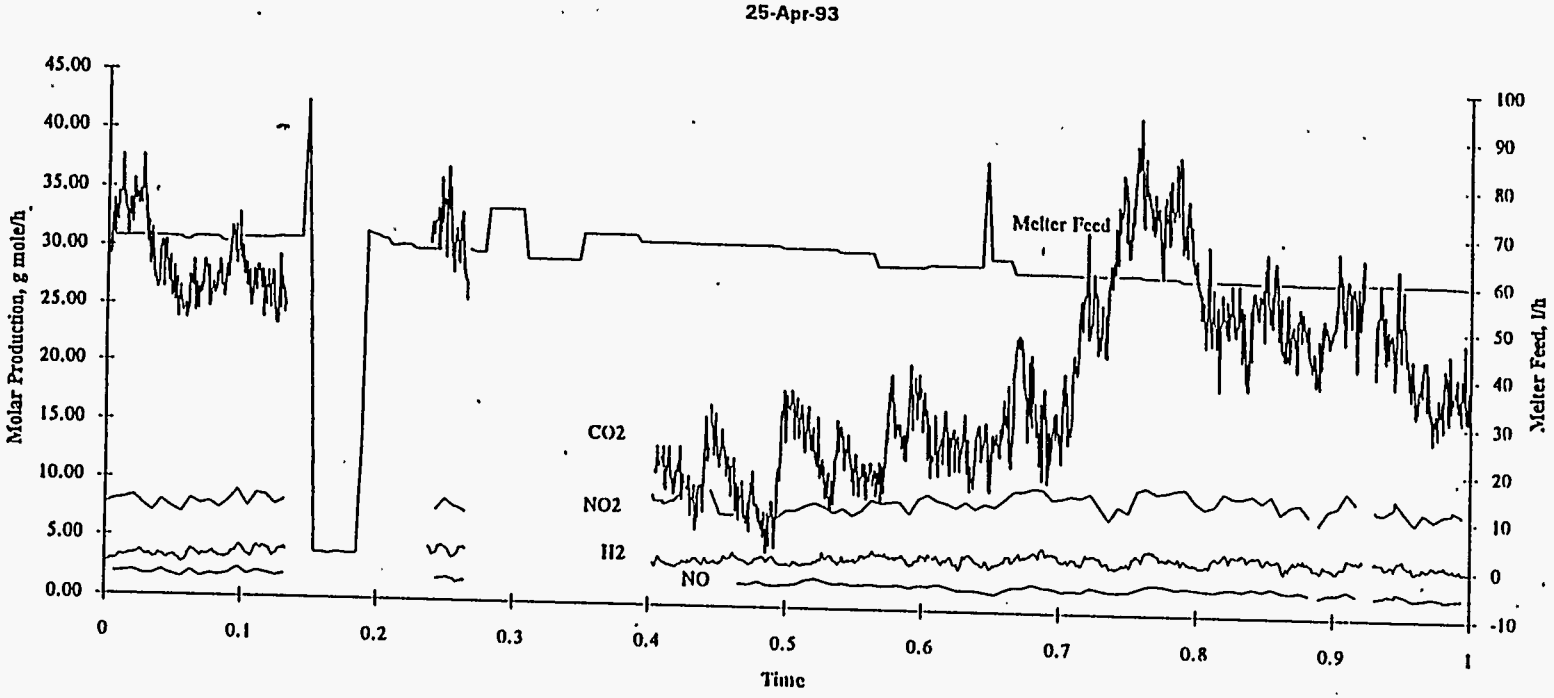
25-Apr-93
Molar Production, g mole/h
Melter Feed, l/h
Time
Melter Feed
CO2
NO2
H2
NO
45.00
40.00
35.00
30.00
25.00
20.00
15.00
10.00
5.00
0.00
100
90
80
70
60
50
40
30
20
10
0
-10
0
0.1
0.2
0.3
0.4
0.5
0.6
0.7
0.8
0.9
1

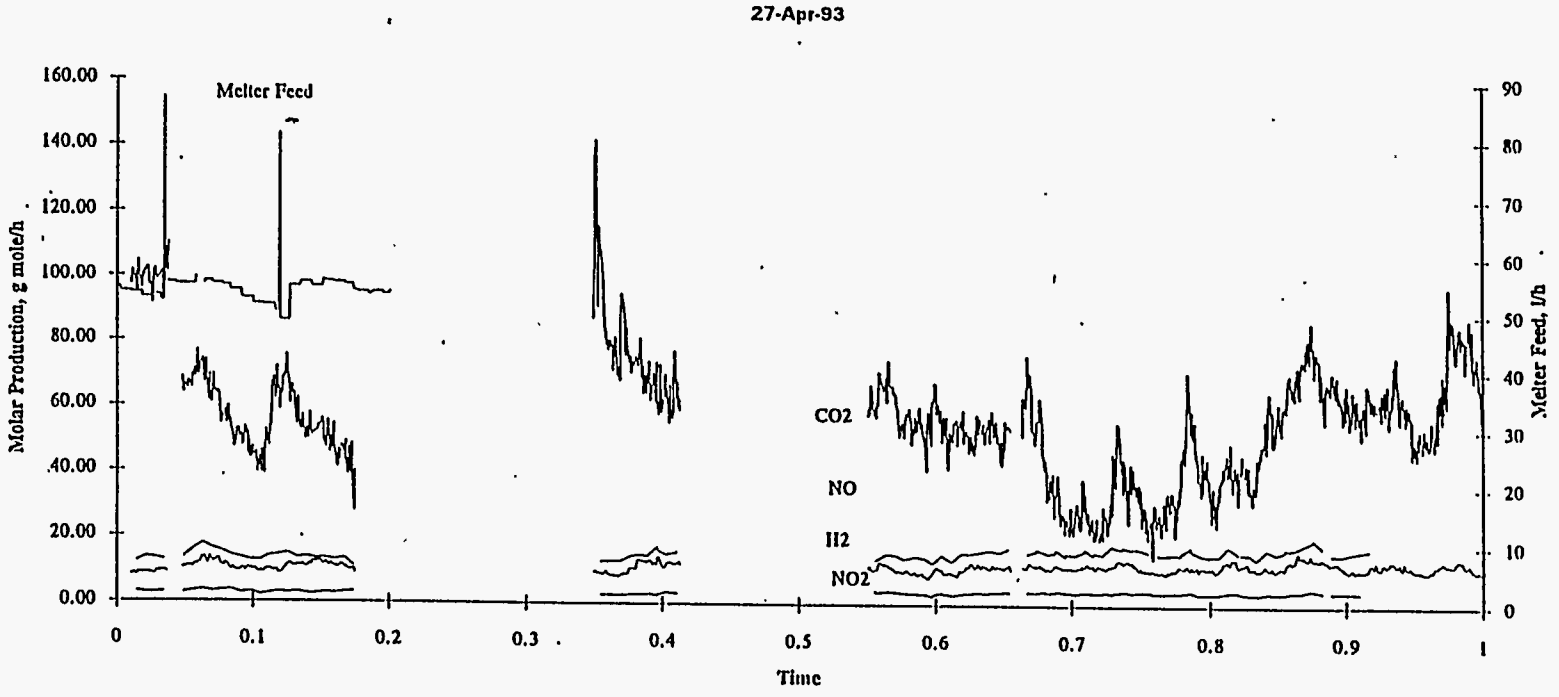
27-Apr-93
Melter Feed
Molar Production, g mole/h
Melter Feed, l/h
CO2
NO
H2
NO2
Time
160.00
140.00
120.00
100.00
80.00
60.00
40.00
20.00
0.00
90
80
70
60
50
40
30
20
10
0
0
0.1
0.2
0.3
0.4
0.5
0.6
0.7
0.8
0.9
1

APR28GAS.XLC

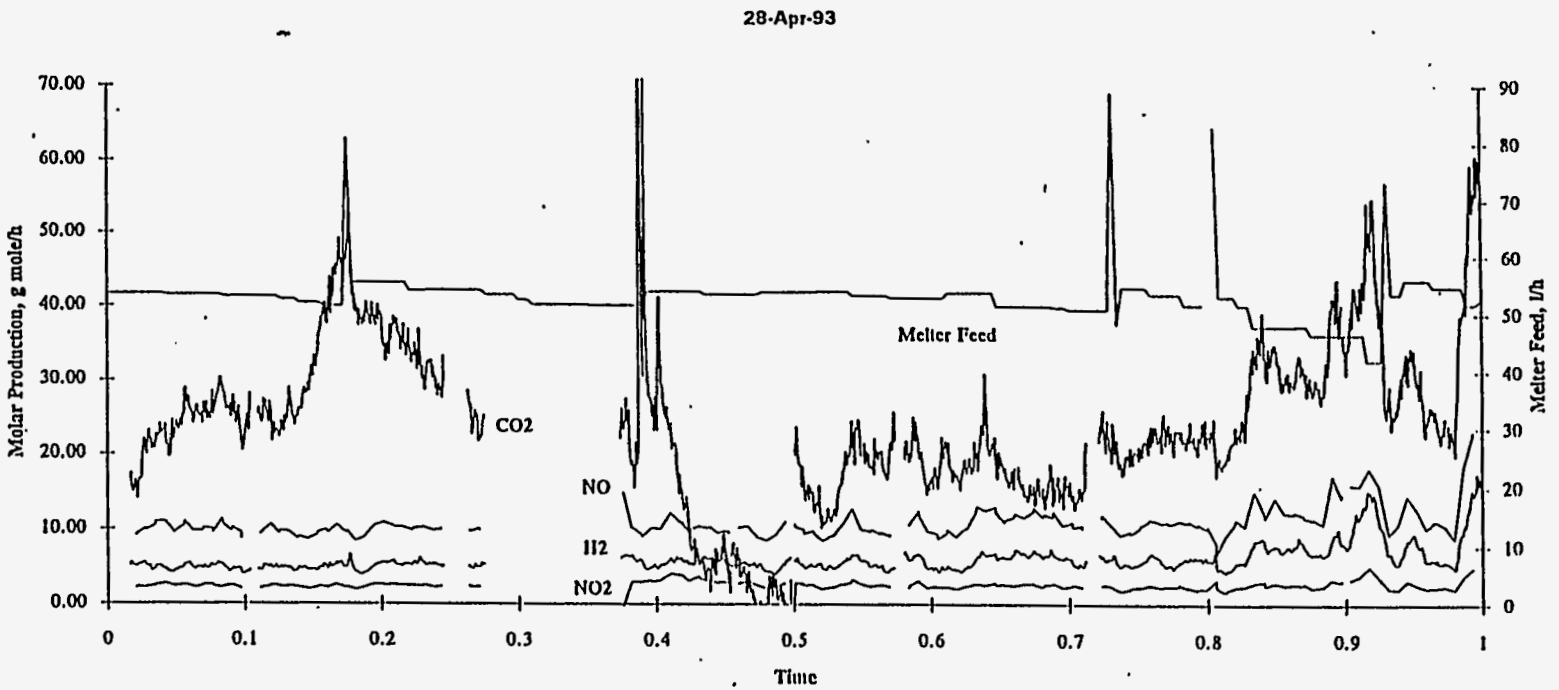

MAY10GAS.XLC

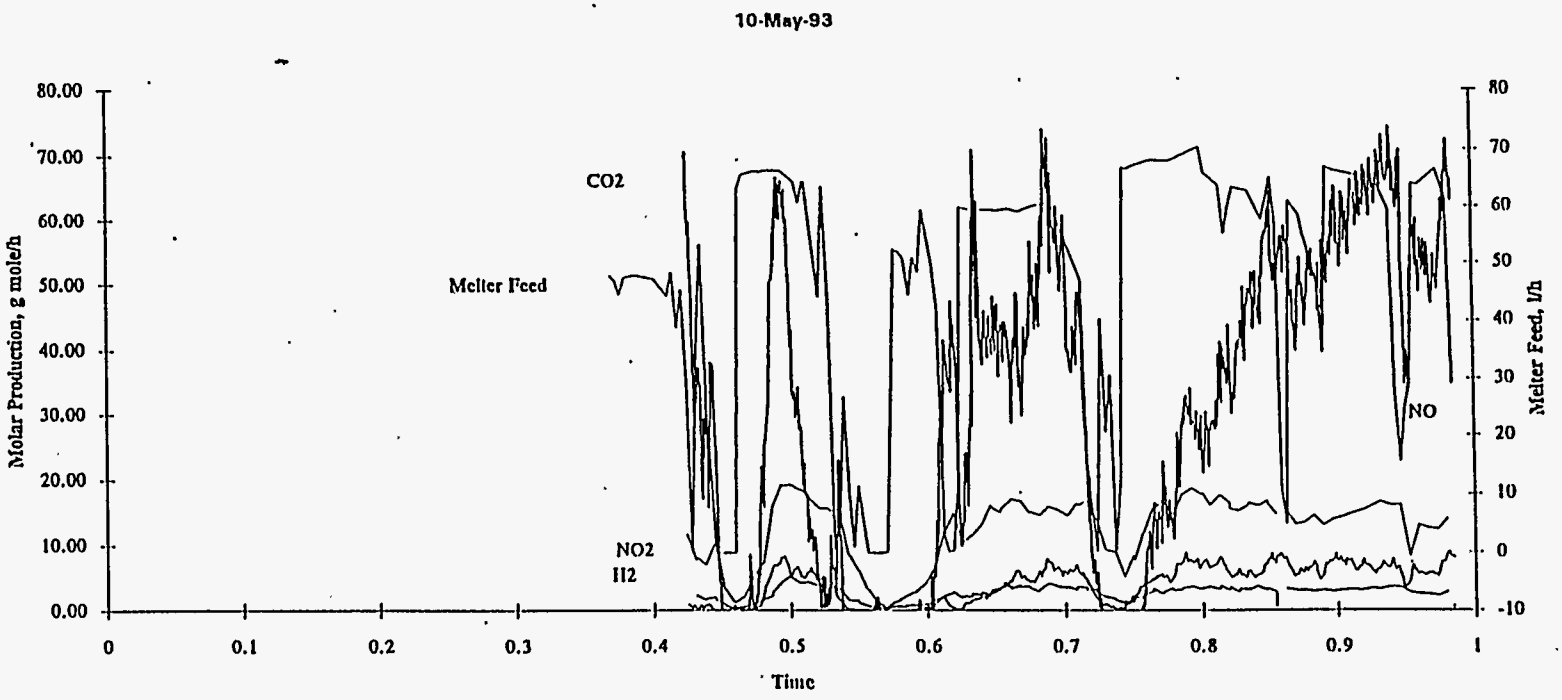

MAY11GAS.XLC

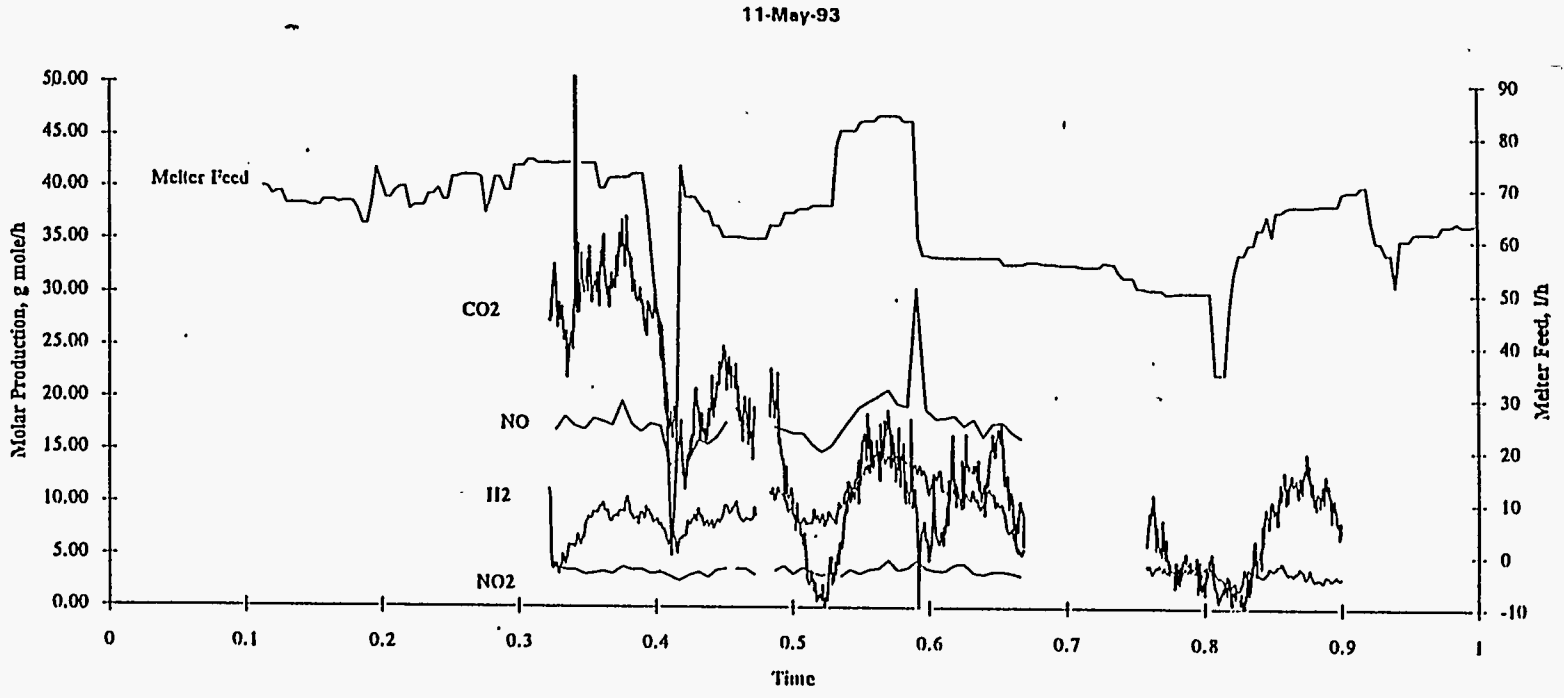

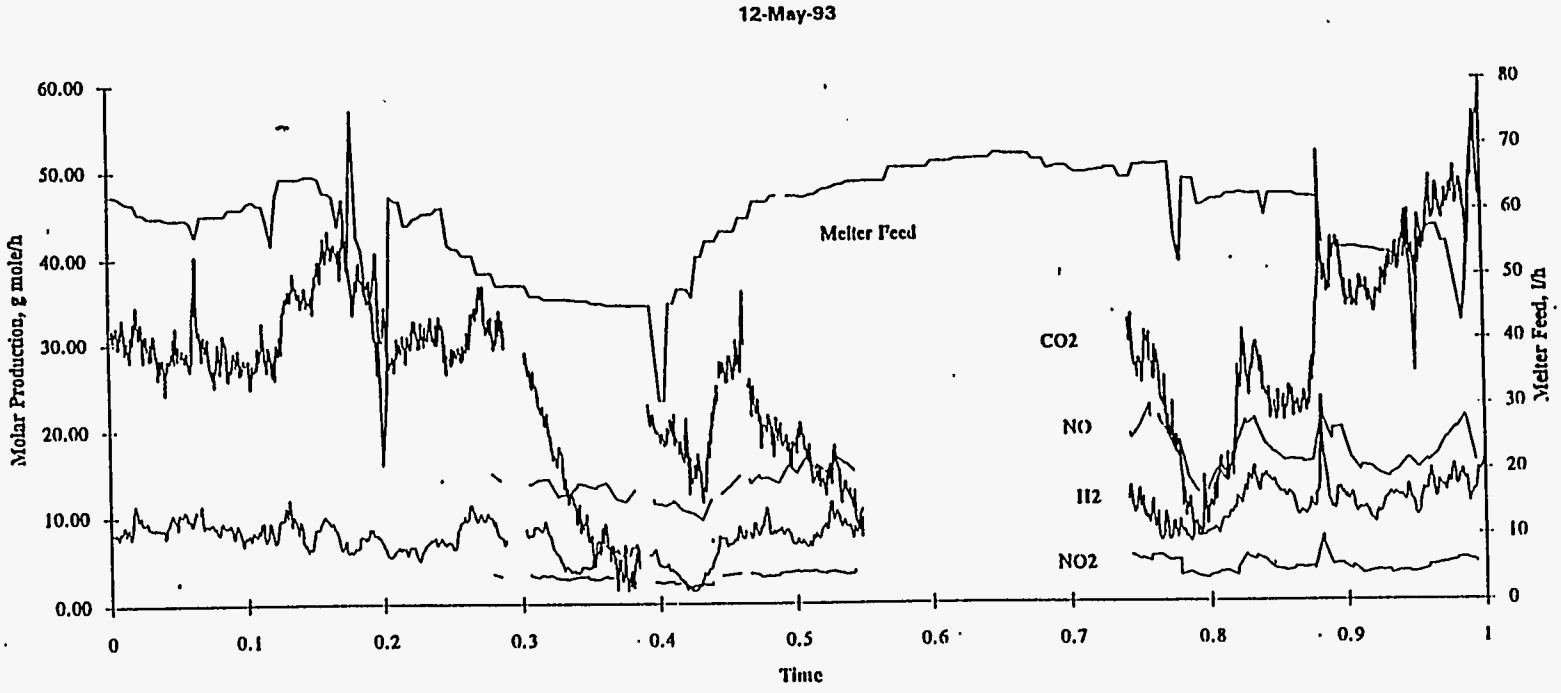
12-May-93
Molar Production, g mole/h
Melter Feed, l/h
Time
Melter Feed
CO2
NO
H2
NO2
60.00
50.00
40.00
30.00
20.00
10.00
0.00
80
70
60
50
40
30
20
10
0
0
0.1
0.2
0.3
0.4
0.5
0.6
0.7
0.8
0.9
1

MAY13GAS.XLC

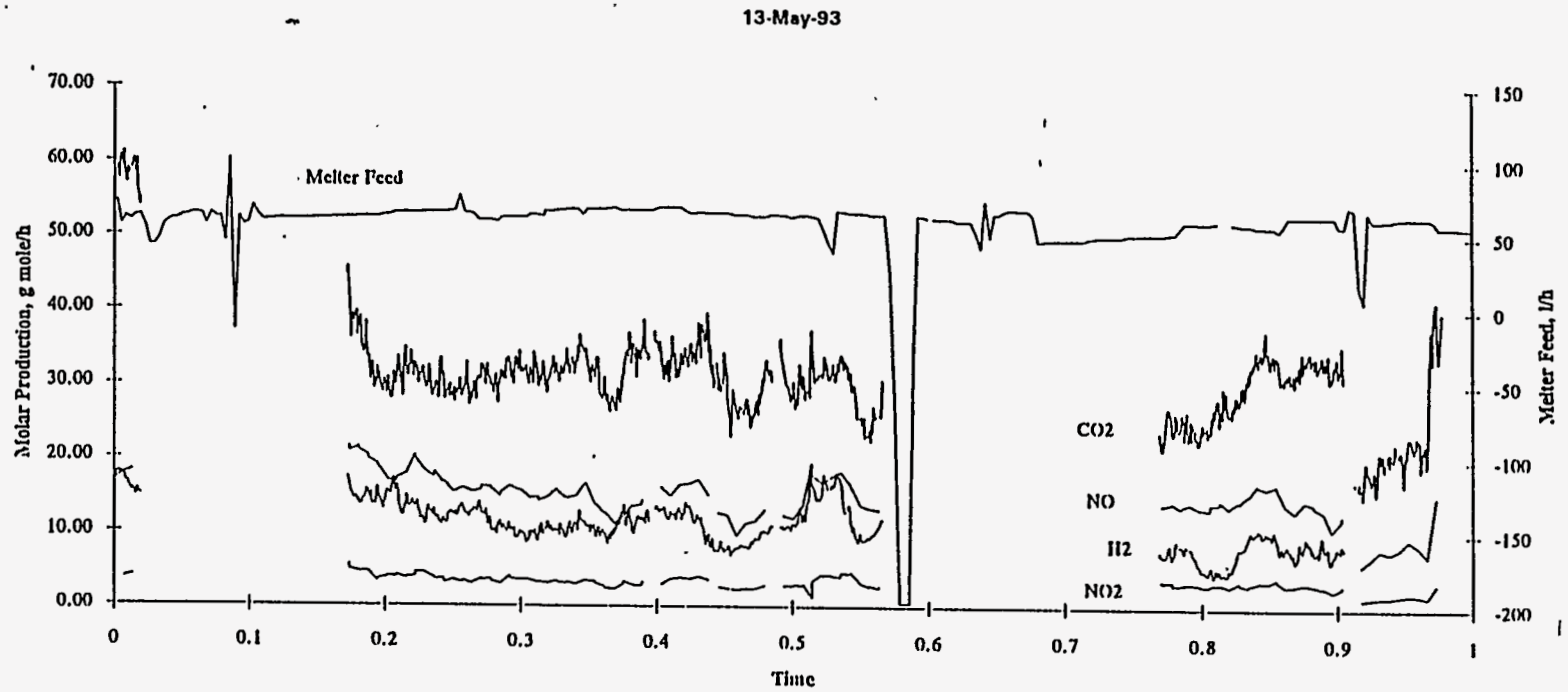

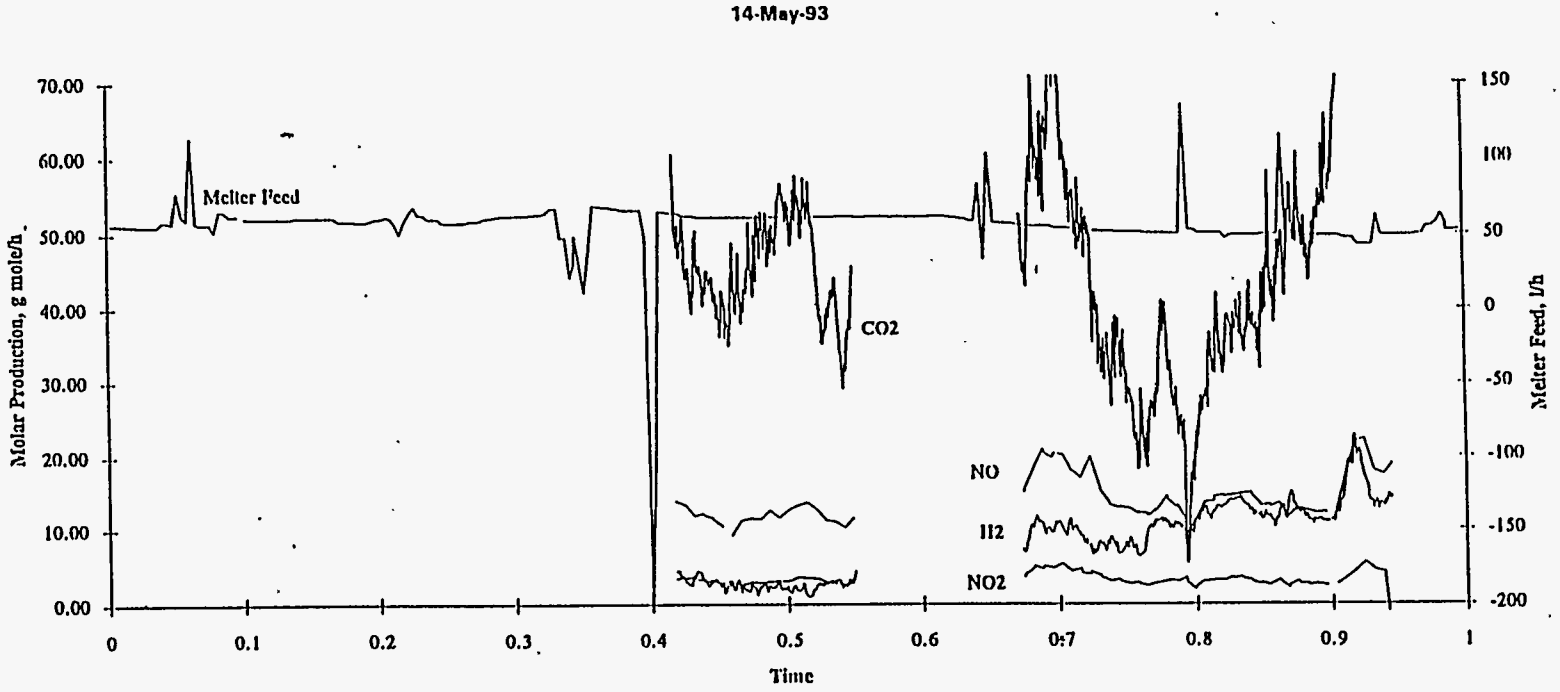
14-May-93
Molar Production, g mole/h
Melter Feed, l/h
Melter Feed
CO2
NO
H2
NO2
Time
70.00
60.00
50.00
40.00
30.00
20.00
10.00
0.00
150
100
50
0
-50
-100
-150
-200
0
0.1
0.2
0.3
0.4
0.5
0.6
0.7
0.8
0.9
1

MAY15GAS.XLC

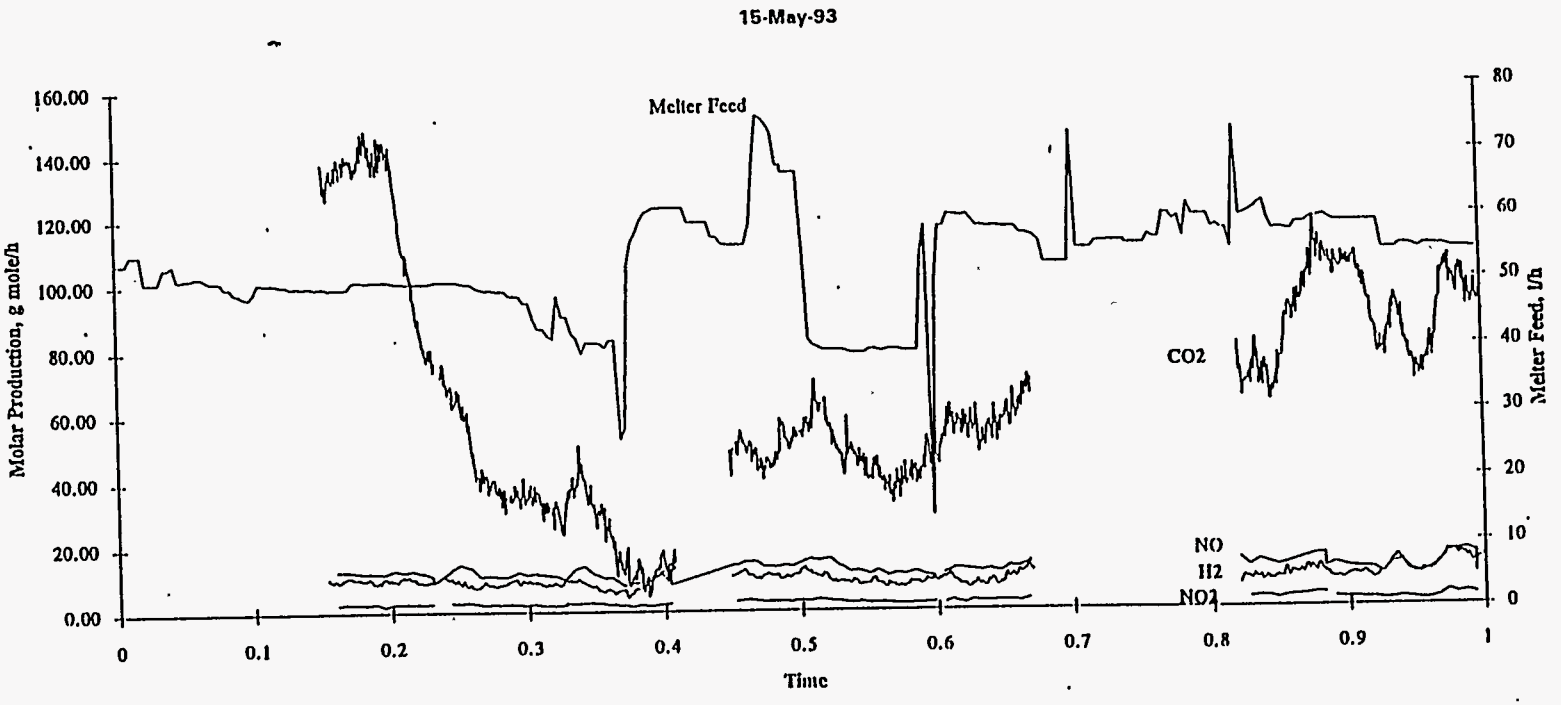

MAY16GAS.XLC